Surface Modification of Hemp Fibres using Low-pressure Plasma Technology

Kunal Shashank Bapat

A thesis submitted in accordance with the requirements for the degree of

Doctor of Philosophy

University of Leeds

School of Chemistry

Leeds Institute of Textile and Colour

July 2025

Intellectual property and publication statements

I confirm that the work submitted is my own, except where work which has formed part of jointly authored publications has been included. My contribution and the other authors' to this work have been explicitly indicated below. I confirm that appropriate credit has been given within the thesis where reference has been made to the work of others.

Reference to publications:

The following articles from this work were published:

1. **Improved colouration of hemp fabrics via low-pressure argon plasma assisted surface modification**
   K. S. Bapat, T. P. Kee, S. J. Russell and L. Lin Cleaner Chemical Engineering 2024 Vol. 10 Pages 100123 DOI:https://doi.org/10.1016/j.clce.2024.100123

This research publication contains experiments and results to achieve the objectives in Chapter 04.

2. **Study of hemp fibre properties modified via long duration low-pressure argon and oxygen plasma treatment**
   K. S. Bapat, Kailas L, Pask CM, T. P. Kee, S. J. Russell
   Under revision ACS Omega

This research publication contains the experiments and results to achieve the objectives in Chapter 05.

Acknowledgements

I extend my heartfelt gratitude to Dr Terence P Kee for his invaluable guidance and support throughout this work. I would like to express my sincere thanks to Professor Stephen Russell for his invaluable support and training.

In connection with Chapter 4, I sincerely thank Algy Kazlauciunas for providing essential training on the SEM equipment. I am also grateful to Dr. Kelvin Tapley for his support and insightful advice during this phase of the work, and to Professor Long Lin for his visionary input.

For Chapter 5, I express my sincere thanks to Dr. Lekshmi Kailas for her assistance with AFM experiments, to Mohammed Asaf for his guidance on FTIR usage, and to Mary Glasper for her instruction in operating fibre processing and testing machinery. I also acknowledge Dr. Chris Pask for his expertise and valuable input in acquiring and analysing XRD data.

With regard to Chapter 6, I wish to thank Martin Fuller from the Faculty of Biological Sciences for his guidance in SEM sample preparation. I am also grateful to Alex Kulak for his help and assistance in SEM and Raman spectroscopy.

In addition, I would like to thank the Chemistry Stores team: Kat, Jordan, Val, and Brian, for their support and friendship throughout. I extend my thanks to my lab mate and a true friend, Sui Hung Lam, for his camaraderie and assistance, and to Alice Hazelhurst from the School of Design for her guidance in the testing laboratory.

A heartfelt thank you to my parents, my uncle and aunt, and all those who have wished me well. Their unwavering faith and support have been a constant source of strength throughout this journey.

List of Figures

List of Tables

Chapter 1

Introduction

This Chapter introduces the foundational context for this research, which begins by exploring the history and background of hemp, tracing its origins, traditional uses, and re-emergence as a sustainable fibre source in modern times. Outlining the unique properties of hemp, such as its mechanical strength, antimicrobial qualities, and biodegradability, which collectively position it as a promising alternative to synthetic and conventional natural fibres. Further, the importance of hemp in the textile industry is highlighted in relation to sustainability and consumer demand for eco-friendly products. Despite various advantages that hemp brings, processing of hemp fibres remains challenging due to their complex structure and chemical composition. These challenges limit the fibre's broader industrial application and necessitate innovative surface treatment techniques. Plasma treatment offers a clean, solvent-free method to modify the surface characteristics of hemp fibres, potentially improving their compatibility with textile processes. The chapter concludes by outlining the aims and objectives of the research, which centre on exploring plasma-assisted surface modification as a means to overcome the limitations associated with hemp fibre processing. Together, these elements provide a comprehensive framework for the thesis and establish the rationale for the experimental work that follows.

1.1 History and general background of hemp

The cultivation and production of hemp fibres date back to 5000-4000 BC and was a highly valued fibrous material used in crafting hats, shoes, and robes for traders and sailors visiting Indian territories [1]. The exceptional quality, strength, and fineness of hemp fibres from this era reflect the sophistication of ancient Indian agricultural tools and textile production techniques. As hemp became an established industrial crop in India and other parts of Asia, it gradually spread to Europe via the Silk Road, where it was widely traded across Mediterranean countries during the Middle Ages. By the 16th century, hemp had been introduced to Chile, eventually reaching North America. Today, hemp is cultivated worldwide, including in France and Great Britain. Its popularity stems from its ability to grow rapidly and efficiently in temperate climates throughout the year, requiring minimal irrigation, pesticides, and chemical fertilisers. However, hemp production declined after the 18th century despite its historical significance. The rise of the Industrial Revolution resulted in the invention of the cotton

gin, and the expansion of industrial agribusiness led to a preference for alternative materials in fabric and paper production [2].

Hemp is widely used in various industries, alongside other bast fibres such as flax and ramie. Bast fibres are derived from the stem of the plants, which are collected from the phloem, the tissue surrounding the stem of certain plants. Figure 1.1 illustrates the internal structure of the bast fibre.

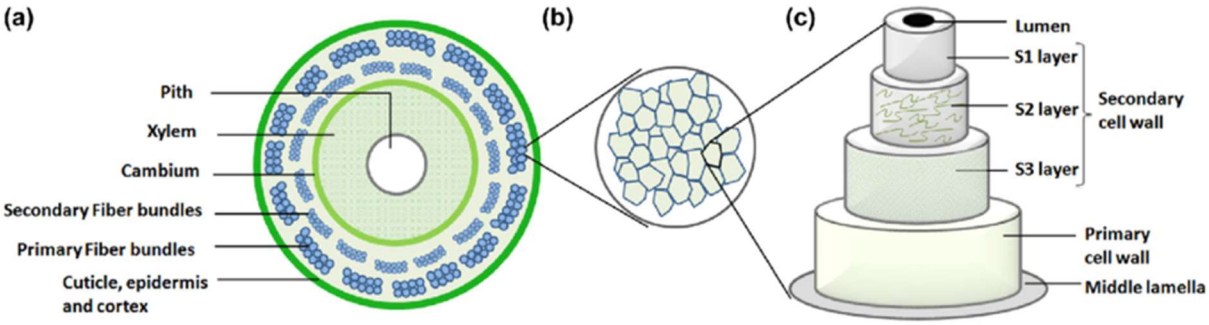

Figure 1.1 Internal structure of hemp [3]

Figure 1.1A illustrates the transverse section of the hemp bast, highlighting the internal anatomical structure. At the centre lies the pith, composed primarily of soft parenchymatous tissue. Surrounding the pith is the xylem, a rigid structure responsible for transporting water and minerals throughout the plant while also providing mechanical strength [3]. Adjacent to the xylem is the cambium, a meristematic layer that drives secondary growth by generating new xylem and phloem cells. External to the cambium lie the primary and secondary fibre bundles, which constitute the hemp fibres utilised in composites and textile applications. The cuticle, epidermis, and cortex form the outermost layers of the stem, offering both protection and mechanical support. Figure 1.1B depicts the primary fibre bundles, characterised by densely packed fibrils, while Figure 1.1C presents the cellular architecture of individual fibres, highlighting their structured and fibrous morphology [3]. The fibres are protected by waxes and other protective substances, with bundles of fibres held together by these waxy substances. Bast fibres are highly oriented in an axial direction and have a low rate of extensibility, a characteristic attributed to the unique structural organisation of the hemp plant [4]. These fibres are promising for use in reinforced composites due to their high tensile and load-bearing capacity. Kenaf, ramie, flax, jute and hemp are among the most commonly used bast fibres for industrial use [5].

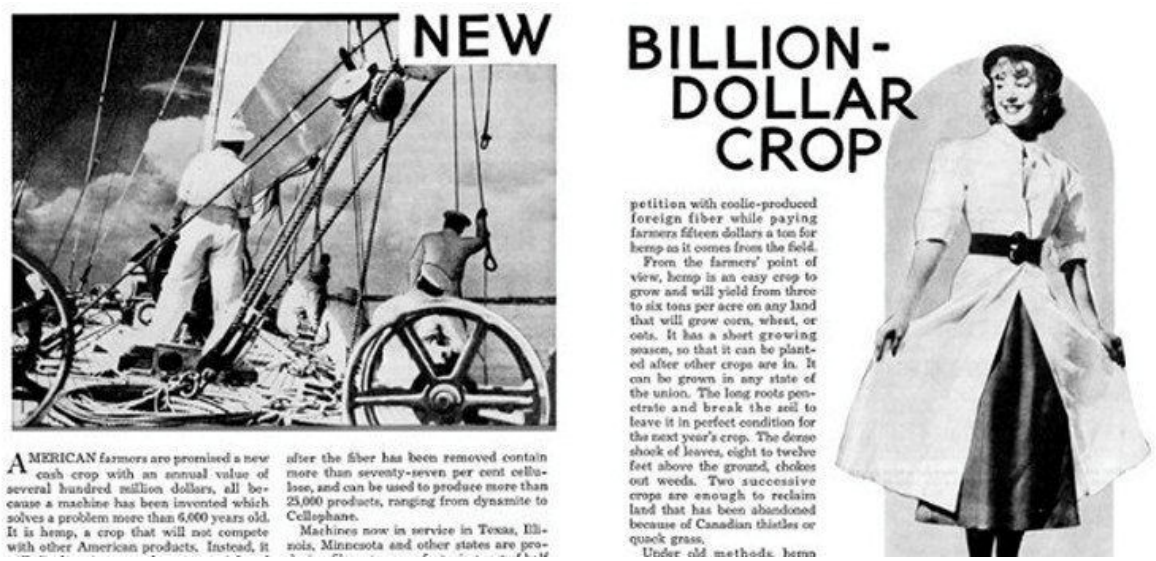

NEW

AMERICAN farmers are promised a new cash crop with an annual value of several hundred million dollars, all because a machine has been invented which solves a problem more than 6,000 years old. It is hemp, a crop that will not compete with other American products. Instead, it after the fiber has been removed contain more than seventy-seven per cent cellulose, and can be used to produce more than 25,000 products, ranging from dynamite to Cellophane.

Machines now in service in Texas, Illinois, Minnesota and other states are pro-

BILLION-DOLLAR CROP

petition with coolie-produced foreign fiber while paying farmers fifteen dollars a ton for hemp as it comes from the field.

From the farmers' point of view, hemp is an easy crop to grow and will yield from three to six tons per acre on any land that will grow corn, wheat, or oats. It has a short growing season, so that it can be planted after other crops are in. It can be grown in any state of the union. The long roots penetrate and break the soil to leave it in perfect condition for the next year's crop. The dense shock of leaves, eight to twelve feet above the ground, chokes out weeds. Two successive crops are enough to reclaim land that has been abandoned because of Canadian thistles or quack grass.

Figure 1.2 Billion Dollar Crop [6]

Hemp has a rich history and is often referred to as the “Billion-dollar crop” because of its versatile uses across industrial, medicinal and agricultural sectors. Following the news article in Figure 1.2, hemp gained widespread attention as a crop with billions of potential applications. It was documented that 5-90% of the world’s paper, including books, Bibles, maps, paper money, stocks and bonds, was made from hemp fibre [7]. From 1890 to 1910, linen textiles were predominantly manufactured from hemp rather than flax. Despite the material's advantageous properties, such as durability, sustainability, and versatility, its contemporary usage has diminished considerably. This decline is primarily attributed to the persistent stigma associated with hemp’s connection to psychoactive substances, which are derived from the plant’s floral components, whereas textile-grade fibres are extracted from the stem.

Industrial hemp, a type of Cannabis sativa, has been successfully developed to contain negligible amounts of tetrahydrocannabinol (THC: the compound in cannabis responsible for its narcotic effects) [8] is now used in a variety of applications, including reinforced composites, concrete, plasticising agents, bio-oils for medicinal use and textiles for commercial use, such as garments and technical textiles. Hemp is one of the fastest-growing plants on earth after bamboo. In Europe, France is the largest producer of hemp for various applications. Hemp’s dense foliage allows it to be planted as a cover crop to suppress weeds in the area. Scientific investigations have shown that hemp is a potential natural source of food, cover, and energy. As the world shifts towards a sustainable and circular economy, hemp may emerge as a key bio-based material to replace petroleum-derived synthetics such as polyester, nylon, and plastic

composites, particularly in industries like textiles, packaging, automotive, and construction [4].

1.2 Overview of useful properties and applications of hemp

Hemp is a highly versatile plant with a wide range of applications across various industries, owing to its unique chemical composition and structural properties. It has been cultivated for centuries for its nutritional, medicinal, cosmetic, textile, energy, and environmental benefits, making it an invaluable resource for sustainable development. Figure 1.3 depicts an overall picture of the various applications of hemp in food, fuel, composite and textile industries.

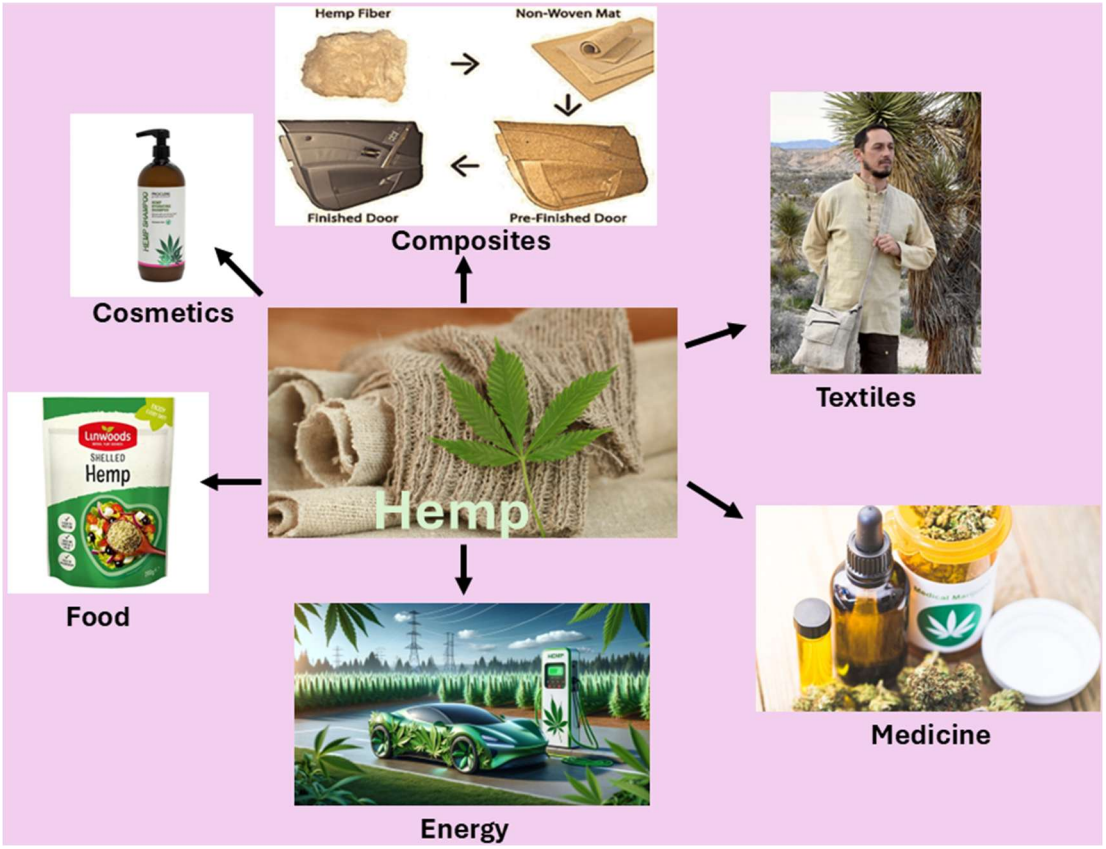

Figure 1.3 Applications of hemp

One of the most significant uses of hemp is in the food industry. Hemp seeds are a rich source of essential nutrients, including proteins, dietary fibres, and fatty acids. They provide an optimal balance of omega-3 and omega-6 fatty acids, which play a crucial role in maintaining cardiovascular health. The oil extracted from these seeds is

commonly used in culinary applications due to its distinctive nutty flavour and health-promoting properties. Furthermore, hemp-derived protein powders have gained popularity among vegetarians and vegans as a plant-based protein alternative, contributing to a nutritious and well-balanced diet [9].

The cosmetic industry has also integrated hemp oil into various skincare and personal care products. Due to its abundance of vitamins A, C, and E, hemp oil serves as a potent moisturising and anti-inflammatory agent. It is widely used in lotions, soaps, and lip balms to enhance skin hydration and protection. Moreover, its non-comedogenic properties ensure that it does not clog pores, making it suitable for all skin types, including sensitive and acne-prone skin [10].

In the pharmaceutical and medical fields, hemp-derived compounds have shown remarkable therapeutic potential. Cannabidiol (CBD), a prominent cannabinoid found in hemp, is recognised for its anti-inflammatory, analgesic, and anxiolytic effects. As a result, CBD has been incorporated into treatments for chronic pain, epilepsy, and anxiety disorders. Unlike tetrahydrocannabinol (THC), which is psychoactive, CBD provides medicinal benefits without causing intoxication, making it a safer alternative for medical applications [11].

Hemp also plays a crucial role in the energy sector. Biomass from the plant can be converted into biofuels, such as biodiesel and ethanol, providing renewable and environmentally friendly alternatives to conventional fossil fuels. Given hemp's fast growth cycle and adaptability to diverse climatic conditions, it presents a viable option for sustainable energy production, reducing dependency on non-renewable resources [2]. Beyond its direct applications, hemp cultivation significantly benefits the environment. Its deep root system stabilises soil and prevents erosion, making it a valuable crop for soil conservation. Additionally, hemp possesses phytoremediation properties, allowing it to absorb heavy metals and toxins from contaminated soils, thereby improving land quality. Furthermore, hemp's rapid growth and ability to sequester carbon dioxide contribute to mitigating climate change, positioning it as an eco-friendly agricultural solution [2].

The construction industry has also embraced hemp-based materials, particularly hempcrete, which is a mixture of hemp hurds and lime. This innovative material provides excellent insulation, is lightweight, and has a negative carbon footprint,

making it an ideal choice for sustainable building projects. Its ability to regulate indoor humidity levels further enhances its suitability for construction purposes [12]. In the paper industry, hemp fibres offer an environmentally sustainable alternative to wood-based paper production. Hemp-derived paper is more durable, resistant to yellowing, and requires fewer chemical treatments compared to conventional wood pulp paper. Additionally, hemp cultivation consumes less water and fewer pesticides, thereby minimising the ecological footprint of paper manufacturing [12]. Hemp fibres are used in the production of fibre-reinforced composites because of their high strength and durability. The resulting composites are used in the manufacturing of automotive components, construction materials, and consumer goods [12].

1.3 Importance of hemp fibre in the textile and composite industries

Hemp fibre stands out among natural fibres due to its remarkable strength, surpassing that of cotton, flax, and nettle. Historically, this durability made hemp a preferred material for producing ropes, rigging, fishing nets, and sails, ensuring reliability in maritime and industrial applications. In addition to its robustness, hemp fibre is valued for its flexibility, resilience, and resistance to water damage, enhancing its practicality for a variety of uses [12]. With advancements in textile technology, hemp is now processed into mainly woven fabrics that not only retain its signature durability but also offer greater softness and comfort. Modern textile manufacturing techniques have led to the production of woven hemp fabrics that outperform cotton in terms of longevity and resistance to deformation. Recognising these advantages, prominent consumer brands such as Adidas and Patagonia have incorporated hemp textiles into their product lines, further promoting their adoption in mainstream fashion [12]. Pure, 100% hemp textiles have gained significant traction in the apparel industry, where they are utilised for making jeans, sportswear, casual clothing, hats, bags, cushion covers, blankets, and accessories. Additionally, hemp's natural breathability and antimicrobial properties make it an excellent choice for summer wear, ensuring comfort and hygiene. Finished textile products such as shoes, socks, and home furnishings often incorporate either 100% hemp or a blend of hemp with other natural or synthetic fibres, expanding their applicability in modern textile production [13].

Beyond clothing, hemp fibre is a key material in interior textiles and composite applications. It is used in manufacturing rugs, pure hemp carpets, and upholstery fabrics, providing durable and eco-friendly alternatives to synthetic materials.

Moreover, its incorporation into composite materials has proven beneficial in the automotive and construction industries, where hemp-based bio composites are increasingly replacing traditional synthetic reinforcements. Despite these advantages, the widespread use of hemp in the textile industry faces certain challenges. However, ongoing research and technological advancements are gradually overcoming these limitations, paving the way for broader industrial adoption of hemp textiles and composites [14].

1.4 Challenges in the utilisation of hemp in textile products

Figure 1.4 outlines the key challenges associated with incorporating hemp into textile products. One of the most significant barriers is governance and regulatory constraints. Extensive documentation, compliance checks, and bureaucratic procedures are required before hemp cultivation can commence, adding to the complexity of its adoption. Additionally, legal restrictions vary across regions, further complicating large-scale production. In India, for instance, only one out of the 28 states has officially approved industrial hemp cultivation, limiting its commercial expansion [1].

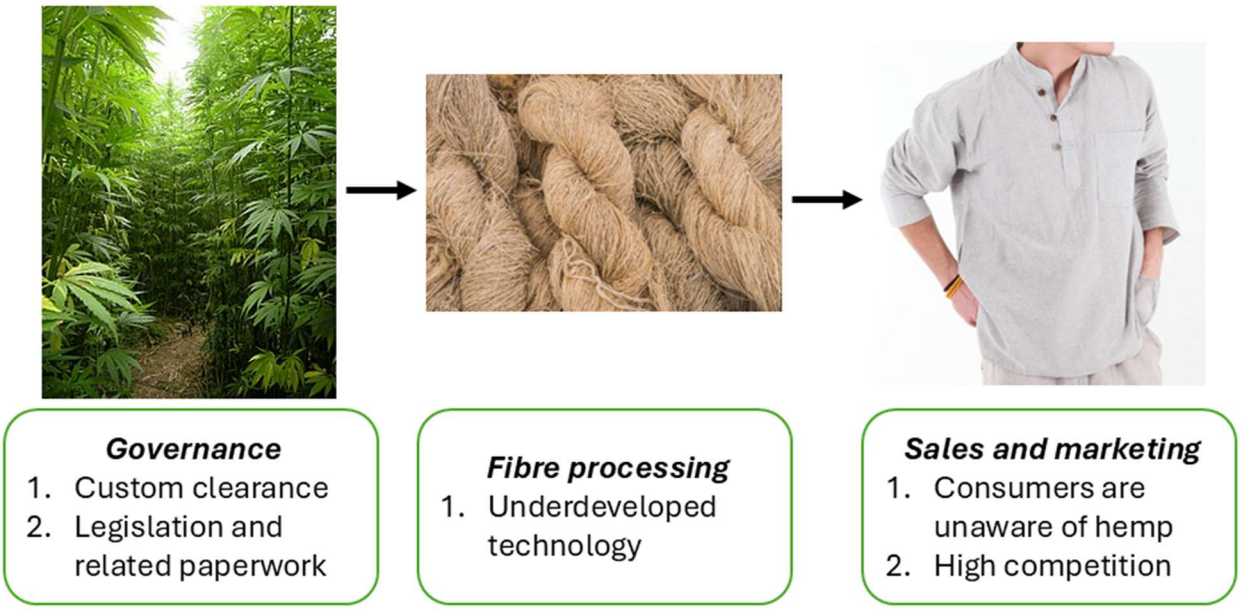

Figure 1.4 General challenges in hemp fibre processing

Major obstacles include laws and regulations on agriculture and hemp production, along with the issue of inadequate fibre processing technology [15]. The equipment

and infrastructure needed for effective hemp fibre processing are still in their infancy when compared to more established sectors like the production of cotton and synthetic fibre [16]. The high production cost and inefficiencies resulting from this technological gap may affect the integration of hemp products into the broader textile market. Additionally, hemp textiles have a low consumer awareness, hindering their market penetration [17]. Some misunderstandings about its connection to psychoactive cannabis fuel these restrictions on hemp-based products, despite its historical prominence as a textile fibre [17]. Hemp clothing and textile products compete with cheap and available synthetic fibres such as polyester and nylon. Additionally, cotton dominates the natural fibre market due to its familiarity and strong market presence. Overcoming these challenges would require targeted efforts in consumer awareness, policy reforms, and advancements in hemp processing technology for hemp to compete in the textile and fibre industries.

1.4.1 Challenges in processing hemp fibre into textiles and composites

The main challenges in processing hemp fibre into composites and textiles mainly include its partially hydrophilic nature and inconsistent fibre length and size, often requiring additional chemical treatments to improve compatibility with the polymer matrix and dyes or finishing agents. In this thesis, hemp is described as a partially hydrophobic substrate, exhibiting a water contact angle of around 60°, which lies between complete hydrophilicity (θ = 0°) and complete hydrophobicity (θ = 90°). The key challenges are as follows [18] [16] [19]:

1. ***Moisture absorption:*** Hemp is hygroscopic in nature, which can affect the processing and performance of fibre reinforced composites and textiles, requiring pre-drying steps before use.

2. ***Poor fibre-matrix adhesion:*** Hemp fibres possess a lignin-rich outer layer that imparts partial hydrophobicity (contact angle ~ 65°) overlying a cellulose core bearing abundant hydroxyl groups. This surface heterogeneity and residual contamination impede consistent wetting and strong interfacial bonding with common polymer matrices (e.g., polypropylene, polyethylene, epoxy).

3. ***Fibre dimensional variability:*** Hemp fibres vary in length, diameter, and morphology depending on the growing conditions and processing methods, potentially impacting the consistency of textile and composite product properties.

4. **Fibre diameter**: Hemp fibres are naturally coarser and stiffer than cotton, which can make them less appealing for certain types of clothing. Such fibre diameter differences can also affect the reflectance properties of fabrics, affecting their visual appearance.

5. **Dye absorption**: Hemp fibres possess a distinct structure compared to cotton, characterised by higher crystallinity and the presence of non-cellulosic components such as lignin and pectin. These features can restrict dye penetration and result in lower dye uptake, making it more challenging to achieve vibrant and uniform colouration without appropriate pre-treatments [19].

6. **Technological differences:** The differing end-use applications of textiles and composites incorporating hemp necessitate distinct processing approaches. Converting hemp for woven textiles involves extensive retting, scutching, and spinning, whereas nonwoven applications for composites demand mechanical or chemical fibre separation methods, complicating standardisation across industries [20].

1.5 Potential for plasma treatment to address these challenges

Plasma is a distinct state of matter where atoms or molecules become electrically, thermally, or magnetically charged, often through ionisation [21]. It is a highly energised state consisting of various particles, including ions, electrons, metastables, and excited states of atoms or molecules. This ionised gas exhibits unique physical and chemical properties compared to its neutral form, making it widely regarded as the "fourth state of matter." Plasma can be categorised into two types: cold plasma and hot plasma [22]. Cold plasma operates at lower temperatures and is predominantly used for material modification, as in this project. Its versatile applications span several industries, including medical plastics, print adhesion, automotive manufacturing, aerospace, microscopy, and water treatment. Plasma treatment can lead to physical or chemical changes in the material's surface through interactions with radicals, ions, or excited-state electrons, resulting in effects like polymerisation or sputtering. Figure 1.5 illustrates the mechanism of plasma treatment, which is commonly used to modify polymers and enhance surface properties such as adhesion, hardening, and cross-linking [22].

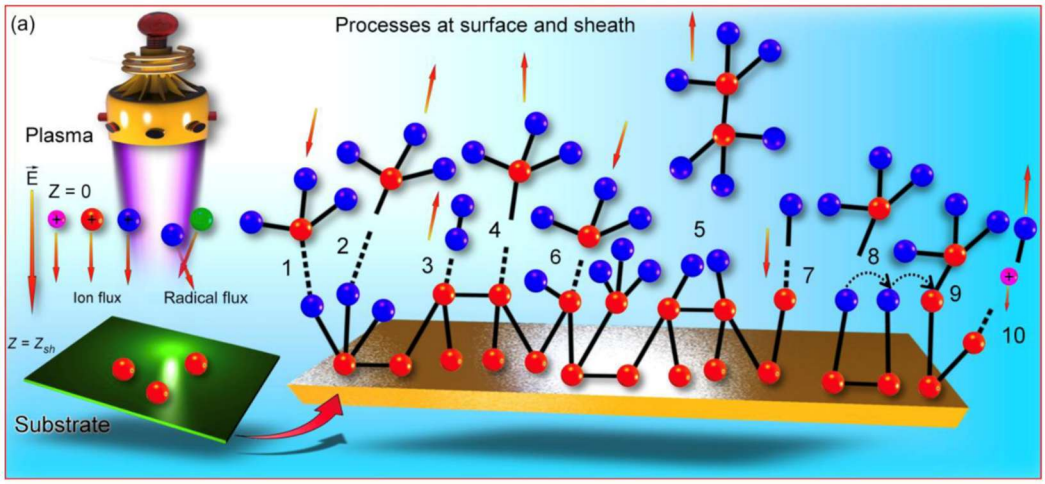

Figure 1.5 Mechanism of plasma treatment of a textile substrate [23]

The advantages of plasma treatment offer significant benefits for polymer surface modification. Firstly, plasma treatment can be limited to the surface layer of the polymer without altering its bulk properties, due to its limited penetration depth, typically in the range of a few nanometres to micrometres, depending on the type of plasma and treatment duration. This ensures that only the outer surface of the fibre is modified, making it ideal for applications where surface functionality is desired without compromising the mechanical integrity of the core structure. Additionally, the excited species in plasma can modify the surfaces of polymers, regardless of their inherent structures and chemical reactivity [24]. Plasma treatment also allows for uniform modification across the entire surface, eliminating the need for wet chemical treatments. In polymer technology, plasma is used to enhance adhesion for reinforcing materials, promote surface ablation, and adjust surface energy by improving hydrophobic or hydrophilic properties depending on the source gas used. The advantages of using plasma treatment to address the key challenges are as follows [19] [25]:

1. ***Enhancing Dye Absorption***: Plasma treatment can increase the surface roughness and introduce functional groups on hemp fibres, improving their dyeability [19]. This leads to more vibrant and consistent colours, overcoming the natural dye absorption challenges of hemp.

2. ***Improving Comfort Properties****:* Plasma-treated hemp fabrics have been shown to exhibit improved air permeability and wickability [26] compared to

non-plasma treated cellulosic fibres, due to increased surface energy and porosity. These enhancements contribute to better moisture management and wearer comfort, making plasma-treated hemp fabrics more comparable to cotton in terms of wearability [27].

3. ***Enhanced Adhesion****:* Plasma treatment improves the bonding strength between the fibres and the matrix in composite materials by modifying fibre surface characteristics. This process increases surface energy, making the surfaces more receptive not just to composite matrices but also to adhesives and coatings, which results in stronger and more durable bonds.

4. ***Surface Activation****:* Plasma treatment introduces functional groups to the surface of composite materials, enhancing their chemical reactivity. This activation improves the interaction between the composite surface and adhesives, leading to better bonding performance.

5. ***Improved Durability****:* By enhancing the adhesion and surface properties of composite materials, plasma treatment contributes to the overall durability and longevity of the final product. This is particularly important in industries such as aerospace and automotive, where high performance and reliability are critical.

Surface properties play a crucial role in determining the effectiveness of textiles in their applications. Although plasma treatment has demonstrated potential in enhancing characteristics such as wettability, adhesion, and absorptivity, there remains a limited understanding of the precise reaction mechanisms involved in plasma-material interactions. While this technology offers significant benefits, research is primarily focused on end-use applications rather than the fundamental chemical and structural transformations induced by plasma treatment.

1.6 Aims and objectives

While there have been various studies of plasma treatment of cellulosic fibres such as cotton, and some bast fibres such as flax, detailed studies of plasma treatment on hemp fibres is less exhaustive due to several factors. Additionally, argon plasma treatment has received considerably less attention than others e.g. oxygen. Therefore, this study aims to bridge existing knowledge gaps in relation to plasma treatment of hemp, by studying the oxygen and argon plasma interactions of different types of

plasma with hemp fibre, and the resulting effects on key properties. Moreover, A distinguishing aspect of this research is the specific focus on low-pressure and long-duration argon plasma treatment.

Specifically, the aim of this research is to evaluate the impact of plasma treatment on woven hemp fabrics, dew-retted fibres, and carded nonwoven fabrics, with an emphasis on both conventional and technical textile applications. The study aims to examine how plasma-induced surface modifications enhance the performance and functional attributes of hemp textiles, broadening their potential applications across diverse sectors**.**

The specific project objectives are:

1. To analyse how oxygen and argon plasma treatment alters the surface properties of hemp fibres and its effect on the dyeability of woven hemp fabrics.
2. To assess the structural and chemical changes in hemp fibres after undergoing argon and oxygen plasma treatments.
3. To evaluate the impact of argon plasma treatment followed by water shock treatment on the properties of nonwoven hemp fabrics.

Chapter 2

Review of Literature

2.1 Introduction

This chapter presents a comprehensive review of existing literature, providing essential background to support the research focus. The cultivation and harvesting of hemp, especially the retting process a critical step in fibre extraction, which involves microbial action to degrade the pectin that binds the bast fibres to the woody core, thereby facilitating fibre separation. The discussion then progresses to the structure and morphology of hemp fibres, highlighting the anatomical hierarchy from stem cross-section to microfibrillar organisation. Due to the presence of approximately 75% cellulose, the complex structure of cellulose and the intermolecular hydrogen bonding have been discussed. Hemp fibres possess impurities such as hemicellulose, pectin and lignin. Lignin acts as a natural binder for the cellulose fibrils in hemp and also imparts strength to the fibre. Lignin is hydrophobic in nature and often hinders textile processing by reducing fibre wettability. Additionally, the presence of impurities such as waxes, pectin, and hemicellulose further limits chemical reactivity, thereby making pre-treatment a necessary step. The chapter further explores various surface modification methods developed to address the processing of hemp into textiles with an emphasis on plasma treatment. This chapter, therefore, builds a critical foundation for the experimental investigations that follow, highlighting both the challenges and opportunities in unlocking the full potential of hemp fibres for modern textile applications.

2.2 Cultivation and harvesting of hemp fibres

Hemp is an annual, fast-growing plant that thrives in diverse climatic conditions, making it one of the most adaptable crops cultivated worldwide. The cultivation and harvesting of hemp are influenced by several factors, including soil conditions, climate, and seed selection, as per the end-use applications. Temperate and subtropical climates are preferred for the cultivation of industrial hemp [28] and a well-drained, nutrient-rich soil, such as deep, loamy soils with high organic matter, having a pH ranging between 6.0 and 7.5 is best for industrial hemp plantation as it facilitates good aeration.

Seed selection plays a crucial role in determining the quality and yield of hemp. Different hemp varieties are cultivated based on their intended use, whether for fibre, seeds, or cannabidiol (CBD) extraction. Certified seeds with high germination rates and disease resistance are preferred to ensure a healthy crop [29]. Sowing is typically done in early spring when soil temperatures reach around 10-15°C. The recommended sowing density for hemp fibre production requires high-density planting. Hemp has a rapid growth cycle, maturing within 70-120 days, depending on the variety and environmental conditions [28]. It exhibits strong weed suppression due to its fast germination and dense canopy formation. Minimal pesticide use is required as hemp is naturally resistant to many pests and diseases. However, nutrient management is crucial, with nitrogen, phosphorus, and potassium being the primary macronutrients required for healthy growth. Crop rotation with legumes or other nitrogen-fixing crops is recommended to maintain soil fertility and prevent nutrient depletion. Industrial hemp fibres are typically harvested 70-90 days after sowing, before the plants reach full maturity. Harvesting at this stage ensures finer and more flexible fibres. Traditional methods involve cutting the stalks using sickles or mechanised harvesters, followed by field retting (dew retting), which is a microbial process that separates the fibres from the woody core [30].

2.2.1 Post-harvest processing of hemp fibres

In the stem of the hemp plant, the elementary fibres are primarily located within the phloem in the form of fibre bundles, and the internal bast fibre structure is illustrated in Figure 2.1. These fibres are embedded in a matrix of parenchymatous cells and are positioned between the outer epidermis and the inner xylem core, aligning parallel to the stem's longitudinal axis [31]. The fibre bundles themselves contain elementary fibres that are interconnected within a network of pectic polysaccharides, which play an essential role in maintaining fibre cohesion and structural integrity [31]. To extract hemp fibres effectively, the plants undergo multiple processing stages. The first stage after harvesting encompasses retting, scutching, hackling, and spinning. Retting is a crucial step which involves microbial or chemical treatment to break down the natural binding materials holding the fibres together [32]. Following the retting, scutching, hackling, and spinning are employed to refine the fibres into usable textile materials. The quality and final characteristics of the extracted hemp fibres are highly dependent on each of these steps, particularly the retting process, which influences fibre fineness, strength, and overall processability. Figure 2.1 illustrates the overall post-harvest processing of hemp fibre extraction.

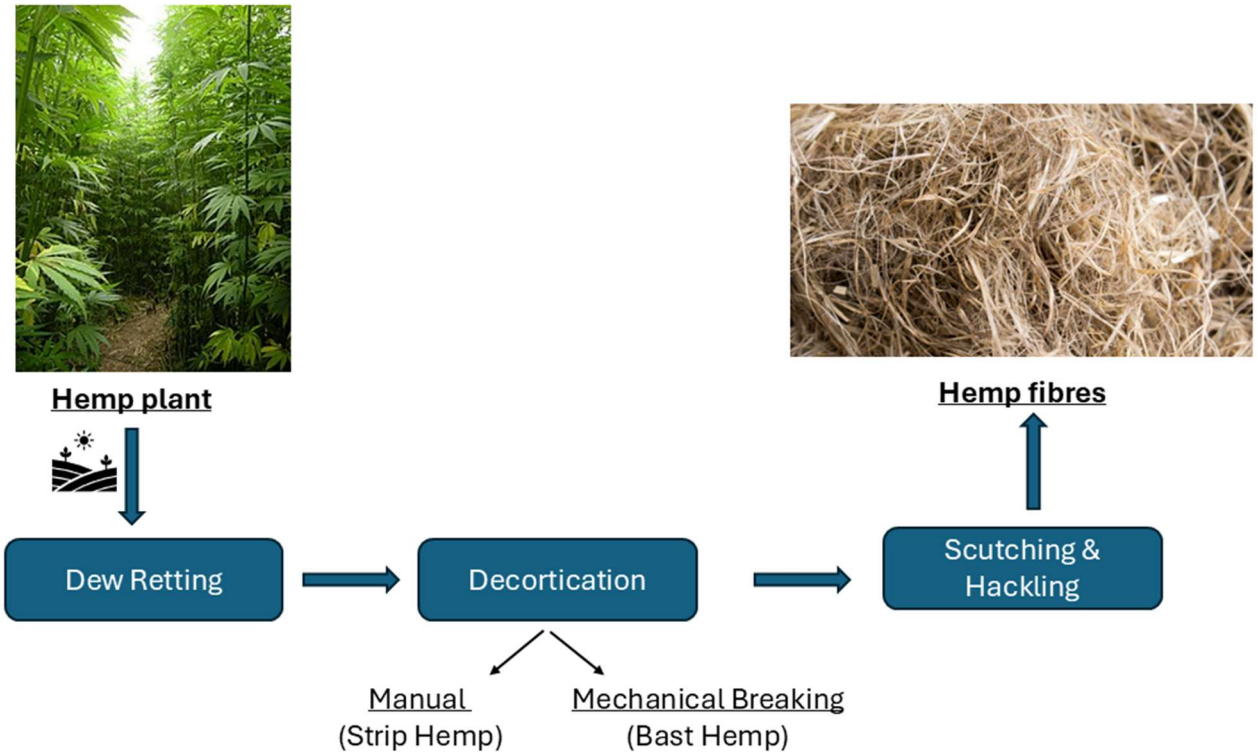

Figure 2.1 Post-harvest processing of hemp

2.2.2 Retting of hemp fibres

Retting is an essential post-harvest treatment that facilitates the separation of fibre bundles from the hemp stalk. Among the various retting techniques, field retting, also known as dew retting, remains the most commonly used method, particularly in European regions [33]. This traditional approach is favoured due to its cost-effectiveness and simplicity compared to other methods such as water, chemical, enzymatic, or mechanical retting. Field retting involves laying the harvested hemp stalks on the ground and allowing natural environmental factors, such as moisture, temperature fluctuations, and microbial activity, to break down the pectin and lignin that bind the fibres to the woody core. This process typically lasts between two and ten weeks, depending on the prevailing weather conditions and microbial efficiency. Microorganisms, including fungi and bacteria, produce hydrolytic enzymes that gradually break down the components of the plant cell wall, mainly targeting the pectin-rich middle lamella, which holds the elementary fibres together [33]. As the pectin deteriorates, fibre bundles loosen, facilitating their subsequent extraction. The effectiveness of field retting is highly dependent on climatic conditions, as environmental factors such as rainfall, humidity, and temperature directly influence microbial activity. Uncontrolled weather variations can lead to inconsistent retting,

resulting in variable fibre quality [34]. The following field retting (dew retting) conditions are most effective for high hemp fibre yield [33, 35]:

1. *Warm Weather*: Optimal temperatures facilitate microbial activity, which is crucial for breaking down the pectin that binds the fibres.
2. *Intermittent Precipitation:* Regular moisture helps maintain the retting process, but it is important to avoid excessive rain, which can lead to over-retting.
3. *Good Air Circulation:* Ensuring that the hemp stalks are well-spread and turned over periodically helps in achieving uniform retting.
4. *Proper Timing:* Retting typically takes 2-3 weeks under ideal conditions. Monitoring the colour change in the stalks from green to pale yellow can indicate the right time to turn them.
5. *Turning Stalks:* Turning the stalks ensures even retting and prevents the bottom layers from over-retting.

Dew retting done in the mentioned conditions produces fibres with relatively good mechanical properties, but can lead to more variability compared to controlled retting methods such as water or enzymatic retting [36]. In some cases, the performance of the fibres is affected by environmental conditions during retting, including temperature, humidity, and microbial activity. Tables 2.1A and 2.1B enlist the chemical and mechanical properties of hemp fibres dew retted at optimal conditions [20].

A Chemical Properties	
Cellulose	60 ~ 80%
Hemicellulose	10~20%
Lignin	5 ~ 15%
Pectin	1 ~5%
Wax and other impurities	0.5 ~ 2%

B Mechanical Properties	
Tensile Strength	~200-900 MPa
Young's Modulus	~10-60 Gpa
Elongation at break	~1.5-3%

Table 2.1 Properties of dew retted hemp fibres

One of the major challenges in retting is achieving the optimal balance between under-retting and over-retting [37]. Under-retting can lead to insufficient fibre separation, making subsequent processing steps more labour-intensive. In contrast, over-retting

weakens the fibre strength due to excessive degradation of cellulose structures [33, 37]. Natural variations in hemp fibre characteristics also contribute to inconsistencies, as factors such as plant variety, soil conditions, and growth environment impact fibre morphology. Poorly managed retting processes further amplify these variations, affecting fibre properties such as fineness, tensile strength, and overall mechanical performance.

2.2.3 Post-retting processing of hemp fibres

Once retting is complete, the fibres undergo a series of mechanical treatments to further refine them. The first step, known as decortication, is done in the decorticator [38]. The process involves breaking and crushing the stalks to fragment the brittle woody core while keeping the fibres intact, which is done by fluted rollers or manually. Following decortication, the scutching process is carried out to remove the loosened woody fragments from the fibres. The hemp scutching process is divided into two stages [39]. The initial process serves to break down the woody stems, while the subsequent step separates the hurd from fibres that remain attached to the bark. Hemp scutching can release two types of fibres: short fibres and long fibres. The short fibres are used for paper, composites production and constructions, and long fibre tends to be used in textiles and for the textile industry. Presently, scutching is done mechanically using sophisticated machinery [39] [38].

The next stage, hackling, ensures the complete removal of woody residues and aligns the fibres into a more uniform structure. The fibres are pulled through a hackling board, which is a wooden base with iron spikes and acts like a comb to align the fibres unidirectionally into a continuous sliver. For composite and weaving applications, hackled hemp is used. Following hackling, the hemp is baled [39] [14].

2.3 Structure and morphology of hemp fibre

Bast fibres such as hemp are collected from the phloem, the tissue surrounding the stem of certain plants. The fibres impart strength to the stem by forming a protective layer around its woody core. The fibres are protected by waxes and other protective substances, with bundles of fibres held together by these waxy substances. Hemp fibres are highly oriented in an axial direction and have a low rate of extensibility [4]. These phloem fibres are promising for use in reinforced composites due to their high tensile and load-bearing capacity. The cells of hemp fibres are tube-like, allowing the

fibres to reach lengths of up to 25mm [40]. A low lignin content in hemp fibres compared to wood contributes to their length and flexibility, which gives them a greater variability than wood. Hemp fibres are found in bundles with a diameter ranging between 100 to 120 μm, and individual fibres possess a diameter between a wide range of 50 to 90 μm. The SEM image in Figure 2.2 reveals the microstructure of hemp fibre having a visible lumen, which appears as hollow voids in the centre of individual ultimate fibre cells. These lumens are a key feature of the closed-cell structure of hemp fibres and play a crucial role in moisture transport and flexibility. The solid regions observed around each lumen correspond to the cell walls, which provide mechanical strength and rigidity to the fibre [8]. The multi-layered composition of these fibres includes the epidermis, phloem, xylem, and pith. Within these layers, the closed-cell structure of the stem has voids at the pith and a distinctive boundary between the phloem and xylem.

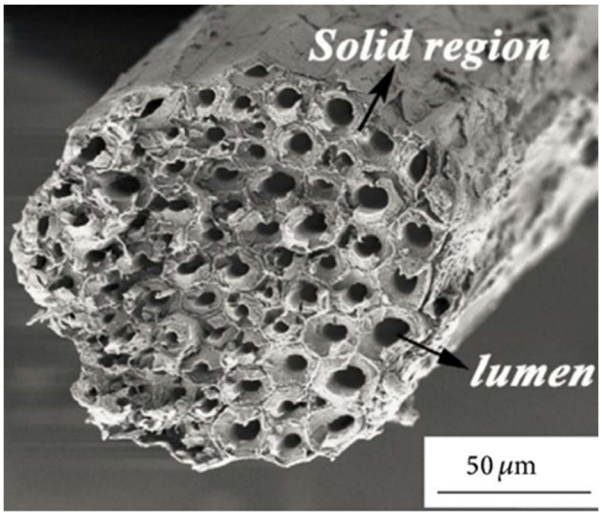

Figure 2.2 Microstructure of hemp fibre [41]

The systematic hexagonal packing of fibre cells governs their mechanical robustness, primarily due to the thick solid wall regions shown in the micrograph [31]. These fibres contain a high cellulose and lower lignin content compared to the xylem and pith layers. The secondary cell walls of hemp fibres are coated with a waxy layer and contain several fibrils with vessels of hemp shiv. Numerous pits can be observed on the secondary cell walls [42] [43].

2.4 Physical properties of hemp

For textile applications, fibres must possess key properties such as cohesiveness, fineness, good tensile characteristics, and aesthetic characteristics. Hemp, as one of the natural fibres which shows promising physical and chemical properties. It is the strongest of the natural bast fibres, boasting high tensile strength ranging between 0.03 to 0.09 GPa. This superior tensile strength is linked to its high degree of crystallinity, with fibres having an axial (unidirectional) orientation. The elongation at break in hemp fibres reflects the amount of stress they can endure before failure, further emphasising their durability and strength for textile use. Hemp fibre has an elongation percentage of 1.6%, indicating its ability to withstand stress along its axis. It has a yellowish colour, like flax, and is known for its durability and resistance to UV rays. With a moisture regain of 12%, hemp exhibits excellent absorbency [44]. Today, hemp is often used as a reinforcement material in polymer matrix composites, valued for its high load-bearing capacity and tenacity. Hemp is also recognised for its good thermal mass, making it an effective insulator. It remains stable up to 250°C of temperature and degrades only between 330-350°C [44, 45]. Due to these physical properties, hemp is increasingly being used to develop energy-efficient composites.

2.5 Chemical properties of hemp

The number of monomer repeat units of cellulose in hemp ranges from 5400 in crude hemp to 2100 in pre-treated hemp [44]. A lower lignin content is an advantage when processing hemp fibres, as hemp contains only about 5 to 15% lignin, which runs axially through the fibre and is strongly bonded with the cellulose; thus, it is difficult to remove. Pectin present in hemp fibres plays a crucial role in adhesion within the bast and aids in hydration [46]. In industrial hemp, the total pectin and fat content ranges from 2% to 6%. The chemical composition of hemp highlights its suitability for various applications due to the specific properties listed in Table 2.2, and the chemical structures of crucial components are given in subsequent sections. In cellulosic textiles, chemical treatments with alkali and acetyl agents can result in the formation of a hydrophilic surface. These treatments increase the number of hydroxyl groups, improving bonding with dyes and polymers. Sawpan et al. [47] demonstrated that hemp fibres treated with 5 wt% alkali achieved a tensile strength of around 600 MPa, compared to 550 MPa for untreated fibres, a negligible improvement of roughly 50 MPa. This improvement is attributed to the removal of non-cellulosic components such as pectin, hemicellulose, and lignin, which increases the relative proportion of crystalline cellulose [48]. Alkali treatment reduces the spiral angle of cellulose microfibrils, which is the angle between the microfibril orientation and the fibre's longitudinal axis. This may lead to a rearrangement of the microfibrillar structure, which

in some cases can result in a decrease in tensile strength due to the disruption of the native alignment [49]. On the other hand, acids have a more detrimental effect on cellulosic textiles, including hemp. Acids catalyse the cleavage of 1-4-glycosidic bonds, leading to a decrease in the degree of polymerisation and the fibre's physical properties.

Composition	Range
Cellulose	65% to 75%
Hemicellulose	15% to 25%
Pectin and Fats	2% to 6%
Lignin	5% to 15%

Table 2.2 Chemical composition of dew retted hemp

2.5.1 Impurities in hemp

Hemp, like other lignocellulosic materials such as wood, consists of cellulose, hemicellulose and lignin as its primary components [50]. Lignin is a crucial biopolymer found in the cell walls of plants, providing structural support, rigidity, and strength [51]. It is an aromatic and complex phenolic polymer with a cross-linked, three-dimensional, amorphous structure. Lignin contains a variety of functional groups, which enable it to undergo chemical or physical modifications, enhancing its applications. Figure 2.3 shows the chemical structure of three primary monomers in lignin, which are namely coniferyl (G), sinapyl (S) and p-coumaryl (H). A higher proportion of guaiacyl units promotes extensive crosslinking and condensed structures, increasing rigidity and recalcitrance. Syringyl units, with two methoxy groups, restrict crosslinking, yielding a more linear and less condensed lignin that is comparatively easier to degrade. Hydroxyphenyl units, being less substituted, are associated with simpler structures and reduced steric hindrance, often enhancing reactivity. Thus, the H/G/S ratio governs lignin's structural complexity, degradability, and interaction with chemical or enzymatic treatments [52].

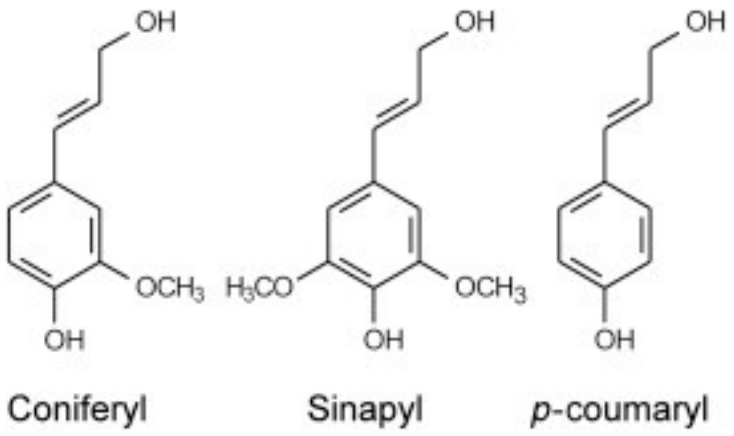

Figure 2.3 Structural monolignols [53]

Lignin is a major impurity in hemp fibres that complicates processing, especially for textile applications [54] [55]. Alkaline treatments are effective in removing lignin and pectin from hemp, though some residual lignin remains. Lignin content in hemp can be analysed using thermogravimetric methods, with degradation occurring across a wide temperature range. In addition to lignin, other impurities in hemp-derived products may include sugars, sugar acids, extractives, and inorganics. These impurities can significantly impact the efficiency of lignin mixtures in various applications, such as their use as dispersants, binders, emulsifiers, and sequestrants [56].

The degumming of hemp fibres is a crucial process for removing non-cellulosic components and individualising fibres. The process of degumming hemp fibre involves pre-treating the tough outer layer of the hemp, followed by mechanical grinding to prepare the fibres for further treatment. Biological enzymes are then used to break down and remove hemicelluloses and lignin that are bound to the fibre surface [57]. The procedure includes repeated mechanical grinding and concludes with washing the hemp fibres to eliminate any remaining hemicelluloses and lignin [58]. The lignin content in hemp fibres varies significantly between degummed and non-degummed states. Typically, non-degummed fibres contain 8 to 10% lignin, in contrast to degummed fibres having 3 to 5% lignin [59]. Removing lignin from cellulosic bast fibres such as hemp can result in a loss of fibre strength, and in some cases, also leads to high water and chemical usage. Recent research has focused on developing eco-friendly methods to minimise this strength loss while reducing water consumption. Zhao et al. introduced an innovative solid-state ethanolamine (ETA) degumming process, which achieved a 33.3% reduction in water usage while removing 87.5% of lignin, simultaneously preserving the fibre strength [58]. Xiang et al. explored a chemo-

enzymatic approach using laccase and hemicellulase, which improved fibre properties by the removal of impurities such as lignin and hemicellulose from the fibre structure without harsh chemicals [60]. Ahmed et al. combined microwave energy with deep eutectic solvents, achieving comparable cellulose content to traditional methods while enhancing UV protection and thermal stability in the hemp fibres [61].

Innovative research over the past few years has increasingly focused on the valorisation of lignin as a structural component, exploring its potential to enhance material properties and create sustainable applications such as bioplastics, 3D-printable inks, and energy storage devices. In recent research conducted by Shong et al., wood-based substrates were first boiled in a solution of sodium hydroxide (NaOH) and sodium thiosulfate ($Na_2S_2O_3$) and then subjected to hot pressing at a high temperature of 100°C [62]. The resulting nanofibers within the wood structure became aligned during the process, leading to the densification of the wood. A comparative analysis between densified and natural wood revealed that the densified version exhibited superior physical properties. Similar studies aim at preserving the lignocellulosic microstructure with an objective to enhance the physical properties of the substrate [63]. These innovative techniques aim to improve fibre quality, reduce environmental impact, and maintain or enhance desirable properties such as strength, fineness, and water uptake, making hemp fibres more suitable for various applications, including textiles.

2.5.2 Structure of cellulose

Hemp differs significantly from cotton in terms of surface, mechanical and chemical properties. As a coarse bast fibre, hemp contains lignin and pectin, which are bonded axially through the stem to provide mechanical support to the plant. Despite these impurities, hemp is composed of a high percentage of pure cellulose, with a notably high degree of crystallinity (~50% to 80%) [64]. The degree of polymerisation in hemp is approximately 2100 cellulose units per chain [65].

Within the cellulose structure, both crystalline and amorphous regions exist. The crystalline regions are tightly bound by intermolecular hydrogen bonds [66], making them more rigid and less flexible. Hemp fibres, being largely composed of these crystalline regions, have less amorphous content compared to other cellulosic fibres like cotton. Native cellulose fibres, such as those found in hemp, are primarily composed of crystalline fibrils, which contribute to the fibre’s strength and durability.

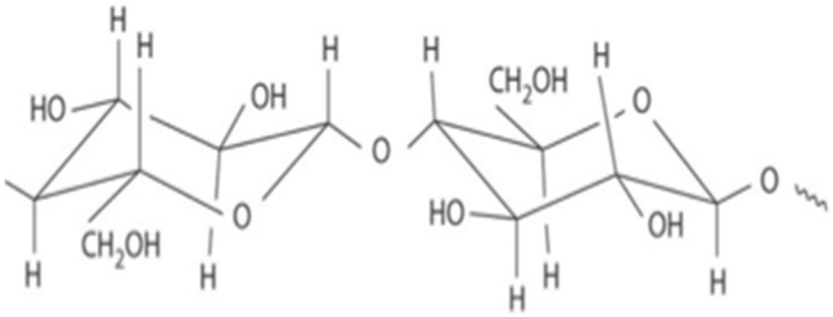

Figure 2.4 Structure of cellulose [67]

Cellulose is a polysaccharide formed as a condensation polymer of β-D-glucopyranose units linked by 1,4-glycosidic bonds [68]. The molecular structure of cellulose is depicted in Figure 2.4. According to the Meyer and Misch theory, the glycosidic bonds are perpendicular to the planes of adjacent rings [69]. However, Herman's model proposes a slightly different arrangement, suggesting that the glycosidic bonds are inclined at small angles, alternating between positive and negative relative to the ring plane. As a result, the chain molecules are extended into flat ribbons with minimal thickness, perpendicular to the planes of the rings [70]. This structural arrangement contributes to its strength and stability.

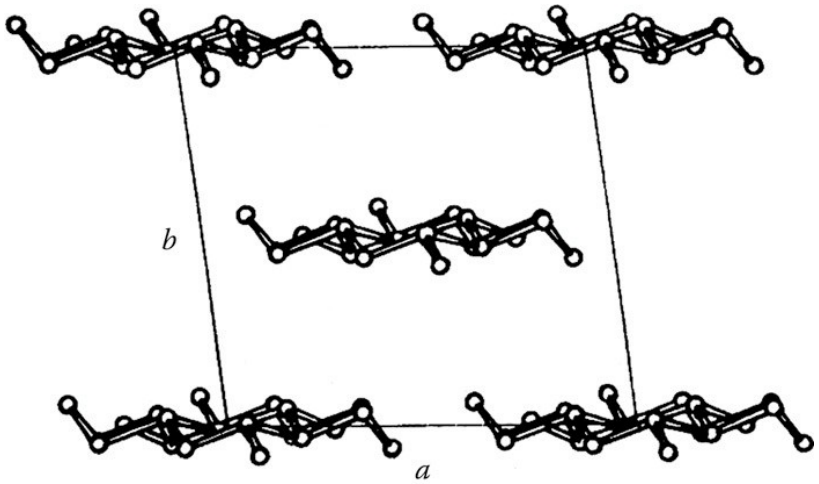

Figure 2.5 Cellulose crystal structure [70]

The flat ribbons of cellulose can be described by a monoclinic unit cell with dimensions of approximately *a=0.82, b=0.79, c=1.03 nm,* and an angle of 97° and are shown in Figure 2.5. As per Meyer and Misch, the chains at the centre and corners of the unit

cell are antiparallel. However, recent evidence suggests that these chains are arranged in parallel, with the centre chains staggered by a distance of 0.26nm [71].

Adjacent chains in the cellulose structure are held by hydrogen bonding in the ac-plane. The staggered, alternating sheets of cellulose chains are linked through hydrogen bonds, with one sheet consisting of corner chains and the other of centre chains. This intricate system of intermolecular hydrogen bonding is shown in Figure 2.6.

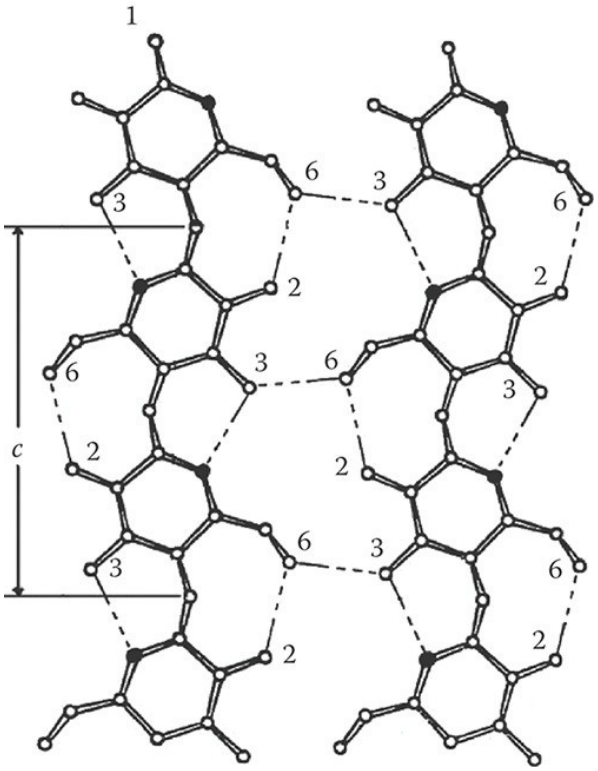

Figure 2.6 Hydrogen bonding in cellulose [72]

Cellulose fibres exhibit a robust network of hydrogen bonds between planes, which makes cellulose resistant to dissolution in most polar solvents. The crystalline regions of cellulose are characterised by strong hydrogen bonding between consecutive planes, as shown in Figure 2.6, while the amorphous regions have weaker hydrogen bonds. In cellulose fibres, the material's structure consists of fringed micelles, where crystalline micelles are embedded within an amorphous matrix. Individual cellulose chain molecules extend through both crystalline and amorphous regions [68]. Thus, the "fringed fibrils concept" implies that non-crystalline regions emerge at various

points along the crystalline fibrils, illustrating a heterogeneous structure of cellulose fibres [73].

2.6 Pre-treatment of hemp fibres

The pre-treatment of hemp fibres is a critical step in processing, having a primary objective to enhance the absorbency of water by eliminating undesirable impurities, such as lignin, hemicellulose and pectin, which otherwise reduce the fibres' ability to absorb liquids. This process ensures that subsequent stages, such as dyeing and finishing, yield optimal results. By effectively preparing the textile surface, pre-treatment enables better penetration of dyes and chemicals, ensuring uniformity, improved quality, and durability of the final product [74]. The pre-treatment process eliminates natural and added impurities, making the textile substrate suitable for subsequent dyeing and finishing stages [75]. Pre-treatment of cellulosic substrates is a vital phase in textile wet processing, where impurities like hemicellulose, lignin, pectin, and sizing oils are eliminated. This multi-step process includes singeing, de-sizing, scouring, and bleaching. Following pre-treatment, the fibre becomes receptive to dyeing as the removal of impurities allows textile chemicals to penetrate the fibre structure more effectively, enabling the formation of chemical bonds.

Common bleaching agents, such as sodium chlorite ($NaClO_2$) and hydrogen peroxide (H_2O_2), are employed to remove residual impurities and transform yellow-grey fabrics into a visually appealing white, providing a clean base for subsequent processing [76]. Pre-treatment of fibres and textiles results in tensile loss due to the decrease in the degree of polymerisation of cellulose. Pre-treatment of hemp and other cellulose fabrics involves four main steps, which are as follows:

1. *Singeing:* The process involves the burning of small fibres which are protruding outside the fabric. Singeing makes the fabric smoother [74].

2. *Desizing:* During fabric production, sizing agents such as polyvinyl alcohol and starch are applied to the warp yarns to minimise hairiness and prevent breakage under the high tension and abrasion they experience during weaving. In the subsequent desizing process, these agents are removed primarily through hydrolysis, using methods such as enzymatic treatments, acids, or, in some cases, chlorinated chemicals [74].

3. *Scouring:* Grey fabric contains non-cellulosic impurities such as lignin, pectin, hemicellulose, waxes, oils, and fats. These surface impurities hinder water

absorbency. Scouring is carried out to enhance the fabric's absorbency through controlled chemical treatments, traditionally involving boiling in a strong alkali solution, typically sodium hydroxide (NaOH) at a concentration of 2-5 wt% (on weight of fabric) [77].

4. *Bleaching and Mercerisation:* Bleaching is a process in which the natural colour of pigments in the cellulosic substrates is removed using peroxides. In mercerisation, the cellulose crystals swell in the presence of an alkali. The dye uptake of the fabric increases, and the fabric looks more lustrous [78].

In addition to traditional chemical methods, modern technologies such as microwave irradiation, plasma treatment, and enzyme biotechnology are increasingly employed. These innovative approaches offer more sustainable and efficient alternatives by reducing the consumption of water, energy, and chemicals, while also improving the overall effectiveness of the pre-treatment process.

Pre-treatment of hemp fibres is crucial for enhancing their properties and performance in composite materials. Various methods have been explored, including chemical treatments with NaOH and EDTA, enzymatic modifications, and innovative approaches using deep eutectic solvents combined with microwave energy [16]. Alkali treatments, particularly with NaOH, effectively remove impurities and improve fibre surface properties, yielding better matrix-fibre interaction for optimal performance in geopolymer composites [79]. Enzymatic treatments have also demonstrated potential, although their effectiveness may vary depending on the pectin structure of hemp fibres [80]. Currently, the pre-treatment of hemp fibres is extensively explored for their use in technical textiles, such as composites.

The surface morphology of fibres changes significantly following pre-treatment, transitioning from a rough to a smoother surface. Among various pre-treatment methods, mercerisation produces a more uniform and less convoluted fibre morphology, thereby enhancing dye affinity, lustre, and the effectiveness of subsequent finishing treatments [81]. This smooth surface improves the overall quality and aesthetic appeal of the treated fabric, making it more suitable for textile applications [77]. Different pre-treatment processes modify the surface morphology of textiles according to the desired outcomes. For applications that require higher dye uptake and enhanced aesthetics, a smooth surface is generally preferred as it allows for uniform dye absorption and a polished appearance. However, certain pre-treatments, such as microwave irradiation, deliberately induce a roughened surface.

This approach can be tailored based on the specific requirements of the textile's final application [82]. For example, the pre-treatment of cotton fabric using ultraviolet irradiation has been shown to result in a 40% higher dye uptake compared to untreated fabric. This demonstrates beyond composites, opening new avenues in the textile and fashion industries where natural and sustainable materials are in increasing demand.

2.7 Methods to modify the tensile and other properties of hemp fibre

To enhance the tensile properties of hemp fibres, various treatment methods have been explored, with chemical modifications being the most widely used approach. One of the most effective techniques involves the application of alkali treatments, particularly sodium hydroxide (NaOH) [83]. This process removes non-cellulosic components such as lignin and hemicellulose, resulting in higher cellulose crystallinity, improved fibre separation, and ultimately, increased tensile strength [84]. Beyond alkali treatments, other chemical modifications can further improve hemp fibre performance. Silane coupling agents, for instance, are commonly applied to improve adhesion between hemp fibres and polymer matrices, particularly in composite materials [85]. This modification enhances interfacial bonding, leading to stronger and more durable composites. Acidic treatments have also been used to alter fibre properties, though they require precise control to prevent excessive degradation of cellulose, which could compromise fibre strength [85] [86]. Emerging research also points to plasma treatment as a promising method for modifying hemp fibres.

Additionally, chemical, physical and blending techniques can be employed to modify the aesthetic properties of hemp fibre. Chemical treatments involve the use of dyes, finishes, and other chemical agents to enhance the colour, texture, and overall appearance of hemp fibres [87] [88]. For example, chemical softening agents can be used to improve the feel of the fabric. Moreover, techniques such as mechanical processing, calendaring, and mercerisation can alter the surface properties of hemp fibres, making them smoother and more lustrous [88]. These methods can also improve the drape and hand feel of the hemp fabric. Another route to enhance the aesthetic properties of hemp is by combining hemp with other fibres like organic cotton, linen, or silk, which can help improve its aesthetic properties. Blending hemp fibres with other fibres can improve softness, sheen, and overall visual appeal while maintaining the durability and eco-friendliness of hemp [89].

2.7.1 Green technologies for modification of hemp fibre

Green technologies for the modification of hemp fibres prioritise environmentally friendly methods aimed at enhancing fibre properties without harming the environment. One notable approach is enzymatic treatment, which utilises enzymes to break down non-cellulosic components such as hemicellulose and lignin [90]. This method operates under mild conditions and is highly specific, making it a sustainable choice. Another effective method involves deep eutectic solvents (DES), which are biodegradable, non-toxic solvents that can dissolve lignin and hemicellulose while also being recyclable [25]. Similarly, ionic liquids (ILs), which are salts in liquid form, can dissolve various materials, including lignocellulosic biomass, and are considered green due to their low volatility and reusability. Mechanical treatments like steam explosion and ultrasound treatment physically alter the fibre structure, facilitating the removal of non-cellulosic components without using harmful chemicals. Additionally, biological treatments that employ microorganisms to degrade lignin and hemicellulose offer a slow but highly specific and environmentally benign alternative [91]. Overall, these green technologies enhance the mechanical properties, thermal stability, and moisture resistance of hemp fibres, making them more suitable for applications in composite materials. Traditional chemical methods like alkali (NaOH) and acetylation involve harsh chemicals that can harm the environment and produce substantial chemical waste [92]. While green methods are effective, they tend to be less aggressive in removing non-cellulosic components compared to traditional treatments, which can provide a more thorough fibre modification. Additionally, green methods may incur higher initial costs due to specialised solvents or enzymes, but they offer long-term savings through reduced waste disposal and the potential for solvent recycling [93]. Traditional treatments, being more established and cost-effective, are easier to scale up but come with higher long-term environmental costs. From a health and safety perspective, green treatments are safer for workers due to the milder reaction conditions, while traditional methods involve greater risks due to the use of toxic chemicals. Overall, green pre-treatment methods are more sustainable and safer, though they may require a higher initial investment and be less aggressive in fibre modification compared to traditional chemical treatments.

UV irradiation, microwave treatment, and plasma technologies are advanced pre-treatment methods that modify the surface and structure of hemp fibres, improving their performance in composite materials [16]. UV irradiation works by exposing hemp fibres to ultraviolet light, breaking down surface impurities and improving surface

roughness and wettability, which enhances bonding with polymer matrices. Microwave treatment heats the fibres using microwave energy, causing the breakdown of non-cellulosic components like lignin and hemicellulose [94] [90]. This results in better fibre separation, improved fineness, and enhanced mechanical properties, making the fibres suitable for high-quality composites. Plasma treatment, on the other hand, involves exposing fibres to a plasma field that generates reactive species, which modify the fibre surface by introducing functional groups [95]. This improves adhesion with polymers and boosts mechanical properties such as interfacial bonding, thermal stability, and moisture resistance. Together, these methods provide environmentally friendly and effective approaches to enhance the properties of hemp fibres for various industrial applications.

2.8 Modification of fibres using plasma treatment

Plasma treatment has been used to modify the surfaces of synthetic substrates such as polyurethanes, polyamides, and polyesters, as well as natural fibres like wool, cotton, and polyester-cotton blends. This treatment can enhance their dyeability and functional properties, including hydrophobicity. For instance, when thermoplastic polyurethane underwent plasma treatment with argon and oxygen gas, its hydrophobic surface was transformed into a hydrophilic one, demonstrating the versatility of plasma treatment in altering surface characteristics [96]. Using noble gases like argon in plasma treatment offers the potential to generate highly energetic radicals capable of breaking C-C, C-H, and hydrogen bonds. Plasma treatment is more effective for surface modification compared to techniques like UV irradiation. For example, plasma treatment of poly(vinyl) alcohol blends increased the surface polarity of the polymer and improved its adhesion properties [94]. The surface modification of a three-dimensional aero graphite network through plasma treatment increased its porosity, creating spaces for oxygen vacancies. This process enhances the material's structural properties, making it more suitable for various applications requiring high surface area and reactivity [97]. Plasma treatment has been successfully applied to cellulose fibres, imparting self-cleaning properties such as superhydrophobicity. Additionally, plasma treatment has provided fire-resistant and water-repellent finishes on cotton and other textile substrates, showcasing its versatility in enhancing textile functionality [98] [99] [100] [101].

The application of plasma treatment to hemp fibres is an emerging research area that bridges material science with environmental sustainability. Various physical and

chemical modifications enhance hemp fibre properties, particularly by improving mechanical strength and adhesion to polymer matrices [102]. Traditional chemical treatments, such as alkali processing, primarily remove lignin and other non-cellulosic components, thereby increasing fibre roughness and improving fibre-matrix bonding [102]. Research has demonstrated that alkali treatments effectively eliminate lignin and hemicellulose, resulting in a lightweight and structurally reinforced fibre [103]. In addition, oxygen plasma treatment introduces controlled oxidation and micro-etching on fibre surfaces, further enhancing their compatibility with polymers [16]. Compared to conventional methods, plasma treatment offers a simple and environmentally friendly alternative, eliminating the need for hazardous chemicals such as strong alkalis and solvents [25] [16]. Argon or oxygen plasma treatment has proven effective in improving fibre adhesion within polymer composites, optimising load distribution, and enhancing overall mechanical properties [103].

Maintaining the intrinsic cellulose structure to enhance compatibility with polymers is essential for diverse industrial applications, including the automotive and construction sectors [104]. Plasma treatments using a variety of gases, such as oxygen, argon, or nitrogen, have been observed to enhance fibre surface morphology and modify moisture absorption, which is crucial for composite and garment manufacturing [85, 105]. Studies examining the properties of plasma-treated hemp fibres suggest that oxygen plasma treatment enhances thermal and oxidative resistance, improving their performance in polymer reinforced composite structures [106]. Parameters such as treatment duration and power significantly influence the extent of fibre property improvements. Incorporating plasma treated hemp fibres into composites has addressed critical challenges such as moisture absorption and thermal degradation [16] [106]. Enhanced adhesion between fibre and polymer improves the resilience of the final material, making it suitable for applications demanding durability under varying environmental conditions [16]. As research progresses, sustainability and environmental impact remain key considerations for fibre treatment methods. Given the rising demand for eco-friendly materials, fibre modification processes must balance performance enhancement with environmental responsibility [107]. Thus, plasma treatment presents a promising approach to enhancing hemp fibre properties for high-performance conventional and technical textiles.

Chapter 3

Materials & Methods

3.1 Introduction

This Chapter provides a detailed account of the experimental techniques employed throughout the study, with an emphasis on the principles and instrumentation of each method. Atomic Force Microscopy (AFM), Scanning Electron Microscopy (SEM), Fourier Transform Infrared Spectroscopy (FTIR), Raman spectroscopy, water contact angle measurements, and tensile strength testing were systematically utilised to characterise the effects of plasma treatment on hemp substrates. A comprehensive explanation of each technique's operating principle is provided. The tapping mode employed in AFM is discussed in detail, alongside the working mechanism of SEM used for evaluating surface morphology. ATR-FTIR and Raman spectroscopy were extensively used to investigate the chemical structure of treated fibres, with their underlying principles and instrumentation thoroughly described. The functioning of the goniometer for assessing water contact angle is also illustrated. Furthermore, the method and principle of tensile strength testing are addressed to evaluate changes in mechanical properties. Plasma treatment was applied to hemp substrates across various experimental conditions. In Chapter 4, woven hemp fabric was plasma treated using argon gas and subsequently dyed using both reactive and vat dyes to assess changes in colouration. In Chapter 5, dew-retted fibres underwent prolonged plasma treatment using oxygen and argon gases ranging from 30 minutes to 4 hours, followed by structural and surface analyses. In Chapter 6, nonwoven hemp fabrics were plasma treated and immediately subjected to a water shock by immersion in ice-cold water. Each treatment scenario was followed by detailed characterisation using the aforementioned techniques to evaluate morphological, chemical, and physical changes induced by plasma and combined treatments. Figure 3.1 thus explains the overall research layout.

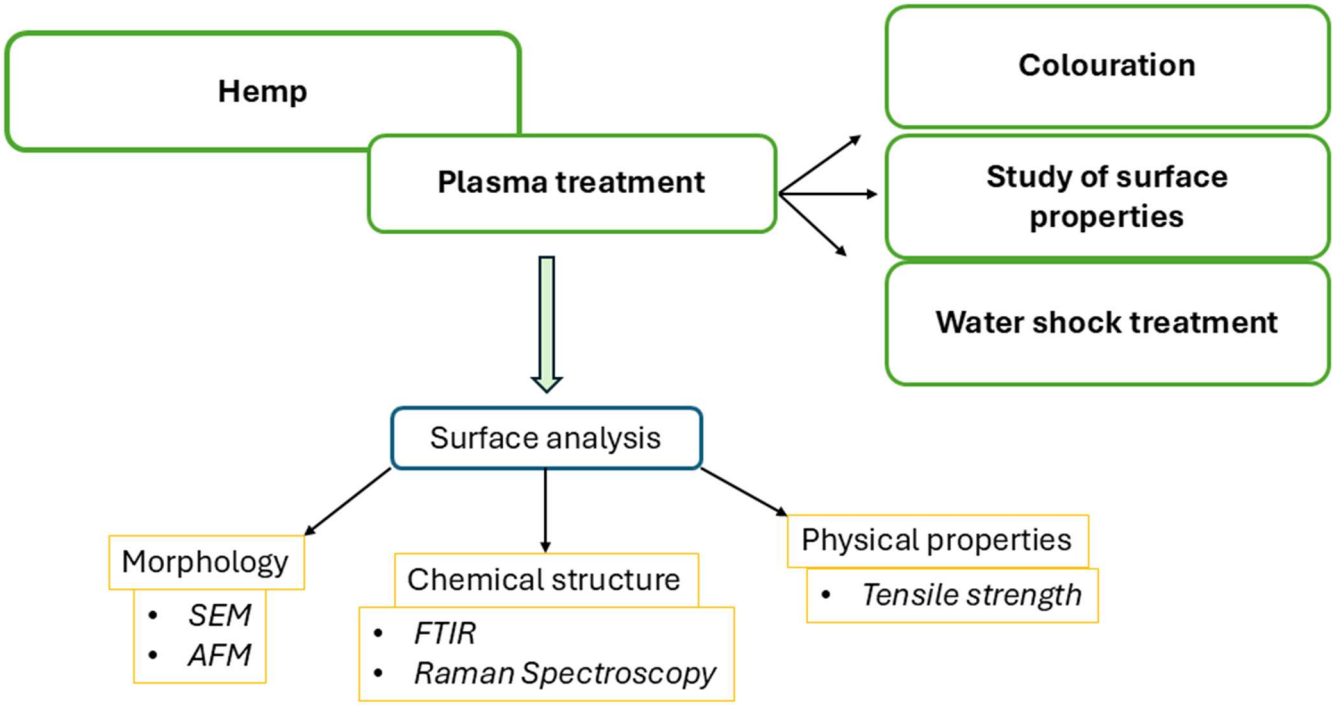

Figure 3.1 Summarised research methodology

3.2 Materials

Three different substrate types were utilised for the plasma-assisted surface modification of hemp (sliver, drylaid nonwoven and woven fabric), as depicted in Figure 3.2. A drylaid nonwoven fabric composed of hemp fibres was manufactured internally using labscale carding, crosslapping and needle-punching facilities. Additionally, a ready-for-dyeing (R.F.D) woven hemp fabric was procured, which was plasma treated and dyed using fibre-reactive and vat type of dyes.

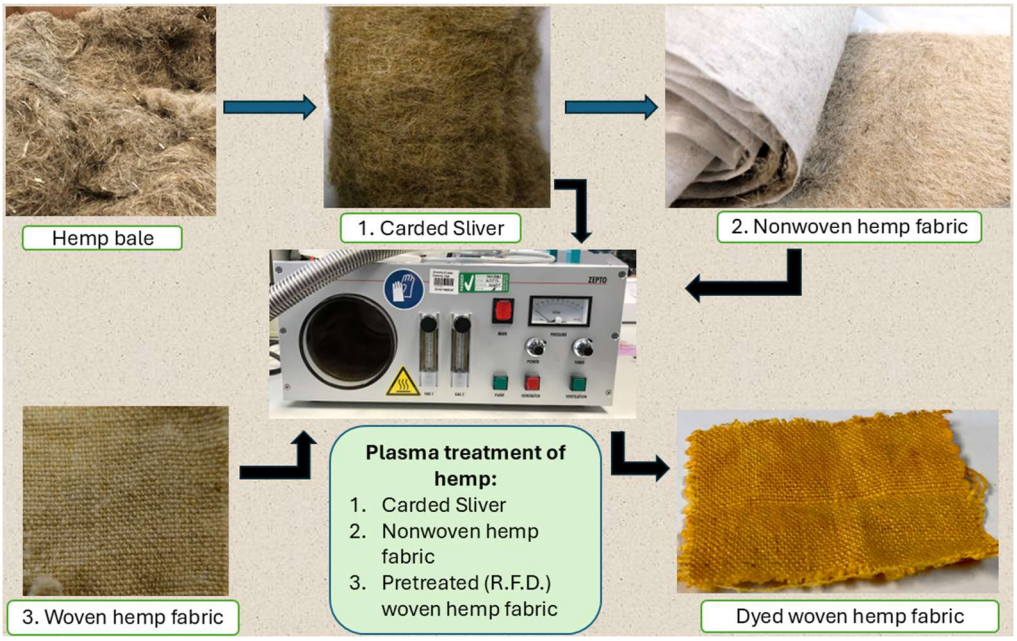

Figure 3.2 Hemp substrates used for plasma treatment

3.2.1 Specifications and source of hemp fibres

A total of 10 kg of hemp fibre bale was sourced from East Yorkshire Hemp [108]. Prior to delivery, the fibres underwent a dew retting process lasting approximately 5 to 6 weeks, followed by mechanical processing steps, including decortication to separate the bast fibres from the woody core, scutching to remove excess hurd, and hackling to refine and align the fibres before being compressed into bales. The hemp fibre bales were passed through a bale opener twice to efficiently loosen and separate the fibres. After this initial processing step, the fibres were subjected to carding, which individualises the fibres and aligns them uniformly, forming a carded web. Following carding, the fibres underwent needle punching, resulting in the formation of a nonwoven hemp fabric. This mechanical process involves repeated piercing of the fibre web with barbed needles, effectively entangling the fibres and enhancing fabric cohesion, strength, and durability.

3.2.2 Equipment used for plasma treatment

The plasma treatment of hemp fibres was conducted using a Diener Electronic Zepto plasma surface treatment machine. Figure 3.3 illustrates the schematic of the low pressure plasma apparatus. The system comprises two copper electrodes, one serving as the cathode and the other as the anode, each embedded with a high-durability insert such as hafnium. Positioned near the gas inlet, these electrodes

initiate plasma generation by producing an electric arc that ionises the gas. In addition to triggering the plasma, the electrodes also help maintain its stability. The chamber is equipped with two gas inlets that introduce the required gases for plasma formation. Before plasma generation, the chamber is evacuated to a pressure of approximately 0.4 mbar. This reduced pressure is critical for achieving a stable plasma state, as it ensures an optimal balance between the gas density and ion collision frequency. Following the treatment process, a vent valve is used to restore atmospheric pressure within the chamber.

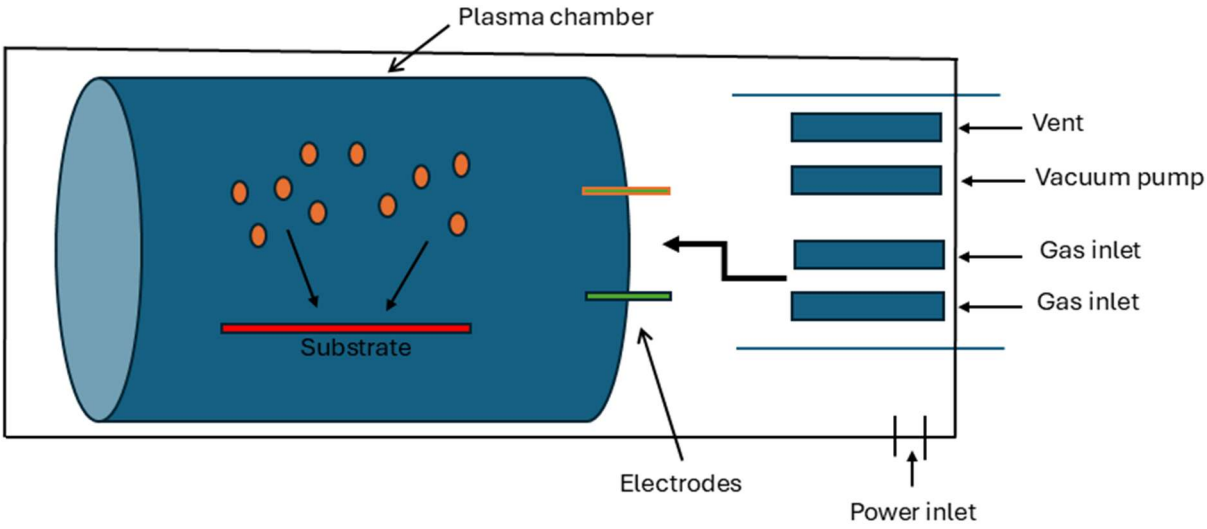

Figure 3.3 Functioning of the plasma machine

This plasma equipment features a quartz glass vacuum chamber with a diameter of 105 mm and a length of 300 mm, offering a total volume of 2.6 litres. The system operates on a 220-240 V AC power supply with a frequency range of 50-100 Hz. Two gases can be supplied through two needle valves, allowing controlled introduction of treatment gases. Pressure measurement is conducted using a Pirani gauge, ensuring precise monitoring of vacuum conditions. The vacuum pump has a capacity of approximately 3 m^3/h, maintaining the necessary low-pressure environment for plasma treatment.

3.3 Method for plasma treatment of hemp

The operational mode of the machine is manual, and it is furnished with a Pfeiffer Duo 3 rotary-vane vacuum pump. For the generation of plasma, argon or oxygen gas cylinders were connected to the plasma system. Plasma treatment of hemp was

executed employing various parameter combinations of power (intensity of plasma frequency) and treatment time (duration). Thus, the R.F.D. woven hemp fabrics underwent plasma treatment for a maximum duration of 10 minutes, and the nonwoven hemp fabrics were plasma treated for 3 hours. The gas supply was maintained at a constant flow rate by setting the gas valve at 1 bar, with a stable pressure of 1.5 mbar within the plasma chamber. After plasma treatment, the hemp fabric/fibre samples were conditioned in a standard textile testing environment having a relative humidity of 65 %, maintained at 20 °C.

3.4 Methods for analysis of surface morphology of hemp fibres

The surface morphology and surface topography of both treated and untreated hemp fibres and fabrics were analysed. Scanning electron microscopy (SEM) was employed to examine the surface morphology, providing detailed insights into fibre structure and surface modifications. Atomic force microscopy (AFM) analyses helped in gathering crucial data regarding the surface roughness and 3D surface projection.

3.4.1 Scanning electron microscopy of hemp

SEM provides high-resolution magnified images of samples by scanning a focused beam of electrons over the sample surface, making it an invaluable tool for material characterisation [109]. The interaction between the incident electron beam and the sample produces secondary electrons (Figure 3.4B), which are detected by the detector to produce an image. The contrast in the image is based on variations in the sample's topography and composition. The secondary electrons emitted by the sample provide detailed morphological information, whereas backscattered electrons help differentiate materials based on atomic number, also known as EDS. Figure 3.4A describes the working of the SEM, which consists of an electron gun, a magnetic lens, a sample holder and a detector.

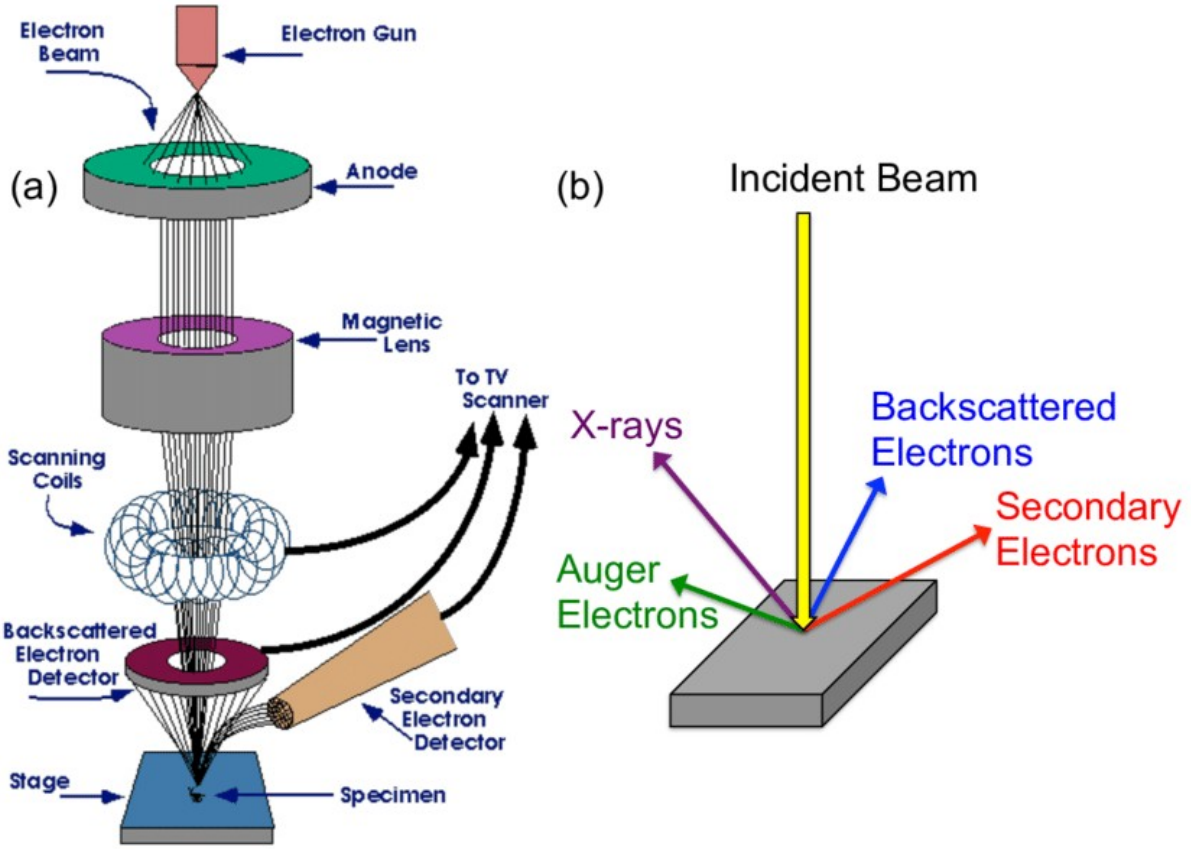

Figure 3.4 Working principle of SEM [110]

SEM is particularly well-suited for analysing hemp fibres because it offers high-resolution images having a maximum magnification of 25000×, allowing for detailed observation of the fibre surface. This technique enables the assessment of structural changes, roughness, and the presence of micro-cracks or defects caused by plasma treatment. For SEM imaging, hemp fibre samples were coated with a 20 nm layer of Iridium using a sputter coater to improve conductivity and enhance imaging quality. Iridium coating prevents electron accumulation on the sample surface, reducing distortions and improving image clarity [111].

3.4.2 Atomic force microscopy of hemp

Atomic Force Microscopy (AFM) is a high-resolution scanning technique used to analyse surface morphology and surface topography at the nanometre scale. It provides 3D-surface profiles by measuring the interaction forces between a sharp probe and the sample surface. AFM operates by scanning a fine tip (mounted on a flexible cantilever) over the sample surface [112]. The tip interacts with surface features through van der Waals forces, electrostatic forces, and mechanical contact.

A laser beam reflects off the cantilever onto a photodetector, which detects deflections and converts them into high-resolution surface maps. A feedback loop maintains a constant force between the tip and the sample surface by adjusting the height of the cantilever based on the detected deflection [112] [113].

Atomic Force Microscopy (AFM) operates in three primary modes: contact mode, tapping mode, and non-contact mode, as illustrated in Figure 3.5. In contact mode (Figure 3.5A), the AFM tip remains in continuous contact with the sample surface, making it most suitable for hard and shear-resistant materials [114]. For this study, AFM analysis of the hemp fibres was performed using tapping mode (Figure 3.5B) in ambient air. In this mode, the tip oscillates at its resonant frequency and intermittently contacts the surface during scanning, enabling high-resolution imaging with minimal sample damage. In non-contact mode (Figure 3.5C), the tip also oscillates near its resonant frequency but does not touch the surface. Instead, image formation relies on detecting changes in the oscillation caused by tip-surface interactions [114].

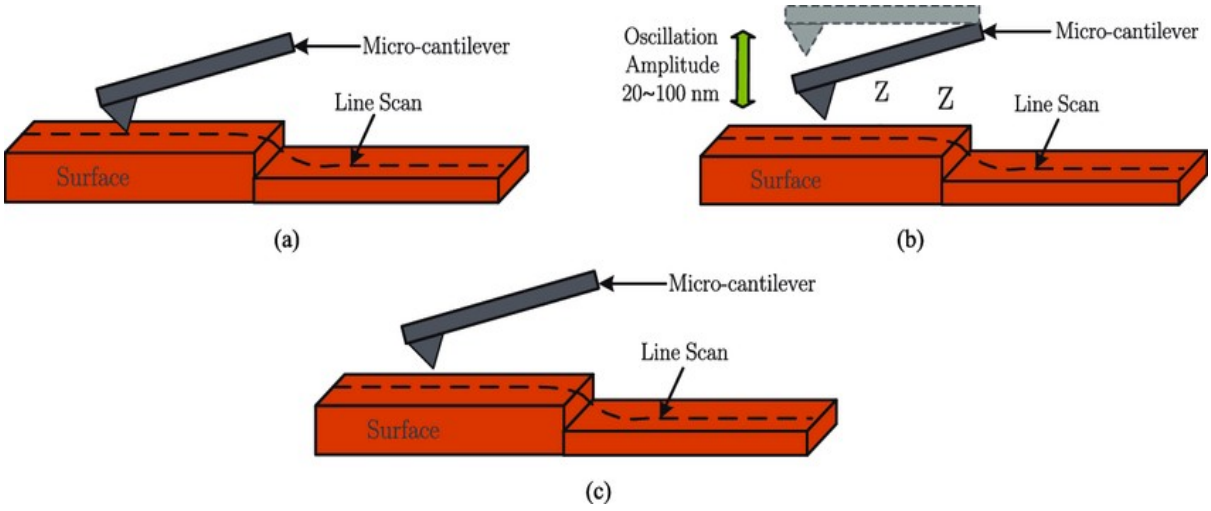

Figure 3.5 Operating modes in AFM: (a) Contact mode, (b) Tapping mode, (c) Non-contact mode [115]

AFM is useful for analysing plasma-treated hemp fibres as it provides quantitative data on surface roughness and topographical modifications at the nanoscale. Unlike SEM, which relies on electron interactions, AFM directly measures surface forces, making it highly sensitive to surface modifications caused by plasma treatment. Precise quantitative measurements of surface roughness (Ra, Rq, Rz) and fibre topography data were extracted using AFM [116].

Sample preparation in AFM is highly important as it determines the quality of resultant images. Thus, the hemp fibre samples were secured onto a flat aluminium disc using double-sided adhesive tape to ensure stability and attachment to mitigate the risk of movement of the sample on the disc due to cantilever oscillation and tapping. Before testing, care was taken to ensure that the fibres were firmly attached and properly flattened on the disc [116].

3.5 Method for analysis of the chemical structure of hemp

To investigate the chemical composition, spectroscopy techniques such as Raman spectroscopy and Fourier Transform Infrared (FTIR) spectroscopy were utilised.

3.5.1 Attenuated total reflectance Fourier transform infrared spectroscopy (FTIR)

ATR-FTIR is an analytical technique used to identify chemical structures and functional groups in materials by measuring their infrared absorption spectra. It works by passing infrared light through the surface of a sample, where specific molecular bonds absorb certain wavelengths. Herein, the penetration depth of the incident rays is up to 500 μm [117]. The absorbed wavelengths are then transformed into an infrared spectrum, which provides insights into the chemical composition of the sample. ATR-FTIR was thus used to essentially determine the presence of chemical functional groups or the induced changes in the absorption spectra of plasma treated hemp fibres and fabrics. Hemp fabrics and fibres, both plasma treated and untreated, were placed on a crystal ATR (attenuated total reflectance) and scanned [118].

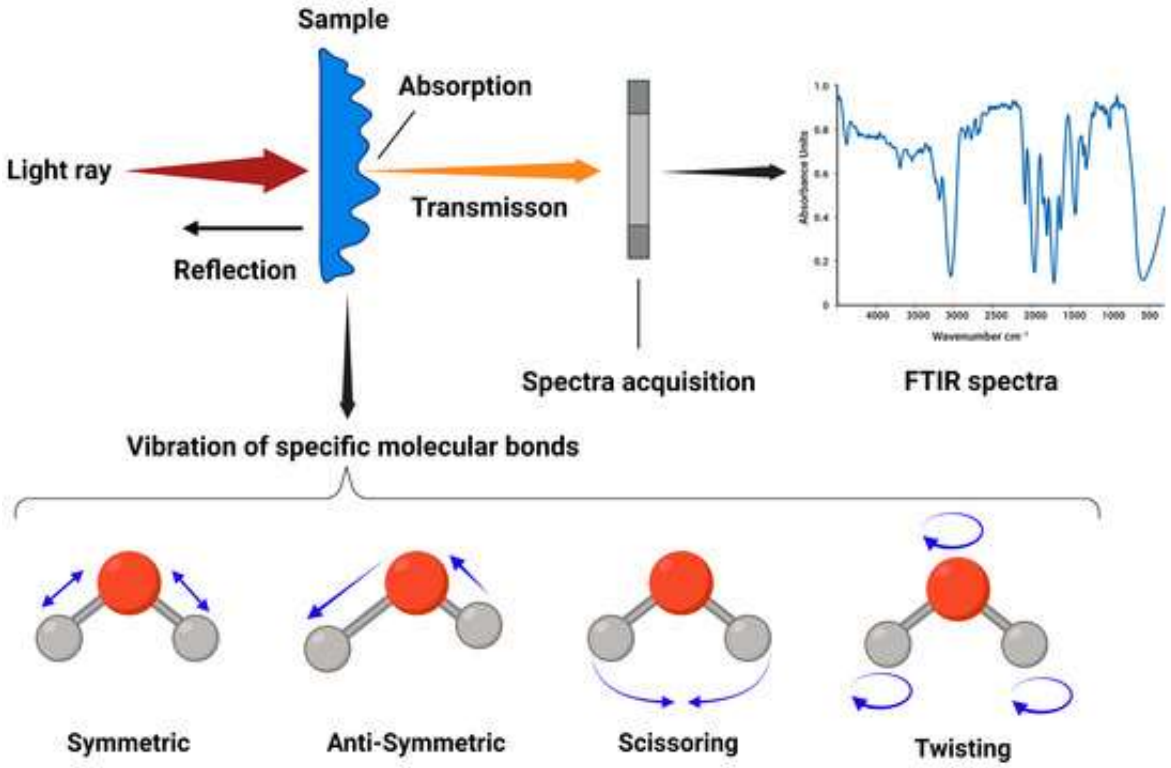

Figure 3.6 Working principle of ATR-FTIR spectroscopy [119]

Infrared (IR) radiation is a type of electromagnetic radiation with wavelengths ranging from 780 nm to 1 mm. Most molecules absorb IR radiation at specific frequencies that correspond to the vibrational modes of their functional groups. Each functional group has characteristic absorption frequencies, allowing molecular identification through IR spectroscopy [119]. Figure 3.6 illustrates the working principle of Fourier Transform Infrared (FTIR) spectroscopy. When infrared radiation is directed onto a sample, certain wavelengths are absorbed while others are transmitted. The transmitted light is captured by a detector, which then generates a spectrum representing the sample's molecular vibrations [120]. Different chemical functional groups absorb infrared light at specific frequencies that correspond to distinct vibrational modes. These include symmetric stretching, where atoms move in the same direction while maintaining the molecule’s symmetry, and asymmetric stretching, where atoms move in opposite directions, disrupting that symmetry. Additional vibrational modes include twisting, which involves changes in bond angles as atoms rotate around the bond axis, and scissoring, where atoms move toward and away from each other, altering the bond angle. These distinct vibrational patterns enable the identification of functional groups within the sample [117].

3.5.2 Raman spectroscopy

Raman spectroscopy is a highly effective analytical method that offers in-depth insights into the vibrational modes of molecules. The technique relies on Raman scattering, an optical process where the interaction between excited light (laser) and a sample results in scattered light. The energy shift of this scattered light corresponds to the vibrational energies of the molecule's bonds. In Raman spectroscopy, a laser beam is directed onto the sample, and the scattered light is detected. Plasma treatment alters the surface characteristics of hemp fibres by changing their chemical composition and structure. Due to its sensitivity to such alterations, Raman spectroscopy is an ideal tool for examining the effects of plasma treatment [121].

Raman spectroscopy is an analytical technique that identifies chemical functional groups through light scattering. When a sample is exposed to a high-energy laser, it scatters the incident light in two ways such as elastic and inelastic scattering. In elastic scattering, known as Rayleigh scattering, the scattered photons retain the same frequency or wavelength as the incident light, indicating no energy exchange with the molecule [122]. In contrast, inelastic scattering, referred to as Raman scattering, involves a shift in the frequency or wavelength of the scattered light, signifying that the molecule has either absorbed or released energy. The Raman spectrum records the intensity of this inelastically scattered light as a function of the Raman shift, which represents the energy difference between the incident laser and the scattered light. Figure 3.7 visually summarises these fundamental concepts [123]. The spectrometer comprises a laser source, a sample holder and a detector. Experiments were done using the 514 nm, 780 nm and 1064 nm lasers depending on the substrate. For natural fibres like hemp, the autofluorescence effects of inherent biomaterials such as lignin may affect the spectroscopy data. In some instances, using the 514 nm laser resulted in fluorescence, as this wavelength falls in the visible light range. Hence, to study the presence of lignin on the fibre surface, they were excited using the 514 nm laser and the images of the fibres were acquired using the confocal Raman microscope.

Confocal Raman microscopy is an invaluable tool to determine a 3D image of the chemical composition of the sample. In this microscope, the laser is focused on the sample and the detector is connected to a microscope to visualise the scattered light. In a few instances, the high-intensity laser may cause fibre burnout [123].

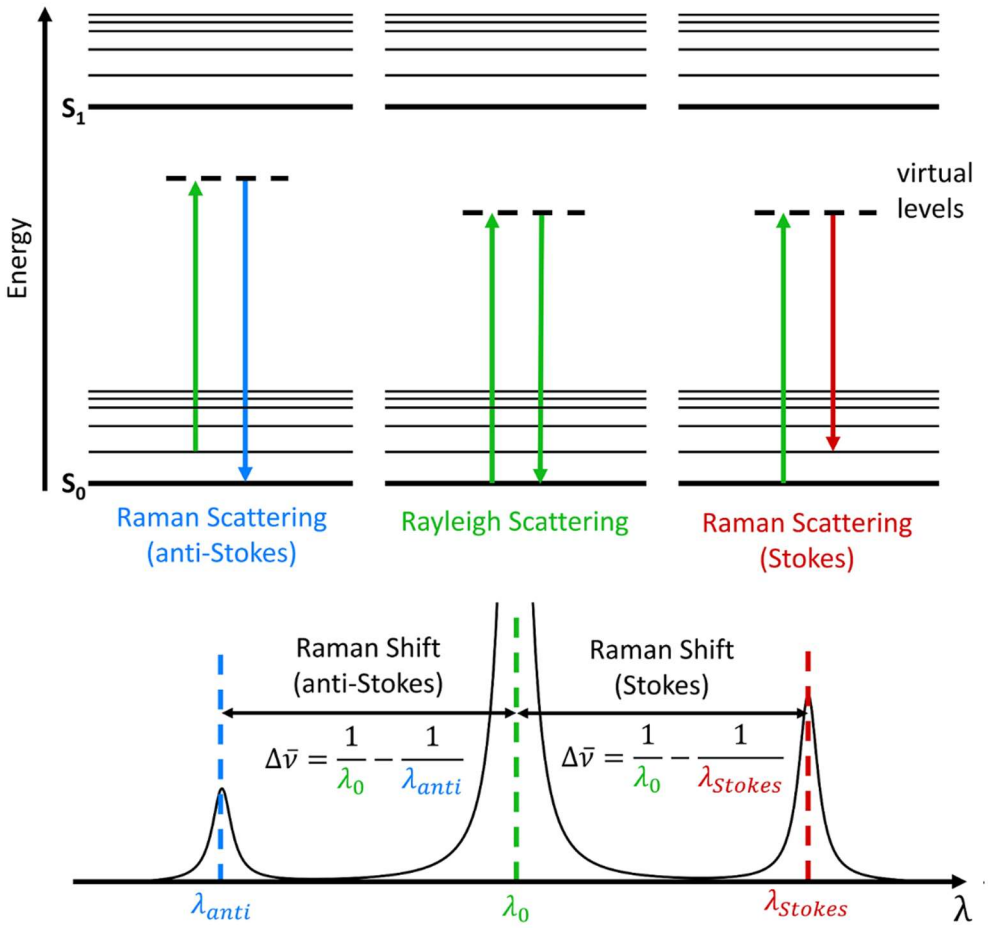

Figure 3.7 Scattering of light

3.5.3 X-ray diffraction (XRD)

X-ray diffraction (XRD) is a widely used analytical technique that provides structural information about crystalline materials. When X-rays are directed at a sample, they interact with the crystal lattice present in the sample, causing the X-rays to diffract at specific angles. The resulting diffraction pattern is unique to the crystal structure and can be used to determine information about the atomic arrangement, crystallinity, and orientation of the material. The angles and intensities of the diffracted rays are measured, and through analysis, one can obtain the crystal structure and other material properties. XRD was employed on both plasma-treated and untreated hemp fibres to analyse the changes in their crystallinity [124].

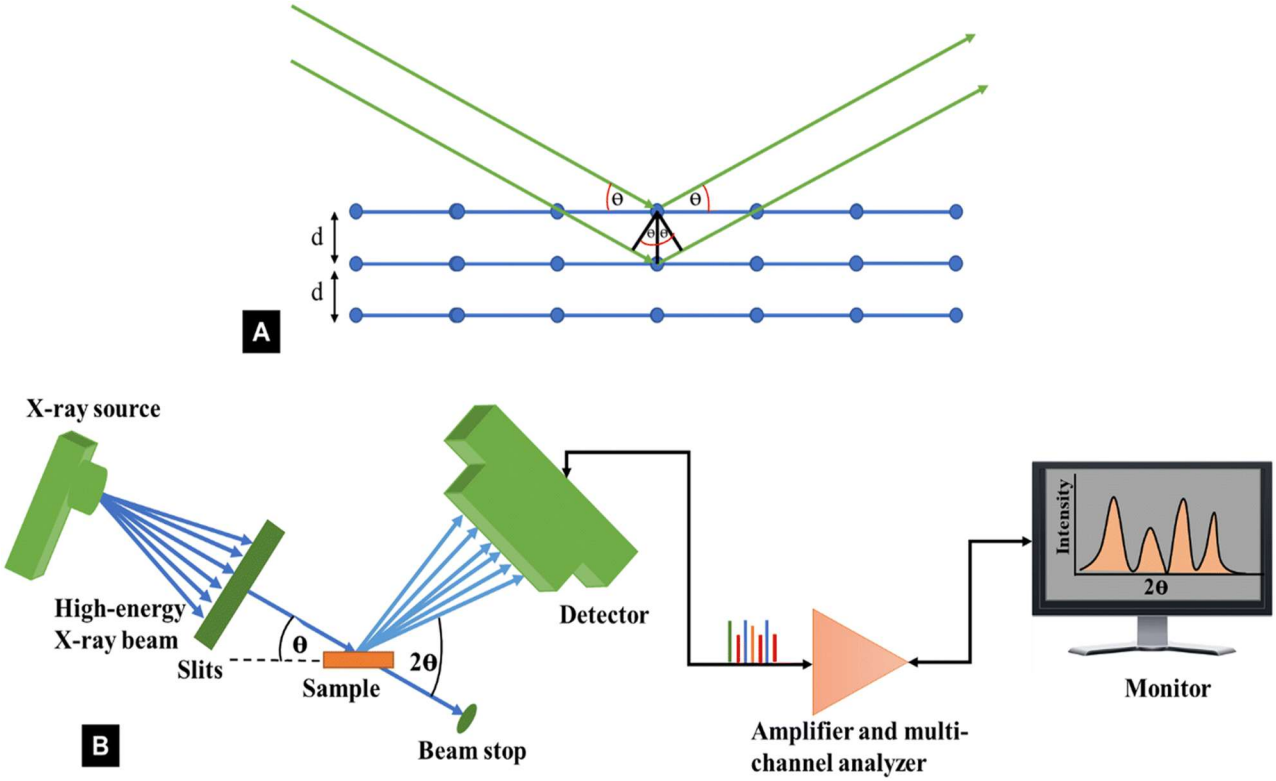

Figure 3.8 A] Bragg's law to determine crystallinity, and B] XRD instrumental set-up [124]

In a crystalline material, atoms are arranged in a well-ordered, three-dimensional pattern known as the unit cell, and the regular repetition of these unit cells forms the crystal lattice. Materials that exhibit a highly ordered and repetitive arrangement of unit cells are considered to have a high degree of crystallinity [124]. In X-ray diffraction (XRD), incident X-rays interact with the crystal lattice and are scattered at specific angles, as illustrated in Figure 3.8A. This scattering behaviour is governed by Bragg's Law, which states that constructive interference resulting in a strong diffraction signal occurs when the difference in the path length of X-rays scattered from adjacent crystal planes is an integer multiple of the X-ray wavelength [125]. When X-rays interact with a crystalline material, they are scattered in specific directions where constructive interference occurs at particular angles (θ), resulting in a diffraction pattern characterised by distinct peaks. These peaks correspond to the interplanar spacings (d-spacings) within the crystal structure and are directly related to the wavelength of the incident X-rays, and the relationship can be explained by the equation.

$$n\lambda = 2dsin\theta$$

wherein n is the order of reflection, λ is the wavelength of incident X-rays, d is the interplanar spacing in the crystal, and θ is the angle of incidence [125]. The

instrumentation for the XRD instrument is described in Figure 3.8B and consists of an X-ray source, a sample holder and a detector [124].

The determination of crystallite size was done using the Debye-Scherrer equation [126].

$$L = \frac{K\lambda}{\beta\, cos\theta}$$

Here, L is the crystallite size, K is a shape factor (usually 0.9), λ is the X-ray wavelength and β is the full width at half maximum (FWHM) in radians and θ is the Bragg's angle [127].

3.6 Method for analysis of surface wetting of hemp

Surface wetting analysis was conducted by measuring the water contact angle. This angle is determined by observing the shape of a small water droplet placed on a surface, using a goniometer to measure the angle formed at the droplet's edge. Water contact angle measurement is a widely used method to evaluate how a surface interacts with water, providing a quick and quantitative assessment of a material's wetting behaviour. The contact angle is defined as the angle formed at the interface where the liquid, solid, and gas phases meet and is illustrated in Figure 3.9. The water contact angle reflects the balance between adhesive forces (between the liquid and solid) and cohesive forces (within the liquid itself) at this three-phase boundary. A low contact angle (θ < 90°) indicates strong adhesion between the liquid and the solid surface, suggesting good wettability. In contrast, a high contact angle (θ > 90°) signifies weak adhesion, implying poor wettability or a hydrophobic surface.

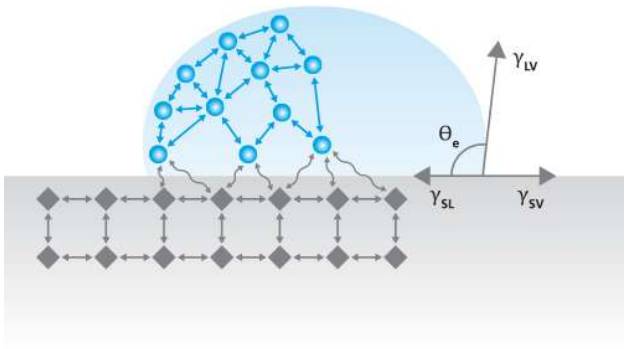

Figure 3.9 Water contact angle and the three-phase boundaries [128]

Wettability is influenced not only by the interaction between the solid and liquid but also by the cohesive forces that cause the liquid molecules to stick together, resisting spreading. If the solid surface is hydrophilic, water molecules will readily adhere, resulting in a low contact angle. Conversely, hydrophobic surfaces resist water adhesion, leading to a high contact angle. Additionally, the interaction between the solid and vapour phases, along with the surface tension at the liquid–vapour interface, plays a crucial role. Liquids with high surface tension tend to minimise contact with the solid, thereby increasing the contact angle.

The surface-wetting characteristics of untreated and plasma treated hemp fibres were evaluated using the Kruss DSA30E contact angle measuring instrument. A contact angle of less than 90 degrees indicates a hydrophilic surface (where water spreads easily), while an angle greater than 90 degrees indicates a hydrophobic surface (where water forms droplets) [19].

3.7 Method for analysis of tensile strength of hemp

A universal tensile strength tester functions by applying a controlled tensile force to a specimen while measuring the resulting deformation. The system typically consists of a load frame equipped with grips to hold the test specimen, a load cell to measure the applied force, and a control unit that manages the test parameters and records data. Figure 3.10 illustrates the main components and working principle of the tensile testing setup.

Figure 3.10 Tensile testing machine wherein 1: Load frame, 2: Software, 3: Load cell, 4: Grip to hold the sample tightly, and 5: Strain measurement [129]

The tensile strength of both untreated and plasma pre-treated hemp fibres was evaluated using a universal tensile strength tester following the BS EN ISO 5079-2020 [130] for individual hemp fibres and ISO 9073-3:2023 [131] for nonwoven hemp fabrics test standard method for testing. Using this process, the tensile strength and modulus of both plasma treated and untreated hemp fibres were determined by recording load and displacement data during the test.

3.8 Spectrophotometry to determine the colour strength of fabric

A spectrophotometer measures colour by quantifying the amount of light reflected or transmitted by a sample across the visible spectrum, ~ 380 nm – 780 nm [132]. In this study, a Konica Minolta spectrophotometer was used to analyse the colour properties of dyed fabrics. The instrument directs a beam of light onto the fabric surface and measures the intensity of light that is either reflected or transmitted, producing a

spectral "fingerprint" that represents the colour characteristics of the sample. Using this data, the amount of colour (dye) present inside the fabric can be quantified [132].

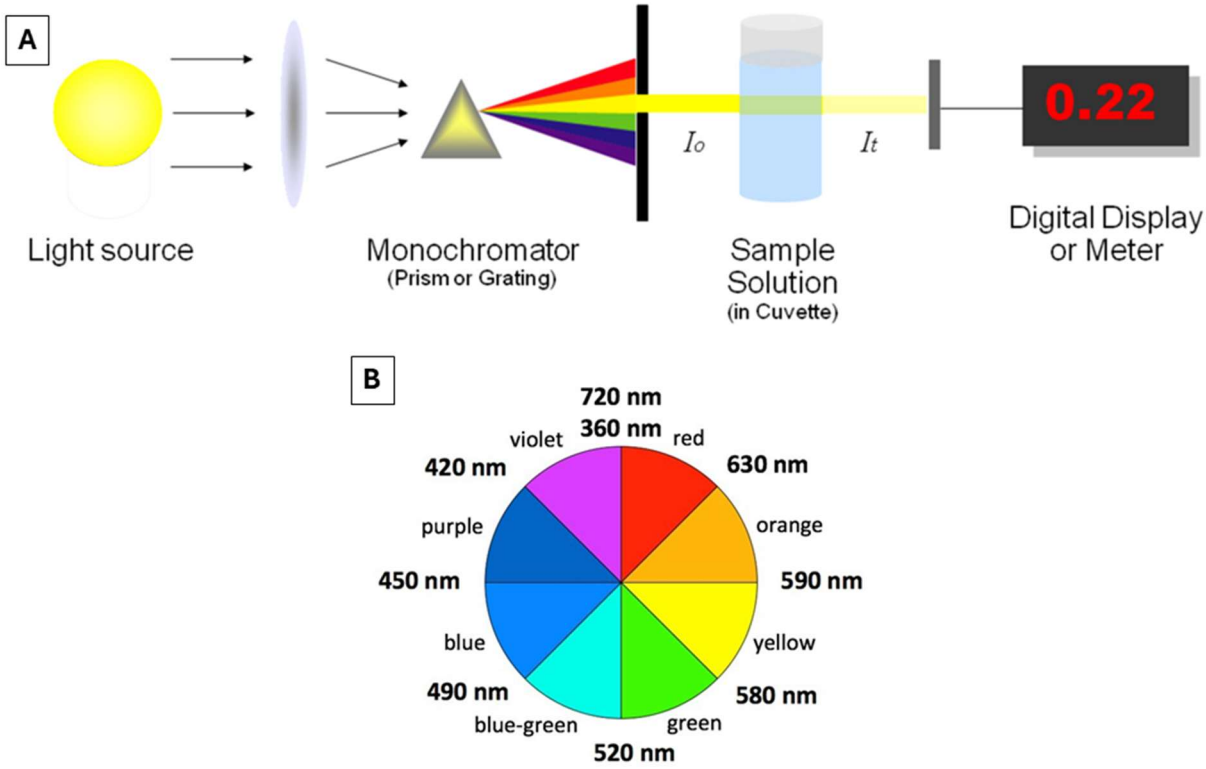

Figure 3.11 Working of a spectrophotometer[A] and a colour wheel [B] [132]

Although Figure 3.11A illustrates the setup of a UV-VIS spectrophotometer, the working principle remains the same for colour measurements in dyed textiles. The spectrophotometer employs a light source, typically a lamp, which emits light across the visible range. The colour wheel in Figure 3.11B shows the specific wavelengths of each colour. As this light interacts with the sample, some wavelengths are absorbed while others are reflected. The reflected light is then collected by a photodetector, which records the intensity of light at each wavelength. By analysing the resulting spectrum, the instrument determines the colour of the sample. For instance, a red-coloured fabric would reflect more light in the red region of the spectrum and absorb more in other regions.

The colour data is commonly converted into CIE L*a*b* values, a standardised colour space developed by the International Commission on Illumination (CIE). In this system, L* represents lightness (ranging from 0 for black to 100 for white), a* represents the red-green axis (positive values indicate red, negative values indicate

green), and b* represents the yellow-blue axis (positive values indicate yellow, negative values indicate blue). These values provide a three-dimensional coordinate for accurately locating and comparing colours.

Additionally, the spectrophotometer can calculate the K/S value, representing colour strength or concentration, using the Kubelka-Munk equation, which relates the sample's reflectance (R) and absorption/transmission (T) properties. A higher K/S value indicates greater dye uptake or colour intensity on the fabric surface. This makes the K/S value particularly useful for evaluating the depth of shade in dyed textiles.

$$\frac{K}{S} = \frac{coefficient\ of\ absorption}{coefficient\ of\ scattering}$$

The L*, a*, and b* values, along with the colour strength (K/S), were measured using a Konica Minolta spectrophotometer, enabling precise quantification of the colour characteristics of the dyed fabrics. Statistical analysis of the collected data was performed using Minitab software to evaluate trends and assess the significance of the results.

Chapter 4

Improved colouration of hemp fabrics via low-pressure argon plasma assisted surface modification

4.1 Introduction

Interest in hemp as a viable cellulosic fibre for clothing has increased, driven partly by its economic benefits and the importance of natural renewable materials in emerging circular economies. However, the colouration and chemical finishing of lignocellulosic fibres such as hemp typically require large quantities of water and chemicals. Argon plasma pretreatment provides a way of modulating the physical properties of hemp fibres to improve the colouration process without compromising other bulk properties such as tensile strength. Such plasma treatments may contribute to alleviating the negative environmental impacts associated with liquid pretreatments, heating, or the use of auxiliary chemicals. Dyeing of hemp fibres is particularly challenging due to its crystalline chemical structure. In this study, low-pressure argon plasma-assisted surface modification of woven hemp fabrics up to 600 s at 40 and 80 Hz was explored for enhanced dyeability, resulting in enhanced dye-fibre bonding. Fourier-transform infrared spectroscopy and Raman spectroscopy of argon plasma pretreated hemp fabrics produced no noticeable changes in the functional groups of the fibres, but a physiochemical modification was observed in terms of the density of polar groups. Scanning electron microscopy (SEM) images revealed marked morphological changes including nano-etching of the fibre surface at certain argon plasma process conditions. The pretreatment process increased fibre hydrophilicity, and enhanced reactivity of the surficial -OH groups towards fibre-reactive and vat dyes, resulting in higher colour strength in dyed woven hemp fabrics. Overall, we envisage such plasma pretreatments may impact positively on the material and energy efficiency of the hemp fabric dyeing process.

Hemp is a natural cellulosic fibre similar to bast fibres such as flax and ramie that are widely used in the textile industry [133]. The fibres are extracted from the internal stems of the *Cannabis sativa L*. plant and comprise primary and secondary walls of long cellulose microfibrils (~72% cellulose [44]) arranged in layered strata, with a distinctive axial orientation [20]. The high crystallinity and axially aligned cellulosic structure confers characteristically high tensile strength and attractive mechanical

properties, such that hemp finds purpose in numerous textile applications, including technical textiles, fibre-reinforced composites and clothing. Opportunities for hemp in clothing are further extended by cottonisation of the coarse fibres extracted from the plant's stem, yielding smaller fibre diameters of ca. 15-20 microns, that are suitable for blending with other fibres such as cotton and spinning into fine count yarns [20]. Given the growing importance of renewable materials in the fashion and textile industry, there is an increasing interest in hemp as an economically attractive fibre for clothing fabrics, but sustainable development necessitates less resource intensive dyeing and colouration processes [134]. Compared to other natural cellulosic fibres, notably cotton, and bast fibres such as flax (linen), there is a paucity of studies relating specifically to the dyeing of hemp.

Conventional dyeing processes in the textile industry can have significant environmental impacts. It has been claimed that for every ton of fabric to be dyed, up to 200 tonnes of wastewater containing salts, dyes, surfactants, peroxides and heavy metals can be generated [135]. To address these issues, alternative colouration methods such as supercritical CO_2 and ultrasonic methods are being studied [136]. Innovative colouration methods also include laser and enzyme processing technologies, particularly in relation to cotton, wool and polyester substrates [137]. However, current research lacks a focus on hemp. The use of hemp in the textile industry is limited primarily due to the dominance of cotton, historical stigma, complex governmental regulations and a lack of awareness about the potential advantages of the fibre [13]. Table 4.1 highlights recent studies where hemp dyeing was accomplished using conventional exhaustion methods.

Substrate	***Dyeing Conditions***	***Summary***	***Reference***
Hemp/Cotton blend	8% w/w dye Material to liquor ratio (MLR)= 1:60 t=1h, T= 60°C	Dyed using common madder and calendula achieving a colour strength of 5.6 after applying tannin as a mordant.	[138]

100% Hemp fabric (GSM:132)	t=2h, T= 70°C	Dyed using plant-based dyes and the ultraviolet protection factor was evaluated.	[88]
100% Hemp fabric	5 % w/w dye shade MLR= 1:20 t=1h, T=60°C	Dyed using reactive dye and compared with cotton fabric.	[139]
100% Hemp yarn	t=70 min, T=60°C	Dyed using the conventional dyeing method and fabric properties were compared with flax, linen, cotton and their respective blends.	[140]

Table 4.1 Recent studies on the colouration of hemp using exhaustion methods

Current research interest in surface-treated hemp fibres is mainly confined to fibre-reinforced composite applications. The aim of the present research is to broaden the scope of hemp usage from composites to clothing applications by addressing two major research gaps related to the study of hemp fibre colouration. First, it addresses the issue of low colour fastness in dyed hemp fabrics, by exploring dye-fibre bonding using pyridine stripping [141]. Second, while numerous studies have reported surface modifications on cellulosic fibres, they often overlook the chemical interactions following these surface modifications [141]. This work investigates both morphological and chemical changes resulting from low-pressure argon plasma pretreatment.

To develop environmentally sustainable colouration techniques for hemp fabrics, it is important to understand the extent to which non-aqueous fabric pretreatments might enhance dyeability. Previously, microwave and UV irradiation of bast fibre cellulosic

fabrics have shown potential to improve the colour strength and fastness of dyed fabrics [82, 142, 143]. However, plasma pretreatment has arguably become the most ubiquitous, non-aqueous pretreatment method for natural cellulosic fibres, providing a means to modulate fibre physical structure and surface chemistry [144]. The advantage of plasma as a pretreatment is that it is a chemically independent technique, which confines its physical and chemical effects to the surface.

Plasma is defined as a state in which a significant number of atoms and/or molecules are either electrically, thermally, magnetically excited or ionised. Plasma treatment may impart physical or chemical changes with the help of radicals, ions or electrons in an excited state. Low-pressure plasma is applied in various fields such as surface cleaning, coating, etching and functionalisation of polymeric materials, with the ability to modify surface fibre morphology and/or chemistry [22]. Plasma treatment can have an etching effect on the surface resulting in a nano-porous structure [145]. The use of noble gases like argon can also produce highly energetic radicals in the plasma state that are able to break C-C, C-H, and hydrogen bonds, and potentially create desirable functional groups [96]. As reported by Thompson et al. [99], plasma treatment of nylon-6 using oxygen gas as a source gas resulted in an increase in the number of polar groups (C=O, C-C, C-OOH), increasing the hydrophilicity of the surface. Comparatively, hemp also has a crystalline structure and is relatively hydrophobic in its parent state.

Previously, plasma treatment of hemp has mainly been confined to studies of bio-composites, specifically fibre-reinforced polymer composites, in which hemp fibres are used as a reinforcing phase [146]. In this context, plasma pretreatment can be used to improve the interfacial bonding between the fibre surfaces and the matrix phase, so as to improve the bulk tensile and shear strengths, as well as the fracture resistance of the bio-composite [147]. Plasma treatment of hemp fibres using argon as a source gas has also been reported to improve the sound absorption of the resulting structures [148].

Low-pressure argon plasma pretreatment of other bast fibres, such as flax, has been found to enhance hydrophilicity leading to strong interfacial bonding with vinyl silane to confer flame retardancy [149]. In the context of fibres derived from bamboo, plasma-assisted surface modification employing gases such as oxygen and argon improved surface wetting and interfacial adhesion, thus promulgating their application as a

reinforcement material in composites [150]. Similarly, jute fibres treated with air plasma, exhibited increased hydrophilicity due to surface etching, subsequently improving interfacial adhesion and thereby rendering them suitable for reinforcement in composites [26] [151].

The potential for argon plasma irradiation as part of a pretreatment process to enhance the dyeing properties of hemp remains a topic that has not been extensively explored in the literature. Radetic et al. studied the low-temperature air plasma and enzymatic pretreatment of hemp for acid dyeing and reported an increase in the dyeing rate, final dye exhaustion and colour yield. The observed effects were attributed to plasma etching and oxidation of hemp fibre surfaces [152]. Argon plasma treatment is believed to promote crosslinking of the polymer chains and fragmentation of polymer chains into lower molecular weight entities, and argon plasma is thought to induce a more enduring hydrophilic transformation than any other gas plasma [153]. Based on the literature survey, it is apparent that there is insufficient study exploring the extent to which plasma pretreatment influences the dyeing of hemp. Dyeing of hemp presents particular challenges due to the high degree of molecular orientation and relatively high crystallinity of the fibres. In such crystalline natural fibres, dye molecules tend to penetrate more easily through the amorphous regions than the crystalline regions [154]. Conventional dyeing procedures take place in an aqueous environment, wherein, water has a competitive role in relation to hydrogen bonding, and given the extensive hydrogen bonding in cellulose, when immersed in water, negative zeta potential arises. Similarly, when reactive dye molecules are solubilised in water, they acquire a negative zeta potential due to the presence of $-SO_3H$ group. Therefore, the addition of salts helps neutralise the negative zeta potential acquired by cellulose, thereby promoting uniform dye adsorption. Lokhande et. al., observed a decrease in a negative zeta potential, leading to proportional dye adsorption in the cellulosic structure [155].

The dyeing of cellulosic fibres such as hemp is an equilibrium reaction, which depends on the temperature, pH and dye concentration, and the extent of dye adsorption hinges on the cohesive forces inherent in the cellulosic structure. When cellulose interacts with water, the water molecules compete for some hydrogen bonding sites. Notably, cellulose carries inherent fixed negative charges that can potentially repel dye molecules, which are also negatively charged, seeking adsorption. The presence of these Coulombic effects inhibits dye adsorption and further dye uptake [156-158]. Accordingly, previous investigations into augmenting the colouration of hemp textiles

have explored the application of mordants such as tannin and alum [138]. A comparable study done by Correia et al. focused on the pretreatment of cotton fabric using cationic ammonium compounds, which were further plasma treated using oxygen gas [159]. Similarly, nitrogen plasma pretreatment can be used to graft silver nanoparticles onto cellulosics such as cotton, viscose and linen to impart antibacterial functionality [160]. In a literature review, Haji et. al summarised major studies in recent years where the colouration of wool, cotton and polyester fibres was achieved [161]. Interestingly, the majority of the studies, aiming to achieve colouration of fibres using plasma, have employed oxygen as their plasma source.

The goal of this research is to utilise an inert, low-pressure argon plasma pretreatment to surface-modify woven hemp fabrics prior to conventional exhaustion dyeing. The extent to which the colour strength of resulting dyed fabrics is affected by the argon plasma pretreatment is studied to assess the potential for effective colouration. Moreover, the impact of power and the duration of argon plasma pretreatment on surface modifications was explored in relation to reactive dyeing and vat dyeing. An analysis encompassing surface morphology, Raman spectroscopy, ATR-FTIR spectroscopy and surface wetting properties was conducted on both untreated and plasma treated hemp fabrics.

4.2 Experimental

4.2.1 Materials

In the experimental work reported here, 100% hemp fabric samples of different woven constructions (H, P1, P2) and yarn linear densities in the warp and weft, were industrially procured (Hemptology Ltd, UK), with material specifications as shown in Table 4.2.

Fibre	Fibre Composition	Woven Fabric Structure	Yarn Linear Density (Tex)		Fabric Weight/unit area ($g.m^{-2}$)
			Warp	Weft	
Hemp	100%	Herringbone (H)	120	120	190

Hemp	100%	Plain (P1)	79	79	100
Hemp	100%	Plain (P2)	35	35	214

Table 4.2 Product parameters of the hemp fabrics

Prior to low-pressure argon plasma pretreatment, all samples were scoured to remove any residual processing chemicals or spin finish. An alkaline boiling process was followed for the scouring of hemp [162]. Thus, hemp fabrics were boiled for 75 minutes in an alkali solution containing 6% o.w.f (on the weight of fabric) NaOH, 3% o.w.f of Na_2CO_3 and 0.5% o.w.f of Na_2SO_3. After the alkaline boiling, the fabrics were neutralised using 10% o.w.f CH_3COOH and were washed thoroughly with deionised water. The scoured fabrics were dried in an air-assisted oven at 90°C. Following drying, the scoured fabrics were stored in a standard textile testing environment with 65% relative humidity at a temperature of 20°C before plasma treatment. Fibre-reactive and vat dyes were procured from Atul Industries Ltd (India). Analytical research (AR) grade reagents, sodium hydroxide (NaOH), sodium dithionite ($Na_2S_2O_4$) and anionic surfactant were acquired from Sigma-Aldrich (UK). Additionally, Turkey red oil utilised for vat dyeing was purchased from Fisher Scientific Ltd (UK).

4.2.2 Surface modification of hemp fibres following argon plasma pretreatment

Argon plasma pretreatment of the hemp fabrics was conducted using a Denier Zepto plasma machine (Diener electronic GmbH & Co KG, Germany). The machine incorporates two needle valves for precise gas supply with gas flow controllers. The operational mode of the machine is manual, and it is furnished with a Pfeiffer Duo 3 rotary-vane vacuum pump. For the generation of plasma, an argon gas cylinder was connected to the plasma system. Argon plasma-assisted surface modification of hemp was executed employing various parameter combinations of power (intensity of plasma frequency) and treatment time (duration). Thus, the hemp fabrics underwent plasma treatment at two power levels of 80Hz and 40Hz at six treatment durations of t= 30s, 60s, 120s, 180s, 300s and 600s. The argon gas supply was maintained at a constant flow rate by setting the gas valve at 1 bar, with a stable pressure of 1.5 mbar within the plasma chamber. Subsequent to argon plasma pretreatment, the fabric samples were conditioned in a standard textile testing environment having a relative humidity of 65%, maintained at 20°C. The design of experiments (DOE) was formulated using the surface response design with two factors such as power (40Hz,

80Hz) and treatment time (30s, 60s, 120s, 180s, 300s, 500s) The results were then analysed using the surface response analysis methodology using the Minitab software.

4.2.3 Analysis of fibre surface modifications

The argon plasma pretreated fabric samples were subjected to surface analysis to investigate any induced alterations in fibre surface morphology, fibre chemical modifications or wetting.

4.2.3.1 Method to study fibre morphological features

The surface morphology of argon plasma pretreated and untreated hemp fibres were investigated by scanning electron microscopy (SEM) images using a Jeol JSM-6610 scanning electron microscope. Using the SE mode, micrographs at magnifications of 25×-8000× were taken of the fibre surfaces for each sample, covering a scale of 1mm to 10μm following the standard method by Juhász et. al [163]. Prior to image capture, the samples were sputter-coated with gold. Subsequently, SEM images were processed using Fiji ImageJ software to analyse fibre morphological features such as surface roughness [164]. To measure the indented features, herein referred to as the 'pore' structure of the fibre surfaces using Fiji Image J, an area of 30 μm on the fibre was selected within the SEM micrograph. Utilising the threshold function, surface pores within the selected area were highlighted enabling the determination of mean porosity. To assess the pore size, the pore analysis option was applied following the threshold function. The porosity measurements were conducted thrice to ensure reproducibility and to obtain consistent results.

4.2.3.2 Methods for analysis of chemical modifications

The chemical structure of argon plasma pretreated and untreated hemp samples were analysed utilising ATR-FTIR and Raman spectroscopy. A Bruker FT-IR spectrometer, which was equipped with an ATR (attenuated total reflectance), was used in the wavenumber range of 600 cm^{-1} to 4000 cm^{-1}. 100 scans were taken at a resolution of 4 cm^{-1} on the untreated and plasma treated samples, referring to the work by Peets et. al [165]. For each fabric sample, three spectra were acquired to ensure the reproducibility of the data. Raman spectroscopy of argon plasma pretreated and untreated hemp fabrics was performed using a Horiba Raman spectrometer equipped

with a microscope and a 785 nm laser source. A total of 32 scans were accumulated per spectrum, having a resolution of 4 cm^{-1} on the untreated and plasma treated samples following a standard method from Rygule et al [166]. For each fabric sample, three spectra were acquired to ensure the reproducibility of the data. The resulting spectra was processed using Origin software to edit, analyse and represent spectroscopic data.

4.2.3.3 Method for analysis of surface wetting

The surface-wetting properties of untreated and argon plasma pretreated hemp were assessed using a Kruss DSA30E contact angle measuring equipment. The static contact angle of the hemp fabric was measured by placing 7μl sessile water droplets of deionised water having a surface tension of 72 N/m on the fabric surface. The droplets were allowed to stabilise for 20s and the contact angle was measured using a built-in camera. Three replicates were taken for H, P1 and P2 fabric types, with each droplet positioned at a different position on the fabric sample to test the reproducibility of the data.

4.2.3.4 Method for dyeing hemp with reactive dyes

To study the effect of argon plasma pretreatment on the dyeing behaviour, a 5% shade on weight of fabric was applied across all the experimental procedures involving exhaust dyeing of each of the hemp fabric samples. The amount of dye solution was calculated using equation 4.1. The dyeing process was conducted with a fabric-to-liquor ratio (MLR) of 1:20 for all samples.

$$Amount\ of\ dye\ solution\ (mL) = \frac{Shad\ \ (\%) \times Weigh\ \ of\ fabric\ (g)}{Concentration\ of\ stock\ solution\ (g/L)} \qquad \text{.....(4.1)}$$

Similarly, the amount of auxiliaries as alkali and salt was calculated using equation 4.2, wherein 20% o.w.f of alkali, namely soda ash and caustic soda, along with 20% o.m.f Glauber's salt were used.

$$Amount\ of\ auxiliary\ (mL) = \frac{Auxiliary\ required\ (\%) \times Weigh\ \ of\ fabric\ (g)}{Concentration\ of\ stock\ solution (g/L)} \qquad \text{.....(4.2)}$$

For the dyeing of the hemp fabric, Glauber's salt, water and dye solution were introduced to a beaker alongside the fabric. Firstly, twenty per cent of the salt was utilised, accompanied by 20% o.m.f of soda ash and 20% o.m.f of caustic soda. Following a 15-minute interval, the dye bath was stabilised at a constant temperature of 75°C. Alkali was then added, and the dyeing was carried out for 60 min under continuous agitation. Figure 4.1 summarises the complete reactive dyeing cycle.

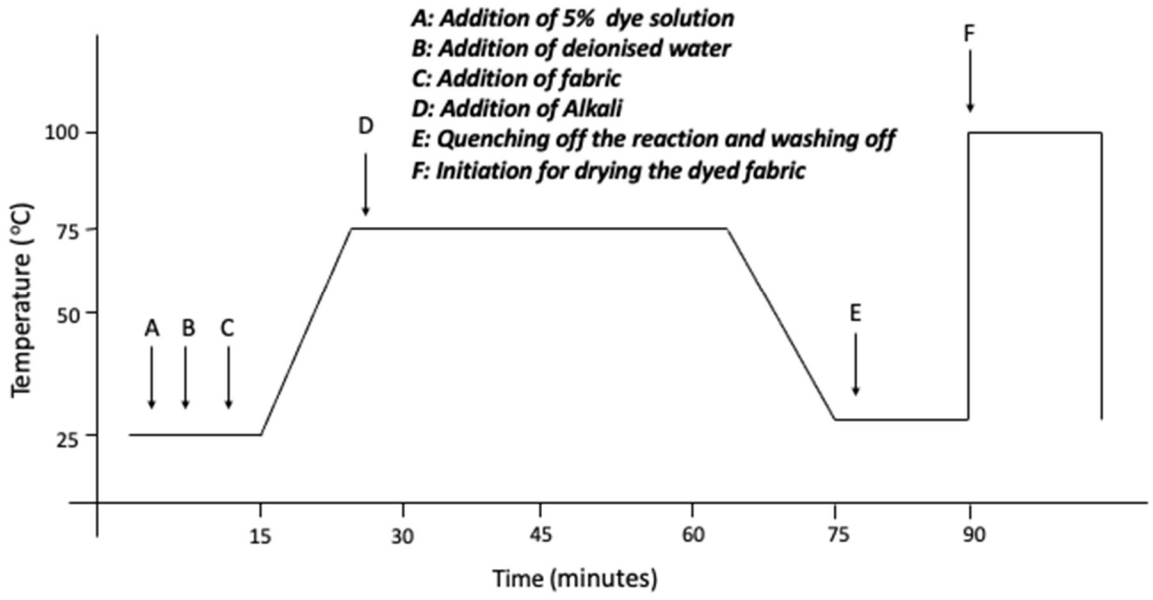

Figure 4.1 Dyeing curve for dyeing of hemp fabric using reactive dye

Subsequent to dyeing, the dyed fabrics were subjected to a soaping process that involved boiling the fabrics in a 5% on weight of fabric anionic soap solution to remove unbound dye molecules. The soaped fabric samples were dried in an air-assisted oven at 90°C for 4 hours. The dyed fabrics were analysed using a Konica Minolta CM 700-d spectrophotometer for colour measurement to ascertain the CIE colour coordinates of the dyed fabrics.

4.2.3.5 Analysis of covalent bonding of reactive dyes

Hemp fabric samples that underwent dyeing with reactive dyes were subjected to a pyridine-stripping process [167]. In contrast to the conventional employment of sodium hydrosulphite and sodium hydroxide for dye-stripping, a solution containing 15 g/L of pyridine was utilised. Thus, the dyed fabrics were subjected to boiling in a solution containing 15 g/L pyridine solution. Following 5-minute boiling intervals, the pyridine

solution was replaced iteratively until achieving a clear solution. The colour strength of the fabrics subjected to pyridine stripping were subsequently measured using a Konica Minolta colour measurement device.

4.2.3.6 Method for dyeing hemp with vat dyes

The vat dyeing process for hemp encompassed three sequential stages: vatting, dyeing and air oxidation. The conventionally known vat dyeing process used in the denim textile industry was followed [168]. Initially, the dye mixture was prepared by combining 1 g of amorphous vat dye with 5 mL of turkey red oil, forming a paste. The turkey red oil (sodium salt of sulphated castor oil) acting as a wetting agent, facilitated this process. 40% o.w.f of sodium hydroxide (NaOH) and 2 gm of sodium dithionite ($Na_2S_2O_4$) were subsequently introduced to the dye paste and stirred until the formation of a homogeneous paste. This process yielded the soluble salt or leuco vat dye. All of the hemp fabric samples were dyed employing a 1% o.m.f shade with a fabric-to-liquor ratio of 1:20. Water, surfactant and alkali were added in accordance with calculations based on the material-to-liquor ratio and the weight of the fabric. The temperature of the dye bath was elevated to 80°C and maintained at this temperature for a duration of 90 min. Upon cooling, the samples underwent washing and air drying to ensure uniform oxidation [168]. The oxidised fabrics were then subjected to a 20 min boiling process in a 15 g/L soap solution, which served the dual purpose of removing excess non-reacted dye molecules and imparting a lustrous appearance to the fabrics. Subsequent to this soaping treatment, the colour strength of the fabrics was assessed following drying. Figure 4.2 illustrates the vat dyeing and reactive dyeing cycle of hemp fabrics used for this research, and Figure 4.3 summarises the employed dyeing profile.

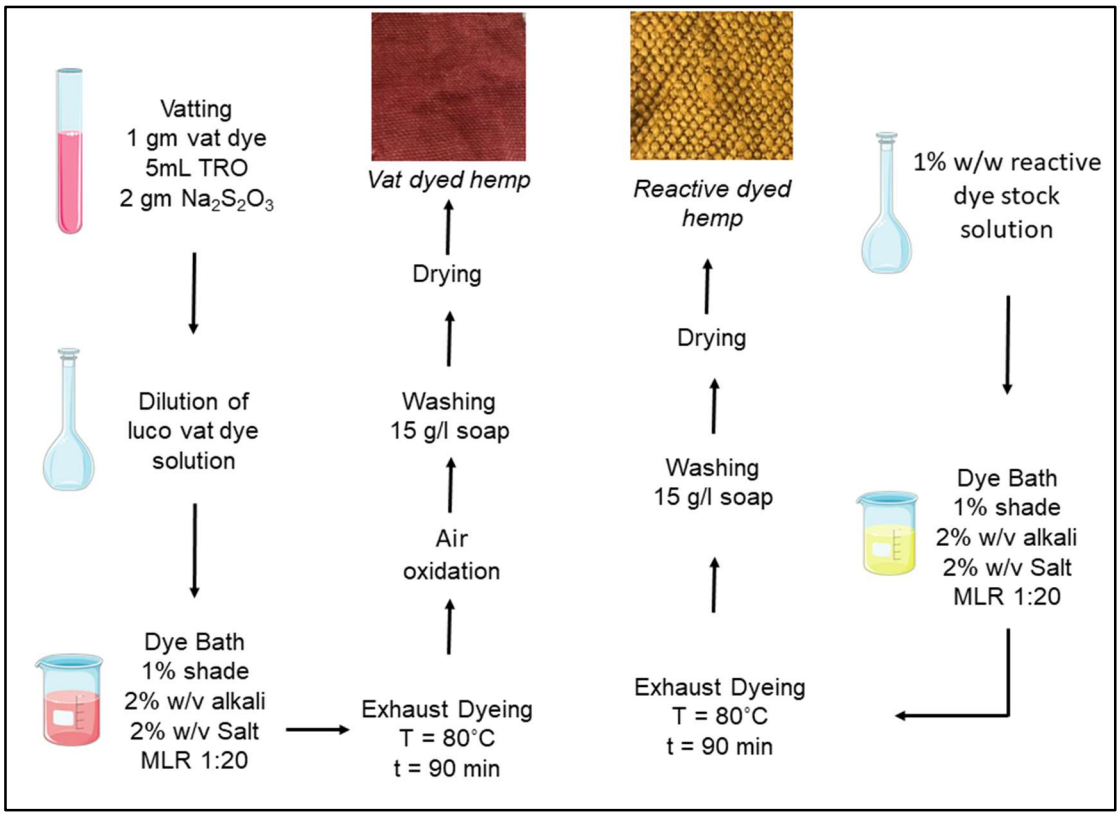

Figure 4.2 Dyeing process for untreated and plasma treated hemp fabrics

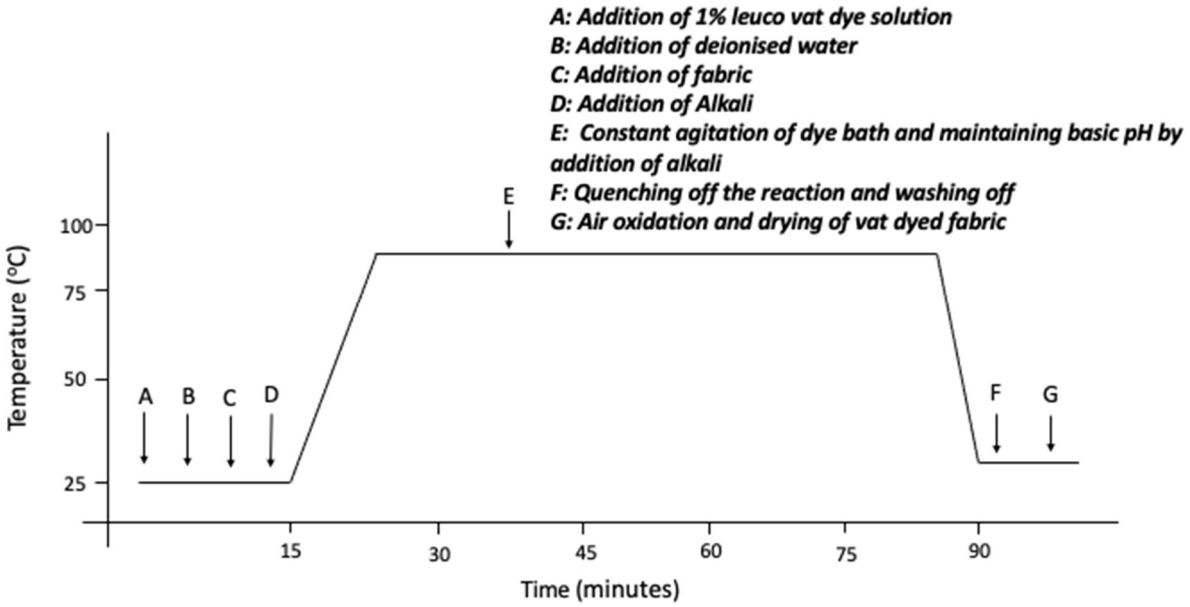

Figure 4.3 Dyeing curve for dyeing of hemp using vat dyes

4.3 Results and discussion

The physical and chemical properties of the hemp fabrics and their constituent fibres were studied before and after pretreatment with argon plasma to determine any structural and chemical effects and their potential influence on the dyeing process.

4.3.1 Influence of argon plasma treatment on hemp fibre surface morphology

The fibre surface morphologies of untreated and argon plasma treated hemp fabrics were investigated by means of SEM (Figures 4.4 A, B, C, D, E and F). Figure 4.4A shows a typical example of the surface morphology of fibres in the untreated sample, having relatively smooth surface. Evidence of dry etching is apparent in hemp fibres that had been argon plasma treated for 600s at 40Hz power (Figure 4.4F). A progressive dry etching can be observed as the argon plasma treatment time increases [169]. The dry etching can be attributed to a chain scission at the surface of the fibre and has been previously observed in plant-based fibres [169, 170] as well as regenerated cellulose fibres such as viscose [150]. This type of effect can be observed, highlighting a high degree of sub-micron surface etching in the argon plasma treated hemp samples (comparing Figures 4.4A and 4.4F).

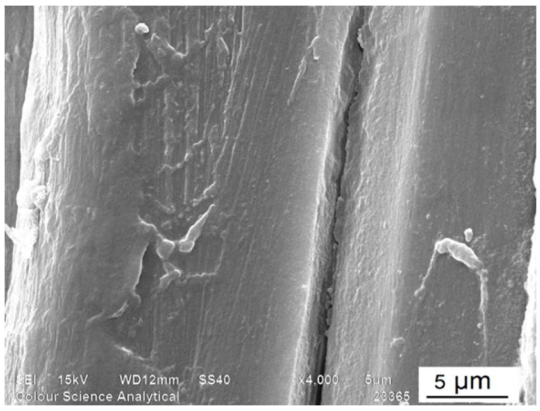

A] Untreated

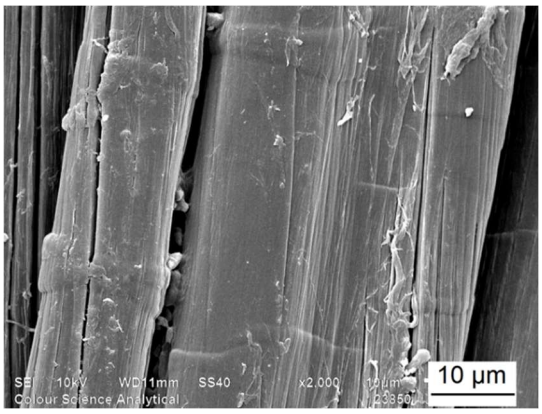

B] P80Hz t60s

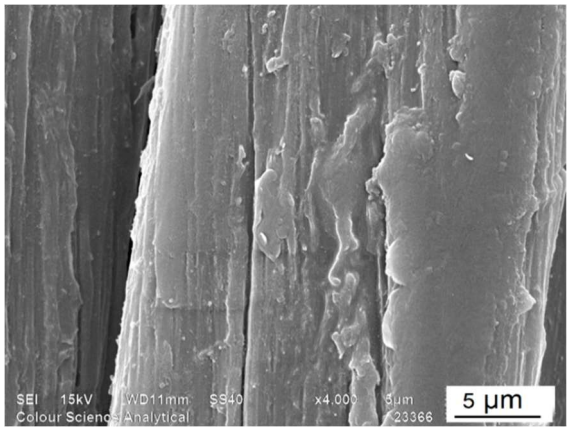

C] P80Hz t300s

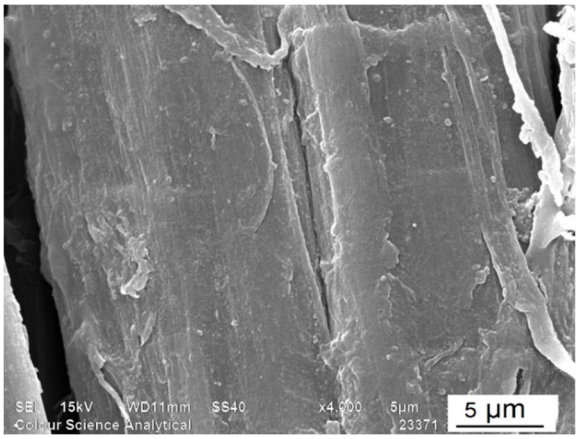

D] P80Hz t600s

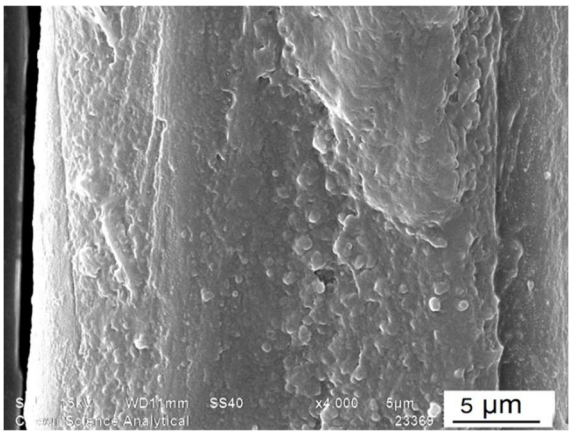

E] P40Hz t300s

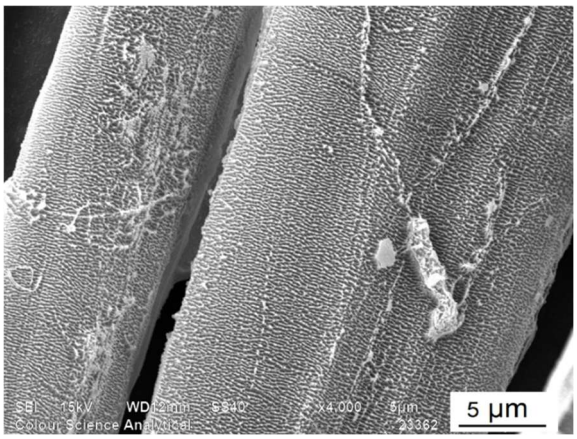

F] P40Hz t600s

Figure 4.4 SEM micrographs showing the surface morphologies of the untreated P1 hemp fibreand the argon plasma treated P1 hemp fibre at different powers (Hz) and treatment times (s) at magnifications of ×2000 (micrograph 4.4B) and 4000× (micrographs 4.4A, 4.4C, 4.4D, 4.4E and 4.4F)

Plasma is known to be capable of nano-etching surfaces [171] and etching at this scale was evident in the argon plasma treated samples at ×4000 (Figure 4.4F). By

means of image analysis (Fiji Image J), the size of 'pores' on the surface of the fibres before and after argon plasma treatment was estimated. It was found that, in the untreated sample, the detectable pore structure covered a very small portion of only 0.5% of the total fibre area of 30 μm, and the mean size of these pores was 3 nm (SD: 0.04). Following argon plasma treatment, the mean pore size increased to 17 nm (SD: 0.01), with the pores covering 24% of the 30 μm fibre area shown in the SEM micrograph. With regard to the change in surface pore structure, the etchant gas, in this case, argon, evidently accelerates onto the surface with a force capable of dislodging atoms or molecules on the surface monolayer. A similar type of nano-porous surface was obtained by the action of argon gas plasma on cellulose paper [172]. In previous research carried out on the surface of diamond, with oxygen and hydrogen as source gases for plasma generation, the etching mechanism was studied using molecular dynamic simulation, and it was concluded that the etching is a layer-by-layer process involving the generation and desorption of gaseous molecules [173]. This type of layer-by-layer etching process can be visible in the micrographs, whereby an initiation in the etching is observed in the hemp fabric plasma treated for a lower treatment time of the 60s (Figure 4.4B).

When argon gas comes in contact with the electrodes in the plasma generator, they govern a type of quasi-neutrality. At this stage, the density of positively charged species and negatively charged species is equal [174]. Ar(18) is a relatively large atom when charged using high-voltage electrodes, it possesses a high potential to be ionised to form Ar^+. Typically, the velocity of travel of an Ar^+ ion is approximately 800m/s [174]. Thus, argon gas plasma can be considered to be in a state of high entropy and highly rapid Ar^+ ions, on reacting with the amorphous or semi-crystalline or crystalline regions present in the hemp fibres, may dislodge atoms and molecules present on the surface monolayer, resulting in an etched surface. Kortshagen et. al has postulated a detailed explanation of the mechanism of nonthermal plasmas [174]. Thus, with reference to the SEM images shown in Figure 4.4, it can be postulated that plasma preferentially etches the amorphous or semi-crystalline regions of the surface monolayer. Such a change in the surface morphology of the fibres may be expected to modulate interfacial properties such as water droplet interaction and, consequently, surface-wetting behaviour.

4.3.2 Chemical properties of hemp before and after argon plasma treatment

In order to investigate the alterations induced in the chemical structure of cellulose, both the untreated and argon plasma treated hemp fabrics were subjected to analysis via ATR-FTIR spectroscopy and Raman spectroscopy.

4.3.2.1 Fourier-transform infrared spectroscopy of hemp fabrics

Prominent peaks corresponding to the stretching vibration of functional groups, namely -OH, -CH and -C-O can be observed within the frequency range of 3500 to 3000 cm^{-1}, 2900 cm^{-1} and 1200 to 1000 cm^{-1} respectively [175]. Figure 4.5 shows the FT-IR spectra pertaining to the untreated hemp fabric and the hemp fabric plasma treated for 600s with 40Hz of power.

In Figure 4.5, the blue FTIR spectrum refers to the P1 fabric (see Table 4.2 for sample details) after argon plasma treatment for 600s at 40Hz power. Sharper peaks of functional groups such as -OH (hydroxyl), corresponding to 3000 cm^{-1} and 2900 cm^{-1} wavenumbers are seen. C-H bond stretching vibration at a wavenumber of 1500 cm^{-1} and a sharp peak at 1600 cm^{-1} can be attributed to the bond vibration of C=O (carbonyl) [176] [177]. The distinct peak of the carbonyl group may have resulted from oxidation induced by the argon plasma. Additionally, the sharp peak at 1000 cm^{-1} corresponds to the vibration of -C-O- group of secondary alcohols and ether bonds within cellulose. There are noticeable alterations in the absorption envelope within these regions of the spectrum, following plasma treatment, suggesting possible modifications to the interaction of the -C-O-vibrational groups.

Following argon plasma treatment for 600s at 40Hz of power, the intensity of -OH, -C=O and -C-O- bond vibration increases leading to prominent sharp peaks associated with polar groups. The presence of these surface active polar groups indicates a strong reactivity of the surface-treated fabric towards dyes. Moreover, it can be hypothesised that after plasma treatment of hemp fabric, the inter and intra-molecular hydrogen bonding in the cellulose molecule was weakened leading to an etched surface and an enhancement in hydrophilicity.

The wetting behaviour of fabric is closely linked to the presence of polar groups on the constituent fibre surfaces, which play a role in attracting water molecules and facilitating liquid spreading through capillary action. The presence of these polar groups signifies that a higher surface energy is to be expected [178]. Concerning

argon plasma treated hemp fabrics, it is apparent that plasma treatment induced a physiochemical modification to the fibre surfaces by increasing the density of polar groups. In a study on oxygen plasma treated carbon nanotubes (CNTs), the wettability of the CNTs increased following plasma treatment because of the surface etching combined with the functionalisation of the CNTs by oxygen plasma [179].

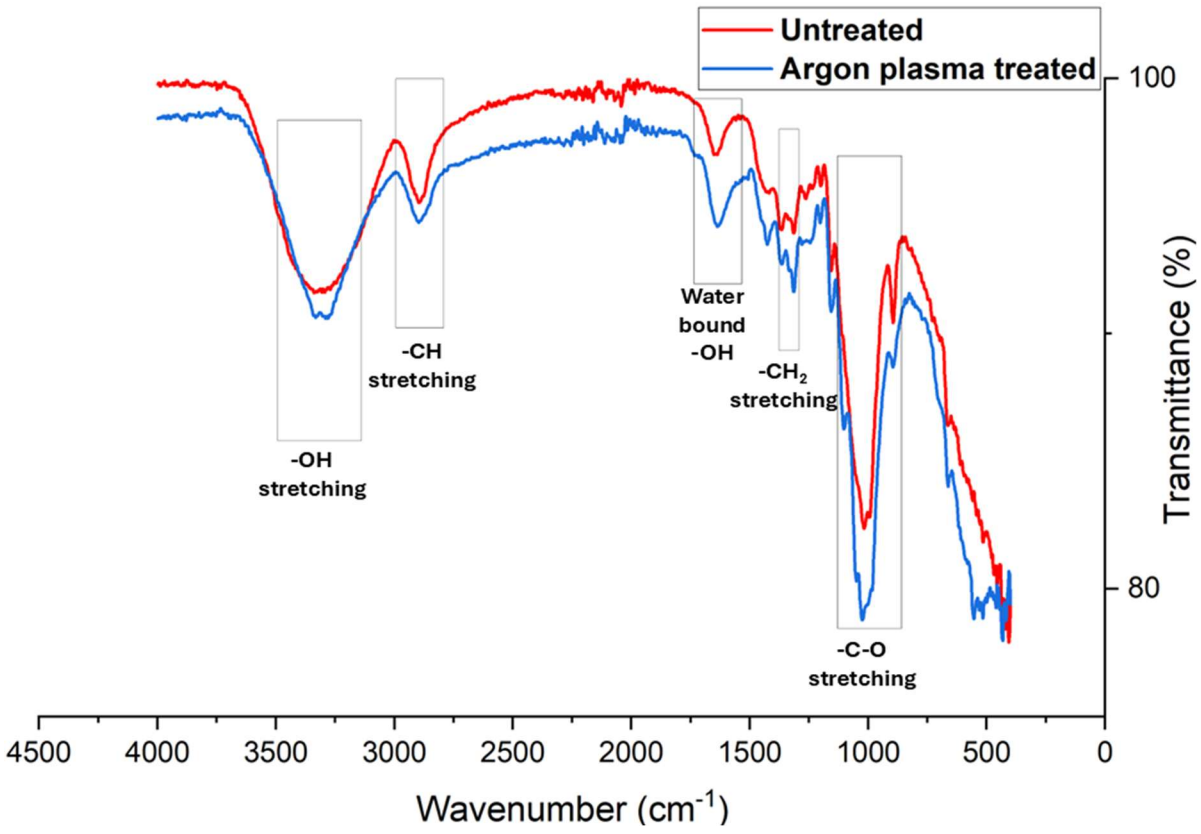

Figure 4.5 FT-IR spectroscopy of P1 hemp fabric before and after argon plasma treatment for 600s at 40Hz of power

4.3.2.2 Raman spectroscopic analysis of argon plasma treated hemp

Raman spectroscopy provides a non-destructive means of identifying surface modifications in textile fabrics. It enables the detection of chemical alterations in surface-modified cellulosic fibres, providing insights into molecular interactions, crystallinity and chemical structure [180]. In Raman spectroscopy, polar molecules with a dipole moment can be detected as they are polarised by a high-energy laser source. To discern the mechanism of plasma penetration and its interaction with either amorphous or crystalline cellulose, Raman spectroscopy was performed on hemp fabrics before and after argon plasma treatment. The frequency of bond vibrations in a Raman spectrum is influenced by the mass of a molecule. To validate the hypothesis

of plasma penetration into the surface monolayer, thereby inducing changes in the masses of surface molecules, Raman spectroscopy was conducted on P1 hemp fabrics treated with argon gas plasma for 600s at 40Hz power. A distinct Raman shift is visible in Figure 4.6A, where the Raman fingerprint spectrum of untreated P1 fabric in black noticeably differs from that of the plasma treated P1 hemp fabric shown in red. The vibrational and stretching frequencies present within the cellulose molecule are manifested in the peaks spanning the range of 1000 cm^{-1} to 2000 cm^{-1} corresponding to the -C-C-C-, -C-C-O-, -C-O-C-, and -C-OH, bonds in the α-D-glucopyranose ring [181].

In the Raman spectra (Figure 4.6), the profound change in peak height is notably observed within the wavelength interval of 0 cm^{-1} to 750 cm^{-1}. These peaks denote the presence of -C-H bending vibration at 330 cm^{-1}, C-O stretching at 490 cm^{-1} and -OH bending of absorbed water molecules visible within the frequency range of 500 cm^{-1} to 650 cm^{-1}. In the case of the plasma treated hemp, a prominent Raman shift is observed with decreasing peak height. This observation suggests that plasma treatment is capable of dehydrating the hemp fibres and can be detected between the wavelength range of 1600 to 1700 cm^{-1} which is the CH_2O bending mode [182].

In Figure 4.6A, a prominent difference can be observed in the frequency range spanning 0 to 600 cm^{-1}. This difference is characterised by a decreasing intensity of bond vibrations in the Raman spectra of the plasma treated hemp, suggestive of alteration in the surface energy [121]. Figures 4.6B and 4.6C showcase the Raman spectrum of plasma treated hemp and untreated hemp fabric across the wavelength frequency range spanning 0 to 1000 cm^{-1}. In spite of plasma treatment, the functional groups inherent to cellulose remain unaltered as observed in Figure 4.5. Noteworthily, Raman shifts are discernible in plasma treated substrates, these vibrations are clearly seen in the Raman spectra belonging to the region of 1200 to 1500 cm^{-1} [182] indicating the presence of acid (-COO) or -C=O (carbonyl) on the surface monolayer. Below 900 cm^{-1}, complex vibrational modes corresponding to C-C-C, C-C-O, C-O-C, O-C-O and C-O-H are detected on the surface of the plasma treated hemp fabric [183]. The shifts in hydrogen bonding are discerned in Raman spectroscopy as peaks transition beyond the 3000 cm^{-1} realm [184]. This phenomenon occurs due to the challenging polarisation of inter and intra-molecular hydrogen bonds in cellulose primarily due to steric hindrance. Additionally, the vibrational frequency of the hydrogen atom changes as it interacts with an electronegative atom like oxygen. Referring to Figures 4.5 and 4.6, it appears that H-OH bonds on the surface monolayer

of the hemp fabric are impacted, leading to the emergence of sharp peaks associated with -OH groups in the IR spectrum and the absence of H_2O bending mode in Raman spectroscopy. This suggests the hypothesis that Ar^+ atoms generated by plasma are capable of cleaving the inter- or intra-molecular hydrogen bonds in cellulose present on the surface monolayer or hemp.

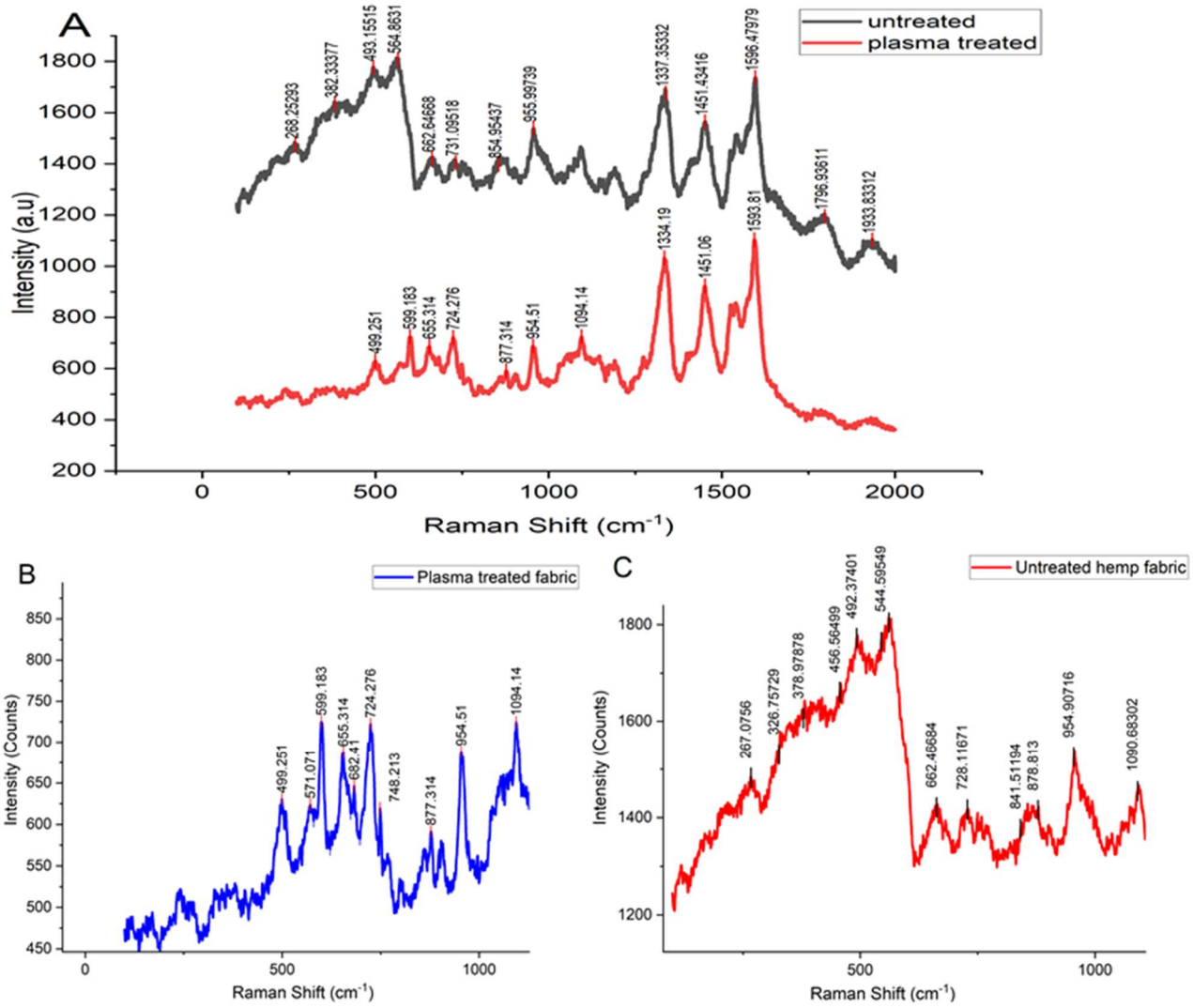

Figure 4.6 A) Raman spectroscopy of P1 hemp fabric before and after argon plasma treatment for 600s at 40Hz power; B) Raman shift in P1 hemp fabric after plasma treatment for 600s at 40Hz power ranging from 0 to 1000 cm^{-1}; and C) Raman shift in P1 hemp fabric in the untreated state ranging from 0 to 1000 cm^{-1}

4.3.3 Wetting characteristics of hemp fabrics after plasma treatment

Water droplet contact angle measurements were made on the H, P1 and P2 hemp fabric samples to assess their surface wettability before and after argon plasma treatment. In their untreated states, all the fabrics exhibited partially hydrophobic ($\theta=60°$) wetting characteristics, evident by the presence of a stable water droplet on the fabric surface, with no lateral spreading. Water droplets on the surface resided for at least 20 min before measurement was concluded. By contrast, argon plasma treatment led to a marked change in hydrophilicity and wettability, with a water droplet contact angle of $\theta=0°$. Lateral liquid spreading was evident in all three argon plasma treated hemp fabrics following wetting, with wetting occurring within >1s from the moment that the droplet made contact with the surface. It was reasoned that argon plasma treatment initiates surface etching (section 4.3.1), thereby increasing the surface energy and contributing to a reduction in the water contact angle. Figure 4.7 illustrates the water contact angle measurements for hemp fabric samples (P1) subjected to plasma treatment for a duration from 0s to 600s based on three replicates for the H, P1 and P2 fabric samples. Line fit curves in Figure 4.7 marked in blue and red for P1 hemp fabric samples treated at 40Hz power and those treated with 80 Hz power follow a decay-type curve. With an increase in plasma treatment duration, a marked decrease in water contact angle is observed and a constant water contact angle of θ=0° is obtained after plasma treatment for a duration of 600s.

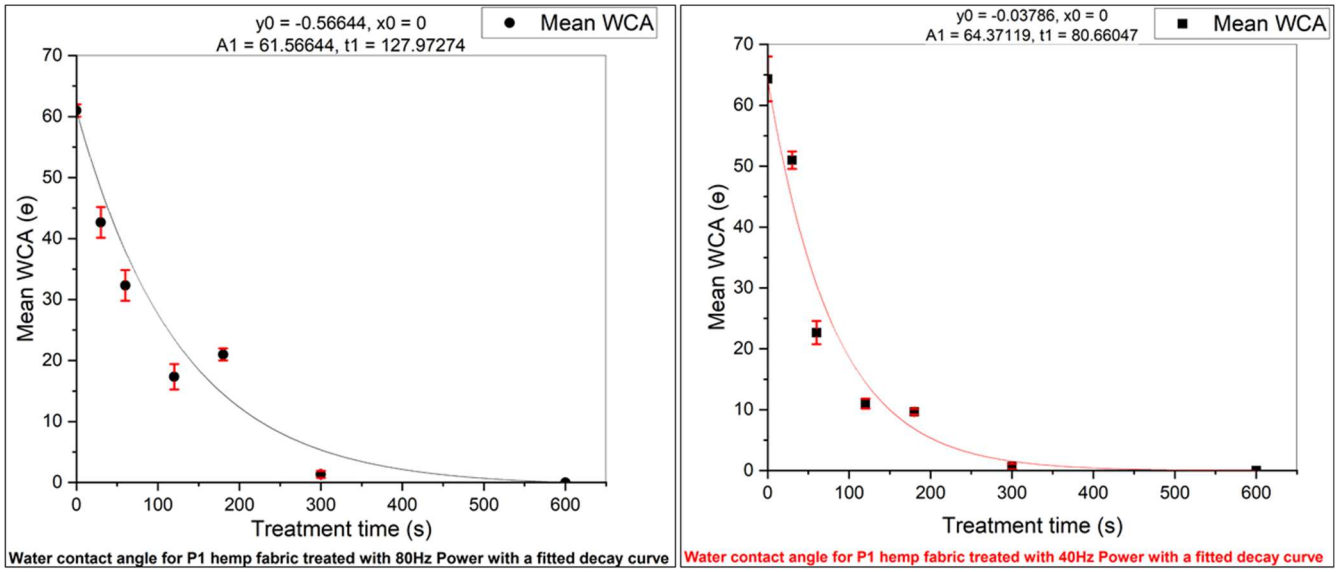

Figure 4.7 Change in fabric water contact angle with the duration of argon plasma treatment

Surface morphology is known to influence wetting characteristics. The role of surface free energy is of key importance in wetting behaviour and the relation is described by

Young's equation for ideal surfaces in which the surface morphologies considered are for smooth surfaces. Following plasma treatment, if a non-ideal smooth surface is modified into a roughened surface, the modified Cassie-Baxter theory can be applied to theoretically analyse the wetting behaviour. Taking into consideration all three models namely, Young's model, Wenzel's equation and Cassie-Baxter theory, it was found that the degree of surface roughness controls the wetting behaviour because of its influence on free energies between the solid-vapour and the solid-liquid phases [185] [186].

Water is a polar liquid possessing a number of forces, specifically London force, dispersion forces and hydrogen bonding. When a droplet of water is applied onto the interfacial monolayer of a fibre surface, attractive forces exist in the phase with higher surficial energy. The interaction between the two phases depends upon the type of individual forces present [187]. Therefore, it can be hypothesised that the increased hydrophilicity observed in argon plasma treated hemp is a consequence of a modulation in fibre surface topography, combined with the increase in the attractive forces of the fibre surface monolayer [188] [151]. Previous research examining the modification in the surface energy of inert materials such as polypropylene following plasma treatment serves as a reference, suggesting that Argon gas plasma has the capability of enhancing the surface energy of the substrate [189]. The extent of surface modification is contingent upon the duration of argon plasma treatment. Consequently, the reduction in water contact angle in a hemp fabric is affected by the duration of argon plasma treatment. Surface modification is notably enhanced with a longer plasma treatment duration as illustrated in Figure 4.4. This is because of an increase in surface etching with pores up to 17nm being formed following plasma treatment.

4.3.4 Influence of argon plasma treatment on the dyeability of hemp

To examine the potential change of the dyeability of hemp fibres following argon plasma pretreatment, both untreated and treated hemp fabrics were dyed using fibre-reactive and vat dye types (Figure 4.2). Fibre-reactive dyes were selected to explore the hypothesis of an increase in the extent of covalent bonding of cellulose surface molecules after plasma treatment. To further explore any potential alteration of bonding sites following argon plasma treatment, hemp fabrics were also subjected to dyeing with vat dyes.

4.3.4.1 Hemp fabrics dyed using fibre-reactive dyes

The impact of argon plasma treatment on H, P1 & P2 hemp fabric, dyed using fibre-reactive dyes was evaluated through the analysis of colour space values. Table 4.3 displays the outcomes of colour space analysis, encompassing L*(brightness), a* (redness or greenness), b* (blueness or yellowness) and K/S (colour strength) for the dyed P1 hemp fabrics that underwent argon plasma treatment under variable conditions. Significantly, the colour strength of the dyed, argon plasma treated hemp increased compared to the untreated hemp fabric. Similarly, the colour strength of the dyed hemp fabrics following a pyridine stripping test was measured and is represented in Table 4.4. It is evident that the colour strength of the untreated hemp fabric after pyridine stripping was markedly lower, indicative of reactive dye being removed by pyridine stripping. However, as the duration of plasma treatment increases, the reactive dye becomes more resistant to washing off, resulting in higher K/S values. This is because of the chemical functionalisation of the surface polymer chains. Ar^+ plasma is capable of generating oxygen-rich groups like -OH following a free radical mechanism [190]. Hence, a greater concentration of hydroxyl groups can contribute to the formation of strong covalent dye-fibre bonds. Upon comparing the data in Table 4.3 and Table 4.4, it becomes evident that the argon plasma treatment strengthens the dye-fibre bonding by making it more resistant to strong alkali as indicated by the similar K/S values before and after pyridine stripping reaction of dyed, plasma treated hemp fabrics.

The effect of plasma treatment on K/S and L* can be seen in Figure 4.8A and Figure 4.8C. Figure 4.8A illustrates that the K/S value increases with extended treatment time, while Figure 4.8C demonstrates that L* increases with higher power (intensity) during plasma treatment. The interaction plots in Figure 4.8B and Figure 4.8C suggest that plasma treatment facilitated an efficient colouration of fabric, particularly in cases where the fabric had a lower yarn count compared to those with densely woven structures. In comparison to the P1 and P2 fabric types, the fabric type H has a herringbone type of weave. Referring to the interaction plots in Figure 4.8B, it is evident that the K/S values for H type sample increased after argon plasma treatment. This can be attributed to the herringbone weave structure, which comprises half warp and half weft yarns, giving a broken twill effect. Consequently, employing a much longer plasma treatment duration can lead to a more enhanced colouration of the herringbone weave [191].

Sometimes, the presence of surface roughness on a fabric can contribute to optical reflection, creating an impression of a deeper coloured dyeing. A rough surface scatters light diffusely, potentially creating a matte-like effect [192]. The colour strength, representing the ratio of the absorbed light to the incident light, is a critical parameter. Therefore, it can be inferred that the observed increase in colour strength is not an effect of optical reflection but is due to the enhanced dyeability of the fabric.

It was hypothesised that plasma treatment improves the diffusion of reactive dyes, which could primarily be due to enhanced penetration of the dye facilitated by the increased surface energy. Such a change in surface energy plays a vital role in facilitating the formation of a strong covalent bond between the dye molecules and cellulose molecules [193]. Furthermore, plasma treatment is observed to result in surface etching as evidenced in SEM micrographs (Figure 4.4). This has effected in the formation of a nano-porous structure, which in turn leads to an increase in surface area of the fabric [194]. As noted by Rattee et al., various factors influence the physical chemistry of dye adsorption, among which surface area plays a critical role. An increase in surface area enhances the uptake of reactive dyes, leading to more uniform dye fixation. This, in turn, results in improved visual attributes of the fabric, such as increased brightness and lustre.

Power (Hz)	Treatment Time (s)	L^*	a^*	b^*	K/S (420nm)
0	0	77	2	14	0.6
40	300	65	28	72	16

Table 4.3 L*, a*, b* and K/S values of the dyed P1 hemp fabrics

Power (Hz)	Treatment Time (s)	K/S (430nm)
0	0	0.2
40	300	12

Table 4.4 Colour strength of the dye-stripped fabrics

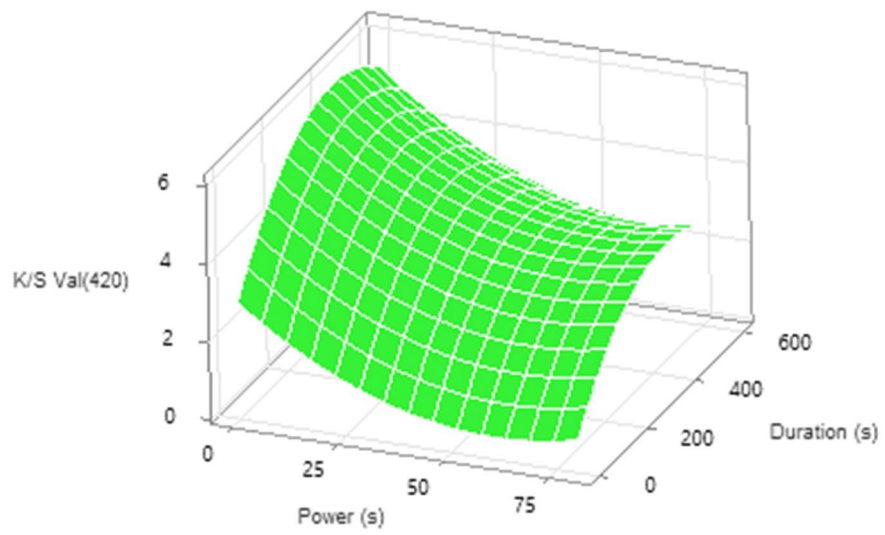

A Surface Plot of K/S Val(420) with treatment time (s) and power (Hz)

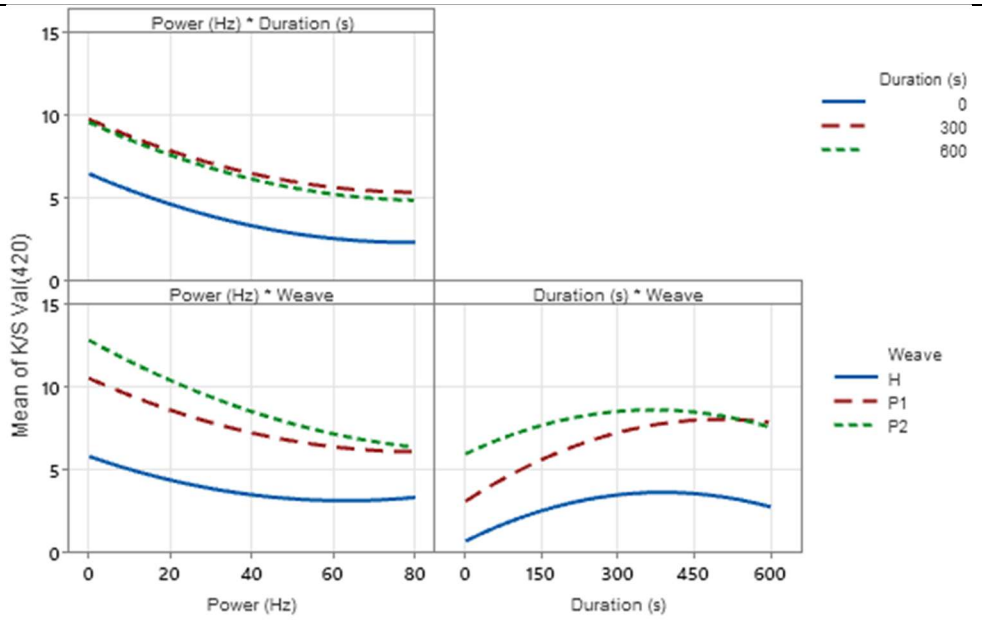

B Interaction Plot for K/S Val(420) with power (Hz) and treatment time (s)

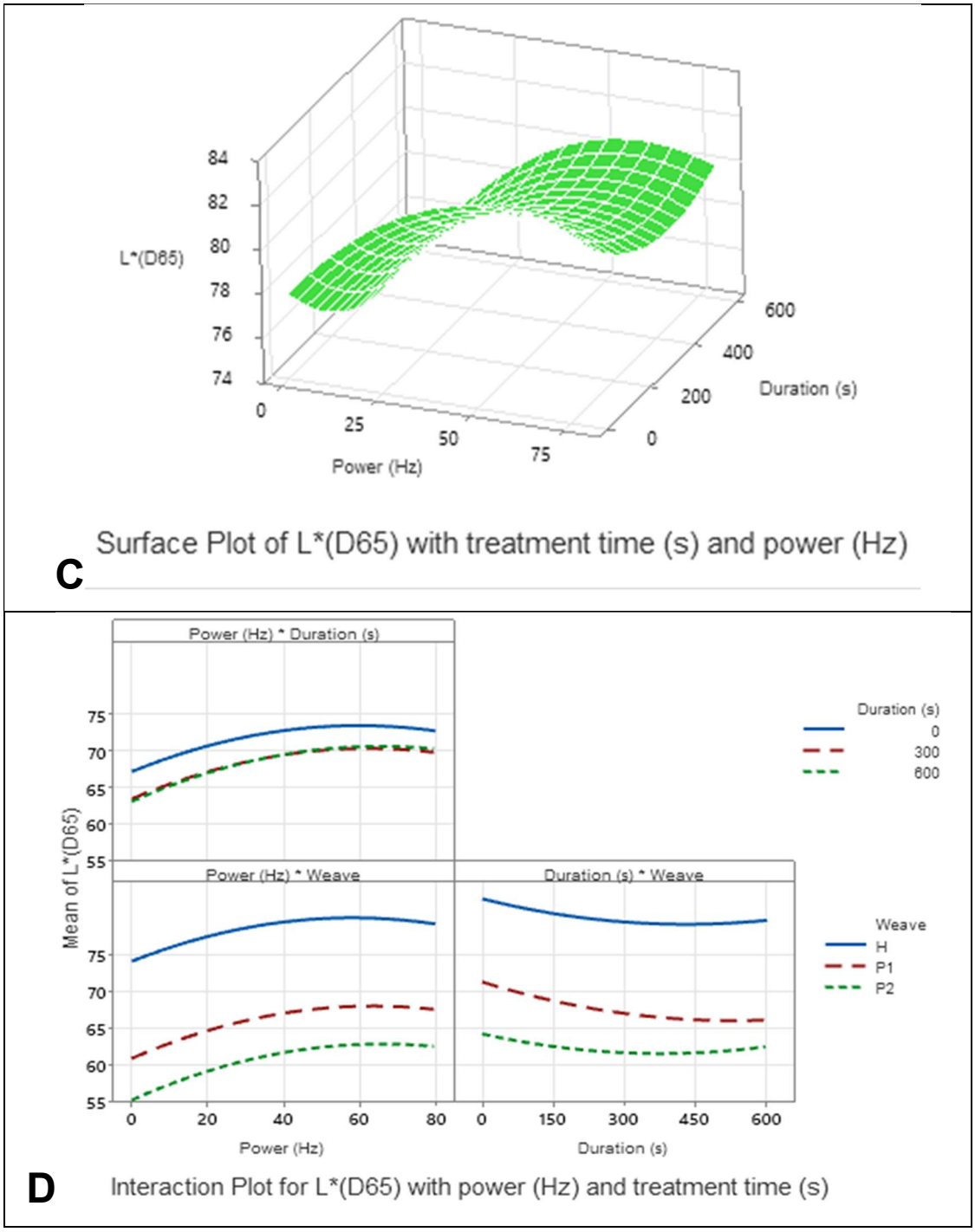

Figure 4.8 The influence of argon plasma treatment parameters (treatment duration and power) on the colour strength (K/S) and brightness (L*) of hemp fabrics dyed with fibre-reactive dyes

Figure 4.9 provides a factorial analysis of the increased colour strength resulting from reactive dyeing on both untreated and argon plasma pretreated hemp fabric. The Pareto chart indicates power (Hz), and weave type have similar impacts on enhancing colour strength. Therefore, it can be concluded that power is a crucial factor that

influences the increased colour strength after reactive dyeing of plasma pre-treated hemp. The statistical analysis for the K/S (colour strength) under the plasma treatment conditions has a standard deviation of 2. The Pareto chart of standardised effects clearly identifies five statistically significant terms: A(Power), B(Treatment time), C (Weave) and two interactions, AC (Power × Weave) and CD (Weave × Gas), all surpassing the critical t-value threshold of 1.965. This suggests that these factors have a meaningful impact on dye uptake or colour depth, with the type of weave and the plasma power being the most influential. The main effects plot supports these findings, where pronounced changes in K/S are observed across varying levels of power, weave, and duration, particularly showing increased K/S values with longer duration and specific weave types. These results collectively demonstrate that, under minimal variability, plasma treatment effectively influences K/S values in reactive dyeing. The analysis of the L* (lightness) response under a higher standard deviation of 3 reveals a significantly variable model. The Pareto chart of standardised effects indicates that none of the factors or interactions surpass the significance threshold (t = 1.965), implying that no single plasma treatment factor independently exerts a statistically dominant effect on lightness. This is further illustrated in the main effects plot, and is true because K/S is a measure of optical density and L* (lightness) is a colour space component representing the brightness of the dyed fabric.

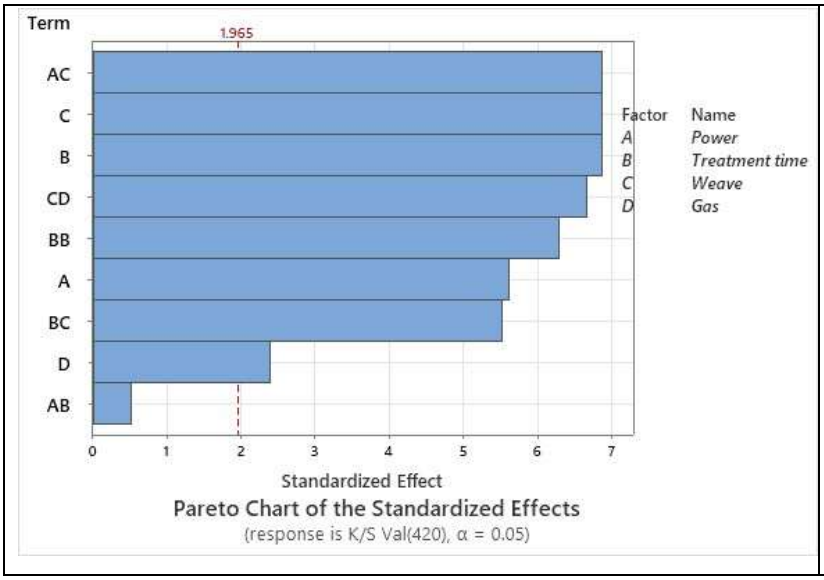

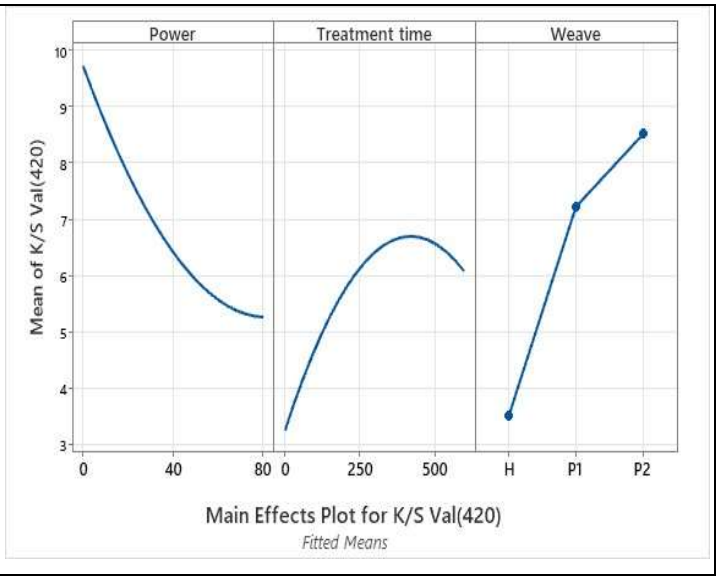

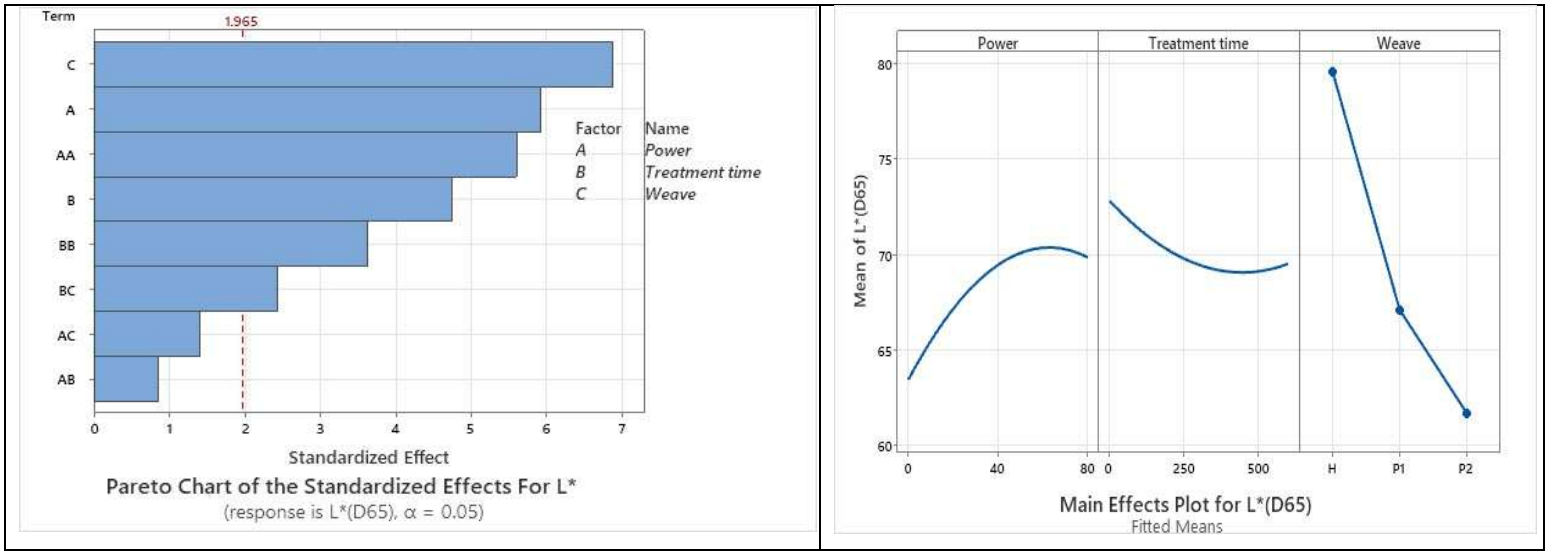

Figure 4.9 Statistical analysis of reactive dyeing using surface response model

4.3.4.2 Hemp fabrics dyed using vat dyes

The impact of argon plasma treatment on the vat dyeing process of hemp fabric was assessed through colour space analysis, and the results are presented in Table 4.4. Notably, the colour strength of the argon plasma treated hemp fabric with a K/S of 22 demonstrates a substantial increase compared to untreated hemp fabric which has a K/S of 6.4.

Figures 4.10A and 4.10C reveal the effect of factors, such as treatment time and power, on the colour strength and the brightness of the dyed fabric. It is evident that, as the duration of plasma treatment is extended, the colour strength of the dyed fabric increases. Similarly, higher plasma power values led to increased fabric brightness. The interaction plots in Figure 4.10B and Figure 4.10D indicate the influence of plasma treatment on the reactivity of hemp towards vat dye molecules. These plots suggest that longer duration and higher power settings in plasma treatment enhance the reactivity of the fabric with vat dye molecules.

It could be considered that the gain in surface energy and concurrent increase in overall surface area due to the change in surface fibre morphology, following plasma treatment, facilitated an enhanced attachment of vat dye molecules to the surface of hemp fibres [189]. A similar increase in the colour strength of vat-dyed cotton was

observed following a surface treatment using ultrasound and microwave treatments [195].

Plasma Parameters		Colour Space Analysis			Colour Strength
Power (Hz)	Treatment time (s)	L* (D65)	a* (D65)	b* (D65)	K/S (510nm)
0	0	37	42.1	20.5	6.4
40	300	47	46	13.5	18
80	300	54	44	3	22

Table 4.5 Colour space analysis of P1 hemp fabrics dyed using vat dye

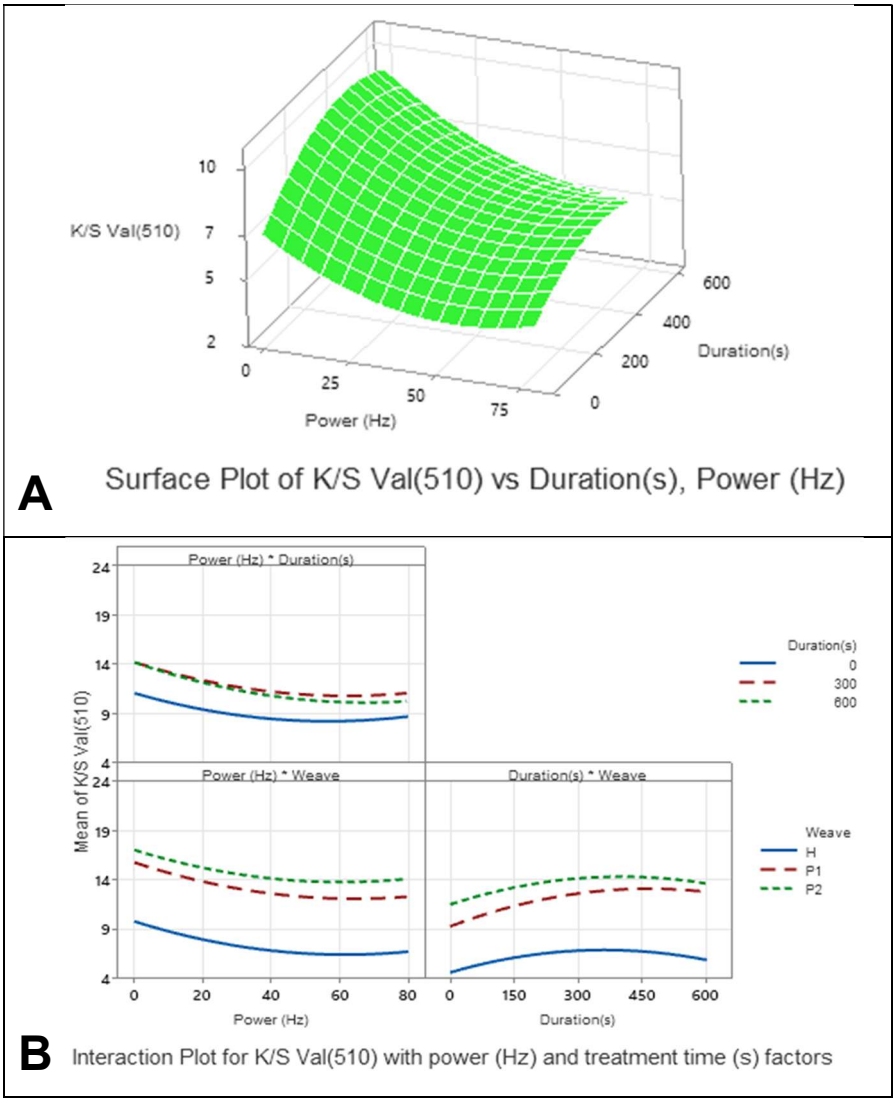

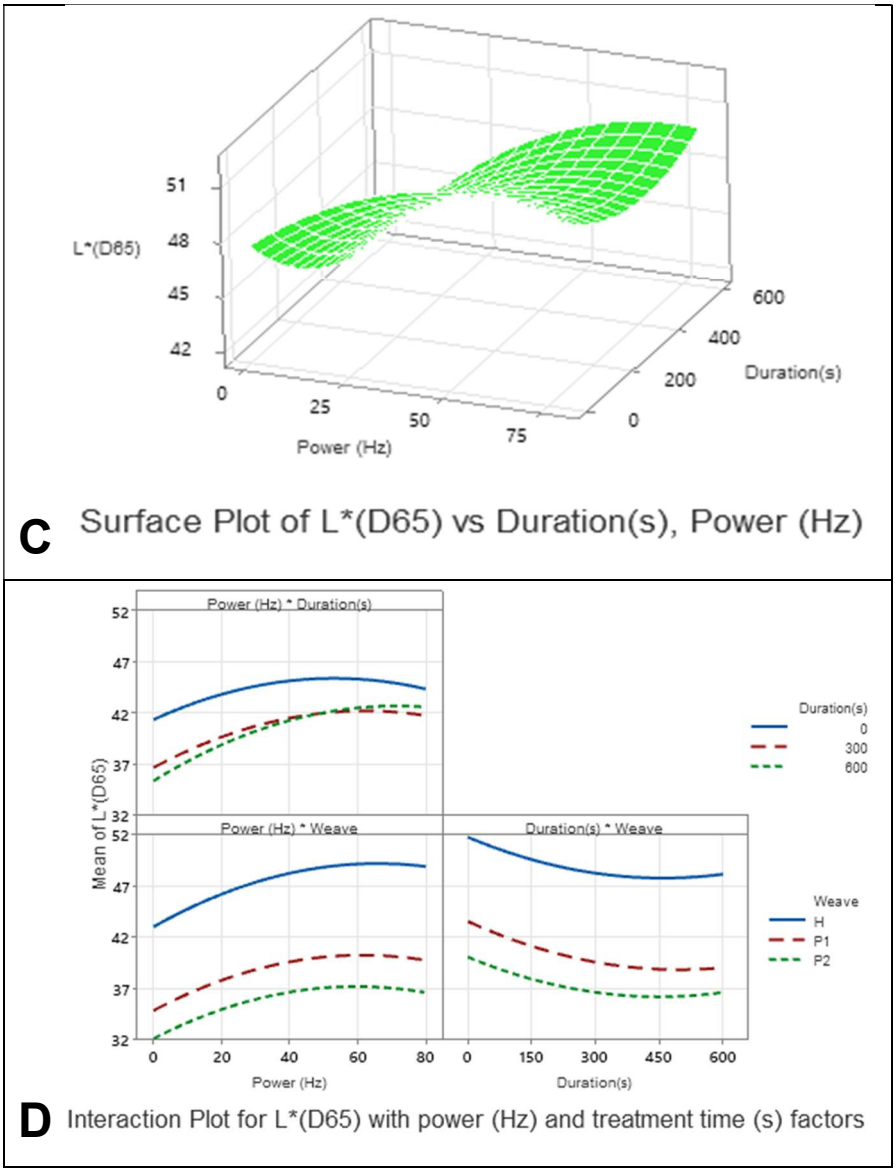

Figure 4.10 The influence of argon plasma treatment parameters (treatment duration and power) on the colour strength (K/S) and brightness (L*) of hemp fabrics dyed with vat dyes

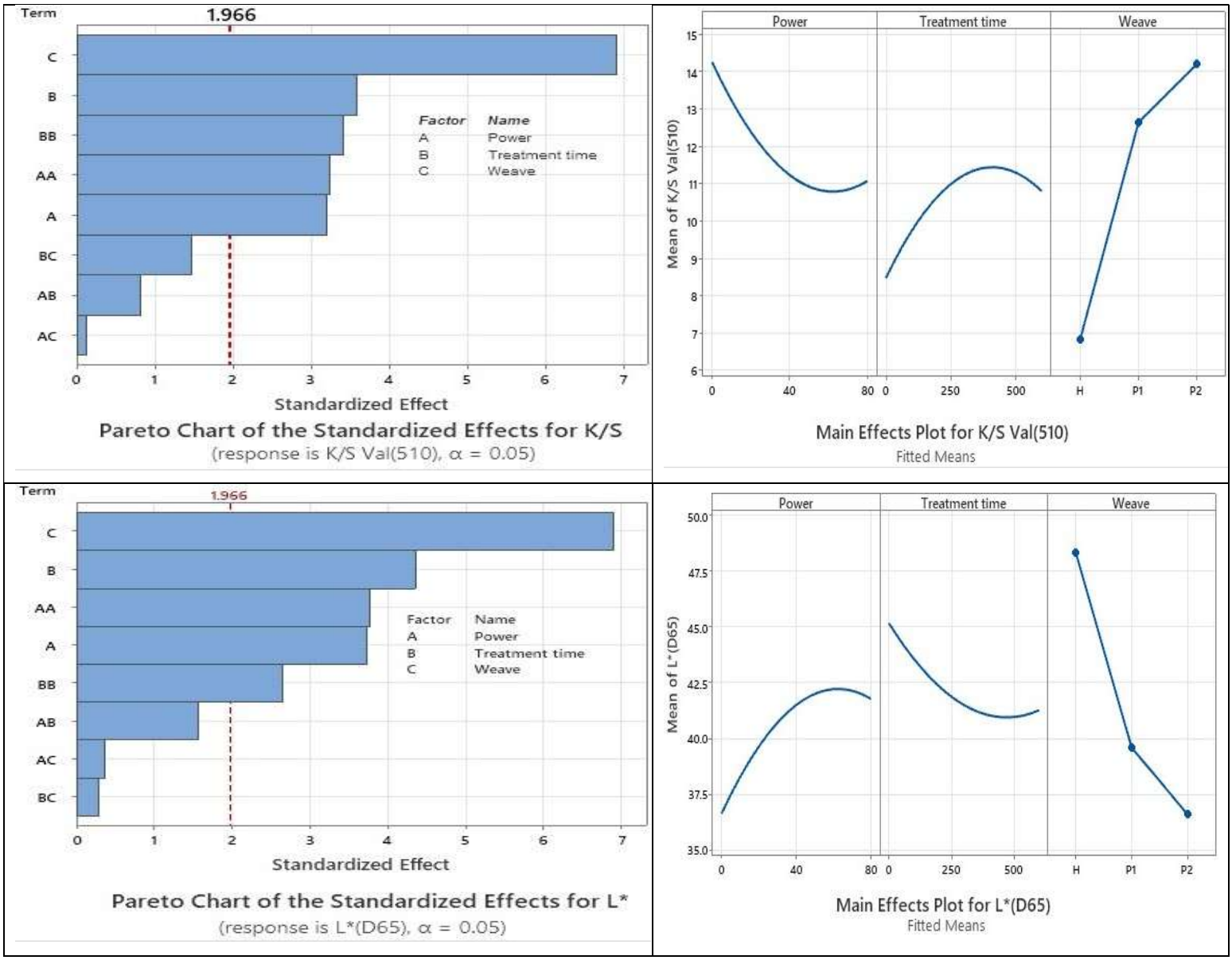

Figure 4.11 Statistical analysis of vat dyeing using surface response model

Figure 4.11 is a factorial analysis that explains increased colour strength following vat dyeing. Factors such as power (Hz), treatment time(s) and the weave type collectively enhance the colour strength. The main effect plot highlights the influence of each factor after vat dyeing of H, P1 and P2 hemp fabrics. Consequently, it can be concluded that the effectiveness of argon plasma pretreatment significantly depends on the weave type and duration of argon plasma treatment. The statistical analysis of the K/S (colour strength) indicates a standard deviation of 3, suggesting a small degree of variation. The Pareto chart of standardised effects identifies four terms that exceed the critical t-value threshold of 1.966, indicating statistical significance for

treatment time and weave. The quadratic term for Power in the Pareto chart (Power × Power) suggests that power input has a nonlinear and strong influence on the dye uptake. The main effects plot reinforces this, showing a positive slope for Power, where an increase in power leads to greater K/S values, while duration and weave have comparatively milder effects. According to the coded coefficients, Power has a significant positive coefficient (-1.586, p = 0.002), confirming its crucial role. L* (lightness) for vat dyed fabrics indicates a higher standard deviation of 4 indicates a weaker influence of plasma treatment factors on L*. The Pareto chart of standardised effects shows that Weave, treatment time and Power × Power(AA) factor crosses the critical significance threshold (t = 1.966), indicating that the three factors have contributed their effects in the modification of L* after argon plasma treatment. Thus, it can be concluded that plasma treatment increases the colouration properties of hemp fabric.

4.4 Conclusions

Low-pressure argon plasma pretreatment of hemp fabrics enhances the colour strength that can be achieved in reactive and vat dyeing. This is attributed to morphological and physiochemical changes to hemp fibre surfaces, specifically nano-etching and an increase in the density of polar groups, which increases aqueous wettability.

Based on the FTIR analyses of the argon plasma treated fabrics, distinct carbonyl (C=O) peaks have been observed at 1500 cm^{-1} signifying oxidation induced by argon plasma. Furthermore, sharper polar group peaks were evident indicating a physiochemical alteration of the substrate. A prominent Raman shift has been observed within the frequency range of 0 cm^{-1} to 1000 cm^{-1} implying a shift in the surface energy of the fibres after argon plasma pretreatment. Moreover, the water contact angle measurements confirmed an increase in the surface energy following argon plasma treatment and the hydrophilicity of hemp gradually increases with longer plasma treatment duration. The morphological modifications using argon gas plasma include the development of a nano-porous fibre surface associated with progressive dry etching. Such a nano-porous surface contributes to an increase in the available surface area for improved dye adsorption. Moreover, the change in surface energy of plasma treated hemp promotes the formation of strong covalent bonds with reactive dye molecules, while also facilitating the attachment of bulkier vat dye molecules to the fibre surfaces.

Given the challenges associated with the colouration of hemp, argon plasma pretreatment represents a potentially valuable means of preparing hemp fabrics for dyeing to maximise colour strength without liquid pretreatments, heating, or the use of auxiliary chemicals. This approach holds promise for addressing some of the limitations and environmental impacts associated with conventional dyeing and wet treatment of hemp fibres to magnify its commercial value. Argon gas plasma treatment offers a method to uniformly dye the hemp fabric by reducing overall treatment time and temperature required for dye-fibre fixation.

Hemp fabrics possess complex surface chemistry and the induced surface modification through low-pressure plasma treatment was detected after colouration of fabrics. Although this study provides significant insights, further investigations on fibre surface topography and surface energy employing specialised analytical equipment would be beneficial in establishing the detailed mechanism involved in the interaction between Ar^{+} plasma and hemp fibres.

Chapter 5

Study of hemp fibre properties modified via long duration low-pressure argon and oxygen plasma treatments

5.1 Introduction

Hemp is a lignocellulosic fibre used in fibre-reinforced composites, technical textiles, and clothing with surface properties that can be modified by plasma to improve processability. In contrast to previous studies reporting the effects of short duration plasma treatment (<10 min), this paper investigates the effects of extended (30 min - 4 h), low-pressure (~0.4 mbar) argon and oxygen plasma treatments on dew retted hemp fibres at varying power levels (40 Hz and 80 Hz). Scanning electron microscopy (SEM) revealed marked surface fibre etching after prolonged treatment, with argon plasma inducing fibrillation and heterogeneous motifs, while oxygen plasma yielded irregular morphologies. Atomic force microscopy (AFM) confirmed a near four-fold rise in surface roughness (70 nm to 270 nm) after 4 h of plasma treatment. All plasma-treated fibres exhibited complete wetting (water contact angle θ=0°) versus θ=62° for untreated controls, based on drop-shape analysis and tensiometry. Fourier-transform infrared spectroscopy (FT-IR) revealed no major chemical shifts, although sharper -OH and -C=O peaks suggested a subtle physicochemical change. X-ray diffraction indicated slightly enhanced crystallinity without crystallite size alteration. Fibre tensile strength remained unaffected across treatments. Fluorescence microscopy suggested a degree of lignin removal, evidenced by reduced surface fluorescence after 4 h of argon plasma treatment. Thus, long duration argon and oxygen plasma treatments distinctly modify hemp fibre surfaces, without substantially altering internal chemistry or crystallinity. These findings highlight plasma treatment as an alternative to wet chemical methods for surficial hemp fibre modification, offering potential for precise surface engineering in textile applications.

Lignocellulosic bast fibres such as hemp are used to produce natural fibre-reinforced composites (FRCs), technical textiles including architectural and building products, as well as fabrics for garments [2, 31]. The attractive tensile strength (~700 – 900 MPa) [16], modulus (~75 GPa) [16] and economics of hemp fibre production have led to its resurgence in eco-conscious fashion and textile products, where the environmental impacts of fibre production, including resource extraction and emissions, are

increasingly scrutinised. Certainly, the precise environmental footprint and physical properties of hemp depend on the agricultural system and conditions used to grow the plant, as well as the fibre processing methods that follow.

To extract industrially valuable hemp fibres from plant stems for textile manufacturing, substantial pre-processing is required, including retting after harvesting. Dew retting, also referred to as field retting, is a cost-effective method where harvested hemp is left in the field for three to five weeks, allowing microbial activity to break down the pectin, hemicellulose, and lignin that binds the integral fibres. Decortication (separating the fibres from the woody core, or shiv), scutching (beating the fibres to remove any remaining woody material), and hackling (mechanical cleaning and fibre separation) are required to produce clean, high-quality fibres [35], [196].

Hemp fibre degumming is typically performed following retting, scutching, and hackling. Fibres obtained through dew retting may require intensive degumming due to residual pectin content [197]. Consequently, the choice of degumming method is tailored to the intended end-use, with chemical and enzymatic approaches commonly employed to produce high-quality textile-grade fibres [197]. Non-cellulosic impurities, mainly lignin, pectin and hemicellulose, can be removed through degumming [57] typically using chemical (normally alkali) [198], enzymatic or eutectic solvent methods [59] [61]. After degumming, hemp fibre comprises mainly cellulose by mass (65%-75%), but residual impurities such as lignin are still present (~9%) axially distributed within the fibre, along with hemicellulose (~20%), pectin and fats, which comprise 3% of the total. During subsequent processing, these impurities adversely affect surface properties such as liquid wetting. However, while lignin removal improves wettability, it often compromises fibre strength, and significant variability in fibre length, diameter, and surface characteristics persists [16], [199], [104]. Strategies for lignin removal include alkaline treatment, oxidative treatments and enzymatic treatments, which can be harnessed to reduce fibre diameter. Cottonisation further reduces fibre diameter, enabling the spinning of fine yarns for textile fabrics suitable for clothing. For the cottonisation of hemp fibres, various methods can be employed, including the use of deep eutectic solvents, urea-etidronic acid treatment, and soda-lye scouring [25]. The combination of deep eutectic solvents and microwave energy enhances impurity removal and enables the efficient extraction of pure cellulose from hemp fibres. In contrast, soda-lye scouring not only refines the fibres but also imparts inherent flame-retardant properties [200, 201]. Deep eutectic solvent (DES) treatments can reduce fibre tensile strength due to the removal of non-cellulosic components such as lignin

and hemicellulose, potentially rendering the fibres more brittle [202]. While DES processing can enhance specific properties desirable for textile applications, it may also compromise structural integrity and alter chemical composition. Therefore, careful optimisation of treatment parameters is essential to balance performance gains with mechanical durability, depending on the intended end use. These wet processes aim for 70-100% delignification, but the processes are associated with significant resource consumption and chemical effluents [199].

Wet oxidation, hydrothermal treatment and steam explosion can also increase the cellulose content in the fibre by up to 15% [203]. Additionally, esterification, alkalisation, silane treatments and UV treatments have been identified as advantageous for improving the mechanical properties of hemp fibre [16]. While aqueous pretreatment methods for hemp are highly effective in removing impurities and increasing the cellulose content, they utilise significant quantities of water, chemical reagents, and energy, having significant effluent management requirements. An alternative approach that obviates the need for wet chemistry and associated drying is therefore attractive if valuable modifications to the fibre surface can still be obtained.

Previously, oxygen [204], atmospheric air [98], nitrogen [205], or argon [150] gas plasma treatment of hemp has been reported as ‘dry’ means for modifying fibre properties such as wetting, chemical functionalisation, and surface cleaning [106]. Sameer et al., treated ramie fibres with atmospheric air plasma for short durations ranging from 60 to 240 s, resulting in significant nanotexturing of the surface. This reduced the water contact angle from 50° to 30°, improving wettability, while the chemical functional groups of cellulose in the fibres remain unaffected [206]. Another study by Biljana et al. examined the sorption properties of hemp fibres treated with atmospheric air plasma for 120 s at different power levels (40W and 80W). A substantial increase in wettability was observed without any significant changes to the chemical or morphological properties of the fibre [27]. A further study on the surface modification of 100% hemp woven fabrics using low-pressure argon plasma revealed nano-etching of fibre surfaces and enhanced wetting and dyeability, together with an increase in the number of polar groups after 10 min of treatment [19].

Plasma treatment is widely recognised for its ability to achieve dry etching [207], resulting in nanoscale surface roughness that can substantially improve both the

surface energy and the functional performance of natural fibres [208]. The formation of roughened surfaces increases the available surface area, which in turn enhances interfacial adhesion in fibre-reinforced composites and strengthens interactions with finishing agents, dyes, and chemical coatings [19]. One of the primary drawbacks of conventional wet chemical and enzymatic treatments is their tendency to compromise structural integrity, often resulting in a measurable loss of fibre strength and flexibility due to uncontrolled molecular degradation [46]. Plasma processing offers a compelling alternative, enabling the achievement of surface modification without altering the bulk fibre properties. The outcome of surface modification via plasma treatment is also strongly influenced by the type of reactive gas used; for example, the use of hexafluoroethane gas as a plasma source leads to the generation of hydrophobic surfaces. In contrast, gases such as argon and oxygen offer pathways for increasing surface polarity and hydrophilicity. Traditional lignin-removal strategies, including scouring and bleaching, frequently reduce fibre strength as a result of cellulose chain cleavage. The current study demonstrates that extended plasma treatments, particularly with argon, can reduce surficial lignin while fully retaining the tensile strength of the fibres, positioning this method as a robust alternative to aggressive chemical pretreatments. Moreover, although argon and oxygen plasmas have been individually explored in previous work, no comprehensive comparison exists evaluating their effects under prolonged low-pressure conditions. This work fills that gap by providing a systematic side-by-side analysis of the modifications in surface morphology, surface chemistry, and wetting behaviour of hemp fibres subjected to extended-duration treatments in both argon and oxygen plasma environments. A process can only be fully understood when studied across its full operational window, from short to long durations. This broad-spectrum approach not only clarifies the range of phenomenological outcomes but also lays the foundation for tailoring treatments for diverse end-use applications.

This work primarily aims to broaden the current scope of literature, which often limits hemp's application to basic garment substrates. Rather than focusing on a single end-use such as dyeing or finishing, the central objective of this study is to explore and understand the underlying mechanism of plasma-fibre interactions. By investigating the morphological, chemical, and physical changes induced through plasma treatment, we present a foundational understanding that can support a wide range of textile applications in both apparel and technical textile domains.

5.2 Experimental

5.2.1 Materials

Raw field-retted hemp fibres were procured from East Yorkshire Hemp Ltd [108] in the UK. Following dew retting process lasting six weeks, a series of mechanical processing was conducted by the supplier to yield fibre, prior to baling. The mechanical processing involved shredders to break down hemp stalk into smaller pieces, decorticator to separate the hemp fibre from the hemp shiv, and lastly, cleaning machinery to remove dust and other debris. Argon and oxygen gas cylinders (supplied by BOC Ltd.) were utilised for plasma treatment, and the gases were used without further purification.

5.2.2 Method for processing hemp fibres before plasma treatment

Retted hemp fibres from the received bale (1 kg) were mechanically opened using a laboratory scale Tatham mini PO30 fibre opener, consisting of a nipped feed roller and single cylinder opener roller, to separate the constituent fibres and remove residual shiv. The hemp fibre was fed through the fibre opening process twice to maximise the fibre separation. The opened fibre was then carded using a lab-scale, single-cylinder, worker-stripper sample card (Haigh), enabling intensive fibre disentanglement prior to web formation and production of a self-supporting sliver for plasma treatment. No additional scouring or chemical pre-processing of the baled fibre or sliver was performed to ensure satisfactory detection of the effects of plasma treatment.

5.2.3 Plasma treatment of hemp sliver

Research-grade pure argon and oxygen gasses were used as a plasma source for the treatment of hemp fibre samples. A Diener Zepto low-pressure plasma machine (Diener Electronic GmbH & Co KG, Germany) was employed for the plasma treatment. The machine is equipped with two needle valves for precise gas supply with gas flow controllers. Operating in manual mode, the system is attached with a Pfeiffer Duo 3 rotary-vane vacuum pump to create a low-pressure environment in the plasma chamber. Plasma treatment was conducted at two power levels (intensity of plasma frequency) of 80 Hz and 40 Hz for treatment durations of t = 30, 60, 120, 180, and 240 min. The gas supply for both gasses was maintained at a constant flow rate, and a fixed pressure of 1 bar, to maintain a stable pressure of 1.5 mbar within the plasma chamber. After plasma treatment, individual fibres (~500 fibres) were taken from the

plasma treated sliver and were conditioned in a standard textile testing environment (ISO 139), with a relative humidity of 65% and temperature of 20°C for a duration of 48 hours, before physical property measurements and chemical analysis.

5.2.4 Fibre Morphology Analysis

5.2.4.1 Scanning Electron Microscopy

The surface morphologies of both untreated and plasma treated hemp fibres were examined using scanning electron microscopy (SEM). Micrographs were captured using a Jeol JSM 6610 SEM operating in secondary electron mode with an accelerating voltage (electron source energy) of 5.00KV, covering a range of magnifications from 25× to 4000×, with a scan size varying from 1 mm to 10 µm × 10 µm following the method referred to by Juhaśz et. al. [163]. Before imaging, the fibres were sputter-coated with gold using a LUXOR gold sputter-coating device to yield a coating thickness of 50 nm.

5.2.4.2 Atomic Force Microscopy

The surface topography of hemp fibres was examined using atomic force microscopy (AFM) (Bruker Dimension FastScan) operating in Tapping mode in air. Individual fibres (n = 3 samples) with an approximate length of 8 mm, were affixed to round stainless steel specimen discs of 15 mm diameter using double-sided adhesive tape to ensure stability and flatness before scanning. FastScan A probes (Bruker) with a nominal spring constant of 18 N/m and resonant frequency of 1.4 MHz were used for imaging each specimen. To ensure the reproducibility of the acquired AFM scans, untreated hemp fibres were initially imaged under the AFM. Three different areas on three different fibres were imaged and scan sizes at 5 μm, 10 μm, 20 μm and 30 μm were collected from each area using the NanoScope 9.4 software. Images were acquired at 768 × 768 pixel resolution at a scan rate of 1 Hz. These same untreated, mounted fibre samples were then plasma treated using the method outlined in section 2.3. Following plasma treatment, the samples were re-examined under the same AFM settings, within the same areas initially imaged. The obtained topographic images were processed with 1st-order flattening and analysed using NanoScope Analysis 1.9 software.

5.2.4.3 Chemical structure of fibres

The crystallinity of untreated and plasma treated hemp fibres was analysed using a Bruker D2 Phaser equipped with a Cu (1.541 Å) source and LYNXEYE detector. The analysis was conducted at a scan speed of 5° per min, with the hemp fibres placed in a 35 × 50 × 5 mm glass sample holder and performed under plateau conditions [209]. The crystallinity index was measured based on the diffractometric method outlined by Chukhchin et. al [210, 211]. Data analysis and peak deconvolutions of the X-ray diffraction pattern(s) were done using the OriginPro software. Additionally, the chemical structure was explored using a Perkin-Elmer ATR-FTIR Spectrum-3 equipped with a single-bounce diamond attenuated total reflection (ATR) accessory. Spectroscopic data were collected at 4 cm^{-1} resolution over 100 scans for untreated and plasma pre-treated samples. OriginPro software was used for data representation of the obtained ATR-FTIR scans.

5.2.4.4 Fibre surface wetting analysis

Surface wetting analysis was conducted on fibres using a Kruss BP100 tensiometer. Prior to analysis, microscopic images with a magnification ranging from 1 mm to 200 μm were taken using a Leica digital microscope, and ImageJ software was employed to measure fibre diameters. To reduce experimental error due to the inherent variation in the diameter of hemp fibres, specimens of fibre were selected with a diameter of 50 μm and cut into 10 cm lengths. The measurements involved assessing the force of attraction of solvents by varying the position of fibre immersion. Hexane, an aprotic solvent, and water, a protic solvent, were utilised for this purpose [212]. The detection speed for the tensiometer was set at 6 mm/min with a detection sensitivity of 5×10^{-4} mN/m. The measuring speed was kept at 3 mm/min with a maximum immersion depth of 5 mm and a minimum depth of immersion of 1 mm. The water contact angle was determined using the data acquired from the tensiometer [213]. In the tensiometer setup, the fibres are suspended from the tip, allowing for the measurement of both the force with which the fibres interact with water and the depth to which they are immersed. The Wilhelmy plate method was applied to determine the water contact angle [214]. In the case of natural fibres such as hemp, which exhibit significant variation in diameter, ensuring reproducibility of results is crucial. Therefore, the water contact angle was also measured using sessile drop measurements with a Kruss DSA30E goniometer [19]. The water contact angle was measured by suspending a 7 μL sessile water droplet of deionised water with a surface tension of 72 N/m on the surface of plasma treated and untreated lignocellulosic hemp fibre. The droplets were allowed to stabilise for 20 seconds, and the contact angle was measured using a built-in camera. From the recorded video, a series of images enabled the water contact

angle to be measured at the point of the droplet's contact with the surface. Three repetitions were taken for each fibre sample.

5.2.4.5 Fibre tensile properties

The tensile strength of both untreated and plasma treated hemp fibres was evaluated using an Instron 5544 universal tensile strength tester following the BS EN ISO 5079-2020 test standard method for fibre testing [130]. The crosshead speed was maintained at 20 mm/min using a gauge length of 20 mm [215]. Before testing, the fibres were mounted on a 30 mm × 30 mm (length x breadth) standard template, which was cut before initiating the test. To ensure consistency, fifteen replicates were tested, and the data averaged. The tensile strength data was analysed statistically using response surface methodology with the help of Minitab software. To minimise the degree of variation, lignocellulosic hemp fibres possessing a 50 µm diameter were selected for testing. Images of the fibres were captured using a Leica optical microscope and analysed with ImageJ software to measure the fibre diameter. Fibre testing was conducted in a controlled textile testing environment maintained at 65% relative humidity and 20°C temperature. To ensure equilibrium with the testing conditions, the fibres were conditioned in this environment for 48 hours before testing.

5.2.5 Fluorescence microscopy

Fluorescence microscopy was employed to visualise lignin within hemp fibres by exploiting its inherent autofluorescence [216]. Comparative analysis was conducted between untreated fibres and those subjected to argon plasma treatment for 4 hours at 80 Hz, focusing on potential changes in lignin distribution and relative abundance. Fibres with diameters of 60 - 80 µm were selected to ensure morphological consistency. High-resolution imaging was performed using a Stellaris 8 confocal microscope, capturing Z-stack images to obtain three-dimensional optical sections of the fibre. Scanning was conducted at 10 µm/min to ensure precise depth profiling. Lignin fluorescence was excited using dual-wavelength illumination at 488 nm and 550 nm [217], delivered at 10% transmission with 30% laser power, parameters optimised to enhance signal intensity while minimising photobleaching. Emission was detected using a bandpass filter (BP530) and a long-pass filter (LP590), allowing selective capture of lignin-specific signals in the green-to-red spectrum. This methodology enabled clear and specific visualisation of lignin distribution, in alignment with established excitation-emission parameters for lignified plant tissues.

5.3 Results and discussion

As-received untreated (dew retted hemp fibre) and plasma treated hemp fibres were examined to explore any differences in physical, morphological and chemical properties.

5.3.1 Morphological analysis of plasma treated and untreated hemp fibres

The SEM and AFM scans (Figure 5.1) on untreated and argon plasma treated hemp fibres (40 Hz power for 30 min and 80 Hz power for 30 min) reveal clear differences in surface morphology. Comparing the SEM images (Figure 5.1 A, D, & G), it is evident that as plasma treatment time and the intensity of argon plasma increases, the degree of surface etching increases, with the maximum surface roughness determined by AFM increasing from approximately 530 nm to around 1.3 µm (Figure 5.1 C, F & I). The surface morphology of the untreated fibre (Figure 5.1A) appears comparatively smooth, while argon plasma-treatment for 30 min at 40 Hz and 80 Hz power (Figure 5.1 D & G) roughens the surface. Morphological distinctions are also visible in fibres treated with argon gas plasma after 30 min when altering the plasma power from 40 Hz to 80 Hz (Fig. 5.1 D & G). Specifically, in the case of D, there appears to be a pronounced surface roughening, most probably caused by the removal of surficial layers associated with the multiple impacts of highly reactive ions, electrons and radicals within the plasma [218]. Sample G, which was treated at 80 Hz for 30 min, also shows evidence of the initiation of fibrillation. Fibrillation appears to be linked to the surface roughness, which leads to the breakdown of the internal structure within the surface layers. This breakdown, however, is not anticipated to be thermally induced, as low-pressure plasma devices operate at low temperatures [219].

With reference to Figures 5.2 A and D, the argon plasma components (consisting of highly energetic atoms and positively charged ions) collide with the lignin-rich fibre surface over a period of 4h, resulting in a highly etched and textured surface with lignin and hemicellulose remnants clinging to the fibre surface. Hemp fibres are relatively coarse in terms of diameter, with lignin strongly bonded throughout their length [220], so it may be hypothesised that plasma treatment facilitates disruption of lignin-cellulose binding interactions resulting in a morphologically heterogeneous, etched surface being observed. In research by Ivanovska et al, similar results were observed

when jute fibres were plasma treated in the presence of atmospheric pressure air plasma [151].

The AFM topographical images over a scan length of 10 μm × 10 μm are given in Figures 5.1 B, E, and H, with their 3D surface projections in Figures 5.1 C, F, & I (untreated and argon plasma treated hemp fibres for 30 min at 40Hz and 80Hz). Additionally, AFM images in Figure 5.2 B & E show hemp fibre samples plasma treated for a substantially longer period of 4 h at 40 and 80 Hz power respectively. The AFM scans of untreated fibres (Figure 5.1 B & C) reveal a relatively smooth surface, with negligible peaks and troughs on the surface, whereas argon plasma treated fibres exhibit a roughened surface texture across the full 10 μm × 10 μm scan and is particularly noticeable in fibres plasma treated for a shorter treatment time of 30 min (Figure 5.1 E & H). Their 3D surface projection illustrated in Figure 5.1 F & I, clearly show a highly textured surface. These topologically altered features on the fibre surface may be attributed to lignin [218]. Previous AFM studies conducted on pre-treated eucalyptus wood, reported similar results to those reported here, albeit with a different material [221]. The textured surface could also be associated with physical disruption of the surface, including fibrillation [222]. Increasing the treatment time to 4 h, led to the formation of deeper valleys, and cracks becoming more pronounced (Figure 5.2 B, C, E & F).

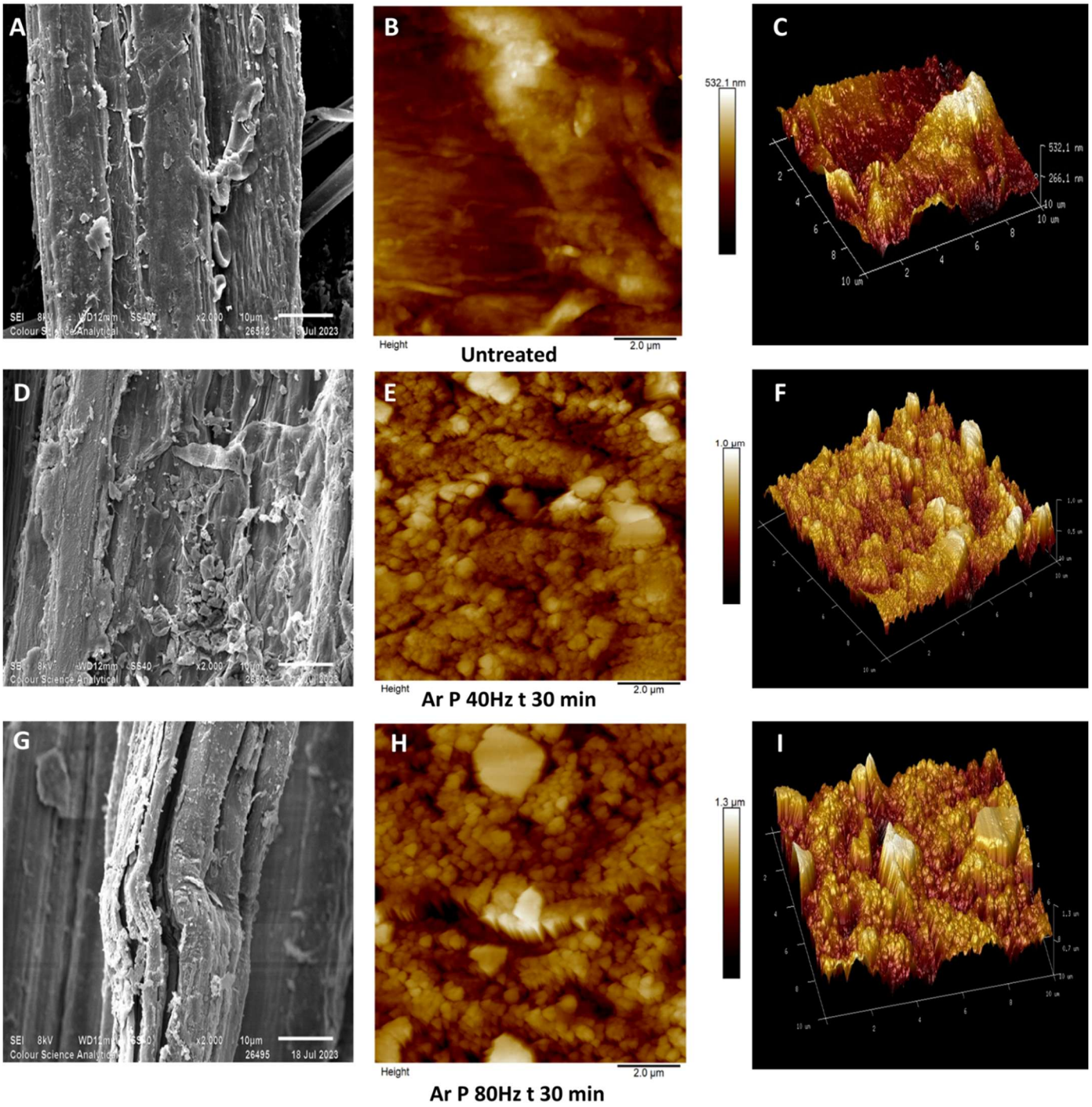

Figure 5.1 Scanning electron micrographs (×2000) and AFM (10 µm × 10 µm) scans of argon plasma treated hemp fibres for a duration of 30 minuites at 80 Hz and 40 Hz power

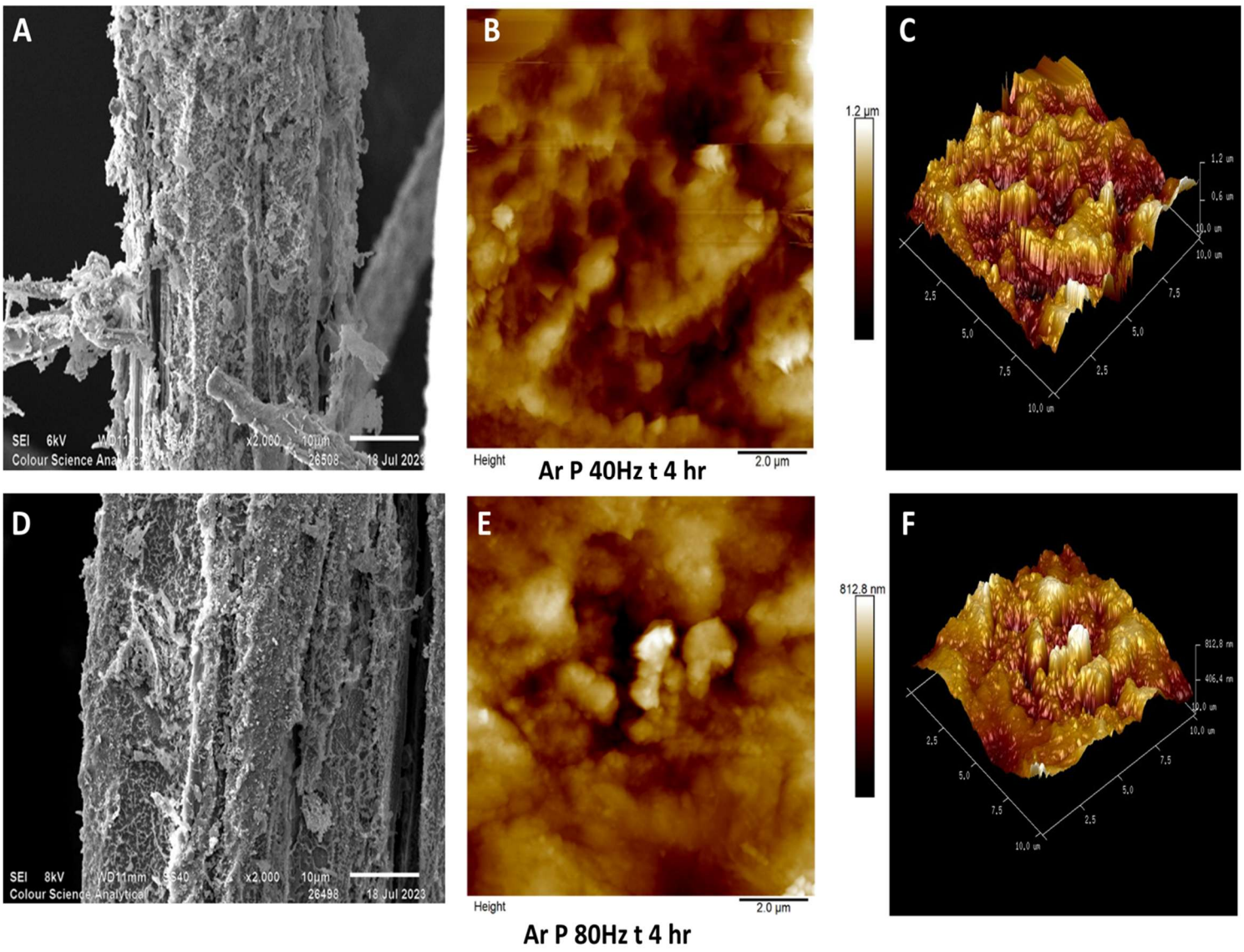

Figure 5.2 Scanning electron micrographs (×2000) and AFM (10 µm × 10 µm) scans of argon plasma treated hemp fibres for a duration of four hours at 80 Hz and 40 Hz power

In Figure 5.3, SEM images, taken at 1200× magnification, alongside 10 µm × 10 µm AFM scans, illustrate the surface morphology and topography of hemp fibres treated with oxygen gas plasma under different conditions. Fibres treated at 40 Hz for 30 min (Figure 5.3A) show a slightly rougher surface than untreated fibre samples, while those treated at 80 Hz for the same duration (Figure 5.3D) display more pronounced surface etching of the fibre surface. Fibres treated for 4 h at 40 Hz (Figure 5.3G) exhibit a highly roughened, network-like surface structure. Farias et al.'s work on oxygen plasma treated coir fibres showed a similar network-like structural morphology [223].

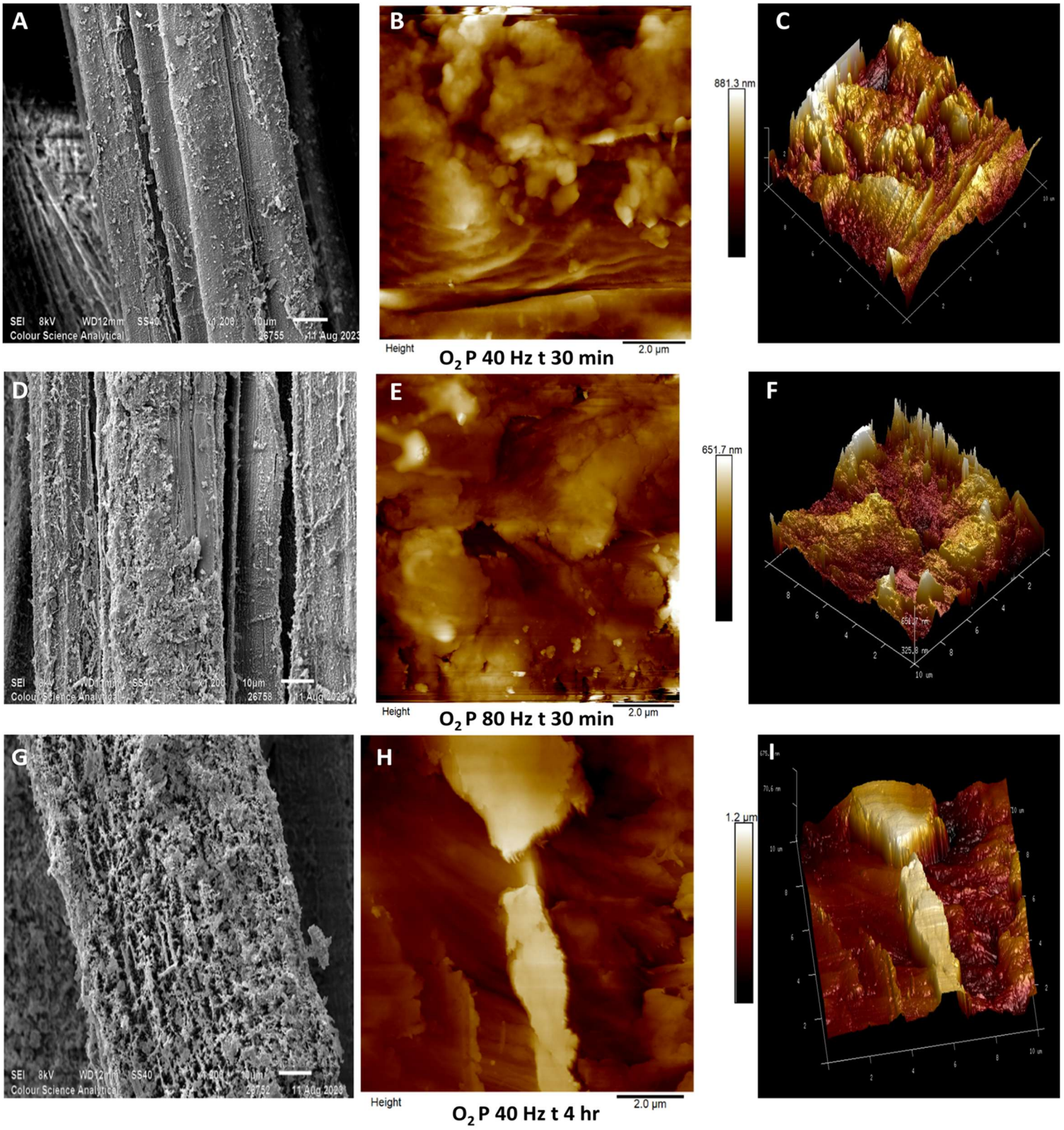

Figure 5.3 Scanning electron micrographs (×1200) and AFM (10 µm × 10 µm) scans of untreated hemp fibres and pre-treated fibres using oxygen gas plasma

Subsequent AFM scans (10 μm × 10 μm) of fibres plasma treated with oxygen gas are illustrated in Figures 5.3 B, E, & H with their 3D surface topography in Figures 5.3 C, F, & I. Note that the roughened surface globular features that were observed in argon plasma treated fibres are less visible in these AFM scans. Lignin consists of complex macromolecular aggregates [224], because of which it can be observed in globular structures similar to those prominently seen in Figure 5.1 E & H. Micic's AFM work on lignin shows similar globular structures [225]. Comparing AFM scans in Figure 5.1(E & H), Figure 5.2 (B & E) and Figure 5.3 (B, E, & H), it may be speculated that oxygen plasma is more capable of lignin removal than argon plasma. Muazzam et al. examined lignin following oxygen plasma treatment and found that lignin underwent oxidation due to the presence of ozone in oxygen plasma [226].

In a study by Edwards et al., the regenerated cellulose fibre lyocell was plasma treated for 20 min at 40Hz power. AFM studies revealed a change in surface roughness from 0.18 nm roughness, in the case of untreated lyocell, to 3.18 nm roughness after oxygen plasma treatment [227]. Chemically, lyocell contains negligible impurities in the form of lignin, hemicellulose and pectin, comprising up to 92% α-cellulose [228]. The marked changes in the surface morphology of hemp fibres observed herein are therefore suggested to be consistent with the removal of impurities such as lignin, hemicellulose and pectin, as well as the sputtering effects during plasma treatment.

Oxygen plasma primarily triggers chemical reactions with O_2 gas, generating a plasma which is rich in reactive oxygen atoms and ozone (amongst others), which contribute to surface modification and surface functionalisation through chemical transformation [229]. In contrast, argon plasma consists of high-velocity Ar^+ ions that modify the surface through primarily physical mechanisms. The resulting differences in surface morphology arise from these distinct processes of oxygen plasma, causing chemical changes and argon plasma, inducing physical alterations. Yamamoto et al. studied the difference in argon and oxygen plasma treatments on gold films and concluded that argon plasma had a physical effect and oxygen plasma had a chemical effect, the latter inducing the formation of Au_2O_3 [230].

Hemp fibres plasma treated using oxygen gas possess a high number of cracks and valleys on the surface, and a prominent difference can be seen in samples treated for 30 mins at 40 Hz (Figure 5.3B) and at 80 Hz (Figure 5.3E). Some features are indicative of globular lignin (Figure 5.3B), whereas increasing plasma power roughens

the surface with deep valleys, hundreds of nanometres in depth (Figure 5.3E). A more substantial change is visible in fibres plasma treated for 4 h at 40 Hz (Figure 5.3H) with an etched surface across the area, resulting in deeper cracks on the surface extending to more than 1 μm in depth, as indicated in the 3D surface projection (Figure 5.3I).

When comparing the effects of argon and oxygen plasma treatment on hemp fibres, it is evident that oxygen plasma produces eroded surface features [231] on the fibres. It can be hypothesised that this is likely due to the presence of oxidising components present in oxygen plasma [232], resulting in more aggressive chemical interactions than in argon plasma. In contrast, argon plasma primarily roughens the surface through an atomic-layer etching process [233], and herein, it can be said that present surface components such as lignin, hemicellulose and pectin are removed one atomic or molecular level at a time [19, 233], exposing textured features [173]. Similar observations can be made referring to the section profile graphs (pages 163 to 166) determined for a 10 nm section in the AFM scan. These graphs with their marked sections on the AFM scans are illustrated in the supplementary information Figures 5.11, 5.12, 5.13.

In the AFM images, lighter colours indicate raised surface features, while darker colours represent recessed or engraved areas. By comparing AFM height images and 3D surface projections across Figures 5.1, 5.2 and 5.3, it can be hypothesised that argon plasma treatment initially removes surface layers up to a certain threshold, after which a smoother surface with reduced roughness is achieved. It can be said that the action of physical sputtering due to the presence of Ar^+ in argon plasma continues only until the reactive material (lignin, hemicellulose or pectin) is fully removed. This type of threshold effect can be hypothesised and will be studied in future. This is evident in Figure 5.2B, where the surface roughness measures ~170 nm, although the surface roughness of argon plasma treated hemp fibre (Figure 5.1D) is approximately double that value, suggesting that the treatment effectively levels out the surface after the removal of the top layers. In contrast, oxygen plasma treated hemp fibres possess a non-uniform, roughened surface topography with deep troughs (with a maximum depth of ~1.2 μm) and peaks.

Plasma is known to be capable of both dry etching and nano-texturing polymer surfaces [171], which is also observed in argon and oxygen plasma treated hemp

fibres. In a recent study, lignin mapping was conducted on lignocellulosic nanofibres using AFM, revealing that lignin covers thin cellulose fibres and presents a grain-like structure [234]. Additionally, AFM analysis on kapok fibre demonstrated similar bundle-like formations with surface roughness being modified by approximately 80% after plasma treatment [235]. In the present study, AFM surface roughness data for both untreated and plasma treated hemp fibres were analysed (Table 5.1). Each roughness measurement is calculated as the average from three AFM scans of 10 µm × 10 µm scan. Referring to Table 5.1, untreated fibres were found to have a surface roughness of around 70 nm, i.e. the surface height range between the highest and lowest topographical points in the imaged area. This increased to ~300 nm following argon plasma treatment at 40 Hz and 30 min duration.

Plasma treatment		Source Gas	Scan size	Surface roughness
Power(Hz)	Duration(min)		µm	nm
0	0	n/a	10	70.4
40	30	argon	10	299
80	30	argon	10	199
40	30	oxygen	10	101
80	30	oxygen	10	182
40	240	argon	10	105
80	240	argon	10	172
40	240	oxygen	10	111

Table 5.1 Surface roughness of untreated and plasma pre-treated hemp fibres measured using root mean square (RMS) method

Figures 5.1, 5.2 & 5.3 suggest that plasma treatment introduces a nano-textured effect on the fibre surface. The surface roughness values in Table 5.1 are root mean square values (RMS). The fibre treated with oxygen gas at 80 Hz power for a treatment time of 30 min produced a surface roughness of 182 nm for a 10 µm × 10 µm scan. Interestingly, the fibre sample treated at 4 h at 40 Hz power using oxygen gas measured a surface roughness of 111 nm in a 10 µm × 10 µm scan. To gain detailed insights into the surface topography, we also used “section analysis” to study the surface. Figures 5.11, 5.12 and 5.13 in the *supplementary information section* represent a section profile (denoted as a white line on the scan) and its surface profile

graph. The most heightened point and the most depressed point are also marked. Surface response analysis and principal component analysis (multivariate analysis) of these three variables (power, treatment duration and gas) as contributors to surface roughness were analysed and are illustrated in Figure 5.14 in the *supplementary information section*. Therefore, the statistical analysis suggests that plasma treatment operates as a synergistic process, where gas type, power, and treatment duration collectively influence surface modification. While each factor holds individual significance, it is the optimal combination of all three parameters that yields the most effective surface roughness outcomes.

The ablation observed in the fibres due to the oxygen gas plasma may be attributed to radical formation [236]. When oxygen gas (O_2) plasma is generated, electrons having a threshold energy of approximately 16.4 eV are produced along with additional metastable states and the total energy of O_2 plasma tends to increase [207]. This causes an increase in the density of electronegative species, due to which the etching on the surface can be observed [237]. Bes et. al. studied the mechanism of oxygen plasma etching on hydrocarbons, concluding that the ablation of surfaces in the presence of oxygen gas plasma is due to the adsorption and desorption of energy-rich species present in the plasma [238] [239]. When oxygen (O_2) gas contacts high-voltage electrodes, the electrical discharges break the molecule into oxygen atoms or ionise the molecule to form $2O^+$ ions. Additionally, oxygen atoms react with oxygen molecules to form O_3, ozone, which is highly reactive and can contribute to dry etching [21, 240]. This complex interaction of plasma species (mixture of reactive components) leads to the observed nano-textured surface modifications in oxygen plasma-treated fibres, resulting in a surface having a roughness of 182 nm. Cao et al. studied plasma-lignocellulose interaction wherein ball-milled wood was plasma treated under atmospheric air. The study concludes that the degradation of plasma treated lignin is mainly due to the cleavage of ether bonds present in lignin [241].

Structurally, hemp fibres have an outer coating of lignin, with the studied fibres containing approximately 9% lignin, which is non-crystalline and amorphous, being hydrophobic [242]. The etchant gas, either oxygen or argon, when in contact with high-voltage electrodes, generates electrons due to ionisation. These electrons are generated rapidly due to frequent collisions, and the electron density in the plasma reactor increases exponentially [243]. These electrons possess high temperatures and have an energy of up to 25 eV. Hence, it can be hypothesised that when these high-energy electrons and other ionised species encounter a relatively weak-bonded

amorphous structure such as lignin bundles, the surface layer of lignin can be readily removed by such energetic impacting, leading to a distinctly etched surface [174]. For fibres pre-treated using argon gas, the surface roughness increased significantly from 70 nm to 299 nm. Argon gas is an inert gas, but when used for plasma generation, it results in the production of Ar^+ along with electrons. Ar^+ ion has a velocity of 800 m/s, and when collides with the lignocellulosic fibre surface results in an etched surface appearing as nano-textured [173]. Etching is a layer-by-layer process, and the progressive etching can be observed as the treatment time increases from 30 min up to 4 h. The etching behaviour of Ar and O_2 plasmas on hemp fibres varies due to their distinct energy distribution profiles. Argon (having a relative mass of ~40 u) delivers high-momentum physical sputtering, increasing surface roughness, while O_2 plasma generates lighter atomic oxygen (with a relative mass of ~16 u), enabling frequent collisions and chemical oxidation of lignin and hemicellulose. Thus, argon plasma can favour mechanical ablation, whereas oxygen plasma may react with a combined physical and chemical etching, and the detailed type of etching can be detected using chemical analysis like ATR-FTIR.

An increase in surface roughness can result in enhanced wetting and an increase in surface energy [244]. Surface morphology plays a significant role in determining wetting characteristics, largely due to its influence on surface free energy, which is a key factor in wetting behaviour. This relationship is traditionally explained by Young's equation [245] [246], which assumes ideal smooth surfaces. However, after plasma treatment, when a smooth surface (~ 70 nm surface roughness) becomes highly roughened (~ 150 to 200 nm), the modified Cassie-Baxter theory [247] characterises the wetting behaviour more accurately. By considering all three theoretical models, Young's model, Wenzel's equation, and the Cassie-Baxter theory, it becomes evident that surface roughness is a crucial factor in controlling wetting behaviour [248]. This is because roughness affects the balance of free energies between the solid-vapour and solid-liquid phases, thus altering the overall wetting properties of the material. Consequently, the modification in the wettability of plasma treated hemp fibres was studied.

5.3.2 Influence of plasma treatment on the surface wetting property of hemp fibres

The wettability of hemp fibres having undergone oxygen and argon plasma treatment for 30 min to 4 h at 40 Hz and 80 Hz power was determined by tensiometry [249].

Advancing and receding contact angles were measured using distilled water and n-hexane as probe liquids. When n-hexane was used as a solvent, all the plasma treated samples, along with the untreated fibre sample, measured a water contact angle of 0°. This is because n-hexane is a non-polar solvent with a surface tension of 18.4 mN/m. In contrast, water, being a polar solvent, has a surface tension of 72 mN/m [250]. For the untreated fibre samples, the measured water contact angle was 65.2°, indicating that hemp fibre before plasma treatment is partly hydrophilic. After plasma treatment (Ar, & O_2) was carried out, the water contact angle reduced to 0°, [67-69]. This modification from a partly hydrophobic surface to a fully wettable surface is arguably due to occurring changes in the combined morphological-chemical alterations leading to an increase in surface energy.

These results were confirmed through water contact angle measurements using a Kruss goniometer. The water contact angle for the untreated fibre sample was recorded at ~69°, and all the plasma treated fibre samples showed a reading of 0°. The surface wetting of a fibre is influenced by factors such as surface roughness and chemical composition [251]. For pure cellulose, the water contact angle typically ranges from 20° to 30° [252]. Interestingly, the experimental data show that 100% wetting was achieved after plasma treatment by both gases, which may suggest that plasma treatment enhances the surface energy of the fibre [151]. Herein, the surface roughness changed from 70 nm to 275 nm (Table 8). These experimental results align with the Wenzel model [248], and a water contact angle of 0° suggests that the surface energy of the fibre is enhanced due to both physical as well as chemical interaction of argon and oxygen plasma with the hemp fibre [227].

This synergistic improvement in surface texture and wettability offers several functional advantages. The roughened nanoscale topography enhances the total surface area, promoting capillary-driven adsorption and absorption of dyes, textile finishes, and functional coatings. Simultaneously, the elevated surface energy resulting from plasma-induced chemical alterations facilitates stronger molecular interactions and bonding with these agents. Such conditions are highly favourable for applications requiring efficient wet finishing, dyeing, or bio-functionalization. To further explore the chemical changes associated with plasma treatment, Fourier-transform infrared spectroscopy (FTIR) and X-ray diffraction (XRD) analyses were conducted. These techniques provide insight into alterations in chemical bonding and crystalline structure, complementing the surface wetting observations and helping to elucidate the underlying plasma-induced modifications.

5.3.3 Influence of plasma treatment on the chemical structure of hemp

ATR-FTIR spectra of untreated and plasma treated hemp fibres are shown in Figure 5.4 (oxygen plasma) and Figure 5.5 (argon plasma), in which prominent peaks for -OH, -CH and -C-O functional groups can be prominently observed in the frequency range from 4000 cm^{-1} to 800 cm^{-1}. Referring to Figure 5.5, the untreated fibres show characteristic peaks at ~3400 cm^{-1} (O-H stretching in cellulose and hemicellulose), ~2900 cm^{-1} (C-H stretching in cellulose), and ~1050 cm^{-1} (C-O stretching in cellulose). After oxygen plasma treatment, the spectra in Figure 5.4 showed sharp -OH and C-O stretching peaks at ~3400 cm^{-1} and ~1050 cm^{-1} wavenumbers. Similarly, ATR-FTIR spectra of argon plasma treated fibres in Figure 5.5 indicates an increase in the intensity of the -OH and C=O functional groups. Although ATR-FTIR probes both surface and near-surface regions, having a penetration depth of ~1- 5 µm, the observed spectral shifts in plasma treated fibres indicate an enhanced fibre polarity [117].

In ATR-FTIR analysis, the peak height (intensity) of a vibrational band is proportional to the concentration of the corresponding functional group as per Beer-Lambert's law [117]. Broad peaks suggest heterogeneity in the molecular environment, often due to interactions like hydrogen bonding, van der Waals forces, or dipole-dipole interactions between functional groups and sharp peaks indicate more uniform environments [117]. Following oxygen or argon plasma treatment, hemp fibres exhibit sharp peaks within the frequency range of 3500 cm^{-1} to 3000 cm^{-1}, indicating two possibilities. The first possibility is surface activation, wherein the number of reactive functional groups (such as -OH) on the cellulose monolayer may increase, leading to sharper peaks [230]. Another possibility is that plasma treatment may be linked to the surficial removal of lignin, hemicellulose, or pectin, resulting in changes in ATR-FTIR spectra of plasma treated fibres showing sharper -OH peaks compared with the untreated fibre [230]. In a recent study undertaken by Kostryukov et. al. plant materials such as hemicellulose, lignin and cellulose were analysed using ATR-FTIR spectroscopy. ATR-FTIR analysis of extracted hemicellulose showed broader -OH peaks than the ATR-FTIR scan of cellulose or lignin, which showed sharp peaks for the -OH group [253].

Regarding oxygen plasma treatment contributing to the functionalisation of the substrate, these results do not show any alteration in the chemical fingerprint of cellulose. The sharp peaks at 3500 cm^{-1}, 1300 cm^{-1}, and 1100 cm^{-1} are evident after

an extended duration of plasma treatment (30 min), which may lead to the breaking of weak surficial hydrogen bonds. A potential reason for the appearance of sharp peaks is ring-opening of the glucopyranose units in the cellulose structure via a pyranosidic ring (C-O-C bonds) splitting mechanism [176]. Although such a ring-opening reaction may be possible in the case of pure cellulose, it is rare for lignocellulosic hemp fibres [232].

Figure 5.5 displays the ATR-FTIR spectra for both untreated and argon plasma treated hemp fibres, revealing noticeably sharper peaks in the -OH fingerprint region (3500 to 3000 cm^{-1}). This suggests that exposure to argon plasma may lead to surface ablation, resulting in sharper peaks. A recent study by Kolarova et al. observed cellulose fibres extracted from cotton subjected to argon plasma for durations between 10 and 300 seconds, finding no evidence of dehydration, as indicated by the consistent -OH peak height [254]. Similarly, Sawangrat et al. investigated chemical changes in bamboo fibres following argon and oxygen plasma treatments and found no notable alterations in functional groups, as the ATR-FTIR spectra for untreated and treated bamboo fibres showed minimal changes [150]. In a recent study, argon plasma treated hemp fabric produced similar findings, with the introduction of polar groups on cellulosic surface evidenced by the appearance of sharper -OH [19].

Non-pre-treated hemp fibres display a yellowish hue due to the presence of lignin, with polyphenolic components such as syringyl and guaiacil being detectable using ATR-FTIR spectroscopy [255]. These lignin components display sharp peaks within the frequency range of 1200 cm^{-1} to 1400 cm^{-1}, belonging to functional groups such as C-C, C-H and C-O [256]. Hence, the use of ATR-FTIR as a primary method for the identification of pretreatment of lignocellulosic fibres is challenging, although sharp peaks associated with these functional groups indicate a physicochemical change in the substrate. In a study by Kabir et. al. [83], the effects of alkalisation on hemp fibres were examined. Higher concentrations of NaOH in the chemical treatment led to increased cellulose content in the hemp fibres, thereby eliminating lignin and hemicellulose [83] and resulting in sharp -OH, -C-H and -C-O peaks [257]. Similar sharp peaks can be observed in the plasma treated hemp fibres illustrated in Figures 5.4 & 5.5, suggesting that the functional groups of cellulose remain unchanged despite the physicochemical modifications. These changes result in more pronounced peaks, particularly in the case of the -OH group, indicating that plasma treatment enhances the visibility of these functional groups without altering their chemical structure [19].

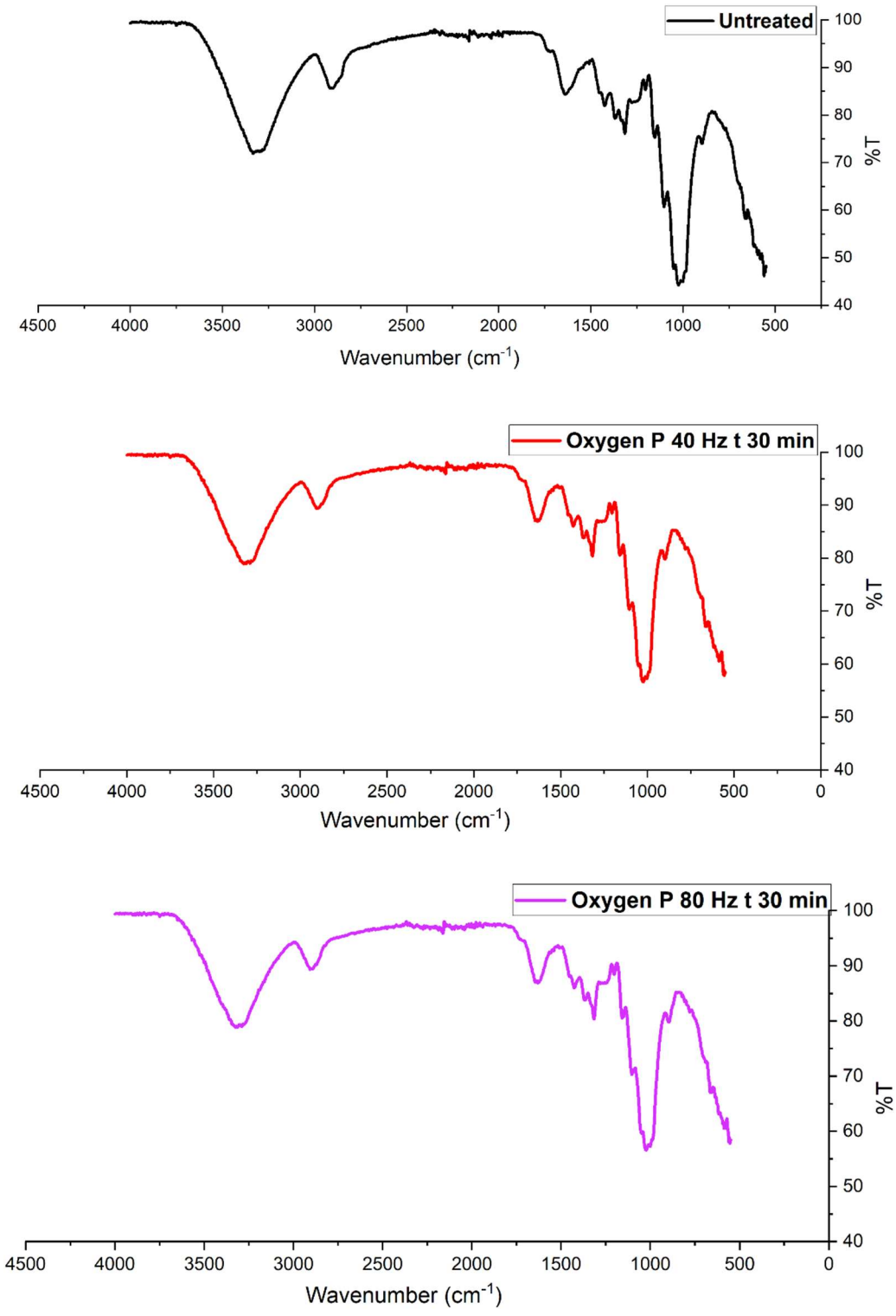

Figure 5.4 FTIR spectrum of hemp fibres before and after oxygen plasma treatment for 30 minutes with 80Hz and 40 Hz power

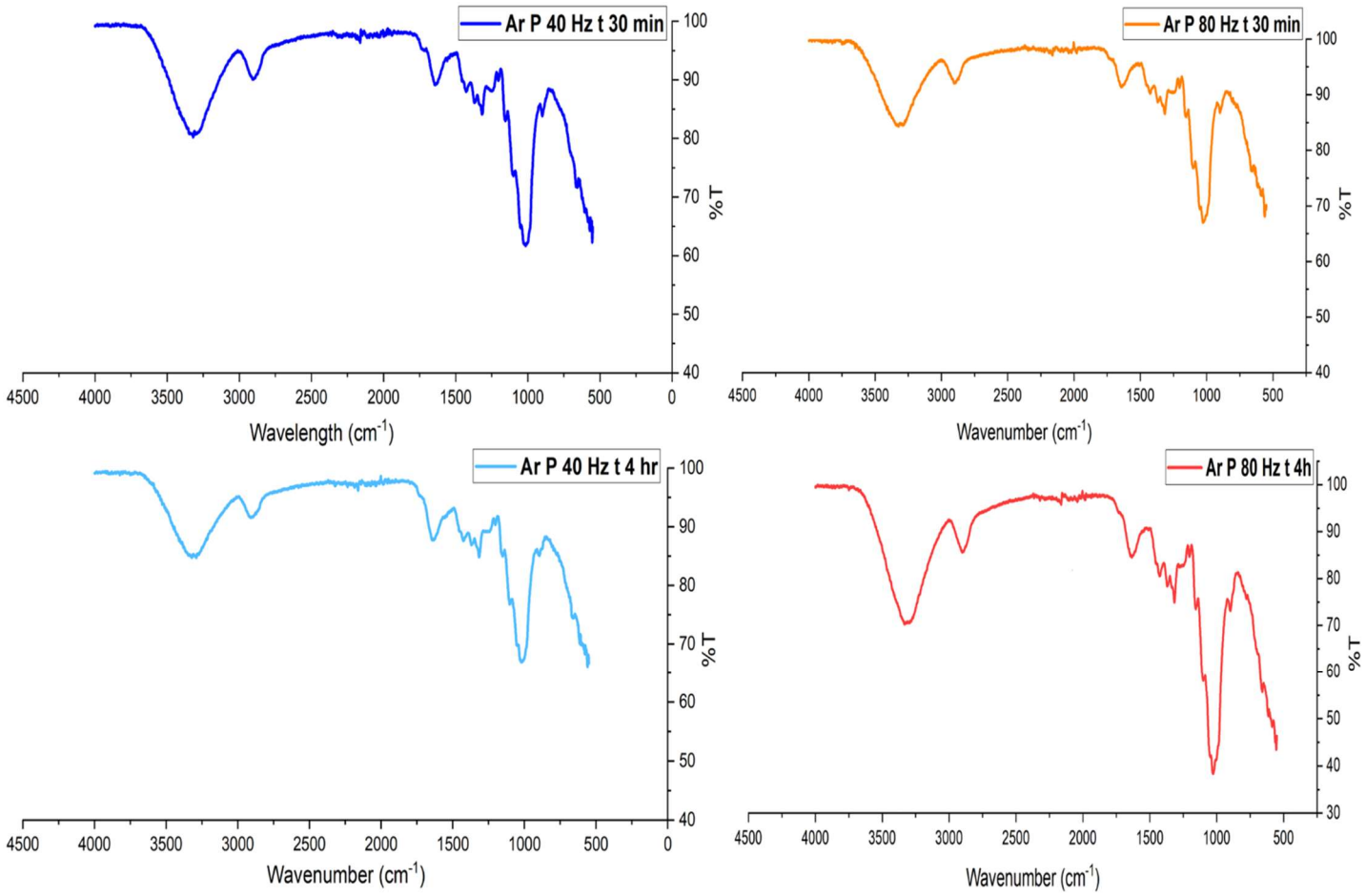

Figure 5.5 FTIR spectrum of hemp fibres before and after argon plasma treatment

5.3.3.1 Principal component analysis of FTIR spectra

Table 5.2 presents the scores of different samples on the first two principal components (PC1 and PC2) obtained from a Principal Component Analysis (PCA). PC1 has a variance of 98.2%, while PC2 has a 1.5% variance. The "Outlier" column indicates whether a sample is considered an outlier based on its position in the PCA space. The PC1 scores show a wide range of values, from -313.04941 to 641.22846. This suggests that PC1 captures a significant amount of variability between the samples. The PC2 scores have a smaller range compared to PC1, indicating that PC2 captures less variability. Two samples, which are outliers, were both plasma treated with argon gas with the same power value of 80 Hz, although differing in the treatment duration, one for 30 min and the other for 4 hr. This suggests that these samples have spectral characteristics that are distinct from the other samples. The wide range of

PC1 scores indicates that the samples exhibit substantial differences in their spectral profiles.

Spectral Names	PC1 (98.2%)	PC2 (1.5%)	Outlier
Ar P40 t30	-188.54242	-23.13473	-
Ar P80 t30	-313.04941	-46.9618	Ar P80 t30
Oxygen P40 t30	-84.72997	31.09819	-
Ar P40 t4h	-274.64974	13.21125	-
Ar P80 t4h	219.74307	69.59966	Ar P80 t4h
Untreated	641.22846	-43.81257	Untreated

Table 5.2 Percentage contribution of each treatment in PC1 and PC2

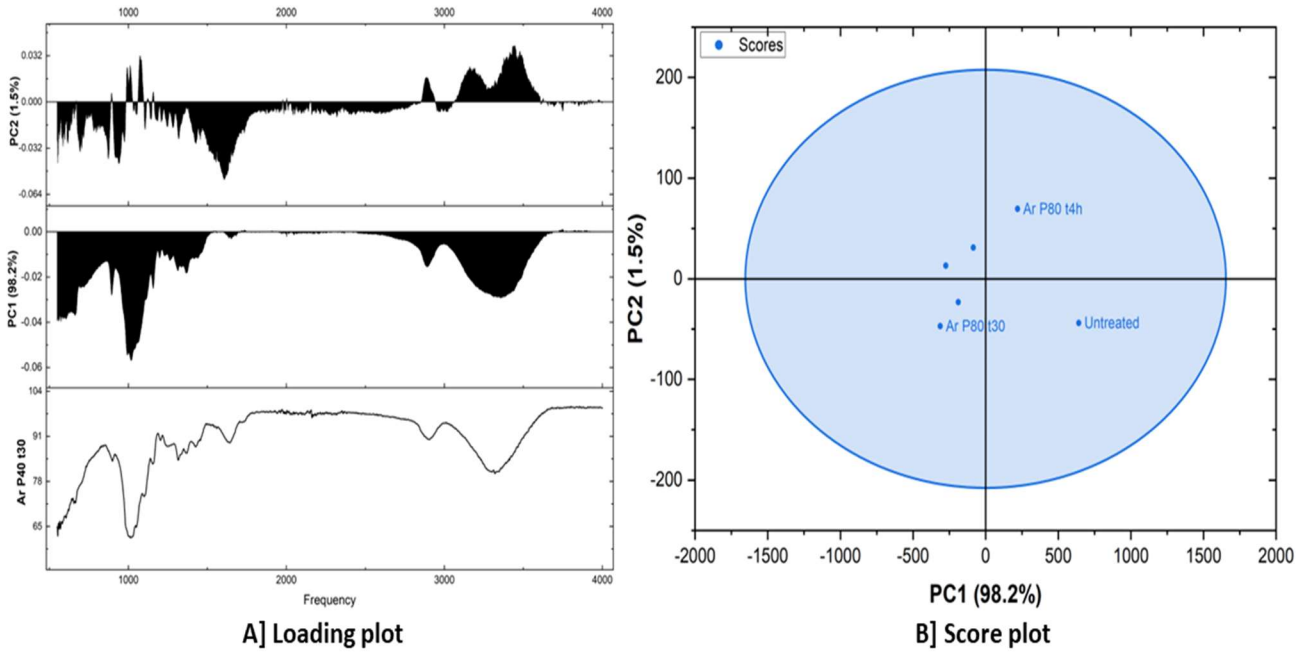

Figure 5.6 Loading plot [A] and score plot [B] which were obtained using PCA analysis of the FTIR spectroscopy data

Figure 5.6A shows a loading plot, which is a technique commonly used in Principal Component Analysis (PCA). It displays the loadings of different variables (in this case,

frequencies) onto the principal components (PCs). Loadings represent the correlation or weight of each variable in contributing to the variance explained by a particular PC. The bottom plot shows the loading of each frequency on the original data (Ar P40 t30). The middle plot displays the loadings of frequencies on the first principal component (PC1). PC1 explains 98.2% of the total variance in the data. Higher loadings indicate that a particular frequency contributes more to the variance captured by PC1. The top plot shows the loadings of frequencies on the second principal component (PC2). PC2 accounts for 1.5% of the total variance. PC1 captures the majority of the variance, representing the overall spectral profile. PC2 captures a smaller portion of the variance, likely representing more subtle spectral variations or features. The score plot (Figure 5.6B) illustrates the relationship between the fibres in this case, untreated, argon plasma treated for 30 mins & 4 h at 80Hz and the principal components. Each point represents a fibre, and its position on the plot reflects its scores on the PCs. The samples appear to cluster together, suggesting that they have similar spectral characteristics. This is supported by the fact that they fall within an ellipse, indicating that they are within the 95% confidence interval. While there's some overlap, there seems to be a slight separation between the untreated fibre sample and the two other fibre samples, which are both argon plasma treated for 4 hr and 30 min at 80 Hz power.

5.3.4 Influence of plasma treatment on the crystallinity of cellulose crystallites in hemp fibres

Cellulose is a semi-crystalline material, comprising both an ordered crystalline structure and an amorphous region. The crystallinity index of untreated hemp fibres and argon plasma-treated fibres was analysed using X-ray diffraction (XRD). Figure 5.7 presents the diffraction patterns for both untreated and plasma-treated hemp fibres. Peak fitting was performed to distinguish between the amorphous and crystalline regions. The cellulose molecule typically exhibits four characteristic peaks in the XRD pattern at approximately 2θ = 15°, 16°, 22°, and 23° [124]. Figure 5.7A displays the XRD pattern of untreated hemp fibres with fitted peaks at these positions. Similarly, Figures 5.7B and 5.7C illustrate the XRD patterns and fitted peaks for hemp fibres treated with argon plasma at 40 Hz and 80 Hz for 30 minutes. Additionally, Figures 5.7D and 5.7E show the diffraction patterns for samples subjected to argon plasma treatment for 4 hours at 40 Hz and 80 Hz, respectively. Figure 5.7F, therefore, represents the XRD pattern comparing argon plasma treated and untreated hemp fibres. The crystallinity index was thus determined using the peak-fitting method

demonstrated in the literature review by Salem et. al [124]. Table 5.3 shows the crystallinity index for untreated and argon plasma treated hemp fibres.

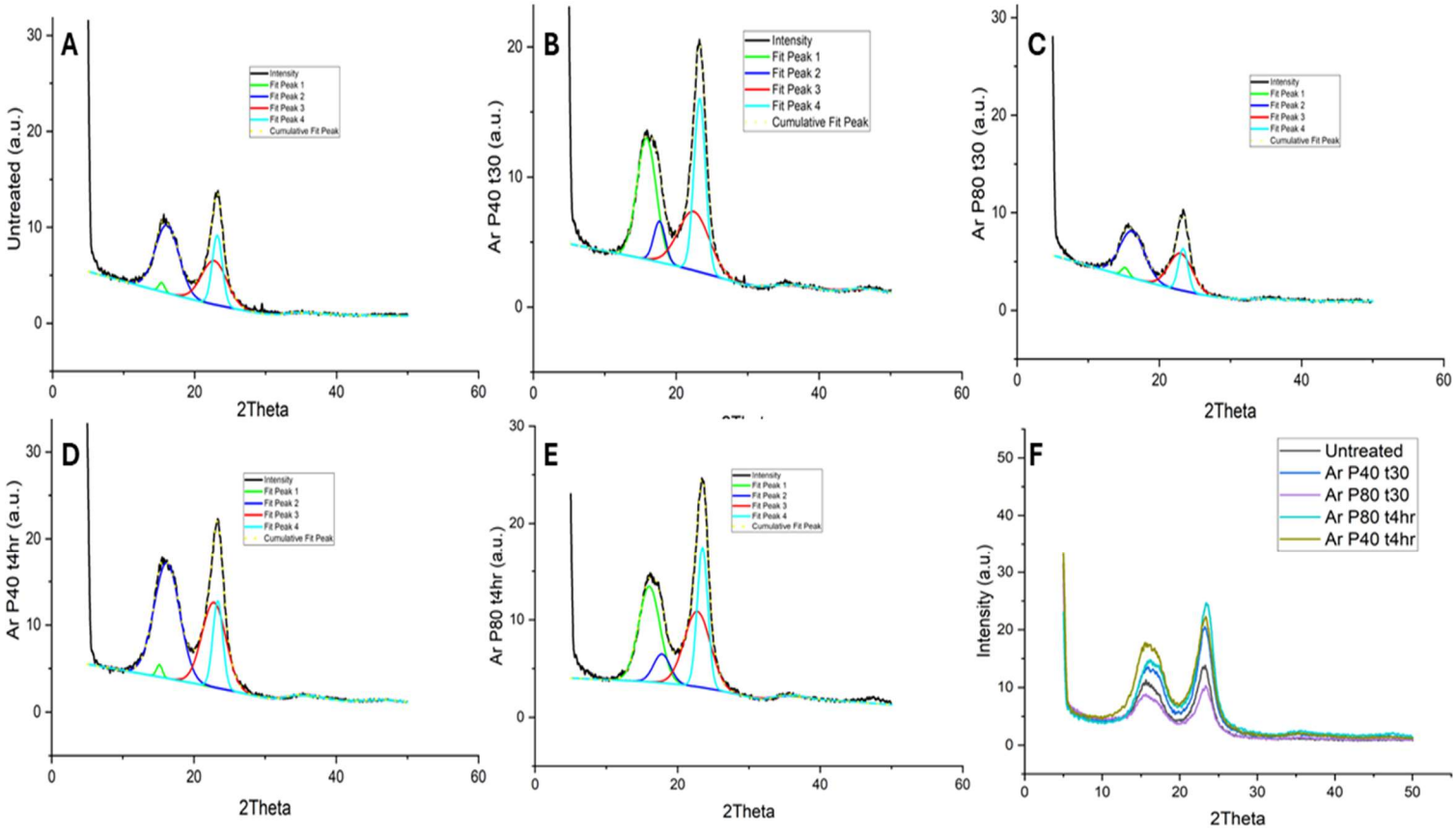

Figure 5.7 X-ray diffraction patterns of untreated and argon plasma-treated hemp fibres with peak fitting for determination of crystallinity

Sample	Crystallinity index (%)	Standard Deviation (%)	Standard Error (%)
Untreated	75	2.6	0.3
Ar P40 t 30	63	3.0	0.5
Ar P80 t 30	86	2.5	0.2
Ar P80 t 4h	55	2	0.2
Ar P40 t 4h	50	2.5	0.3

Table 5.3 Crystallinity index of untreated and plasma treated hemp fibres

Interestingly, hemp fibres treated with argon plasma at 80 Hz for 30 minutes exhibited the highest crystallinity of 86%, whereas prolonged exposure (4 hours) led to a significant reduction in crystallinity (~50%) compared to untreated fibres (75%). Jasti et al. analysed the crystallinity of hemp fibres using the peak fitting method, reporting a crystallinity range of 49% to 85% [258]. A higher degree of surface etching was observed after 4 hours of argon plasma treatment, suggesting that the removal of weakly bonded amorphous components such as lignin, pectin, or hemicellulose may facilitate the ordering of cellulose crystallites. This reorganisation could contribute to sharper diffraction peaks while simultaneously decreasing the overall crystallinity of the fibre [124]. Additionally, argon plasma treatment may induce the realignment of cellulose microfibrils along specific orientations, further enhancing peak sharpness [124]. Fibres which underwent argon plasma treatment for 30 minutes at 40 Hz power show a surface roughness of 300 nm, which can thus be attributed to the decrease in overall crystallinity.

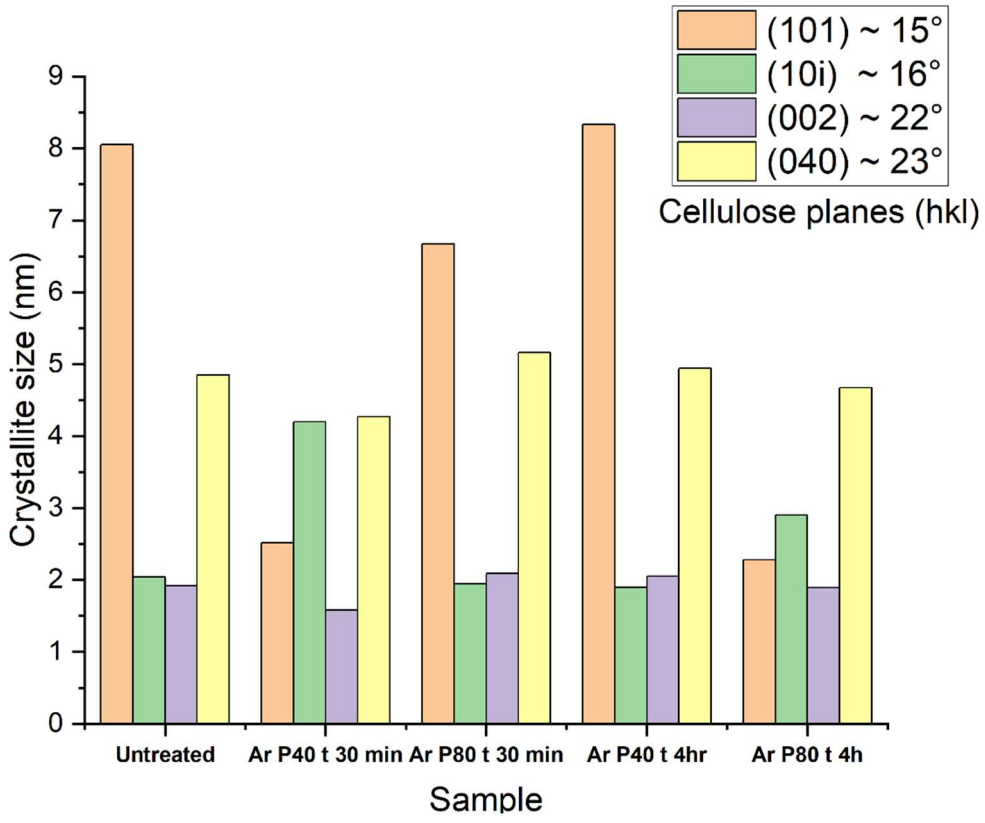

Figure 5.8 Crystallite size of untreated and argon plasma treated fibres

Crystallite size was calculated using the Debye-Scherrer equation to understand these structural changes better. Figure 5.8 presents the four identified crystallites along with their respective sizes in nanometres. The (002) plane, which is found at 2θ = 22°, is strongly related to cellulose crystallinity, representing the stacking of cellulose chains along the fibre axis [68]. Referring to Figure 5.8, it can be observed that the crystallite size has no significant change, indicating that argon plasma treatment is confined only to surficial interaction.

Cellulose crystals at the (101) and (10$\bar{1}$) planes indicate the lateral packing of cellulose chains, with a notable variation observed in fibres treated with argon plasma for 4-hours at 80 Hz, suggesting localised reordering. In contrast, the (040) plane, which appears at approximately 2θ = 23° [68] corresponds to intermolecular hydrogen bonding within cellulose sheets. Notably, no significant changes were observed in this crystalline region, and crystallite size remains unchanged across all the plasma treatments. This suggests that argon plasma treatment is mainly confined to the fibre surface. As the degree of crystallinity is related to the mechanical properties of the fibre, the tensile strength of untreated and plasma treated hemp fibres was determined.

5.3.5 Influence of plasma pretreatment on the tensile strength of hemp fibres

Figure 5.9 shows representative stress-strain results for untreated and plasma treated hemp fibres. As shown, both argon and oxygen plasma treatment for 30 minutes do not affect the tensile strength of the fibres. Notably, fibres subjected to argon plasma treatment at 80 Hz for 30 minutes closely follow the stress-strain curve of the untreated fibres, suggesting no adverse effect on the tensile properties. Additionally, these fibres have 85% crystallinity, suggesting that the fundamental cellulose crystalline structure remained largely intact, preserving strength loss.

In cellulose, the (002) crystal plane plays a crucial role in governing longitudinal stress transfer. The (101) and (040) crystal planes are associated with intermolecular hydrogen bonding, along with the (10$\bar{1}$) plane exhibiting the largest crystallite size among all tested samples which may play a critical role in reinforcing fibre structure, along with (101) and (10$\bar{1}$) planes contributing to fibre rigidity and tensile strength. The crystallite size for the (002) plane (Figure 5.8) does not show a substantial difference

from that of the untreated fibres, indicating that argon plasma treatment remains confined to the surface. Fibres treated with argon plasma at 40 Hz for 30 minutes exhibit a slightly reduced tensile strength (~0.09 GPa) than untreated fibres (Figure 5.9) and have a crystallinity of 63%. Such a slight reduction in the tensile strength may be correlated with the reduced crystallite size for the (002) plane (Figure 5.8). These findings indicate that argon plasma treatment could enhance the strength of intermolecular hydrogen bonds, ultimately preserving the mechanical performance of hemp fibres, although advanced research is needed for concrete evidence.

Hemp fibres plasma treated with oxygen gas for a duration of 30 minutes at 80 Hz power show a tensile strength (~0.12 GPa) similar to the untreated fibres. This indicates that oxygen plasma treatment remained confined to the surface without penetrating the bulk structure of the fibre. Moreover, FTIR analysis of oxygen plasma treated fibres confirms this as the chemical fingerprint of cellulose remains unchanged. Similarly, in the case of argon plasma treated fibres, although a higher surface roughness was observed at a micrometre scale, it does not alter the tensile properties. Hence, to confirm the hypothesis of lignin removal, fluorescence microscopy was done on untreated and argon plasma treated hemp fibres.

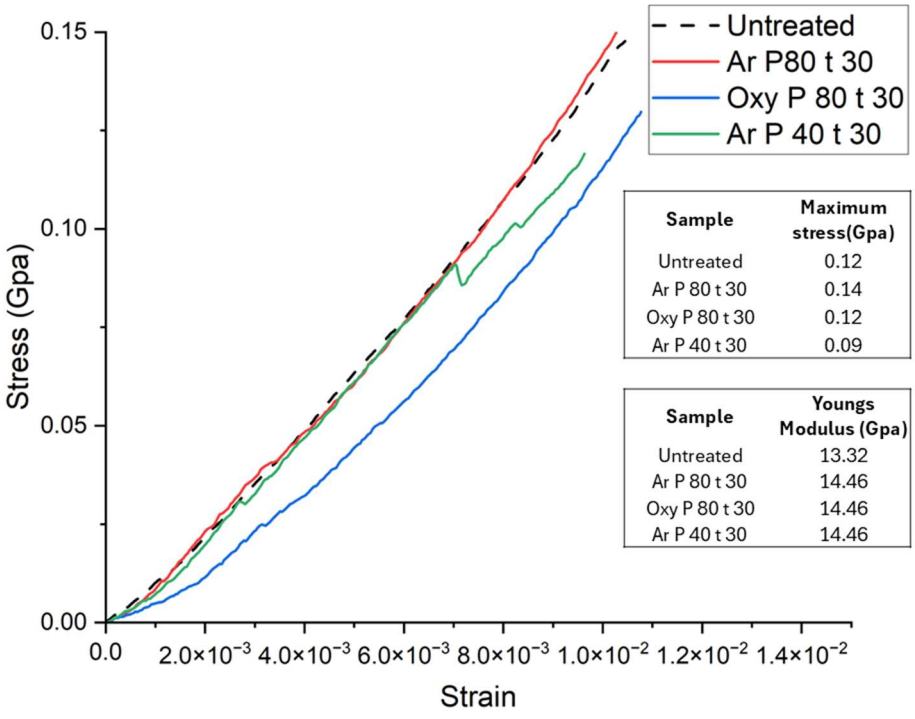

Sample	Maximum stress(Gpa)
Untreated	0.12
Ar P 80 t 30	0.14
Oxy P 80 t 30	0.12
Ar P 40 t 30	0.09

Sample	Youngs Modulus (Gpa)
Untreated	13.32
Ar P 80 t 30	14.46
Oxy P 80 t 30	14.46
Ar P 40 t 30	14.46

Figure 5.9 Stress-strain results for hemp fibres along with surface response analysis where Ar P80Hz t 30 min represents argon plasma treatment for 30 min at 80 Hz power and Oxy P80Hz t 30 min represents oxygen plasma treatment for 30 min at 80 Hz power

5.3.6 Influence of plasma treatment on fluorescence of lignin

Lignin naturally exhibits autofluorescence when excited at a wavelength of 488 nm [217]. Therefore, autofluorescence microscopy was utilised as a confirmatory test to assess lignin removal following plasma treatment [259]. This technique offers high sensitivity and specificity, enabling precise identification and localisation of lignin within plant tissues.

A z-stack is a series of images captured at different focal planes along the Z-axis (depth) in a sample. The microscope captures multiple images at incremental depths (z-positions). The resulting stack of images can be used to analyse fluorescence intensity at different depths. Figure 5.10 presents both fluorescence and transmission images of untreated and plasma-treated fibres (treated for 4 hours at 80 Hz power), along with the corresponding fluorescence intensity profile along the depth (z-axis). A comparison between the fluorescence image of the untreated fibre (Figure 5.10B) and the plasma-treated fibre (Figure 5.10D) reveals that the plasma-treated fibres exhibit lower fluorescence intensity than the untreated ones. A noticeable difference is observed in the fluorescence intensity peaks, with the plasma-treated sample exhibiting lower fluorescence intensity and a shallower peak. The z-stack imaging method used in fluorescence microscopy thus confirms the hypothesis that plasma treatment removes or modifies surface lignin.

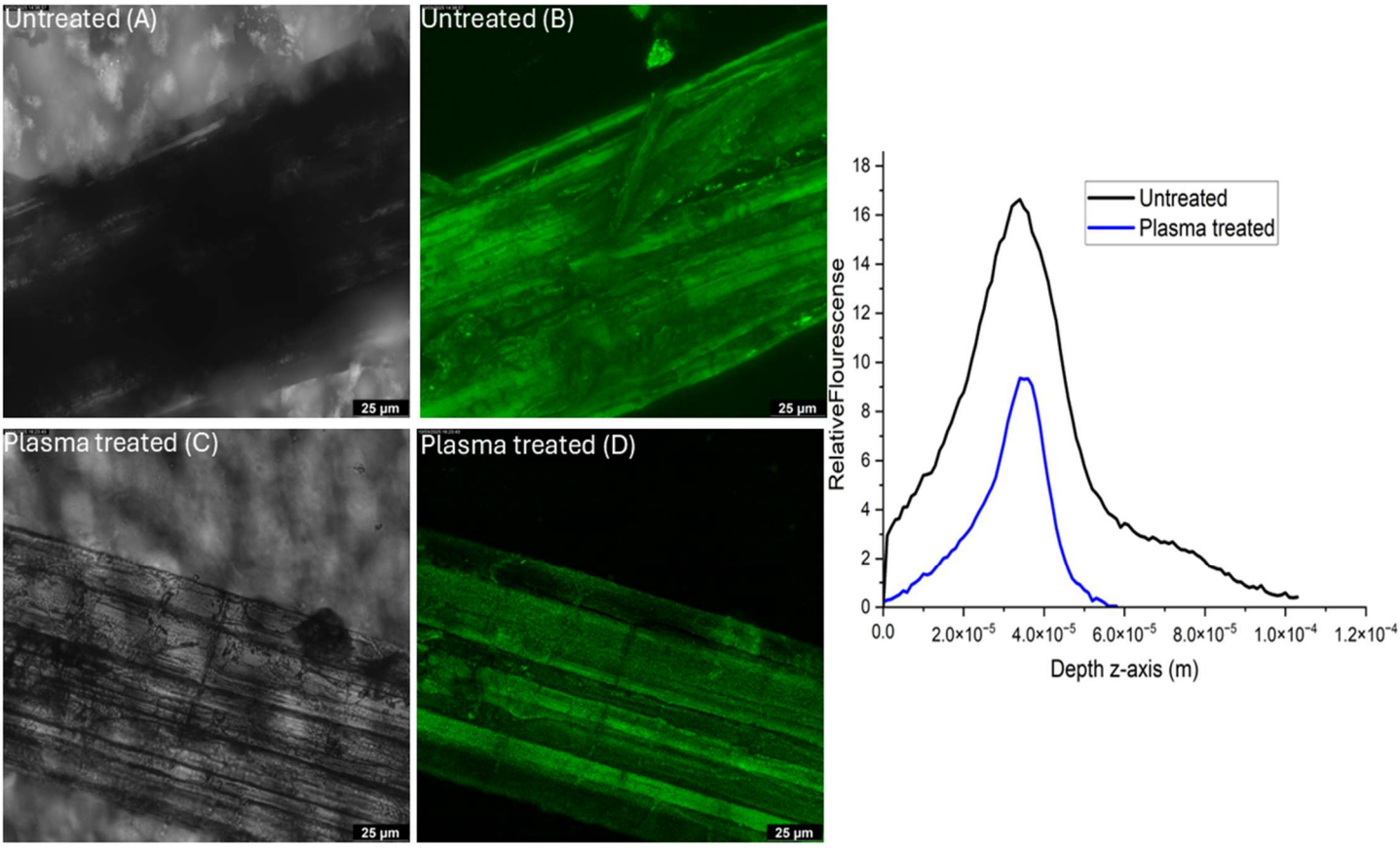

Figure 5.10 A] transmission image of untreated fibre, B] Auto fluorescence image of untreated fibre, C] transmission image of plasma treated fibre and D] auto fluorescence image of plasma treated fibre along with relative autofluorescence intensity vs depth (z-axis)

5.4 Conclusion

In conclusion, this study highlights some physicochemical impacts of argon and oxygen plasma treatment on hemp fibres, offering a valuable approach to surface fibre modification. Results demonstrate that both the treatment duration and the type of plasma gas significantly affect the degree of surface etching, with surface roughness increasing from around 70 nm to approximately 299 nm, according to AFM measurements. The texturing observed on the fibre surface is attributed to surface degradation and fibrillation of cellulose, with etching probably proceeding in a layer-by-layer manner. These results highlight the potential of plasma treatment as an environmentally friendly method to enhance the functional performance of natural fibres such as hemp. The induced surface morphological changes observed via SEM

and AFM can significantly improve surface reactivity, thereby broadening the fibre's applicability across both apparel and technical textile domains.

Auto-fluorescence mapping also points towards lignin loss as a result of the plasma treatment. The water contact angle of untreated hemp fibres, of about 69˚, is reduced to 0˚ following plasma treatment with both argon and oxygen, signifying a marked increase in surface energy resulting from surface roughening. FTIR analysis of argon plasma treated hemp fibres shows no major functional group changes, although changes to peak envelope suggest physicochemical modifications consistent with changes to the bound-cellulose water levels. Similarly, oxygen plasma treatment indicates possible surface functionalisation without alteration in the bulk cellulose structure. X-Ray diffraction analysis suggests a decrease in crystallinity after a 4-hour argon plasma treatment. Analysis of crystallite suggests that plasma treatment remained confined to the fibre surface without altering the crystallite size of the fibres, with the tensile strength of the fibres being unchanged after 30 min plasma treatment.

Overall, plasma treatment may prove to be a viable, low-chemical-contact technique for the manipulation of hemp fibre surface morphology, achieving surface modification with minimal water and chemical consumption while preserving the bulk properties of the fibre. These findings position plasma treatment as a sustainable and potentially impactful method for advancing the utility of natural fibres like hemp in diverse applications.

Chapter 6

Alteration in the microstructure of hemp fibres via the aid of low-pressure argon plasma treatment

6.1 Introduction

Enhancing the intrinsic strength of lignocellulosic fibres, particularly bast-type fibres like hemp, remains challenging due to the strong bonding of lignin, hemicellulose, and pectin with cellulose. The microstructure of dew-retted hemp fibres is such that the individual fibres are held together by lignin and pectin. Moreover, the majority of the cell wall is composed of lignin and hemicellulose. This preliminary study explores an innovative surface modification technique for dew-retted nonwoven hemp fabric through argon plasma treatment, followed by an immediate water shock process. The water shock treatment involves immersing fabric samples in an ice-water bath (approximately 4 °C) immediately after undergoing plasma treatment, which is applied for durations ranging from 30 minutes to 3 hours at power settings of 40 Hz and 80 Hz. Comparative analysis of untreated, plasma treated, and cold water shock treated fabric samples was conducted using scanning electron microscopy, tensile strength testing, Raman spectroscopy, and ATR-FTIR spectroscopy. Findings reveal no statistically notable changes in tensile strength for plasma treated hemp fabric, with a remarkable fourfold increase in samples subjected to the water shock (~0.49 MPa) compared to untreated fabrics (~0.09 MPa). The tensile strength of individual fibres remains largely unchanged after plasma treatment; however, a significant increase is observed following the water shock treatment, with values rising from approximately 20 MPa to 80 MPa. The porosity of the fabric decreases as stress increases after water shock treatment, indicating densification in the structure. Scanning electron micrographs of hemp fibre microstructure indicate distinct structural alterations, showing fibrillation in plasma treated fibres and a densified-compressed architecture in samples after a water shock treatment. Raman spectroscopy of plasma treated fabrics reveals a lower Raman shift than untreated samples; however, sharper peaks with increased Raman shift are observed for water shock treated samples, particularly in the crystal lattice region, indicating the formation of stronger intermolecular and interfibrillar hydrogen bonds. Similarly, prominent –OH peaks are evident in the FTIR spectra of water shock-treated samples, further supporting enhanced hydrogen bonding. This approach demonstrates promising potential for enhancing the strength of pure hemp fibres through surface modification using low-pressure argon plasma

treatment, without relying on synthetic resins commonly used in composite manufacturing. It presents a sustainable alternative to conventional fibre-reinforced composites, with potential applications in the development of lightweight and environmentally friendly materials.

Most research aimed at developing high-strength materials from cellulosic substrates primarily focuses on wood [260]. This is because wood is abundant, possesses outstanding mechanical and physical properties, and has a wide range of applications across various industries such as architecture and construction, packaging, sports equipment and transportation [261]. In comparison to wood-based high-strength materials, bast fibres such as hemp, flax, and jute offer several advantages, including lower density, higher flexibility, and faster renewability. Additionally, bast fibres require fewer processing steps and lower energy input for extraction and refinement, making them more sustainable alternatives. Their superior tensile properties, biodegradability, and compatibility with polymer matrices further enhance their potential for applications in textiles, biocomposites, and lightweight structural materials. Despite these advantages, bast fibres remain underutilised in high-performance material applications due to challenges such as variability in fibre quality, the presence of non-cellulosic components like lignin and pectin, and limited research on their structural optimisation.

Recent studies on lignocellulosic substrates, mainly involving wood, aim at developing mechanically efficient products to help transition from a fossil-fuel-dependent linear economy to a circular economy [262] [263]. Tian et. al developed a thermally insulating wood-based material capable of transmitting sunlight [264]. A microbial fuel cell (MCA) made of a wood-based anode was developed by Huang et. al for its application in wastewater treatment [265]. Similar product development can be seen for wood-based materials being applied in water distillation [266], energy conservation [267] and numerous other applications [268]. Hence, wood remains a versatile substrate capable of varied applications.

Innovative strengthening processes like structural densification by delignification, crosslinking, and composite manufacturing have proven beneficial in developing high strength wood-based materials [261]. In bast fibres such as hemp, these processes are less explored due to a lower lignin (~9%) and high cellulose content (~75%) [2]. Additionally, it is unknown if such fibres would respond to such treatments in a similar

way to wood. Hence, this preliminary study sought to explore the extent to which hemp fibre assemblies, as well as the integral fibres, would respond to a structural densification treatment. Structurally, wood contains microfibrils having crystalline and amorphous regions of cellulose. In the crystalline region, cellulose molecules possess strong intermolecular hydrogen bonding [269]. These intrinsic properties are advantageous in developing mechanically strong wood-based materials. Horikava et al employed alcoholysis and hydrogen peroxide bleaching on natural wood, resulting in transparent wood without altering chemical functional groups present in cellulose and preserving the 3D microfibrillar structure of wood [270]. In recent research by Tang et al, the natural crystalline-amorphous structure of wood was utilised to produce W-paper exhibiting exceptional mechanical properties. This was achieved by steaming wood samples in sodium chlorite solution for 5 hours at 80˚C, followed by deionisation and air-drying, resulting in a self-densifying wood structure [271]. Song et al used this concept to process bulk wood samples into a material having a specific strength higher than most alloys and metals. This was achieved by boiling wood in a strong alkali solution to partially remove lignin and hemicellulose, followed by hot pressing.

Xiao et al developed an innovative method to modify wood into a strong and flexible material using a water shock treatment [63]. Wood samples were boiled in sodium hydroxide and sodium sulfite solution for 48 hours, followed by washing and air drying for 30 hours, forming a shrunken wood intermediate, which was then immersed in water for 3 min, which is the “water shock treatment”. Being inspired by this methodology and having studied the interesting results from Xiao et al’s work, in this research, we have used a similar approach of using water shock treatment with the objective to densify the hemp fibre microstructure, aiming to enhance tensile properties.

The primary component in wood and hemp is cellulose, amounting to approximately 80% in both. Wood has a multi-layered cell wall structure composed of cellulose, hemicellulose (35%) and lignin (20%), with a thick primary cell wall and thinner outer cell wall giving wood its strength [53]. Hemp fibres are bast-type fibres with single-layered thin cell walls composed of cellulose (~70%), lignin (~10%) and hemicellulose (~20%) [272]. Thus, due to a lower lignin content compared to wood, hemp fibres are flexible and fit for applications in fibre-reinforced composites, textiles and architecture [273]. This study focuses on examining the morphological and mechanical characteristics of nonwoven hemp fabric treated with argon plasma, with an emphasis on maintaining the inherent structural integrity of the hemp fibres. Nonwoven fabrics

produced through needle-punching techniques generally exhibit low tensile strength, a limitation primarily attributed to the random arrangement of fibres and the inherent mechanical properties of the fibres themselves. The research aims to enhance the strength of these fabrics using argon plasma treatment and study their surface morphology and microstructure along with their tensile performance, at both the fabric and individual fibre levels.

The majority of research done on the strengthening of bast fibres such as hemp is confined to fibre-reinforced composites [274], although there lies a tremendous gap in modifying pure hemp fibres in high tensile strength materials without polymeric reinforcement [106] [275]. A recent literature review by Gallos et al [276] mentions the vast scale of work done on incorporating lignocellulosic fibres like hemp in fibre-reinforced composites [276]. In a study by Raja et al, hemp fibres were immersed in an alkali solution for 2 hours, following washing and drying, with the resulting tensile strength being increased over untreated [277]. In a literature review by Siouta et al, novel methods such as acetyl treatment, enzyme treatment and acetone treatments are mentioned, which are useful in protecting the cellulosic structure and removing impurities such as hemicellulose and lignin [278]. Additionally, nano-enhancement by incorporating nanocellulose in natural fibre-reinforced composites proves to be a helpful method for achieving high strength in composite materials [279]. In this study, we give a novel approach to enhance the tensile properties of hemp fibres using a microstructure densification mechanism.

Argon plasma treatment is proven to be useful in surface cleaning, surface modification and surface functionalisation of polymer substrates [280]. One relevant study investigated the effect of argon and air plasma treatments on flax fibres to improve the mechanical properties of flax fibre-reinforced unsaturated polyester composites. The research found that plasma treatment modified the fibre surface, enhancing adhesion in composite materials. However, this study primarily focused on composites rather than pure fibres [281]. Another study investigated the efficacy of plasma treatment on the mechanical properties of natural fibre composites and their interfacial interactions with the matrix in the composite. The findings indicated that plasma treatments optimised the surface structures of the fibres without decreasing tensile strength, suggesting potential benefits for fibre reinforcement in composites. Nonetheless, this research also centred on composite applications [282]. Numerous studies have concluded that employing argon plasma is beneficial in enhancing the fibre-matrix interaction in a composite [283]. Currently, there is a limited amount of

research focused on enhancing the tensile strength of pure hemp fibres and fabrics through sustainable processing methods such as argon plasma treatment. While argon plasma is recognised for its ability to induce surface etching and activation, its specific impact on the internal microstructure of hemp fibres, particularly in terms of fibril alignment, remains insufficiently explored. Additionally, non-cellulosic components such as lignin, pectin, and hemicellulose play a crucial role in determining the mechanical and chemical properties of hemp fibres. However, the extent to which argon plasma treatment modifies these components and influences overall fibre/fabric performance is not yet well understood. Therefore, the objective of this study is to investigate the potential of argon plasma treatment, both independently and in combination with the additional processing step of a water shock treatment, to enhance the structural integrity and tensile strength of hemp fabrics.

6.2 Experimental

6.2.1 Materials

Dew-retted (also known as field-retted) hemp fibres were procured from East Yorkshire Hemp Ltd [108] in the UK. Following a dew retting process lasting six weeks, a series of mechanical processing was conducted by the supplier to yield fibre, prior to baling. The mechanical processing involved shredders to break down hemp stalk into smaller pieces, a decorticator to separate the hemp fibre from the hemp shiv, and lastly, cleaning machinery to remove dust and other debris. Argon gas cylinder (supplied by BOC Ltd.) was used for plasma treatment, and the gas was used without further purification.

6.2.2 Method used to produce nonwoven hemp fabric

Dew-retted hemp fibres from a 1 kg bale were mechanically processed using a Tatham mini PO30 fibre opener, which includes a nipped feed roller and a single-cylinder opener roller, to separate the individual fibres and remove any remaining shiv. The fibre was passed through the opener twice to ensure maximum separation. Following this, the fibres were carded using a lab-scale single-cylinder worker-stripper sample card (Haigh), facilitating thorough disentanglement before forming a web. This process was repeated twice to ensure uniform fibre web formation. Following double cross-lapping, the carded fibre web was processed through a sample needle loom (Bywater Ltd.). This needle-punching loom is equipped with felting needles of 15GG gauge and

lengths ranging from 9 to 16 inches, featuring a twisted (ROT) configuration. Weight assessments were conducted at each processing stage to maintain a consistent GSM of 500. Figure 6.1 illustrates the steps involved in the production of the nonwoven hemp fabric.

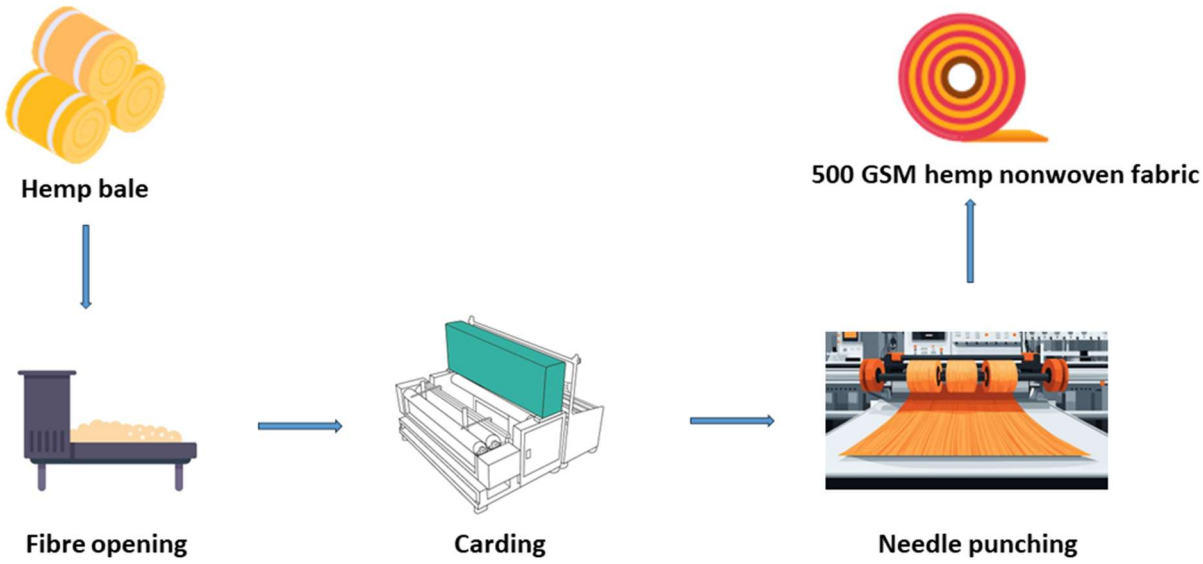

Figure 6.1 Steps in the production of drylaid nonwoven hemp fabric samples (basis weight = 500 g/m^2)

No additional scouring or chemical pre-processing was performed on the nonwoven hemp fabric to ensure that the effects of plasma treatment could be accurately observed. Additionally, plasma treatment itself provides a surface-cleaning effect [24].

6.2.3 Method of surface modification of nonwoven hemp fabric

6.2.3.1 Argon plasm assisted surface modification

Research-grade pure argon gas was used as a plasma source for the treatment of hemp fabric samples. A Diener Zepto plasma machine (Diener Electronic GmbH & Co KG, Germany) was employed for the plasma treatment. The machine is equipped with two needle valves for precise gas supply with gas flow controllers. Operating in manual mode, the system is attached to a Pfeiffer Duo 3 rotary-vane vacuum pump to create a low-pressure environment in the plasma chamber. Hemp fabric samples with approximate dimensions of (35×25) cm were subjected to argon plasma treatment. The argon plasma treatment was conducted at two power levels (intensity of plasma

frequency) of 80 Hz and 40 Hz for treatment durations of *t* = 30, 60, 120, and 180 min. The gas supply for argon gas was maintained at a constant flow rate of 8 standard cubic centimetres per minute (sccm), with a stable pressure of 1.5 mbar within the plasma chamber. After plasma treatment, the fabric samples were conditioned in a standard textile testing environment (ISO 139), with a relative humidity of 65% and a temperature of 20°C for a duration of 48 hours, before characterisation.

6.2.3.2 Method for immediate water shock treatment of hemp fabric

Additional swatches from the produced nonwoven fabric were subjected to plasma treatment under the same parameters, with power levels of 40 Hz and 80 Hz, and treatment durations of 30, 60, 120, and 180 minutes. Immediately after the argon plasma treatment, the samples were immersed in an ice bath (T = 4°C) containing 65% ice and 35% water for exactly 5 minutes. After immersion, the samples were dried in a hot air oven at 40°C until completely dry. The dried samples were then conditioned in a standard textile testing environment (ISO 139), with 65% relative humidity and a temperature of 20°C for a duration of 48 hours, before characterisation.

6.2.4 Method for the evaluation of tensile strength of hemp fabrics

The tensile strength of the hemp fabrics was evaluated following the standard test ISO 9073-3:2023 [131]. Specimens were prepared according to the test, ensuring uniform dimensions and consistent handling to minimise variability. The weight and thickness of each fabric sample were measured before tensile testing. For the tensile strength testing, an Instron material testing system 3366 was used. The gauge length and crosshead speed were set according to the standard, with the gauge length typically at 200 mm and the crosshead speed at 100 mm/min, having 45% break detection. The jaw scheme used for all the tests was J25, with a jaw pressure of 100 psi. For each test, 25 specimens were measured to ensure statistical reliability of the results. The maximum force and elongation at break were recorded, and the stress and strain were determined by the Instron in-built software. All tests were conducted in a controlled environment, adhering to ISO 139 conditions (20°C and 65% relative humidity). The results were analysed using Origin Pro software, and statistical analysis of the data was done using Minitab.

6.2.5 Method to determine the tensile strength of individual fibres

For a deeper insight into the fibre mechanics, the individual hemp fibres were separated from the nonwoven fabric and subjected to fibre tensile strength analysis. The tensile strength of hemp fibres was measured twice, first with a gauge length of 20mm and then with a gauge length of 10 mm. An Instron 5544 universal tensile tester in accordance with the BS EN ISO 5079-2020 standard [130] was used for fibre testing. The test was conducted with a crosshead speed of 20 mm/min. For each treatment variation, n=25 replicates were tested, and the results averaged. Statistical analysis of the tensile strength data was performed using Minitab software. Associated fibre diameters were measured using images captured with a Leica optical microscope and analysed with ImageJ software. All fibre testing was conducted in a standard textile testing environment, maintained at 65% relative humidity and 20°C.

6.2.6 Method to identify alteration in fibre microstructure

The cross-section of fibre samples was analysed under a scanning electron microscope. The sample preparation to capture the internal cross-section of fabric morphology under the SEM involved curing of the fibre bundle in a resin, followed by precision cutting with a microtome. Three different types of resins, Araldite, SPURR resin, and LR White resin, were used. To ensure thorough impregnation, the fibres were immersed in the respective resin solutions and left to soak overnight. This extended immersion period allowed the resin to fully penetrate the fibre structure, ensuring a uniform distribution throughout the material. Following the curing process, the resin-embedded fabric blocks were carefully sectioned using a microtome equipped with a sharp glass blade. This precision cutting technique provided thin, consistent 0.5 μm slices of the resin-fibre composite, suitable for scanning electron microscopy. These samples were then sputter-coated with iridium with a thickness of 20 nm. A Bruker Nova Nano Scanning Electron Microscope was used in a SE mode covering a range of magnifications from 25× to 4000×, with a scan size varying from 1 mm to 3 μm, following the method referred to by Juhaśz et al. [163].

6.2.7 Method to identify chemical alterations in nonwoven hemp fabric

Raman spectroscopy was conducted on the untreated and treated hemp fabrics using a Horiba Raman spectrometer with a microscope. A 785 nm laser source was used to eliminate autofluorescence effects due to components such as lignin, which emit light at wavelengths lower than 600 nm. Each spectrum was obtained by accumulating 32 scans, with a resolution of 4 cm^{-1}, following the standard method outlined by Rygula

et al [166]. To ensure data reproducibility, three spectra were collected for each fabric sample. Additionally, the chemical structure was explored using a Perkin-Elmer FT-IR Spectrum-3 equipped with a single-bounce diamond attenuated total reflection (ATR) accessory. Spectroscopic data were collected at 4 cm^{-1} resolution over 100 scans for untreated, plasma treated and water shock treated samples. The acquired spectra were processed using OriginPro software, which facilitated the editing, analysis, and representation of the spectroscopic data.

6.3 Results and discussion

6.3.1 Fabric tensile strength

The tensile strength of untreated and plasma treated nonwoven hemp fabrics was evaluated and is illustrated in Figure 6.2. Argon plasma treatment appeared to increase the tensile strength of the nonwoven hemp fabric, but the difference was not statistically significant ($P>0.05$). Hemp fibres, especially those which were only dew-retted, exhibited inherent variabilities, most notably in fibre length. Fibre bridging effects may occur during fabric tensile strength testing, potentially resulting in artificially elevated tensile strength values. To maintain consistency, such outliers were excluded during data analysis.

Argon plasma treatment is known to roughen the fibre surface [19], thereby potentially enhancing inter-fibre cohesion and friction. However, this effect could also introduce variability in the results, as surface roughness is influenced by both the duration and intensity of plasma exposure. Argon plasma treatment effectively removes surface impurities such as lignin, hemicellulose, and pectin from dew-retted hemp fibres [19]. It can be hypothesised that the elimination of these non-cellulosic components facilitates stronger inter-fibre friction, leading to improved fibre entanglement and mechanical interlocking. Since tensile strength in nonwoven structures is largely governed by frictional resistance between fibres, variations in plasma treatment parameters can significantly affect the outcome. In a recent study by Sadeghi et al., the tensile strength of dew-retted hemp fibres was evaluated, revealing that a decrease in fibre diameter corresponds to an increase in specific strength per unit area [284]. The strength of a nonwoven fabric is significantly influenced by the properties of its constituent fibres, particularly when those fibres exhibit a high density of imperfections like hemp.

Finer fibres, which are found in nonwoven fabrics made from synthetic materials such as Nylon or PET, possess a higher surface area-to-volume ratio than hemp [285], which reduces the likelihood of large surface flaws or cracks [286]. As fibre diameter decreases, the probability of critical defects diminishes, thereby enhancing the mechanical performance of the fabric. Since the critical stress a material can withstand before failure is directly related to the size of its largest imperfection, fibres with smaller flaws are capable of sustaining higher tensile stresses before rupture [287].

Tensile testing is conducted under controlled environmental conditions, maintaining a relative humidity of 65% and a temperature of 20°C. Prior to testing, the fabrics undergo a 24-hour conditioning period within the testing environment to ensure equilibrium. The argon plasma treatment alters the fibre surface from partially hydrophilic to fully hydrophilic, enhancing moisture absorption [19]. This increased moisture uptake may, in turn, strengthen cohesive forces within the fabric structure, contributing to improved mechanical performance [288].

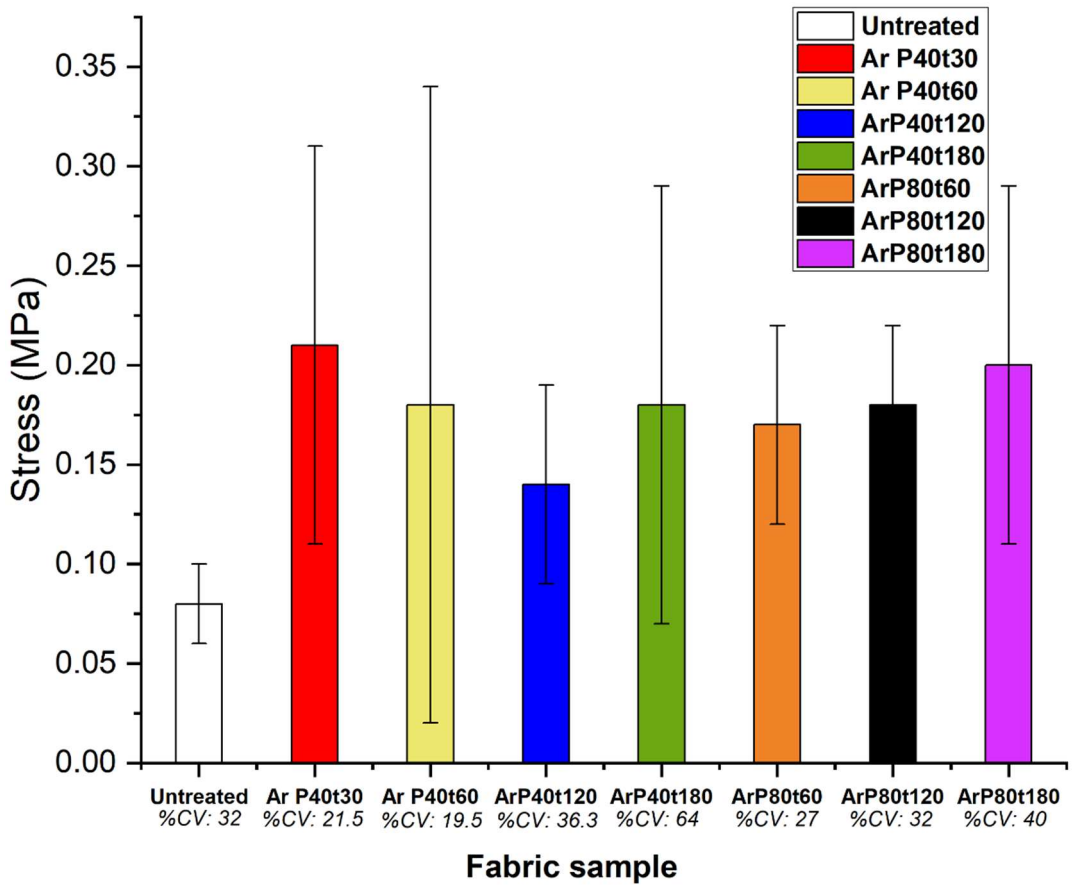

Figure 6.2 Tensile strength of argon plasma treated hemp fabrics, where ArP40t120 resembles argon plasma treatment at 40Hz power at 120 minutes

Table 6.1 presents the key fabric properties, including thickness, GSM, fabric density, porosity, and tensile strength of plasma treated hemp fabrics. Notably, the tensile strength of untreated hemp fabric, averaging approximately 0.08 MPa, demonstrates a promising increase to 0.21 MPa following argon plasma treatment at 40 Hz power for 30 minutes. Despite the comparable standard deviations (0.03 MPa in untreated vs. 0.04 MPa for ArP40t30), this substantial rise highlights that specific treatment parameters could improve the mechanical performance of the nonwoven hemp fabric. This suggests that a 30-minute plasma treatment at 40 Hz power establishes an optimal balance between fibre surface activation and structural integrity, resulting in increased tensile properties.

Argon Plasma Power	Argon Plasma Treatment time	Fabric Thickness	Fabric Basis Weight	Fabric Density	Fabric Porosity	Fabric Stress at Break	Standard Deviation for Fabric Stress at Break
Hz	min	mm	g/m^2	kg/m^3	%	Mpa	Mpa
0	0	5.6	552	99	90	0.08	0.03
40	30	5.5	514	110.8	90	0.21	0.04
40	60	5.5	514	92.5	92	0.18	0.09
40	120	6.15	583.3	95.0	92	0.14	0.09
40	180	4.07	447	109.8	90	0.18	0.06
80	60	5.6	601	105.4	91	0.17	0.06
80	120	5.6	619	109.6	90	0.18	0.06
80	180	4	556	139.3	88	0.2	0.08

Table 6.1 Physical properties of argon plasma treated hemp fabrics

Referring to Table 6.1, a 30-minute argon plasma at 40 Hz power maintains the porosity while improving the strength. As porosity increases, the tensile strength decreases due to a reduction in inter-fibre contact [289]. Argon plasma treatment for a duration of 180 minutes at 80 Hz power results in a fabric having high density with low porosity. This indicates excessive etching or increased compaction in the fabric structure. In a recent study of synthetic fabrics, the release of fibrils from polyester fabric was investigated. The results concluded that fabrics treated with oxygen plasma exhibited lower fibrillation compared to untreated fabrics [290].

Figure 6.3 represents the relationship between fabric tensile stress at break and porosity. Comparing the data in Figure 6.2, Figure 6.3 and Table 6.1 collectively, it can be concluded that the tensile strength of nonwoven hemp fabrics is heavily influenced by fibre-to-fibre interactions [291] as this influences frictional resistance. As the fabric density increases, for example, in the case of fabric plasma treated for 180 minutes at 80 Hz power, the tensile strength shows a notable improvement (~ 0.2 MPa), having a lowest porosity of 88%. This can be due to a higher frictional resistance between the fibres. Lower porosity increases the number of fibre contact points, enhancing the load distribution across the fabric, and increasing the tensile strength [292]. Additionally, this inverse relationship can also be supported by the negative slope of the linear fit in Figure 6.3. The linear regression plot yielded a y-intercept of 0.871 and a slope of -0.0078, indicating a linear decrease in stress with increasing porosity. The extrapolated x-intercept was ~112%, which, while not physically attainable (as porosity cannot exceed 100%), suggests that stress approaches zero at complete porosity. This supports the interpretation that plasma treatment progressively weakens the internal fibre structure [292].

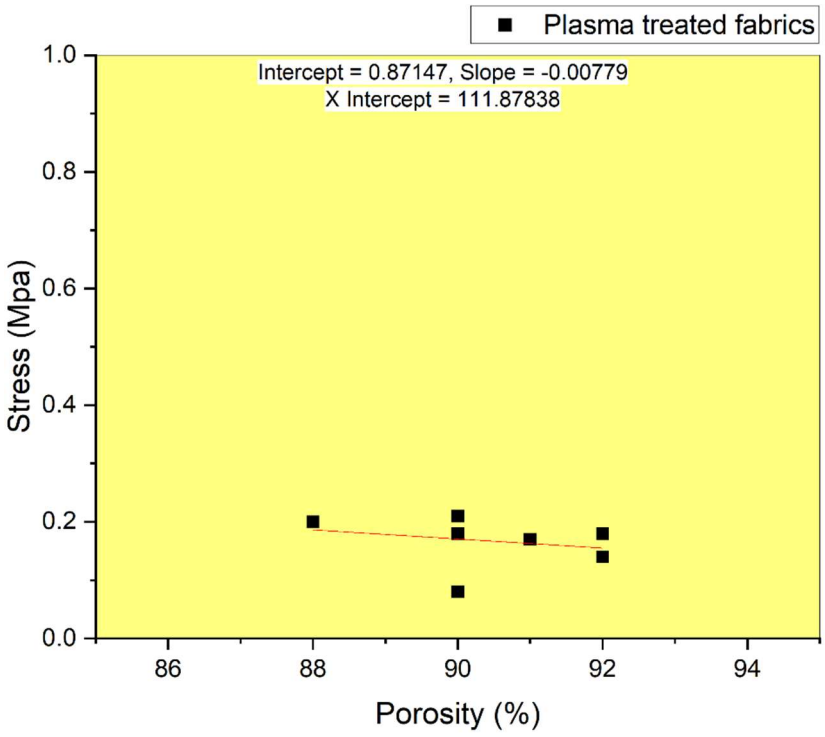

Figure 6.3 Relationship between stress and porosity of argon plasma treated fabrics

In a study done on polypropylene nonwoven fabrics, atmospheric air plasma treatment increased porosity, thereby lowering the tensile strength of the fabric [293]. In a recent

study performed on silicon carbide composites, it was found that pores create stress concentrations leading to failure in the axial direction [294]. The effects of argon plasma treatment on bamboo plant fibres and sisal fibres were investigated by Mosquera et al [295], revealing that a treatment duration of 20 minutes resulted in the highest Young's modulus for the fibres.

A further enhancement in tensile strength is observed when an immediate water shock treatment is applied immediately after argon plasma treatment. Figure 6.4 represents the corresponding tensile strength results for these ‘water-shocked’ fabrics. The tensile strength of these fabrics in Figure 6.4 shows a large increase for one sample compared to the results of argon plasma-only treated fabrics in Figure 6.2. Additionally, the increase in tensile strength is evident from the low standard deviation observed in water shock treated fabrics. However, the fabric that was plasma treated for 180 minutes at 40 Hz power and subsequently immersed in ice-cold water shows a standard deviation of 0.11 MPa, compared to 0.02 MPa for the untreated fabric, which was also immersed in ice-cold water. This suggests that prolonged plasma treatment alters the fibre structure, leading to increased variability. This conclusion is supported by the cumulative variation of 64% observed for this sample. Comparing Figure 6.4 and Figure 6.2, it can be said that the tensile strength increases by approximately fourfold following the additional water shock treatment, suggesting a bulk property change in fibre/fabric structure.

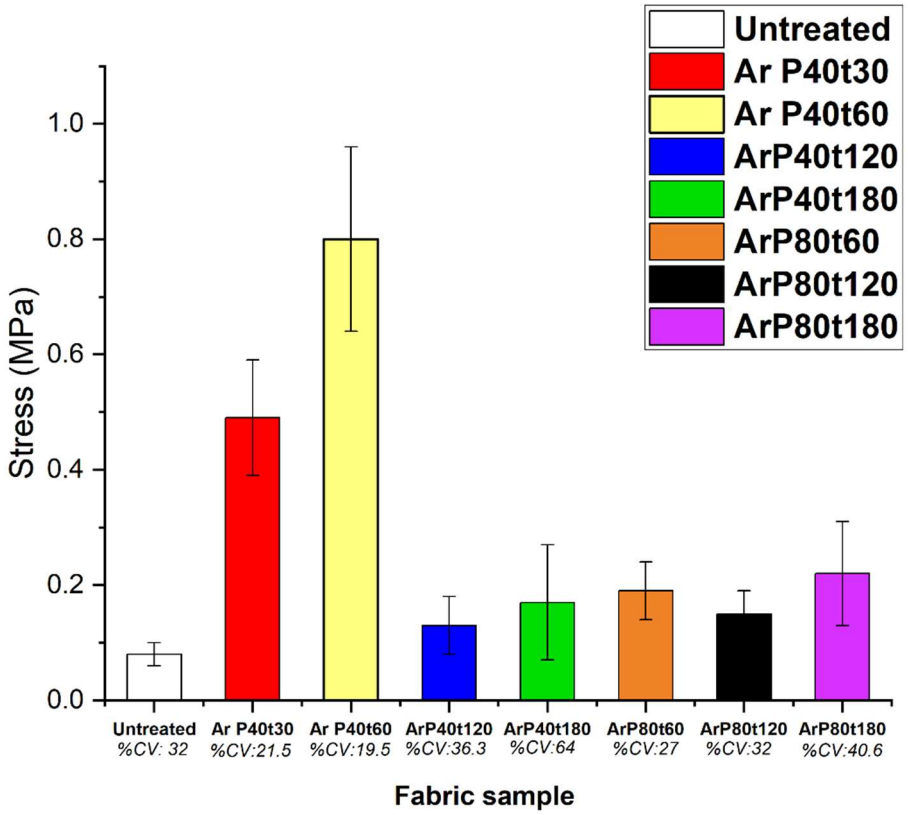

Figure 6.4 Tensile strength of fabrics following water shock treatment where ArP40t30 represents the fabric plasma treated for 30 mins at 40Hz power and then immediately immersed in ice-cold water

Figure 6.5 shows the relationship between fabric porosity and fabric tensile strength for nonwoven hemp fabrics subjected to additional water shock treatment. A steeper slope compared to Figure 6.3 indicates a stronger porosity dependence. Such a slope of -0.027 and a higher stress range (0.5 MPa at 85 % porosity down to 0.1 MPa at 95% porosity) suggests that the additional water shock treatment preserves the modified fibre structure and contributes to densification of the fabric structure. While it is reasonable to expect the fabric to densify when immersed in water, it is unclear if there is any corresponding change in the hemp fibre morphology that contributes to the increased fabric tensile strength. Certainly, the large differences in fabric strength that were observed in fabrics with similar porosities (Figure 6.6), suggest that some other factor contributes to the effect

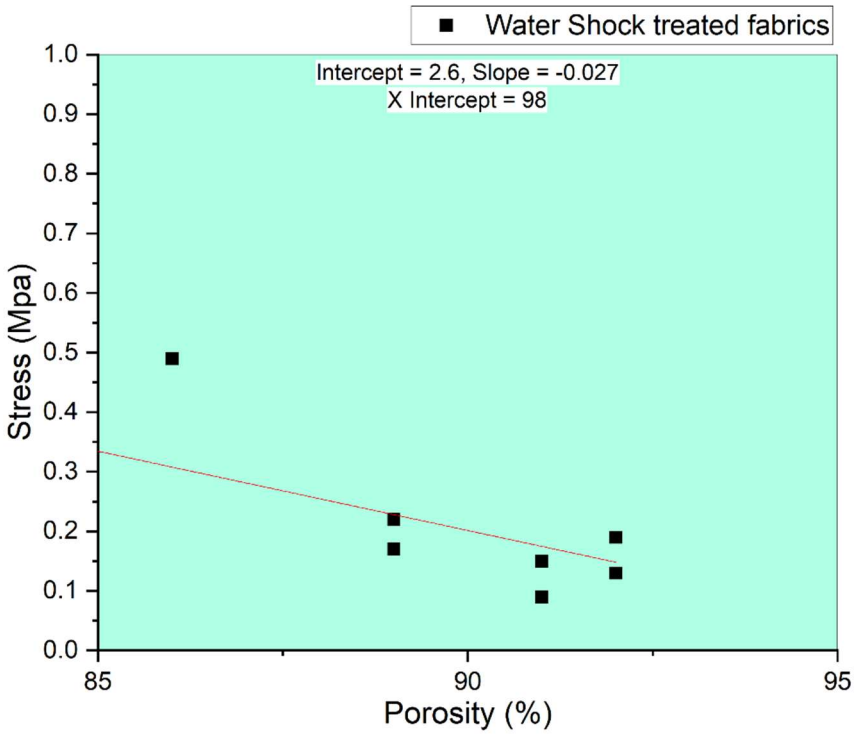

Figure 6.5 Relationship between stress and porosity of water shock treated fabrics

In a study on epoxy, polyurethane, and polypropylene-based composites, the effect of water immersion was investigated. Polypropylene-based composites retained their tensile strength after being immersed in distilled water for 30 days, which was attributed to the strengthening of molecular chains that enabled more efficient load distribution [296]. Another study investigated the water absorption and mechanical properties of epoxy reinforced with bamboo fibres. After immersion in water at various temperatures, the composite exhibited a decrease in tensile strength, indicating that fibre–matrix interactions and water-induced swelling can significantly alter the bulk properties [297]. The study also suggests that the reduction in mechanical performance with increased liquid uptake may result from the formation of hydrogen bonds between cellulose fibres and water molecules [297]. However, since plasma treatment alters the water contact angle from 60° to 0° [19], plasma-treated samples are likely to absorb a greater amount of water compared to untreated ones. The presence of water molecules (-H-OH-) within the fabric structure increases the mobility of macromolecular chains in the amorphous phase, as liquid uptake may act as a plasticiser. This plasticisation leads to significant changes in mechanical behaviour, as evidenced by the increased tensile properties [298]. When water sorption and water solubility tests were performed on resin-based composites for use in dentistry, it was

observed that water helps in filling the voids, however, a prolonged water immersion lowers the tensile properties [299].

Argon Plasma Power	Argon Plasma Treatment time	Fabric Thickness	Fabric Basis Weight	Fabric Density	Fabric Porosity	Fabric Stress at Break	Standard Deviation for Fabric Stress at Break
Hz	min	mm	g/m^2	kg/m^3	%	Mpa	Mpa
0	0	5.6	552	98.2	91	0.09	0.02
40	30	5.05	500	161.4	86	0.49	0.10
40	60	1.4	569	406.7	66	0.81	0.16
40	120	5.2	492.64	94.5	92	0.13	0.05
40	180	2.8	351	126.1	89	0.17	0.11
80	60	4.7	440	93.8	92	0.19	0.05
80	120	4.6	453	98.06	91	0.15	0.04
80	180	3.5	439.5	130.5	89	0.22	0.09

Table 6.2 Physical properties of water-shock treated hemp fabrics

The post-plasma water shock treatment can resemble a cold quenching reaction followed by controlled drying. Such a treatment may increase fibre bonding and structural integrity. Table 6.2 shows the fabric properties of nonwoven hemp fabric after the water shock treatment. A significant increase in strength is seen from 0.09 MPa for the untreated fabric to 0.81 MPa after the water shock treatment. The maximum tensile strength was recorded for hemp fabrics which underwent a water shock following a 60-minute argon plasma treatment at 40 Hz power. In this sample, the fabric density increased, and porosity decreased to 66% along with a drastic reduction in the thickness. This is suggestive of a densification of the fibre structure due to extreme fibre compaction. For the fabrics with an increased plasma treatment time (>120 min), an increase in porosity is seen with a reduction in strength, indicating that fibres may have lost structural integrity. Interestingly, argon plasma treatment for 180 minutes at 80 Hz power showed a moderate tensile strength of 0.22 MPa due to an increase in fabric density, suggesting a compaction in the structure, which can be evidenced by the low thickness of 3.5 mm.

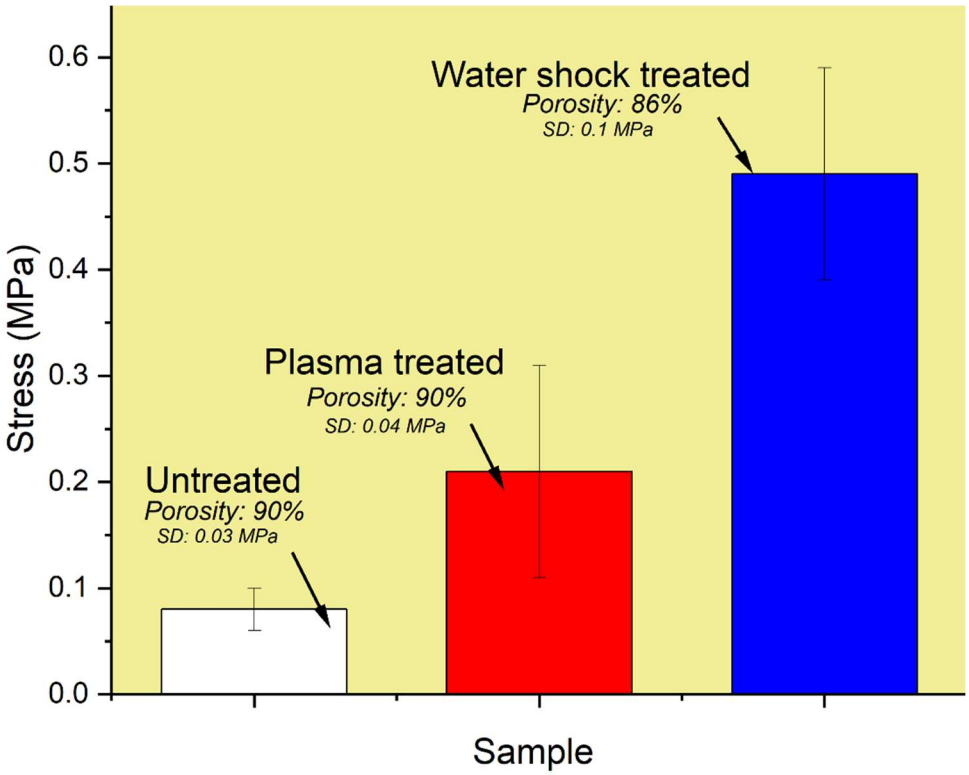

Figure 6.6 Tensile strength of untreated, plasma treated and water shock-treated fabric samples

Figure 6.6 compares the tensile strength of fabric samples across treatments, and all had similar porosities. The plasma treated fibres correspond to those subjected to argon plasma treatment for 30 minutes at 40 Hz power. Similarly, the water shock-treated fabric refers to samples that underwent plasma treatment under the same conditions (30 minutes at 40 Hz power) but were immediately exposed to a water shock post-treatment. These samples were further analysed to determine their chemical and morphological properties.

Argon plasma treatment activates the surface, introducing thermal and chemical stress in the hemp fabric. The immediate immersion of argon plasma treated fabric in cold water may result in rapid stress relief, helping the fibres align and reorganise into a more stabilised structure. This can improve load distribution across fibres, increasing overall strength. In a study performed on hydrated nanocellulose, it was observed that water molecules (H–OH) can replace some of the internal hydrogen bonds within the cellulose chains, initially leading to mechanical weakness. However, as the hydration time increases, the presence of moisture facilitates more uniform stress distribution across the nanocellulosic structure, ultimately increasing tensile strength [300]. Thus,

it can be assumed that residual water molecules may act as a temporary plasticising agent, promoting flexibility and enhancing load transfer within the hemp fabric.

Argon plasma treatment modifies the hemp fabric into a hydrophilic fabric, increasing the ability to absorb water [19]. It can be assumed that water molecules may plasticise the fibre, resulting in a more compact and dense structure having an increased concentration of hydrogen bonds. As the fabric gradually dries at 40°C, these hydrogen bonds formed between adjacent fibres are reinforced, resulting in a strong fabric with a dense architecture. Sinko et. al concluded that cellulose nanocrystals having a high density of intramolecular hydrogen bonds have greater tensile properties [301]. Argon plasma treatment is known to enhance the adhesion properties of a substrate [96]. Additionally, cellulose possesses the inherent ability to form hydrogen bonds [67], which can further contribute to improved interfacial interactions. In a recent research, molecular dynamics simulations were used to investigate the wood structure. The findings revealed that cellulose microfibrils play a dominant role in the longitudinal mechanical properties of wood, particularly in its strength. Additionally, hemicellulose and lignin are susceptible to moisture-induced weakening because of their swelling behaviour [302]. Hence, it can be concluded that argon plasma treatment for 30 minutes etches and activates the lignin–hemicellulose rich surface layer, thereby increasing the specific surface area. This modification also facilitates swelling of the constituent fibres when the fabric is immersed in water immediately after plasma treatment. Subsequent gradual drying at 40°C promotes the formation of hydrogen bonds within the predominantly cellulosic fibre structure. As a result, elevated tensile strength is observed following the water shock treatment.

Hence, to validate these hypotheses, tensile strength tests on individual fibres and microstructural analysis using SEM were done. The samples treated with argon plasma for 30 minutes at 40 Hz power were selected for further analysis as they demonstrated an optimal balance between fibre surface activation and structural integrity, as indicated by the significant improvement in tensile strength. Similarly, for the water shock-treated samples, the same plasma treatment parameters (argon plasma for 30 minutes at 40 Hz power) were maintained to ensure consistency in processing conditions. This allowed for a direct comparison of the additional effects introduced by the immediate water shock treatment, providing a clearer understanding of how this combined approach influences the mechanical and structural properties of the fabric.

6.3.2 Fibre tensile strength

Fibre tensile properties highly influence the tensile strength of the bulk nonwoven fabric. Strong individual fibres can bear more load, which enhances the overall strength of the fabric [303]. In needle-punched fabrics, the mechanical bonding (physical fibre entanglement) between corresponding fibres may be weak, or if the fibres are not well-aligned in the direction of loading, the fabric may not fully utilise the collective strength of the individual fibres [304]. Thus, to understand the extent to which the treatments had influenced fibre tensile properties, individual fibre tensile strength tests were performed with gauge lengths of 20 mm and 10 mm were performed on the fibres. Figure 6.6 reports the stress-strain curves for individual hemp fibres obtained at a gauge length of 20 mm.

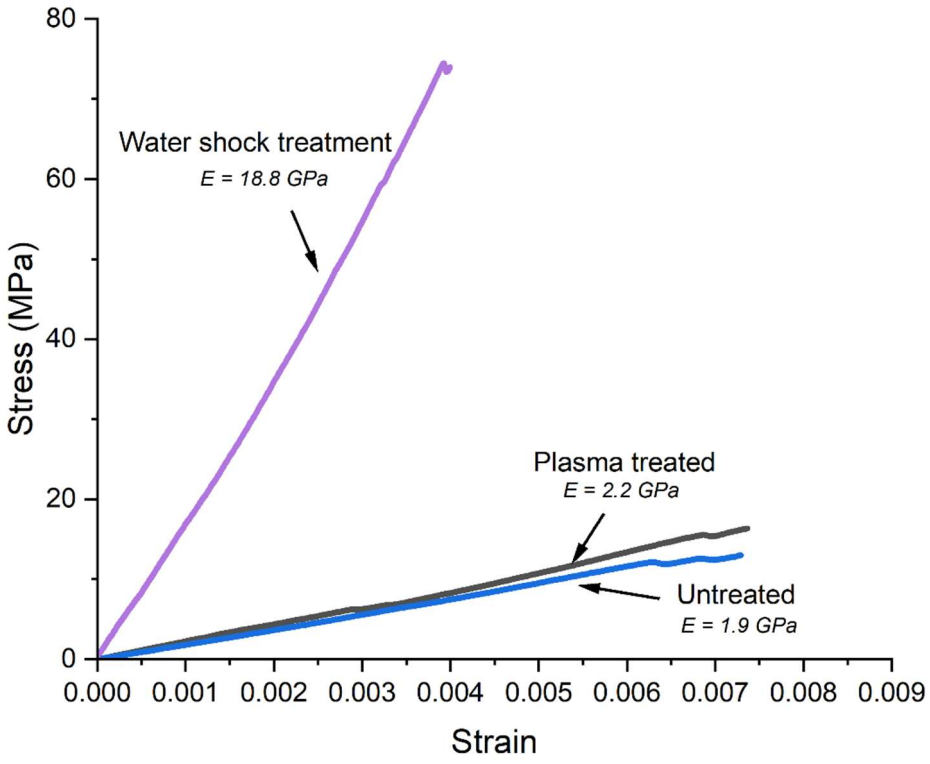

Figure 6.7 Tensile strength of untreated, as well as argon plasma treated hemp fibres before and after cold water shock treatment (gauge length = 20mm)

Referring to Figure 6.7, it can be inferred that the tensile strength of untreated and plasma treated fibres both have a similar tensile strength of ~20 MPa. Interestingly, water shock treated fibres have a tensile strength of ~80 MPa, suggesting a four-fold increase. In Figure 6.7, “E” represents the Young’s modulus. The modulus remains relatively unchanged after plasma treatment, at approximately 2 GPa. However, it increases markedly to around 18 GPa following the water shock treatment. In a study

done on alkali-treated hemp fibres, it was observed that alkali treatment increases the Young's modulus due to the removal of lignin and hemicellulose in the fibre structure [305].

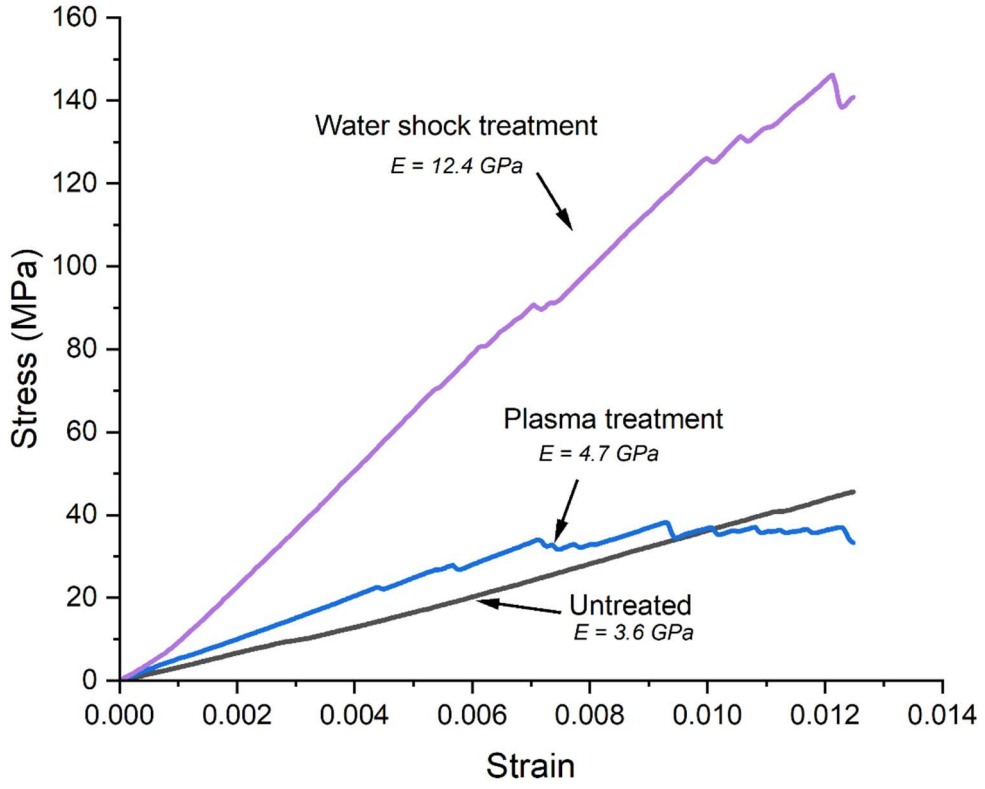

Figure 6.8 Tensile strength of untreated, as well as argon plasma treated hemp fibres before and after cold water shock treatment (gauge length = 10mm)

Figure 6.8 shows the stress-strain curves for tensile strength testing of individual hemp fibres with a shorter gauge length of 10 mm. Testing with shorter gauge lengths reduces the effect of weak places along the fibre length from affecting the results and ensures that the load is more evenly distributed across the fibre, leading to a more precise determination of its strength [306]. As observed at the longer 20 mm gauge length (Figure 6.7), the tensile strength of untreated and plasma treated fibres remains relatively unchanged. However, in 10 mm gauge length test (Figure 6.8), a sevenfold increase in fibre tensile strength is observed in fibres subjected to the water shock treatment, reaching approximately 140 MPa. Moreover, a decrease in Young's modulus to around 12 GPa is observed when compared to the value obtained from the 20 mm gauge length test. This reduction may be attributed to variability in fibre diameter, as supported by Placet et al. [307], or to gauge length sensitivity. Nevertheless, this does not alter the conclusion that individual fibres are indeed strengthened as a result of the water shock treatment.

Prominent stick-slip effects (a change of frictional resistance without a decrease to zero) are observed in plasma-treated samples, and these effects are also evident in water shock treated samples in Figure 6.8, compared to the fibre tensile strength results at a 20 mm gauge length shown in Figure 6.7 [308]. At shorter gauge lengths, such as 10 mm, the testing apparatus is more likely to detect localised variations in surface topography, resulting in intermittent contact and slippage. In contrast, longer gauge lengths like 20 mm provide an averaging effect over a greater length of fibre, which helps smooth out these local irregularities and reduces the prominence of stick-slip behaviour. Zhang et al. studied the stick-slip behaviour in cellulose nanocrystals and found that it primarily arises from the presence of dense hydrogen bonds within the structure. During mechanical testing, these hydrogen bonds act like shock absorbers, initially resisting the applied force and resulting in a "stick" phase. When the applied force exceeds a certain threshold, the hydrogen bonds undergo rotation around their axes and eventually break, leading to a "slip". This cyclical stick-slip mechanism is a key contributor to the observed mechanical response in cellulose-based materials [309]. Hence, referring to Figure 6.8, it can be inferred that the hydrogen bonds in plasma treated fibres may be relatively weak compared to those formed in water shock treated fibres. The stronger hydrogen bonding in water shock treated fibres helps resist stick-slip behaviour more effectively. This enhanced resistance likely contributes to the observed increase in Young’s modulus for these fibres.

These fibre tensile strength results suggest that plasma treatment remains confined to the surface without modifying the internal structure of dew-retted hemp fibres [19]. In contrast, the water shock treatment greatly strengthens the fabric as well as the fibre, suggesting a modification in the internal structure of the fibre and also the fabric. For all fibres, a shorter gauge length test like the 10mm test (Figure 6.8) shows a higher tensile strength than the 20mm test. However, in the case of water shock treated fibres, an increase from 80 MPa to 140 MPa suggests that there can be densification of the fibre structure resulting in such an increase. To gain a deeper understanding of the structural modifications, scanning electron microscopy (SEM) was performed on both the cross-section and surface morphology of the fibres. Additionally, a diameter analysis was conducted to assess any changes in fibre dimensions resulting from the treatments.

6.3.3 Analysis of fibre diameter

Figure 6.9 presents the diameters of untreated, plasma-treated, and water shock treated hemp fibres. Although hemp fibres naturally exhibit considerable variation in diameter, the data in Figure 6.9 clearly show a significant reduction in diameter following water shock treatment. Untreated fibres have an average diameter of approximately 220 μm, which decreases to around 180 μm after plasma treatment. This reduction indicates that plasma treatment induces surface-level modifications without significantly affecting the internal structure of the fibre. Given the inherent variability in hemp fibre diameter, such a difference is considered negligible, as also noted by Placet et al. [307]. Therefore, it can be concluded that plasma treatment primarily roughens the fibre surface by forming 'nanopores', rather than altering its internal microstructure.

A reduction in fibre diameter is observed in the case of water shock treated fibres, measuring approximately 100 μm. This suggests that hemp fibres undergo swelling when immersed in water immediately after surface activation and etching by argon plasma, followed by shrinkage during drying at 40°C. In a recent study on microfibrillated cellulosic paper, it was observed that cellulose fibres, when in a swollen state, tend to rearrange into a more aligned configuration, resulting in a mechanically stronger and more resistant structure [310]. A similar mechanism may be occurring in this case, as plasma treatment creates additional surface voids [311], potentially allowing more water molecules to penetrate the cellulosic structure. This enhanced water uptake could lead to greater swelling than usual, promoting the realignment of cellulose fibrils. Gradual drying at 40°C may then facilitate the formation of new hydrogen bonds in this reorganised structure, contributing to the improved mechanical properties observed after water shock treatment.

Theoretically, the strength of the fibre is influenced by the microscopic defects, particularly the diameter in this case. As the diameter of the fibre increases, the possibility of such defects increases, failing to resist stress. A study using Weibull analysis on sisal fibres demonstrated an inverse relationship between tensile strength and fibre diameter. Sisal fibres with diameters less than 50 μm exhibited the highest tensile strength. Such an inverse relationship suggests that fibres with smaller diameters possess greater strength [312], which can be concluded from the results in Figures 6.7, 6.8 and 6.9. Similarly, another study on hemp fibres found that fibre diameter significantly influences tensile properties, particularly the Young's modulus. This dependency is primarily attributed to microstructural deficiencies. Lower tensile

strength may also indicate a higher microfibril angle, which is the angle at which cellulose microfibrils are oriented within the fibre wall, and is often associated with reduced crystallinity and, consequently, weaker mechanical performance [307].

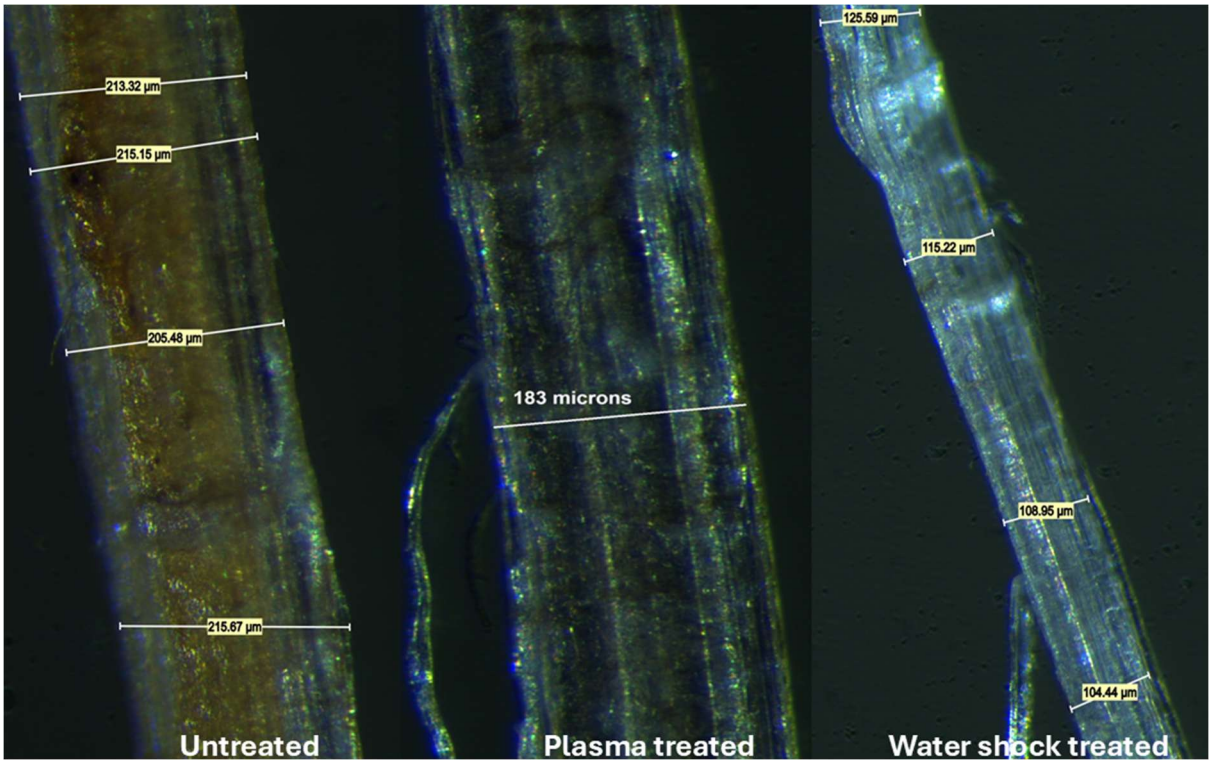

Figure 6.9 Comparison of hemp fibre diameter before and after argon plasma treatment for 30 mins at 40 Hz power and cold water shock treatment

Following an immediate water shock treatment, the diameter reduces to an average of 100 µm. This suggests an extreme contraction, i.e. internal densification of the structure, which could also be consistent with the greater alignment and proximity of adjacent cellulose fibrils. It can be hypothesised that the rapid cold water shock may shrink the cellulose fibrils, resulting in a densified structure. In biological materials such as hemp, which is a plant-based fibre, there is an inherent ability to change shape through the absorption or release of water. This phenomenon is known as hydro-actuated deformation [313]. Structurally, hemp fibres consist of a cell wall made up of lignin and bundles of cellulose microfibrils. The cellulose microfibrils, which are aligned axially, are stiffer compared to the surrounding lignin matrix. When hemp absorbs water, the cellulose microfibrils swell, and as the water is gradually released, the structure undergoes shrinkage [314].

6.3.4 Internal morphology of hemp fibres

Figure 6.10 presents SEM micrographs depicting the internal morphology of the hemp fibres. Hemp fibres possess a multi-layered fibrillar structure, which is evident in the micrographs of untreated samples. Referring to Figure 6.10, these fibrils are bound together by an outer cell wall primarily composed of lignin, with the core structural component of the fibres being cellulose [315]. The cross-sectional view in Figure 6.10 distinctly reveals the arrangement of internal fibrils, providing insight into the hierarchical organisation of the fibre structure. In plasma-treated fibres, the SEM micrographs reveal the presence of multi-layered fibrils with noticeable fibrillation, indicating surface etching and structural modification. However, this fibrillation is absent in water shock-treated samples. Instead, the water shock-treated fibres exhibit a densified structure with fused fibrils, suggesting that the immediate water shock promotes compaction and structural reinforcement rather than fibrillation.

The diameter of the untreated fibre is about 220 μm, having a multilayered fibrillar internal structure with a tensile strength of approximately 20 MPa. This indicates that the fibre has numerous weak points where fibrils can slip or break. Argon plasma-treated fibres exhibit an average diameter of 180 μm, with noticeable fibrillation observed in cross-sectional micrographs. Despite this fibrillation, the tensile strength remains comparable to that of untreated fibres, suggesting that argon plasma primarily etches the fibre surface, increasing surface area and fibrillation without significantly altering the internal structure. In contrast, water shock treated fibres display a reduction in diameter, with fibrils appearing fused in the cross-sectional micrographs. This structural densification indicates that water shock treatment promotes fibre compaction, likely due to an increase in inter-fibre hydrogen bonding during the gradual drying phase following the sudden cold water immersion. Argon plasma treatment plays a crucial role in this process by activating the fibre surface and inducing fibrillation. When immediately subjected to ice-cold water, newly formed hydrogen bonds contribute to fibril fusion. The significant enhancement in both fibre and fabric tensile strength can be attributed to rapid fibre shrinkage and compaction, reinforcing the overall structural integrity. These structural and mechanical modifications were observed in wood and are discussed in the review by Singh et al. [316]

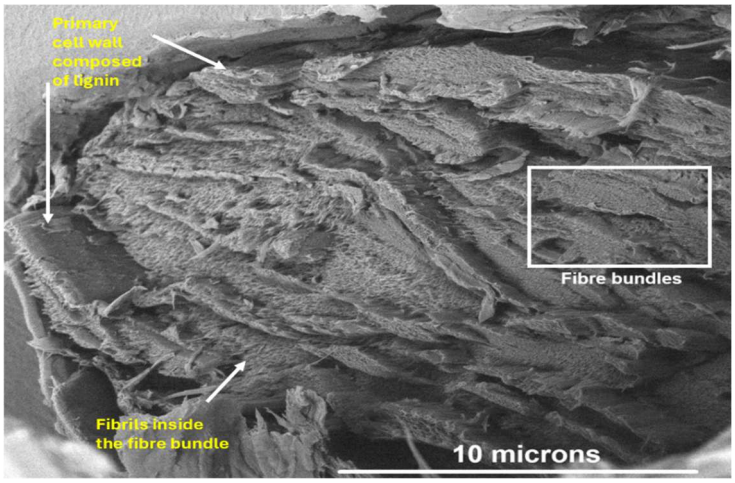

A)Untreated (5000×)

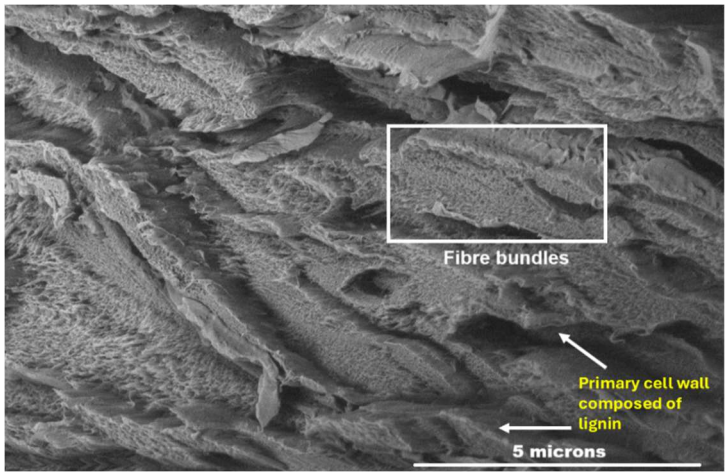

B)Untreated (10000×)

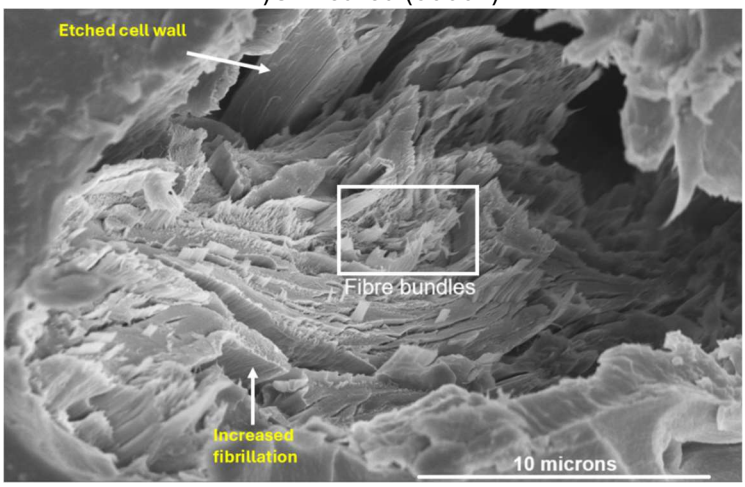

C)Argon plasma treated (5000×)

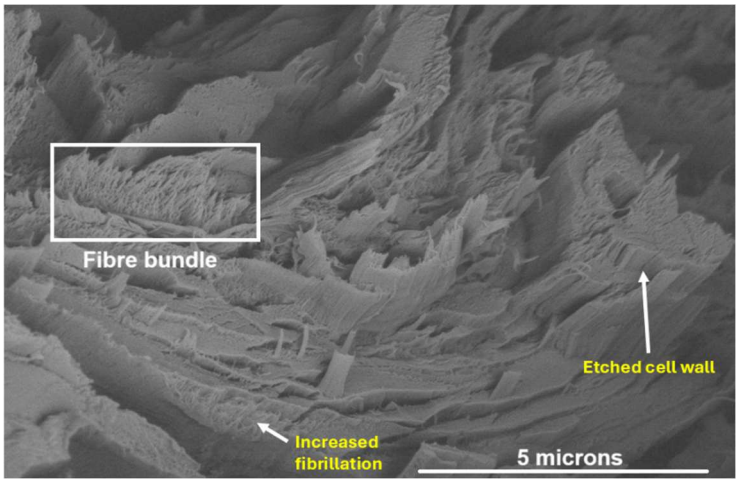

D)Argon plasma treated (10000×)

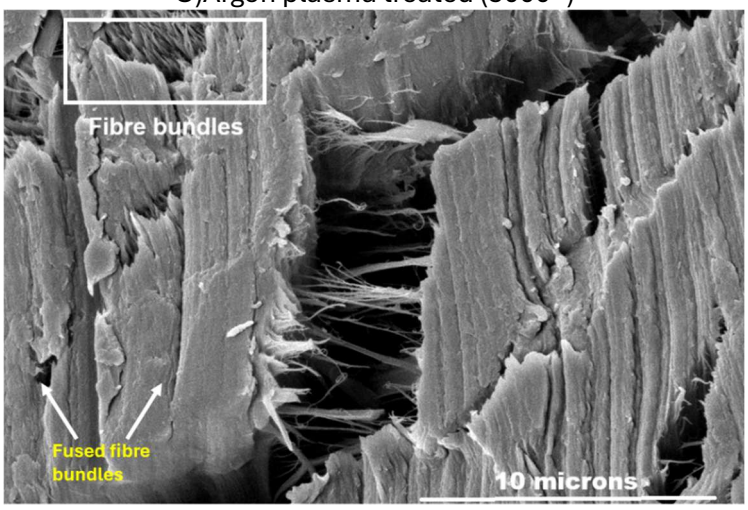

E)Water shock treated (5000×)

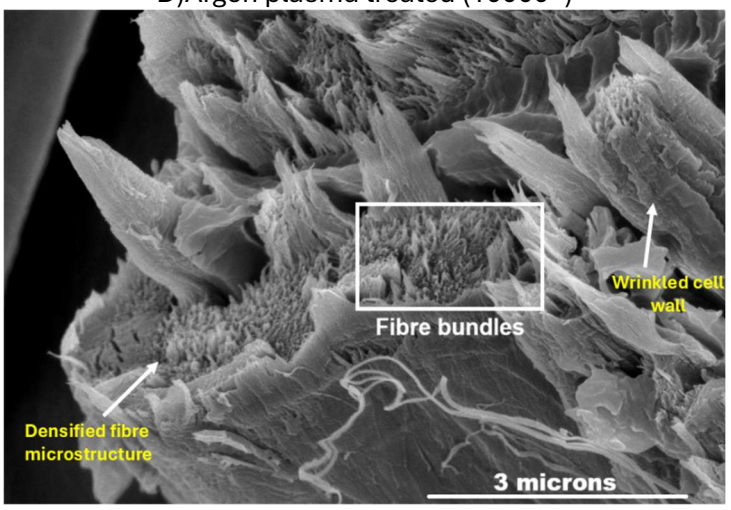

F)Water shock treated (10000×)

Figure 6.10 10µm and 5µm SEM micrographs of the internal structure (cross-section) of untreated, argon plasma-treated (Power = 40Hz; t = 30 mins) and cold water shock treated (Power = 40 Hz; t = 30 min following immediate immersion in cold water) fibre

To gain a deeper understanding of the surface morphology of untreated, argon plasma-treated, and water shock-treated fibres, SEM micrographs were captured and analysed.

6.3.5 Surface morphology of untreated, argon plasma treated and cold water shock treated hemp fibres

Figure 6.11 presents SEM micrographs illustrating the surface morphology of untreated, argon plasma-treated, and water shock-treated hemp fibres. The untreated fibres (Figure 6.11A) exhibit a relatively smooth surface, characteristic of dew-retted hemp fibres, which is further confirmed at higher magnification in Figure 6.11B. Following a 30-minute argon plasma treatment, SEM images (Figure 6.11C) reveal noticeable fibrillation with etching at low magnification, while a highly porous and etched pattern becomes evident at higher magnification (Figure 6.11D). Argon plasma is known to etch fibre surfaces, creating a nanoporous structure. This observation aligns with the porosity measurements in Table 6.1, which show a slight increase in porosity compared to untreated fabric, suggesting the formation of nanopores due to plasma treatment. Similar fibrillation and etching effects were reported in a prior study where a 10-minute argon plasma treatment induced nanopore formation on woven hemp fibres [19]. The water shock-treated fibres exhibit a distinctly different morphology. At low magnification, a densified and fused fibre structure is observed, indicating compaction. However, at higher magnification, while nanopores remain visible, distinct layered structures appear on these pores, suggesting a structural transformation induced by the rapid immersion in water (Figure 6.11F).

SEM micrographs of both the lateral section (Figure 6.10) and longitudinal section (Figure 6.11) provide insight into the structural transformations occurring in water shock treated fibres. Similar structural changes were observed in the water shock treatment study done on wood [63]. Kumar et al., in a literature review [317], points out the positive influence on the delignification of wood mechanically and structurally [317]. The SEM images of untreated, plasma treated, and water shock treated fibres show a modification, and the analysis supports the assumption of structural densification. To gain insight into the chemical structure of the fibres, Raman and FTIR spectroscopy were performed.

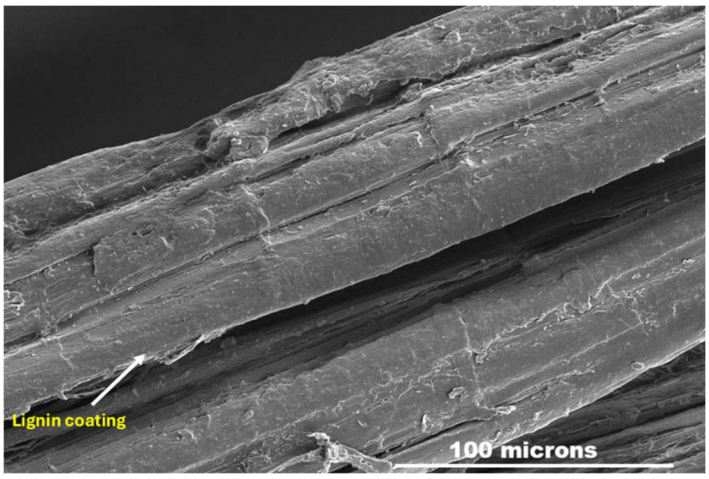

A]Untreated(500×)

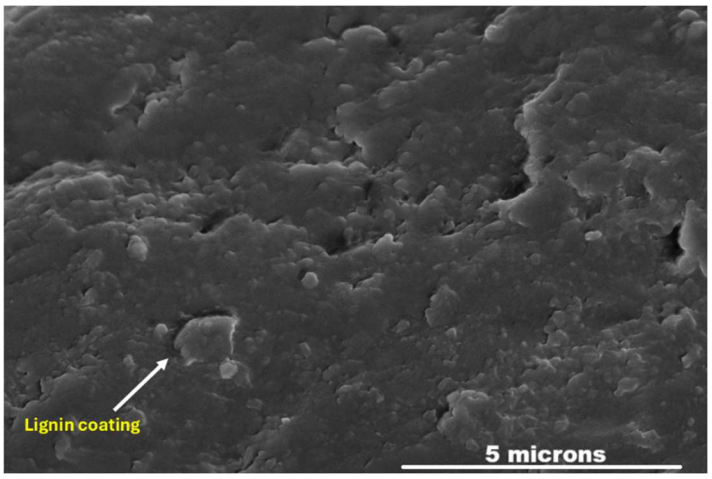

B]Untreated(10000×)

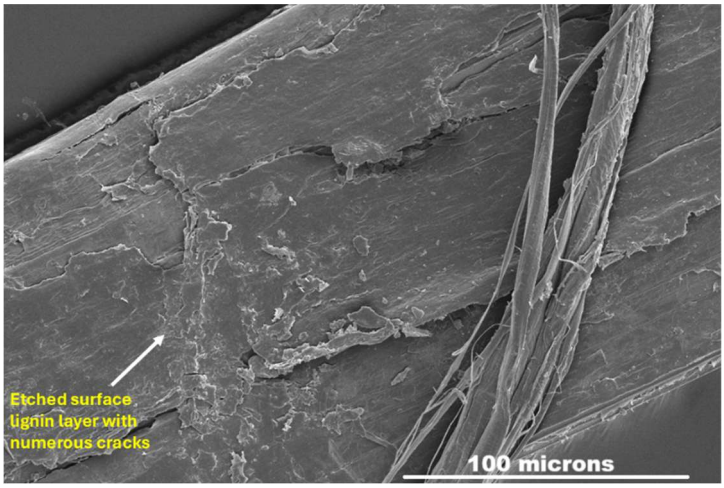

C]Plasma treated (500×)

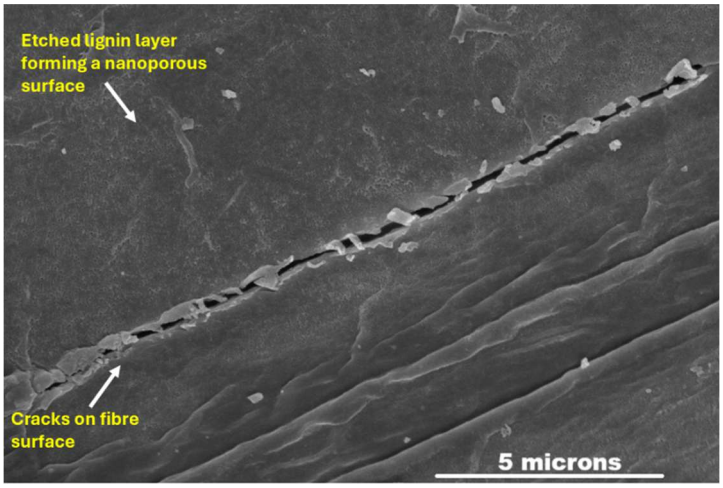

D]Plasma treated (10000×)

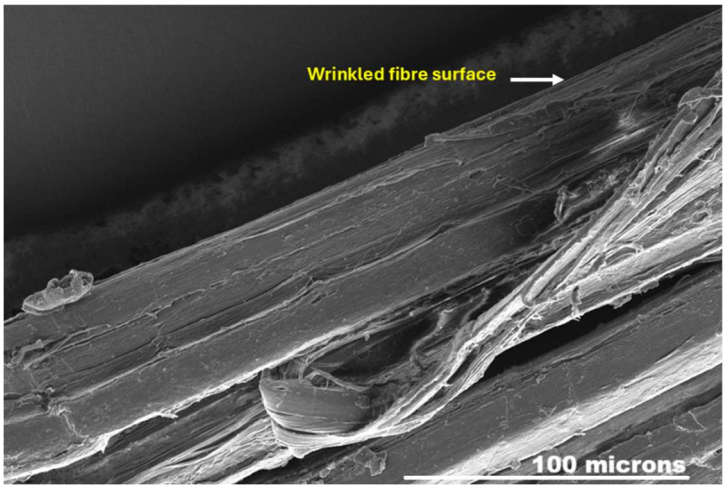

E]Water shock treatment (500×)

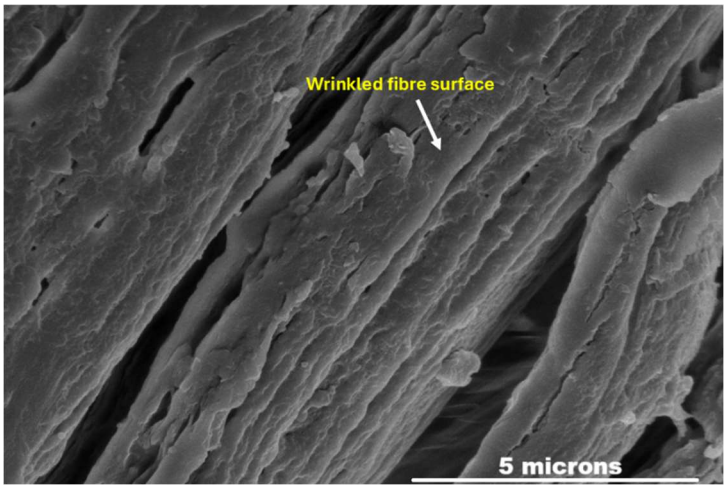

F]Water shock treatment (10000×)

Figure 6.11 SEM micrographs showing the surface morphology of untreated, argon plasma treated (Power = 40Hz; t = 30 mins) and cold water shock treated (Power = 40 Hz; t = 30 min following immediate immersion in cold water) fibres at a magnification of 500× and 10000×

6.3.6 Raman spectroscopy of fibres

Figure 6.12A presents the Raman spectra of untreated, argon plasma treated (for a duration of 30 minutes at 40 Hz power), and cold water shock treated hemp fabrics. To provide a more detailed analysis, Figure 6.12B highlights an enlarged view of the spectra within the wavelength range of 0 to 400 cm^{-1}, capturing subtle structural variations. Similarly, Figure 6.12C focuses on the wavelength range of 500 to 900 cm^{-1}, allowing for a closer examination of characteristic vibrational modes associated with molecular changes induced by plasma and water shock treatments. Notable broad peaks can be seen for water shock treated fabric. Untreated and plasma treated fabrics exhibit similar peak heights.

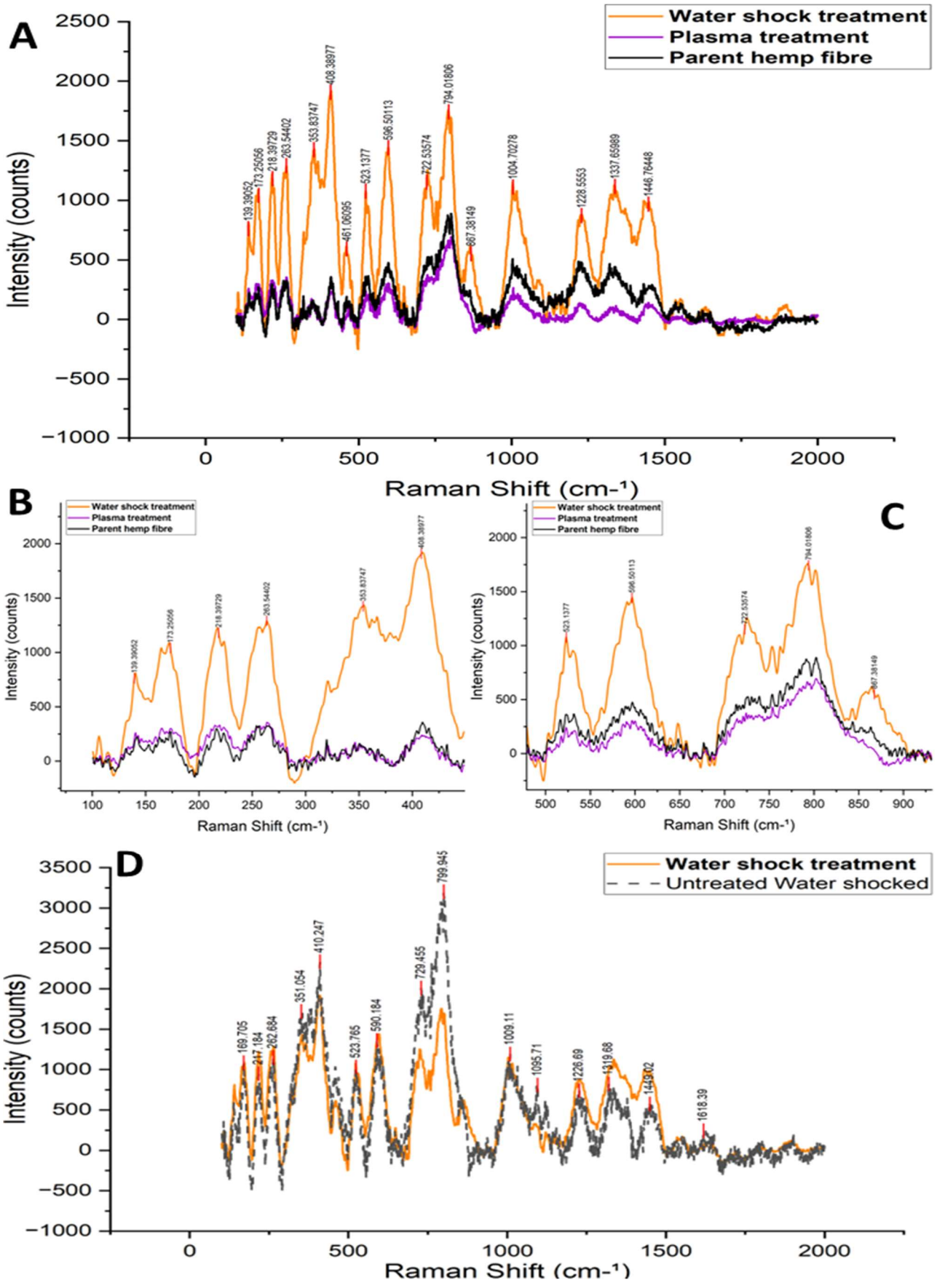

Figure 6.12 Raman spectra of untreated, plasma treated and water shock treated hemp fabric

Hemp fibres primarily consist of cellulose, and the vibrational frequencies associated with cellulose predominantly fall below the 1500 cm^{-1} range [121]. Consequently, the Raman spectra presented in Figure 6.12 can be attributed primarily to cellulose-related molecular vibrations [121]. In the fingerprint region (0 - 400 cm^{-1}), bond vibrations correspond to lattice movements, -C-O-C bending modes, and C-C stretching modes [318]. As shown in Figure 6.12B, distinct peaks appear at 139 cm^{-1}, 173 cm^{-1}, 218 cm^{-1}, 353 cm^{-1}, and 408 cm^{-1}. These peaks can be assigned to COH bending, CCC, COC, OCC, and OCO skeletal bending modes, respectively. Additionally, the characteristic glucopyranose ring breathing mode is evident within this spectral region [121] [318] [319]. Spectral bond vibrations in the fingerprint region of 400 to 650 cm^{-1}, as shown in Figure 6.11C, are primarily associated with -C-C and -C-H bonds. Prominent peaks are observed at 523 cm^{-1}, 596 cm^{-1}, 722 cm^{-1}, 794 cm^{-1}, and 867 cm^{-1}. These peaks correspond to CH_2 rocking, COC skeletal stretching, which is characteristic of lignin and C-C ring breathing vibrations [121, 318]. The spectral region between 1000 and 1400 cm^{-1} is indicative of C-O stretching, C-C stretching, and CH_2 asymmetric bending, all of which are associated with the cellulose polymeric chain. Peaks corresponding to these vibrational modes are observed in Figure 6.12A at 1000 cm^{-1}, 1228 cm^{-1}, 1337 cm^{-1}, and 1446 cm^{-1}. Additionally, lignin and hemicellulose contribute to this region, as CH_2 wagging and CH bending signals appear within the 1250 to 1450 cm^{-1} frequency range. Similar peaks in Raman spectra were seen in densified wood after water shock treatment [63].

A noticeable variation in bond vibration intensity is observed between argon plasma treated and untreated fabrics, with argon plasma treated (30 minutes at 40 Hz power) samples exhibiting slightly lower Raman intensity. This suggests that argon plasma treatment may enhance surface energy, potentially leading to a reduction in Raman signal intensity [19]. Additionally, as illustrated in Figure 6.11, argon plasma induces etching on the fibre surface, which could result in increased diffusion of the scattering signal, further contributing to the observed decrease in Raman intensity. Conversely, a significant increase in peak heights is evident in water shock treated fabrics. This can be attributed to a higher concentration of molecular bonds within the densified fibre structure. A recent study investigated the densification of SiO_2 glass using Raman spectroscopy. The findings revealed that with increasing densification, the Raman shift also increased, accompanied by higher peak intensities, particularly in the glass samples subjected to the highest pressure [320]. Hence, when a high-intensity laser

interacts with the compacted structure of water shock treated hemp fabric, the densely packed bonds within a confined area produce stronger bond vibrations, resulting in a pronounced Raman intensity.

The Raman spectra reveal a notable increase in intensity across multiple peaks for water shock treated fibres compared to both plasma treated and untreated fibres. This suggests significant structural modifications at the molecular level, potentially indicating enhanced intermolecular interactions, such as stronger hydrogen bonding [321]. In contrast, argon plasma treated fibres exhibit only slight intensity variations relative to untreated fibres, reinforcing the observation that plasma treatment primarily affects the fibre surface without substantially altering the internal molecular structure. The observed decrease in Raman shift can be attributed to the interaction of argon plasma with the lignocellulosic surface, leading to the formation of reactive species such as $OH^{\cdot}$ radicals or OH^{-} ions. In a recent study, glucose was treated with atmospheric gas plasma composed of Ar, O_2, and N_2, and the results showed that glucose underwent oxidation following the plasma treatment [322]. However, similar oxidation may not occur in the case of hemp fibres due to their highly complex and heterogeneous structure, which differs significantly from the simpler molecular structure of glucose. Additionally, when correlated with the SEM images, the presence of nano-pores formed due to argon plasma does not indicate drastic changes in molecular bonding. Although the pronounced intensity variations in water shock treated fibres imply a distinct molecular reorganisation, likely driven by fibril densification observed in SEM micrographs [63]. This structural transformation correlates with the enhanced tensile properties observed in mechanical testing, where the tensile strength increased significantly, reaching up to 140 MPa in tests conducted with a 10 mm gauge length. This improvement can be attributed to the reinforcement of intermolecular interactions and the fusion of fibrils, ultimately contributing to a more compact and robust fibre structure.

Figure 6.12D presents the Raman spectra of water shock-treated fabrics (argon plasma-treated followed by immediate ice water immersion) and untreated water shock-treated fabrics (untreated fabric subjected to ice water immersion). The presence of identical peaks in both spectra confirms that water acts as a driving force for the observed high-intensity peaks [323]. However, as indicated by the tensile strength results, the strength of untreated water shock treated fabric remains comparable to that of untreated fabric. This suggests that while water alone influences the molecular structure, it does not enhance mechanical strength. Instead, argon

plasma treatment plays a crucial role by activating the fibre surface, facilitating the formation of strong intermolecular bonds upon ice-water immersion. These strong bonds thus transform the fibre and the fabric into a strenuous material.

6.3.7 ATR-FTIR spectroscopy

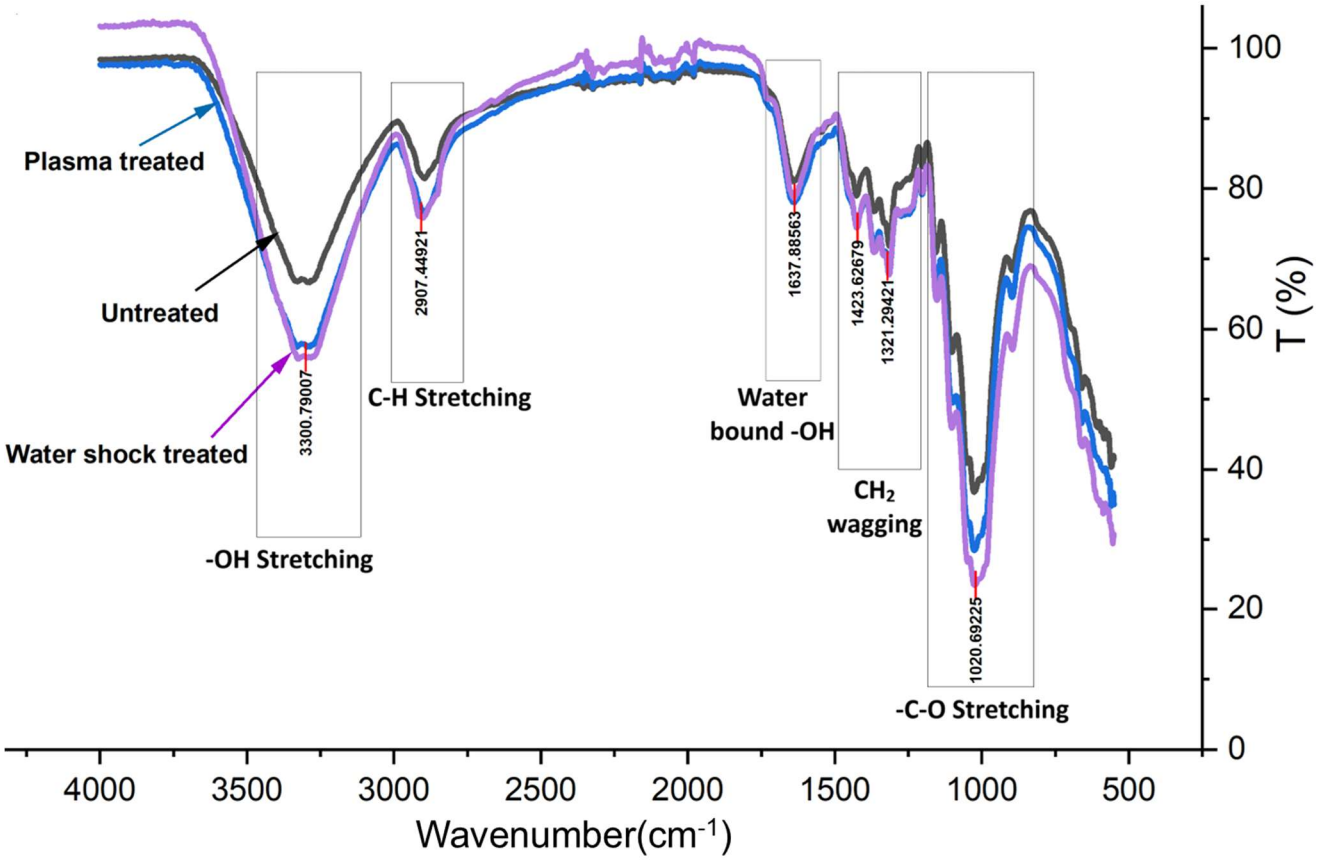

Figure 6.13 ATR-FTIR spectra of untreated, argon plasma treated and cold water shock treated hemp fibres

Figure 6.13 presents the ATR-FTIR spectra of untreated, argon plasma treated, and cold water shock treated fibres. The results indicate clear chemical modifications following both treatments, with notable changes observed in the -OH functional group region. In hemp fibres, -OH stretching vibrations typically appear between 3200 and 3600 cm^{-1} [177]. The sharpness and intensity of this peak reflect the density of -OH groups. Plasma treatment appears to polarise the surface -OH groups, making them more detectable by ATR-FTIR. Water shock treated fibres exhibit an -OH peak of the same intensity, suggesting a slight alteration in the density of hydroxyl groups, likely due to structural rearrangements and increased hydrogen bonding facilitated by the

treatment. Moreover, intermolecular hydrogen bonding in cellulose chains can also be detected in this region [324]. The -CH stretching peak at approximately 2900 cm^{-1} also shows increased intensity following plasma treatment, which becomes even more pronounced after water shock treatment. This enhancement is attributed to the structural densification observed in Figure 6.10, and the ATR-FTIR spectra further support the trends noted in the Raman analysis. The intensification of this peak is likely due to the surface etching effect of plasma treatment, which forms nanopores on the fibre surface (as shown in Figure 6.11), leading to the removal of amorphous impurities and resulting in sharper, more defined spectral features. A recent study on oxygen plasma-treated sisal fibres reported similar findings, where plasma etching enhanced the surface structure and ATR-FTIR spectra exhibited sharper peaks around the 2900 cm^{-1} region [223].

The peak observed at 1637 cm^{-1} corresponds to the bending vibration of water-bound –OH [325]. This peak shows a significant increase in intensity for water shock treated fibres compared to untreated fibres. Such a change is likely due to an increase in intermolecular hydrogen bonding within the cellulose structure following water shock treatment, indicating enhanced chemical and structural reorganisation at the molecular level. The peaks observed in the frequency range of 1400 to 1200 cm^{-1} correspond to CH_2 wagging, COH in-plane bending which is a type of asymmetric stretching, and tertiary CH vibrations that are typically associated with crystalline cellulose. Such bond vibrations related to crystalline cellulose were also observed in the Raman spectra (Figure 6.12) of the fibres. Lastly, the prominent peak at 1020 cm^{-1} is attributed to -CO stretching, which is inherent to cellulose because of its glycosidic bonds [326]. The increase in peak height for water shock treated fibres indicates the combined effect of plasma treatment and water shock treatment. In case of plasma treated fibres, the increase in peak height compared to untreated fibres can be a result of surface etching [223]. These results align with the notable increase in tensile strength and Young's modulus, further supporting the hypothesis that enhanced surface functionalisation induced by 30-minute argon plasma treatment and increased density of hydrogen bonds following cold water shock treatment contribute to improved fibre cohesion and more efficient load transfer. The densified architecture observed in SEM images, along with the reduced porosity (66%), likely intensifies these functional group interactions. Additionally, the thermogravimetric analysis and crystallinity analysis illustrated in the supplementary information support this conclusion.

6.3.8 Effects of prolonged plasma treatment on hemp fabric

Recent research on wood-based materials has suggested that partial lignin removal can contribute to structural strengthening [63] [62] [327]. In the present study, an increase in tensile strength is observed following an immediate water shock treatment after a 30-minute argon plasma treatment. However, the data so far does not provide concrete evidence of lignin removal. To gain deeper insight into the potential of argon plasma to remove lignin from the fibre structure, fibres treated with plasma for 3 hours were examined using SEM and ATR-FTIR analysis.

Figure 6.14 presents the ATR-FTIR spectra of untreated fibres, fibres argon plasma treated for 3 hours at 40 Hz, and fibres subjected to cold water shock treatment following the same plasma conditions. The water shock treated fibres show an approximate 20% decrease in transmittance, suggesting increased light absorption, which may indicate partial degradation of the fibre structure [147]. Despite this, the primary chemical functional groups characteristic of cellulose present in hemp fibres remain unchanged. Notably, more pronounced peaks are observed for -OH, -CH, and -C-O groups, indicating possible structural reorganisation or pronounced polarisation of these groups [19]. For fibres subjected to a 3-hour plasma treatment, the ATR-FTIR spectra show a sharp -OH peak around 3200 cm^{-1}, which becomes more pronounced after the water shock treatment. However, since lignin and cellulose share similar functional groups, it is difficult to definitively conclude lignin removal based on ATR-FTIR alone. Referring to Figure 6.15, which presents the tensile strength data for fabrics plasma treated for 3 hours and subsequently water shock treated, it can be statistically inferred that extended plasma exposure weakens the fabric structure. The high cumulative variation of 64% supports this conclusion, indicating significant structural degradation. In contrast, an immediate water shock treatment following the 3-hour plasma exposure appears to mitigate this effect, potentially through the reorganisation and reformation of disrupted bonds. This is supported by the reduced cumulative variation of 30%, which matches that of the untreated fabric. SEM images in Figure 6.16 reveal the longitudinal section of the hemp fibres, showing a severely etched surface after 3-hour plasma treatment. Additionally, fibres subjected to the subsequent water shock treatment appear highly wrinkled and shrunken, which indicates that the immersion of water helps preserve the fibre structure from further degradation.

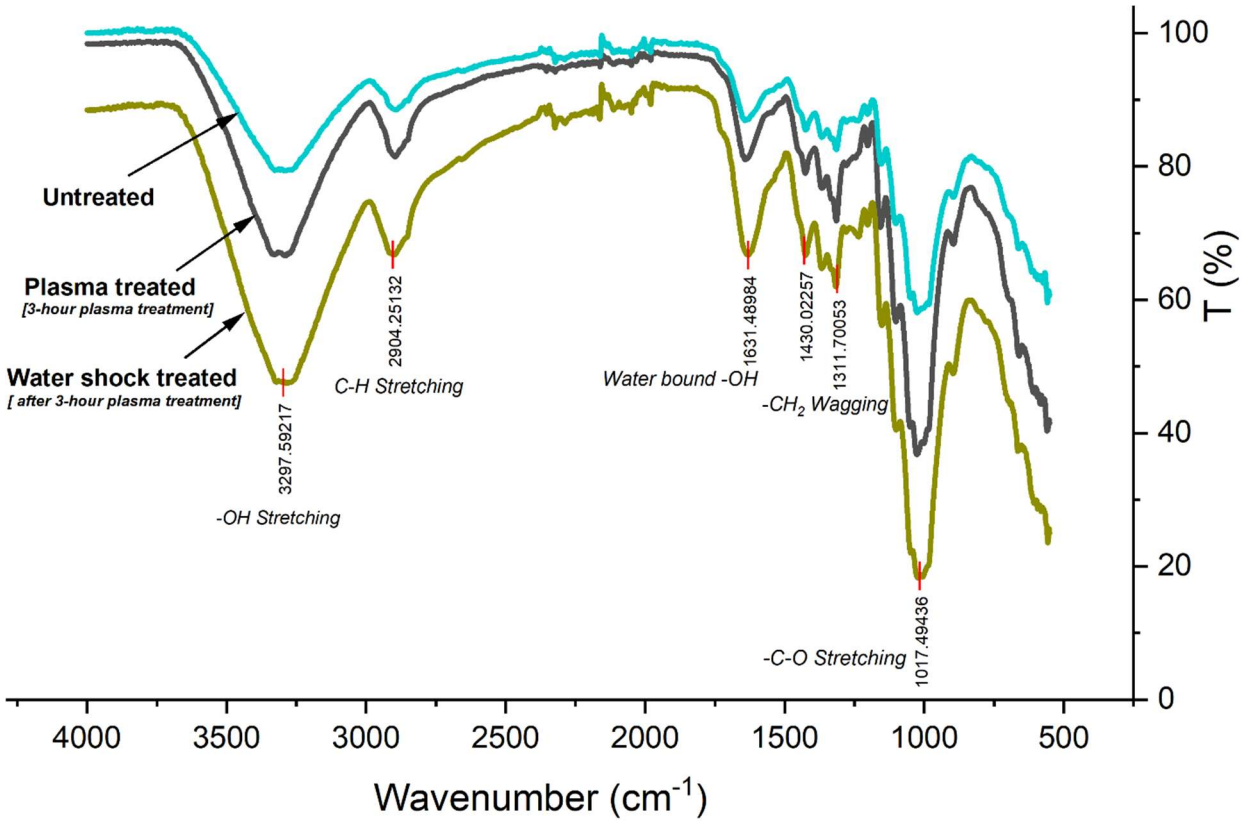

Figure 6.14 FTIR spectra of untreated, 3-hour argon plasma treated and cold water shock treated (immediately after 3-hour argon plasma treatment) hemp fabric

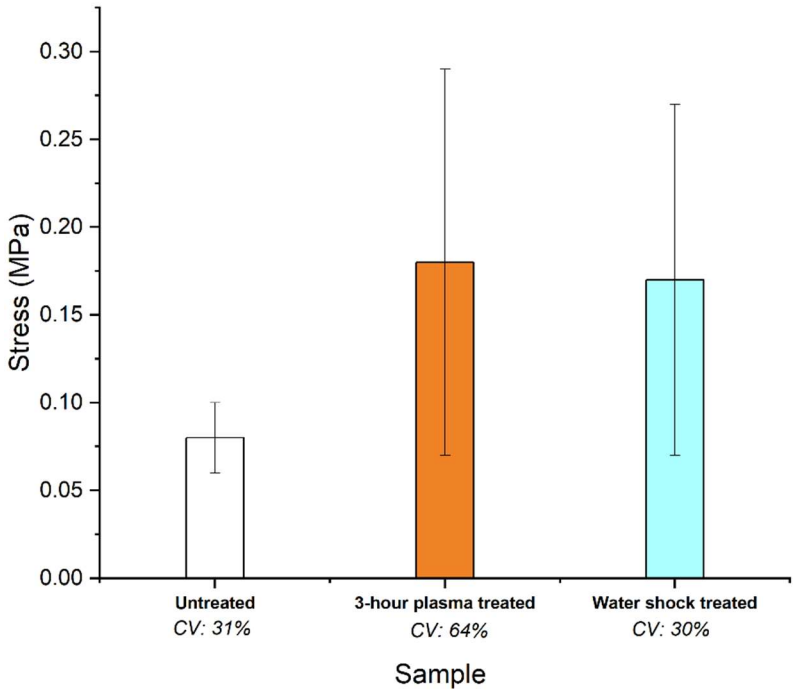

Figure 6.15 Tensile strength of prolonged argon plasma treated (3 hour argon plasma treatment at 40 Hz Power) and cold water shock treatment following same plasma treatment conditions hemp fabrics

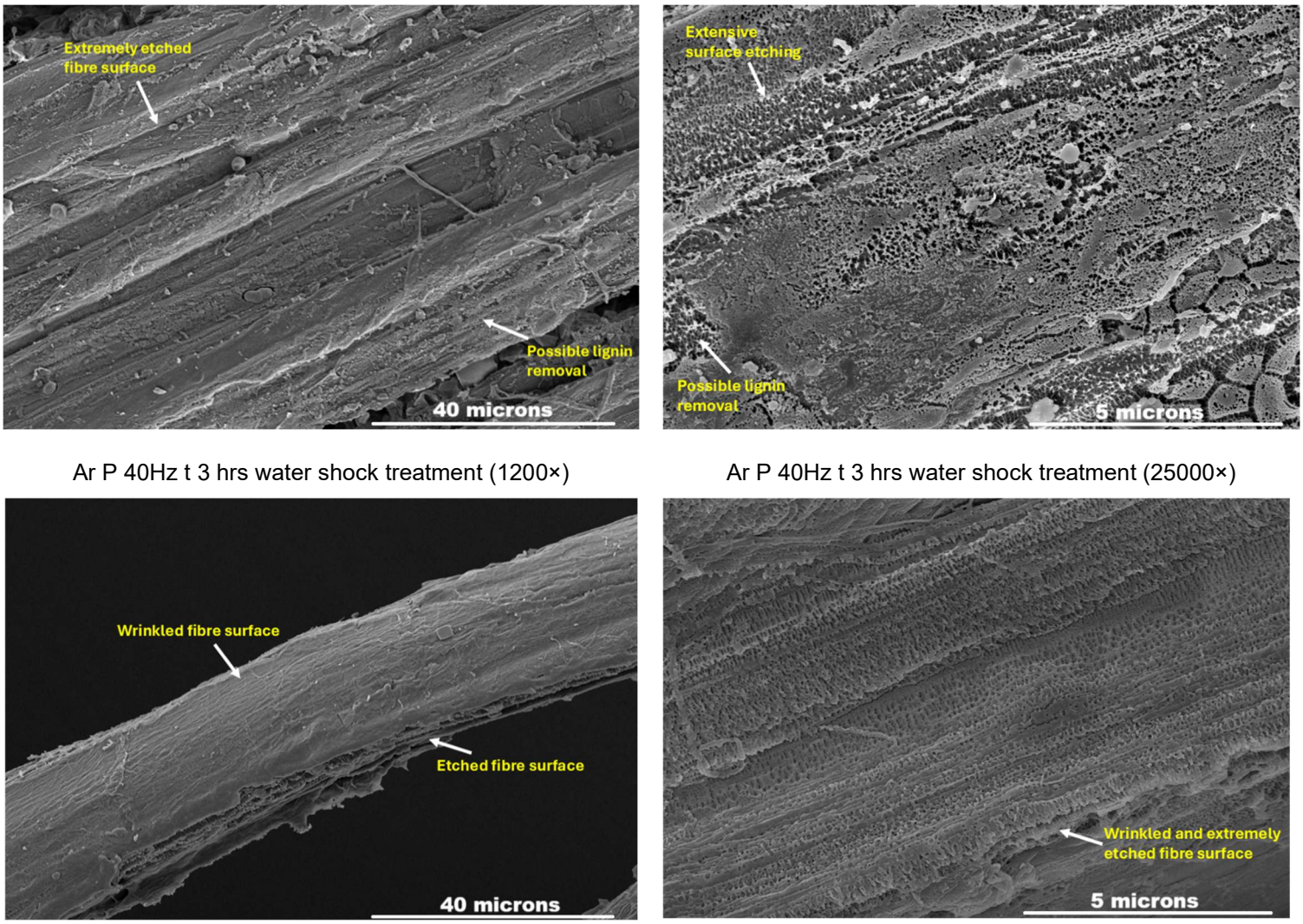

Ar P 40Hz t 3 hrs water shock treatment (1200×)

Ar P 40Hz t 3 hrs water shock treatment (25000×)

Ar P 40Hz t 3 hrs water shock treatment (1200×)

Ar P 40Hz t 3 hrs water shock treatment (25000×)

Figure 6.16 SEM images of prolonged plasma treated fibres

6.4 Conclusion

This study investigated the effects of argon plasma treatment and cold water shock treatment on the mechanical and structural properties of needle-punched nonwoven hemp fabrics and their integral fibres. The results reveal significant modifications in fibre morphology, fabric porosity, and both fibre and fabric tensile strength, providing valuable insights for enhancing the performance of hemp fibres in sustainable textile applications.

The tensile strength of untreated nonwoven hemp fabric was measured at approximately 0.09 MPa. Argon plasma treatment resulted in fibre surface modification, as evidenced by SEM analysis, where surface nano-pores were observed. However, while plasma treatment induced slight fibrillation and reduced fibre diameter (from 220 μm to 180 μm), the fibre's tensile strength remained unchanged (~20 MPa) for individual fibres. This suggests that plasma primarily affects the surface characteristics rather than fundamentally altering the fibre's internal structure without altering the Young's modulus of the fibre (~2 GPa). In contrast, water shock treatment led to remarkable changes in fibre tensile strength with a Young's Modulus of ~18 GPa. SEM analysis of fibre longitudinal sections showed a denser structure with fibrils being fused, resulting in a more cohesive internal fibre structure. This was accompanied by a substantial reduction in fibre diameter (to 100 μm).

Raman and FTIR spectroscopy showed no change in the constituent functional groups in hemp, although enhanced peak heights were seen for water-bound -OH, indicating an increase in intermolecular hydrogen bonding. Especially in the case of Raman spectra, wherein pronounced peaks were observed in the crystal lattice region. These results are reflected in porosity and density measurements. Argon plasma treated samples exhibited higher porosity due to surface etching, whereas cold water shock treatment induced fibrillar fusion, decreasing porosity and increasing fibre density.

A prolonged plasma treatment of 3 hours weakens the hemp fabric due to excessive surface etching of the fibres, leading to fibre degradation. Therefore, it can be concluded that an optimal treatment duration of 30 minutes is more suitable for enhancing the fabric's mechanical strength.

Overall, this research highlights the potential of combined argon plasma treatment and water shock treatment as a novel and eco-friendly method to enhance the mechanical properties of hemp fibres.

Chapter 7

Conclusions and Future Outlook

This research systematically investigated the effects of low-pressure, long duration (≥30 min) argon plasma treatment for enhancing the surface, structural, and mechanical properties of both hemp fibres, and the effects on bulk properties of hemp fabrics.

The experiment sections detailed in Chapters 4, 5 and 6 consider the underlying mechanisms, and their evidence to support the proposition that argon plasma-assisted surface modification can provide an efficient strategy to improve the performance of hemp-based textiles in terms of both colouration and tensile properties. This aligns with industry trends towards sustainable development of textile manufacturing by reducing dependency on water-intensive methods and aqueous chemical treatments.

This research addressed three specific objectives, each contributing to a scientific foundation for plasma treated hemp fibres:

- **Analysis of the impact of plasma treatment on fibre surface properties and the dyeability of woven hemp fabrics.**

  Chapter 4 demonstrated that low-pressure argon plasma pretreatment significantly improved colour strength in reactive and vat dyeing. Argon plasma treatment effectively transformed the partially hydrophobic hemp fibre into a fully hydrophilic material, thereby enhancing dye penetration into the fibre structure. Additionally, the nano-scale morphological modifications, such as surface etching and increased porosity, led to a greater specific surface area, which promoted the formation of stronger dye-fibre interactions due to enhanced dye bath penetration.

  Scanning electron micrographs revealed that argon plasma-induced etching is a time-dependent process. With increasing treatment duration, progressive surface etching was observed. Notably, samples treated for 10 minutes exhibited a distinct nano-porous morphology, with pores averaging approximately 12 nm in diameter. Spectroscopic analyses using FTIR and

Raman spectroscopy confirmed significant physicochemical modifications on the fibre surface, including an increased density of polar functional groups. Despite these changes, the intrinsic chemical structure of cellulose remained largely intact following a 10-minute argon plasma treatment. FTIR spectra revealed enhanced intensity of characteristic peaks such as -OH, C=O, and -C-O-, indicating successful surface functionalisation. Additionally, a noticeable reduction in Raman shift for the plasma treated hemp fibres suggested alterations in surface energy and the occurrence of nano-scale surface etching. This increase in surface energy was confirmed by water contact angle measurements, which suggested that argon plasma treatment modified a partly hydrophobic ($\theta = 60°$) surface into a fully hydrophobic ($\theta = 0°$) surface.

Hemp fabrics treated with argon plasma exhibited significantly higher colour strength (K/S) values following reactive dyeing. Furthermore, when subjected to dye-stripping, the colour strength remained largely unaffected, indicating that plasma treatment promotes the formation of highly stable covalent bonds between the reactive dye molecules and the fibre. Statistical analysis using surface response methodology revealed that both the weave type and the duration of plasma treatment are critical factors influencing colour strength. Additionally, the model showed a low standard deviation, suggesting that the experimental data are statistically robust and the results are reliable. Hemp fabrics treated with argon plasma and subsequently dyed with vat dyes exhibited a notable increase in colour strength, rising from 6.4 in untreated samples to 22 in treated ones. This significant enhancement suggests that argon plasma treatment not only facilitates stable dye-fibre covalent bonding (in case of reactive dyes) but also increases the surface activity through physical interactions such as van der Waal's forces, allowing vat dye molecules to more effectively adhere to cellulose surface. The improved surface characteristics, including enhanced roughness and porosity, likely contribute to better retention of the relatively bulky vat dye molecules, enabling more effective dye adhesion to the fabric surface. Statistical analysis using surface response methodology for vat dyed fabrics revealed that "power" is the most significant factor influencing the increase in colour strength. Furthermore, the low standard deviation associated with the experimental data indicates that the process is consistent, and the results are statistically reliable.

These results position argon plasma as a clean and efficient alternative to conventional wet pretreatments, achieving uniform and intensified colouration without auxiliary chemicals or high temperatures.

Future outlook:
The present study has primarily focused on identifying the morphological and chemical modifications induced by argon plasma treatment and their impact on the colouration of hemp. While the findings highlight significant improvements in dye uptake and stability, further research is required to gain a deeper mechanistic understanding of plasma-assisted dyeing. For instance, systematic studies using dyes with well-defined chemical structures would allow precise elucidation of dye–fibre bonding mechanisms. Advanced analytical methods such as UV–Vis spectroscopy could be employed to quantitatively assess dye wash-off, thereby providing greater insight into the fixation efficiency and fastness properties of plasma-treated hemp.

Moreover, investigation of dyeing kinetics on plasma-treated fabrics would help clarify how plasma-induced surface modifications influence dye diffusion, adsorption, and fixation rates. Such studies could contribute to the optimisation of plasma parameters for specific dye classes and weave structures. Expanding this work to include different dye types, particularly natural dyes and low-impact synthetic alternatives, would strengthen the relevance of plasma technology in sustainable textile processing.

- **Assessing structural and chemical changes in hemp fibres post-plasma treatment**

Chapter 5 examined the effects of argon and oxygen plasma treatments on dew-retted hemp fibres. This novel investigation into prolonged plasma exposure revealed that both argon and oxygen plasma treatments induced notable physicochemical modifications, primarily characterised by surface roughening. Moreover, following both argon and oxygen plasma treatment, the intrinsic chemical structure of cellulose and the bulk properties of hemp fibre, such as tensile strength and crystallinity, remained unaltered.

SEM micrographs of untreated and plasma-treated fibres revealed morphological changes, with surface roughness increasing progressively with longer treatment durations. In the case of argon plasma treatment, a 30-minute

exposure resulted in noticeable surface roughening and the initiation of fibrillation. After a prolonged 4-hour argon plasma treatment, significant surface etching was observed, along with the presence of residual surficial impurities such as lignin and hemicellulose clinging to the fibre surface. Additionally, SEM micrographs of fibres treated with oxygen plasma revealed significant surface roughening after a 30-minute plasma treatment. Following a 4-hour exposure to oxygen plasma, the fibre surfaces exhibited a distinct network-like structure. Surface topography analysis using AFM revealed a substantial increase in surface roughness for dew-retted hemp fibres following plasma treatment. For fibres treated with argon plasma, roughness values increased from approximately 70 nm in untreated samples to around 300 nm, while oxygen plasma treatment resulted in a maximum roughness of 182 nm. This difference can be attributed to the greater mass and physical impact of argon gas. Furthermore, AFM scans of argon plasma-treated fibres (30-minute duration) displayed distinct textured features, corresponding to lignin bundles. These features were absent in the 4-hour treated samples, suggesting that prolonged plasma exposure may have contributed to the removal of lignin from the fibre surface. Section analysis of the AFM scans indicated that oxygen plasma treatment had a more localised and pronounced impact on surface topography, characterised by the formation of deeper valleys. In contrast, argon plasma treatment resulted in a more uniform roughening across the entire fibre surface. This distinction highlights the differing surface modification mechanisms of the two gases, with oxygen plasma inducing more targeted surface erosion and argon plasma promoting widespread nano-texturing. Hence, the type of gas, treatment duration and power all influence the surface roughness, which can be confirmed using principal component analysis.

Water contact angle analysis suggested that both argon and oxygen gas plasma treatments help transform the partially hydrophobic fibre surface (~69°) to fully hydrophilic (0°), which is mainly due to a roughened surface morphology and increased surface energy. ATR-FTIR spectroscopy highlighted distinct physicochemical changes, particularly in argon plasma treated samples. Compared with the untreated fibres, plasma treated fibres with both argon and oxygen gas showed sharp peaks due to surface functionalisation and surface removal effect due to lignin removal. Although the intrinsic structure of cellulose remained unaltered following plasma treatment. Moreover, fibres treated with oxygen gas plasma fell in PC2 as observed in PCA analysis, suggesting that oxygen plasma treatment etched the fibre surface without extreme oxidation.

Following a plasma treatment of 30 minutes with both gases, the tensile strength remained unchanged, mainly because of the action of plasma being confined to the fibre surface, which was confirmed using crystallite size analysis and crystallinity index. Fluorescence microscopy revealed effective surface lignin removal for 4-hour argon plasma treated fibres, suggesting that plasma treatment is capable of lignin removal.

Hence, this study not only contributes to a deeper understanding of plasma-induced surface modifications in hemp fibres but also demonstrates the value of employing novel characterisation tools such as fluorescence microscopy to visualise surficial modifications. Furthermore, the findings suggest that both argon and oxygen plasma treatments may serve as effective strategies for improving the processability of hemp as well as for other lignin-rich natural fibres. This work thus reinforces the potential of plasma technology as a sustainable, non-chemical alternative for enhancing fibre functionality in textile processing.

Future outlook:

While this chapter has demonstrated the influence of argon and oxygen plasma on surface roughness, wettability, and lignin removal in dew-retted hemp fibres, further investigations are required to refine our understanding of plasma-fibre interactions. One immediate avenue for exploration is the introduction of finer experimental intervals between 30 minutes and 4 hours. By incorporating intermediate treatment durations (e.g., 45, 60, 90, and 120 minutes), a more complete profile of surface roughening, wettability alterations, and lignin removal can be developed. Such an approach would allow a more precise correlation between plasma exposure time and the onset of key morphological and chemical transformations. Furthermore, evaluating surface energy in relation to surface roughness could support the use of plasma-treated hemp fibres in high-performance applications, such as aerospace and automotive components, where strong adhesion with advanced or complex coatings is required.

To gain mechanistic insights into the plasma-fibre interface, advanced surface-sensitive techniques such as secondary ion mass spectrometry (SIMS) and X-ray photoelectron spectroscopy (XPS) could be employed. The use of fluorescence microscopy in this study has proven highly effective in visualising

surficial lignin removal. Expanding this technique to include fluorescence spectroscopy could enable quantitative assessment of lignin content across different treatment conditions. In the longer term, integrating these advanced analytical approaches with process optimisation studies will contribute to a more comprehensive understanding of plasma treatment mechanisms

- **Evaluating the combined effects of argon plasma treatment and cold water shock treatment on nonwoven hemp fabrics**

  As a preliminary study into strengthening nonwoven hemp fabrics, Chapter 6 explored the sequential application of argon plasma and cold water shock treatment on needle-punched nonwoven hemp fabrics. The results indicate that a cold water shock treatment immediately after argon plasma treatment helps enhance the fabric as well as the fibre tensile strength.

  The tensile strength of argon plasma treated hemp fabrics remained statistically unaffected across varying plasma treatment parameters, likely due to inherent structural inconsistencies within the hemp fibres. However, with increasing argon plasma treatment duration, a gradual increase in fabric density was observed, contributing to an enhancement in fabric tensile strength. The reduction in fabric porosity associated with plasma treatment also led to a higher stress at break. Notably, the application of a cold water shock treatment immediately after argon plasma treatment resulted in a fourfold increase in tensile strength, accompanied by a lower standard deviation across all treatment groups. Specifically, the untreated hemp fabric exhibited a tensile strength of 0.08 MPa, which increased to 0.21 MPa after argon plasma treatment and further to 0.49 MPa after the combined cold water shock treatment.

  Individual fibre tensile strength of hemp fibres remained unchanged following argon plasma treatment, having a constant Young's modulus of 2 GPa. However, cold water shock treated hemp fibres showed a sevenfold increase in their tensile strength and Young's modulus measured up to 18 GPa. Individual fibre tensile strength with a lower gauge length of 10 mm showed a stick-slip effect in water shock treated fibres, indicating an increased number of hydrogen bonds in the fibre structure.

Scanning electron micrographs of cold water shock-treated hemp fibres revealed a markedly densified microstructure, with fibre bundles appearing fused together compared to the untreated fibres in which these fibre bundles were distinctly visible. Argon plasma treated fibres exhibited increased fibrillation, and surface etching was also observed, indicating progressive surface modification. A significant reduction in fibre diameter from approximately 200 μm in untreated fibres to 100 μm in cold water shock treated hemp fibres was observed, suggesting substantial structural compaction induced by the immediate thermal shock. SEM micrographs of the longitudinal sections of fibres further supported these findings, wherein untreated fibres displayed relatively smooth surfaces, compared to argon plasma treatment, which resulted in a nano-porous surface. In the case of cold water shock treated fibres, a highly wrinkled and shrunken surface morphology was observed, providing strong visual evidence for the densification model proposed in this study.

Spectroscopic analysis using Raman and FTIR showed sharp peaks following cold water shock treatment, confirming structural densification without altering the intrinsic cellulose structure. Raman spectra for argon plasma treated fibres showed a lower Raman shift than untreated fibres, suggesting a surface degradation effect and an enhanced surface energy. Moreover, sharp peaks in the crystal lattice region were observed in the case of water shock treated fibres thus indicating densification of the structure.

Hemp fibres treated with argon plasma for 3 hours exhibited a highly etched and degraded surface morphology, as observed in SEM analysis. Corresponding FTIR spectra showed reduced transmittance, indicating surface removal, though the intrinsic cellulose structure remained intact. In contrast, fibres subjected to cold water shock after 3-hour plasma treatment displayed less pronounced etching, with a distinctly wrinkled surface. FTIR spectra of these samples revealed sharp -OH peaks, confirming the introduction of polar functional groups. These findings suggest that prolonged argon plasma treatment primarily affects the surface layer, while water shock treatment moderates the extent of degradation.

Hence, this novel preliminary study demonstrates that the immediate application of cold water shock following argon plasma treatment significantly enhances the tensile properties of both fibre and fabric. Plasma introduces

polar groups and nano-pores, while rapid water absorption followed by drying induces structural compaction, resulting in a densified, high-strength microstructure. These findings open new possibilities for sustainable enhancement of natural fibres in technical and performance-based textile applications.

Future outlook

Further experimentation could focus on investigating the high standard deviation observed specifically in plasma-treated nonwoven hemp fabrics. A detailed study of the structural inconsistencies within hemp fibres could help optimise plasma treatment parameters to achieve more consistent tensile strength improvements.

A comprehensive investigation into end-use applications is essential to translate these findings into practical solutions. The sharp peaks observed in Raman spectra suggest potential for advanced material characterisation using a 554 nm fluorescence laser. If water shock-treated fibres exhibit high fluorescence, they could be developed into lightweight, reflective materials for applications such as safety textiles or optical sensors. Additionally, the significant increase in tensile strength and Young's modulus of treated fibres makes them ideal candidates for integration into polymer matrices to create high-strength, lightweight composites. These composites could find applications in industries such as automotive, aerospace, or construction, where sustainable, high-performance materials are in demand. Moreover, research specifically aimed at using these fibres in the geotextile and filter fabrics sector can be beneficial, thus positioning hemp as a suitable material in every textile sector, from garment to technical textile.

Collectively, the findings demonstrate that low-pressure and long duration (≥30 min) plasma treatment, particularly with argon gas, is a versatile tool for enhancing hemp fibre performance. The increased surface energy, surface nano-texturing, and improved wettability achieved through plasma treatment enhanced dye uptake and aspects of fibre functionality.

The novel use of cold water shock treatment was found to further improve mechanical properties such as fibre and fabric tensile strength, potentially widening the applications for treated hemp fabrics in technical textile applications. The research establishes plasma treatment as a transformative approach for sustainable fibre engineering. The ability to selectively modify surface characteristics without compromising the bulk structure of hemp fibres highlights the precision and efficacy of this technology. Moreover, the successful combination of plasma and water shock treatments opens new possibilities for developing structurally robust, high-performance nonwoven hemp textiles, with potential applications in composites, technical fabrics, and eco-conscious apparel.

Future Outlook

While this work provides a strong foundation for understanding argon plasma and hemp fibre interactions, several avenues for future research are recommended to further advance the field, which are as follows:

- *Advanced Surface Characterisation:* Employing techniques such as X-ray Photoelectron Spectroscopy (XPS) or Time of Flight Secondary Ion Mass Spectrometry (ToF-SIMS) could provide deeper insights into the chemical states and elemental composition of plasma-treated surfaces, elucidating transient states and modification kinetics.

- *Industrial Scalability:* Pilot-scale and industrial trials are essential to adapt laboratory-scale plasma processes to commercial textile production, ensuring scalability and cost-effectiveness.

- *Fibre Blends and Fabric Constructions:* Exploring the effects of plasma treatment on hemp-based blends (e.g., hemp-cotton, hemp-polyester) and diverse fabric constructions could broaden the applicability of this technology

Supplementary Information

For Chapter 5

Study of hemp fibre properties modified via long duration low-pressure argon and oxygen plasma treatments

Section analysis of AFM scans

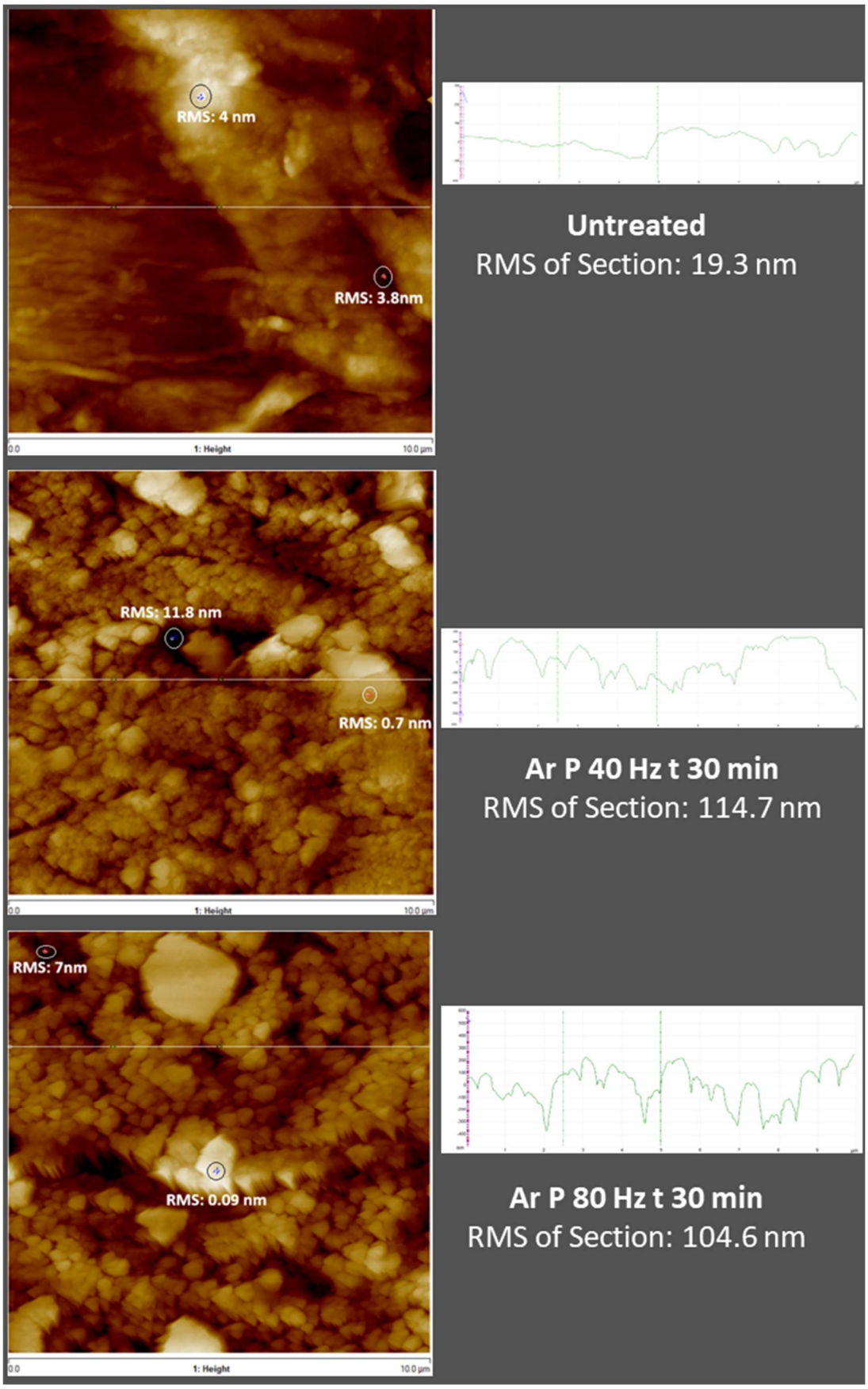

Figure 5.11 AFM section analysis of untreated and argon plasma treated hemp fibres for 30 min at 40 and 80 Hz power

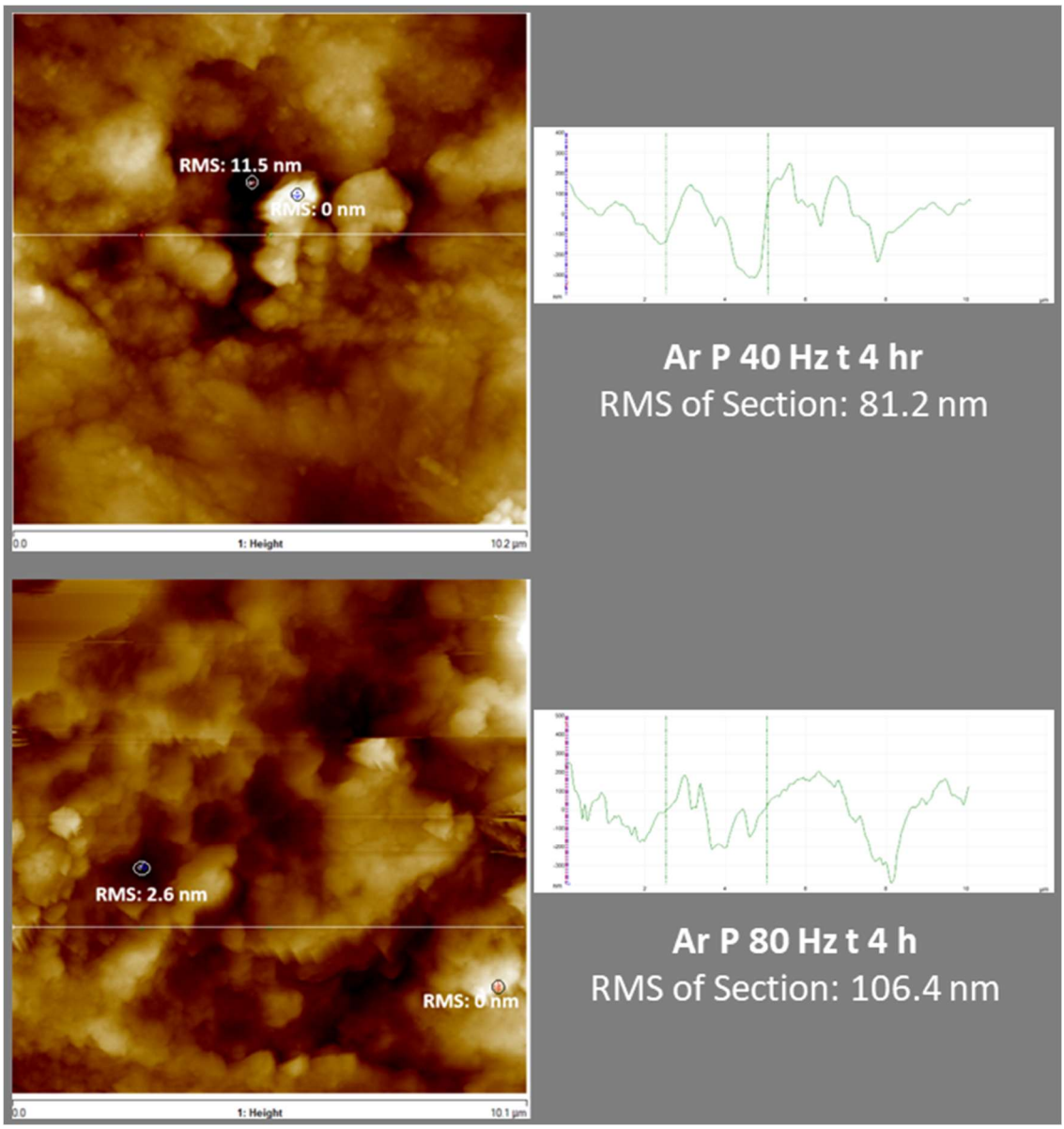

Figure 5.12 AFM section analysis of argon plasma treated hemp fibres for 4 hr at 40 and 80 Hz power

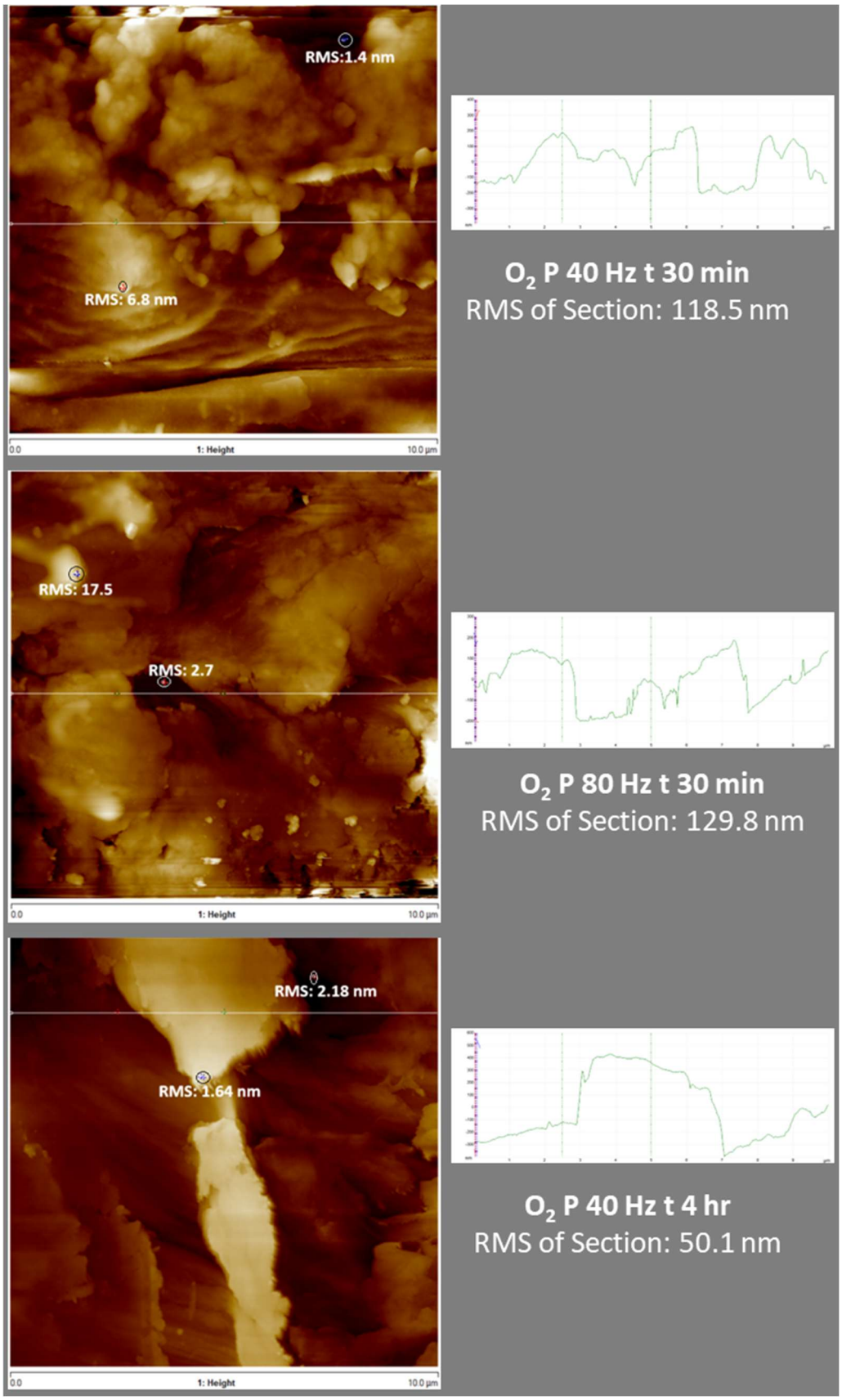

Figure 5.13 AFM section analysis of oxygen plasma treated hemp fibres for 30 min at 40 and 80 Hz power along with 4 h oxygen plasma treated fibres at 40 Hz power

Statistical analysis of fibre-surface roughness

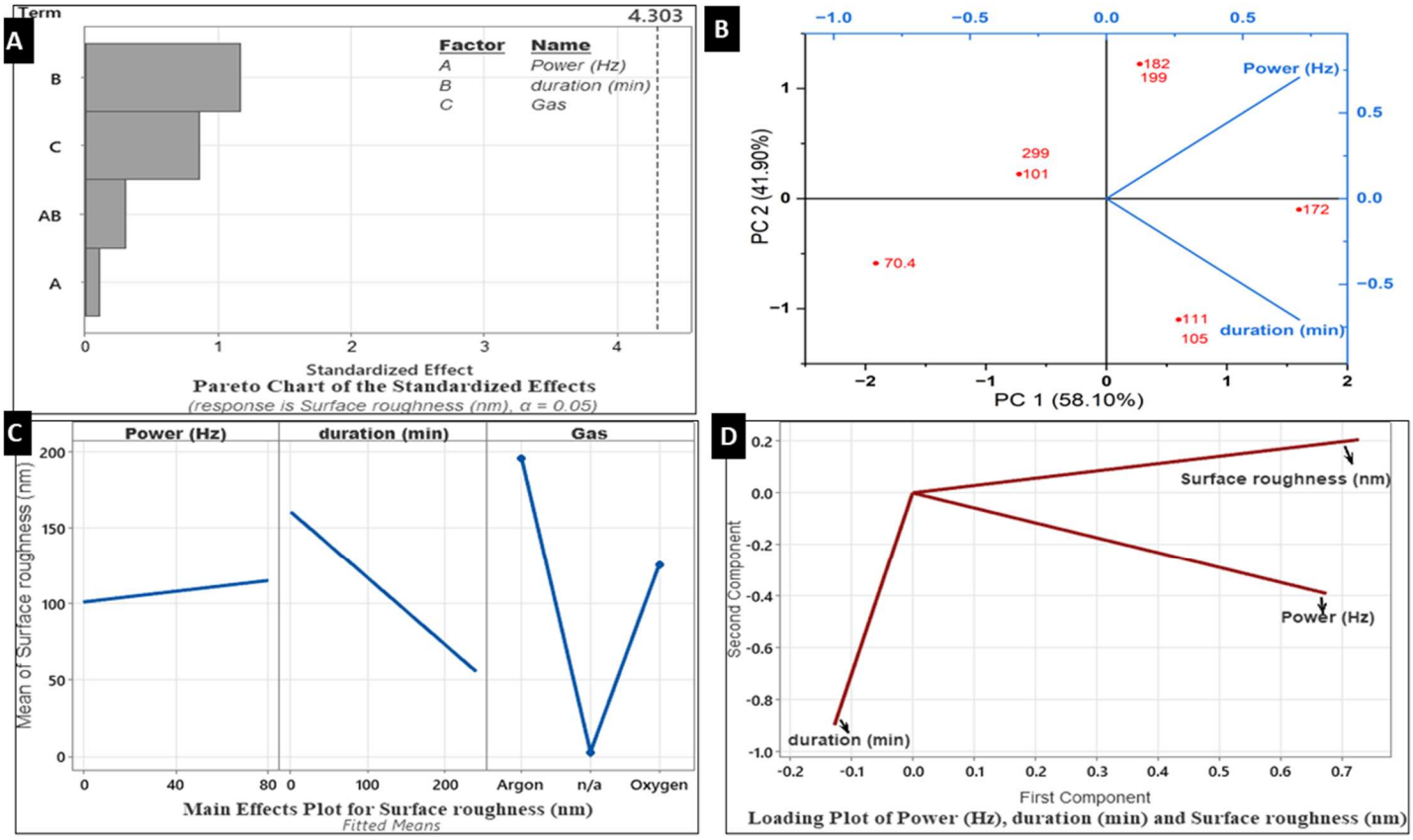

Figure 5.14 Surface roughness (RMS) of hemp fibres along with surface response analysis

Figure 5.14 presents the statistical analysis for the surface roughness (RMS) data derived from AFM scans of untreated and plasma-treated fibres, incorporating surface response analysis and multivariate analysis to evaluate the influence of various treatment parameters. Figure 5.14A shows a Pareto chart of standardised effects, where factors influencing surface roughness (nm) are analysed. The factors include Power (Hz) [A], Duration (min) [B], and Gas type [C]. The chart reveals that Power (Hz) has the strongest influence on surface roughness, aligning with the principal component, PC 1, which accounts for 58.10% of the variance, as confirmed in Figure 5.14B. The PCA analysis suggests that higher power settings may result in greater surface roughness. Additionally, duration of plasma treatment is the second most significant factor, associated with PC 2, accounting for 41.90% of the variance. Interestingly, plasma treatment for shorter durations of about 30 min corresponds to higher roughness, while longer durations of 240 min may lead to smoother surfaces, indicating an inverse relationship. Among gases, plasma generated using argon gas

consistently leads to higher surface roughness compared to oxygen gas under similar conditions. For instance, hemp fibres plasma treated at 40 Hz power for 30 min with argon gas result in a surface roughness of 299 nm, while fibres treated with the same conditions but using oxygen gas result in a fibre having 101 nm of surface roughness. Notably, high power (80 Hz) combined with short duration (30 min) plasma treatment results in high surface roughness ~199 nm for argon gas plasma and ~182 nm for oxygen gas plasma. In contrast, low power (40 Hz) with extended duration (240 min) yields lower roughness, ~111 nm for oxygen gas plasma, ~105 nm for argon gas plasma. This highlights that extended treatment duration can mitigate the roughness induced by higher power levels. Thus, referring to Figure 5.14B, it can be concluded that Power (Hz) and surface roughness are closely aligned along PC 1, demonstrating a positive correlation. Duration (min) aligns oppositely along PC 2, showing a negative correlation with surface roughness, which aligns well with the previous interpretation. Figure 5.14C shows the main effects plot, where the influence of individual factors on surface roughness is shown. The Duration panel illustrates a declining trend, which suggests that longer treatment leads to smoother surfaces. The Gas panel emphasises significant differences in roughness depending on gas type, with argon gas plasma leading to the roughest textures and oxygen gas plasma resulting in moderately rougher surfaces compared to untreated fibre. The Power panel shows an upward slope, indicating that higher power increases surface roughness, albeit to a lesser extent compared to gas and duration. Figure 5.14D shows the PCA loading plot, where the vector for surface roughness closely aligns with Power (Hz), indicating a strong positive relationship. In contrast, the vector for duration points in the opposite direction, suggesting a strong negative correlation with surface roughness. The angle between the power and duration vectors suggests a weak correlation between these two parameters. These relationships reinforce earlier findings that surface roughness increases with power but decreases with treatment duration. Therefore, the statistical analysis suggests that plasma treatment operates as a synergistic process, where gas type, power, and treatment duration collectively influence surface modification. While each factor holds individual significance, it is the optimal combination of all three parameters that yields the most effective surface roughness outcomes.

Supplementary Information

For Chapter 6

Alteration in the microstructure of hemp fibres via the aid of low-pressure argon plasma treatment

X-ray diffraction analysis of treated and untreated hemp fibres

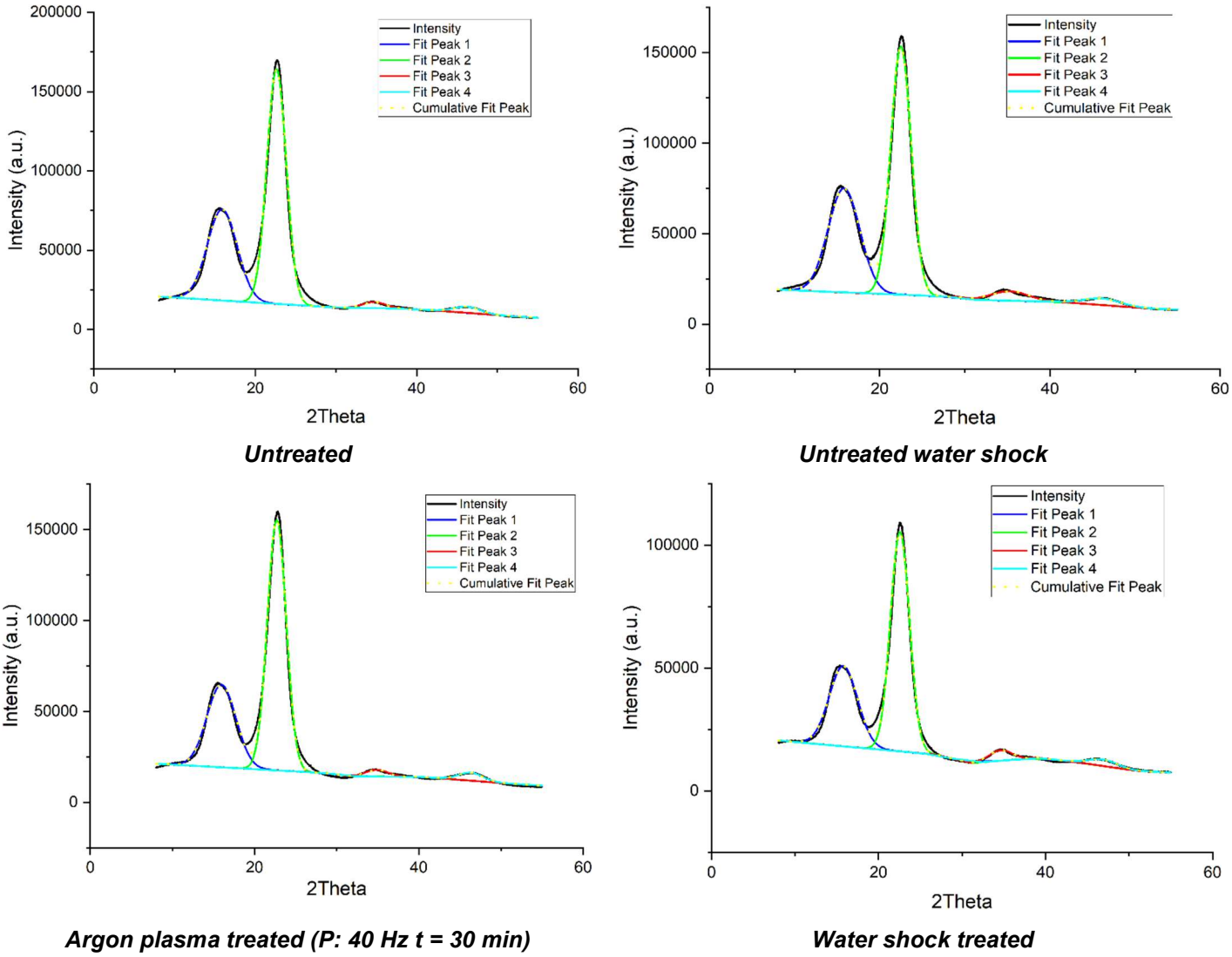

Figure 6.17 Deconvoluted X-ray diffraction peaks of untreated, argon plasma treated (for a duration of 30 minutes at 40 Hz power) and cold water shock treated hemp fibres

.

.

.

Sample	Crystallinity (%)	SD
Untreated	68	0.001
Untreated Water shock	71	0.002
Plasma treated	65	0.004
Water shock treatment	58	0.001

Table 6.3 Crystallinity index of untreated, argon plasma treated (for a duration of 30 minutes at 40 Hz power) and cold water shock treated hemp fibres

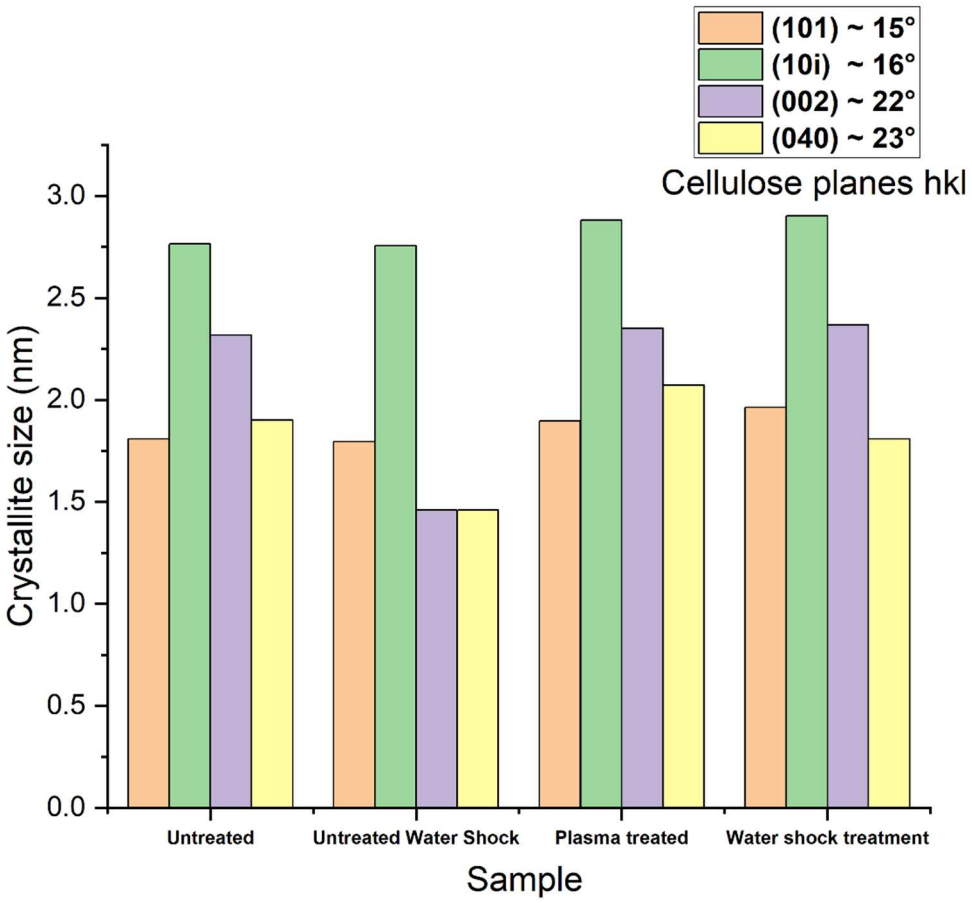

Figure 6.18 Crystallite size of untreated, argon plasma treated (for a duration of 30 minutes at 40 Hz power) and cold water shock treated hemp fibres determined using the Debye-Scherrer equation

Thermogravimetric analysis of untreated and treated hemp fibres

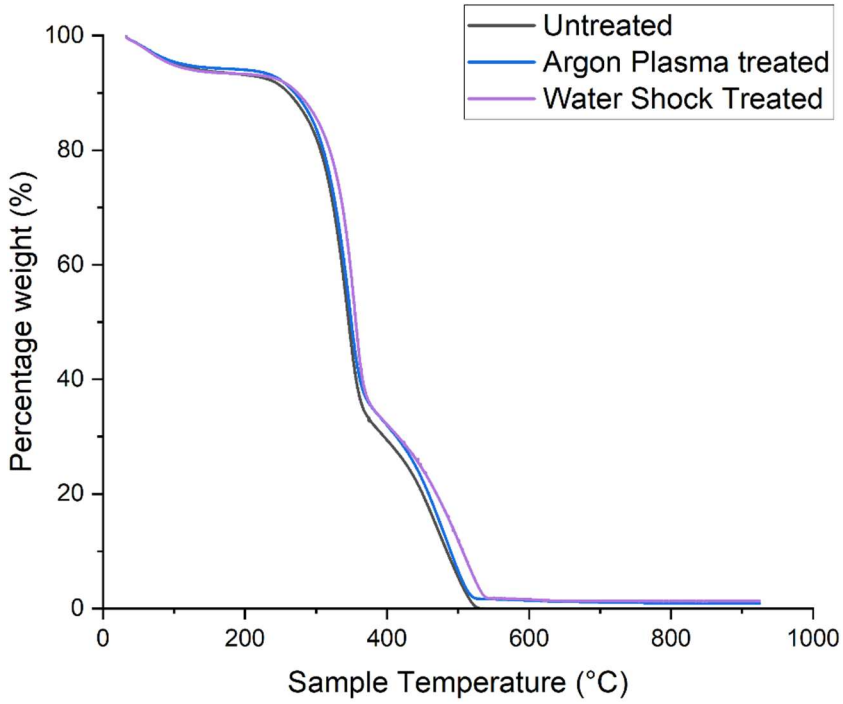

Figure 6.19 Thermal decomposition profile of untreated, argon plasma treated (for a duration of 30 minutes at 40 Hz power) and cold water shock treated hemp fibres

Figure 6.17 shows the x-ray diffraction pattern for hemp fibre without any treatment, non-plasma treated but water shock treated fibre, argon plasma treated and water shock treated fibres. Table 6.3 gives an overview of the crystallinity index in these samples. It is observed, that in the case of untreated fibres, the crystallinity remains unchanged, indicating that water shock treatment does not alter any changes in the crystal lattice structure shown in Figure 6.18. Although, the Raman spectra for untreated water shocked fibres showed sharp peaks, a low tensile strength proves the fact that the crystal structure remains unaffected. Similarly, fibres subjected to a 30-minute argon plasma treatment showed no significant change in crystallinity, suggesting that plasma-induced modifications are confined to the fibre surface without affecting the bulk structure. However, a 10% decrease in crystallinity was observed in fibres that underwent plasma treatment followed by immediate cold water immersion, resulting in a final crystallinity of 58%. This reduction is likely due to structural reorganisation triggered by thermal shock.

Upon plasma treatment, the fibre surface undergoes functionalisation and nano-scale etching, leading to increased surface stress. The immediate application of a cold water shock is believed to induce fibre shrinkage, as evidenced by the reduced fibre diameter shown in Figures 6.9 and 6.10. The consistent crystallite size across all samples (Figure 6.18) suggests that while the structural changes are subtle, they contribute meaningfully to the observed enhancement in tensile strength. Furthermore, the unchanged thermal behaviour observed in Figure 6.19 across all samples confirms that no significant compositional modification occurred.

References

1. Sengupta, S., et al., *Characterization of Indian hemp (Canabinus sativa L.) fibre and study for potentiality in textile application.* Cellulose, 2024. **31**(11): p. 7053-7066.
2. Ahmed, A.T.M.F., et al., *Hemp as a potential raw material toward a sustainable world: A review.* Heliyon, 2022. **8**(1): p. e08753.
3. Deshmukh, G., *Advancement in hemp fibre polymer composites: A comprehensive review.* Journal of Polymer Engineering, 2022. **42**.
4. Karche, T. and M.R. Singh, *The application of hemp (Cannabissativa L.) for a green economy: a review.* Turkish journal of botany, 2019. **43**(6): p. 710-723.
5. Zhao, X., et al., *Industrial Hemp—an Old but Versatile Bast Fiber Crop.* Journal of Natural Fibers, 2021: p. 1-14.
6. Preston, B., *High noon: the mayor of Grand Forks aimed to make his town hemp central. Then came the showdown.* Saturday night (Toronto, Ont. : 1963), 1998. **113**(9): p. 27.
7. Andre, C.M., J.-F. Hausman, and G. Guerriero, *Cannabis sativa: The Plant of the Thousand and One Molecules.* Frontiers in plant science, 2016. **7**: p. 19-19.
8. Strzelczyk, M., M. Lochynska, and M. Chudy, *Systematics and Botanical Characteristics of Industrial Hemp Cannabis Sativa L.* Journal of natural fibers, 2021. **ahead-of-print**(ahead-of-print): p. 1-23.
9. Alonso-Esteban, J.I., et al., *Hemp (Cannabis sativa L.) Varieties: Fatty Acid Profiles and Upgrading of γ-Linolenic Acid–Containing Hemp Seed Oils.* European journal of lipid science and technology, 2020. **122**(7): p. 1900445-n/a.
10. Promhuad, K., et al., *Applications of Hemp Polymers and Extracts in Food, Textile and Packaging: A Review.* Polymers (Basel), 2022. **14**(20).
11. Naeem, M.Y., et al., *Hemp: An Alternative Source for Various Industries and an Emerging Tool for Functional Food and Pharmaceutical Sectors.* Processes, 2023. **11**(3): p. 718.
12. Crini, G., et al., *Applications of hemp in textiles, paper industry, insulation and building materials, horticulture, animal nutrition, food and beverages, nutraceuticals, cosmetics and hygiene, medicine, agrochemistry, energy production and environment: a review.* Environmental Chemistry Letters, 2020. **18**(5): p. 1451-1476.
13. Gedik, G. and O. Avinc, *Hemp Usage in Textile Industry*, in *Revolutionizing the Potential of Hemp and Its Products in Changing the Global Economy*, T. Belwal and N.C. Belwal, Editors. 2022, Springer International Publishing: Cham. p. 69-95.
14. Mariz, J., et al., *Hemp: From Field to Fiber—A Review.* Textiles (Basel), 2024. **4**(2): p. 165-182.
15. Kaminski, K.P., et al., *Opportunities, Challenges, and Scientific Progress in Hemp Crops.* Molecules, 2024. **29**(10).
16. Palanikumar, K., et al. *Targeted Pre-Treatment of Hemp Fibers and the Effect on Mechanical Properties of Polymer Composites*. Fibers, 2023. **11**, DOI: 10.3390/fib11050043.
17. Stanković, S., *Consumer Awareness and Textile Sustainability: Sensory Evaluation of Hemp Textiles by Consumers as a Prospective Market*

Research Method for New Textile Products, in *Consumer Awareness and Textile Sustainability*, S.S. Muthu, Editor. 2023, Springer Nature Switzerland: Cham. p. 117-135.
18. Salmins, M., F. Gortner, and P. Mitschang, *Challenges in Manufacturing of Hemp Fiber-Reinforced Organo Sheets with a Recycled PLA Matrix.* Polymers (Basel), 2023. **15**(22).
19. Bapat, K.S., et al., *Improved coloration of hemp fabrics via low-pressure argon plasma assisted surface modification.* Cleaner Chemical Engineering, 2024. **10**: p. 100123.
20. Zimniewska, M., *Hemp Fibre Properties and Processing Target Textile: A Review.* Materials (Basel), 2022. **15**(5).
21. Kan, C.-w., *A Novel green treatment for textiles : plasma treatment as a sustainable technology*. Sustainability contributions through science and technology. 2015, Boca Raton: CRC Press.
22. Chan, C.M., T.M. Ko, and H. Hiraoka, *Polymer surface modification by plasmas and photons.* Surface Science Reports, 1996. **24**(1-2): p. 3-54.
23. Levchenko, I., et al., *Plasma and Polymers: Recent Progress and Trends.* Molecules, 2021. **26**(13): p. 4091.
24. Boehm, D. and C. Canal, *Application of Plasma Technology in Bioscience and Biomedicine.* Applied Sciences, 2021. **11**(16).
25. Liu, M., et al., *Targeted pre-treatment of hemp bast fibres for optimal performance in biocomposite materials: A review.* Industrial crops and products, 2017. **108**: p. 660-683.
26. Ullah, M.H., et al., *Surface modification and improvements of wicking properties and dyeability of grey jute-cotton blended fabrics using low-pressure glow discharge air plasma.* Heliyon, 2021. **7**(8): p. e07893-e07893.
27. Pejić, B.M., et al., *Effect of plasma treatment on chemical composition, structure and sorption properties of lignocellulosic hemp fibers (Cannabis sativa L.).* Carbohydrate polymers, 2020. **236**: p. 116000-116000.
28. Liu, M., et al., *Effect of harvest time and field retting duration on the chemical composition, morphology and mechanical properties of hemp fibers.* Industrial Crops and Products, 2015. **69**: p. 29-39.
29. Ramesh, M., *Hemp, jute, banana, kenaf, ramie, sisal fibers*, in *Handbook of Properties of Textile and Technical Fibres*. 2018. p. 301-325.
30. Ramesh, M., et al., *Physical Modification of Bast Fibre Surface and Their Effects*, in *Bast Fibers and Their Composites: Processing, Properties and Applications*, G. Rajeshkumar, et al., Editors. 2022, Springer Nature Singapore: Singapore. p. 65-80.
31. Sadrmanesh, V. and Y. Chen, *Bast fibres: structure, processing, properties, and applications.* International materials reviews, 2019. **64**(7): p. 381-406.
32. Ventorino, V., et al., *Water retting process with hemp pre-treatment: effect on the enzymatic activities and microbial populations dynamic.* Applied microbiology and biotechnology, 2024. **108**(1): p. 464-464.
33. Jankauskienė, Z., et al., *Chemical composition and physical properties of dew- and water-retted hemp fibers.* Industrial crops and products, 2015. **75**: p. 206-211.
34. Chabbert, B., et al., *How the interplay between harvest time and climatic conditions drives the dynamics of hemp (Cannabis sativa L.) field retting.* Industrial crops and products, 2023. **204**(117294): p. 117294-11.

35. Bou Orm, E., A. Bergeret, and L. Malhautier, *Microbial communities and their role in enhancing hemp fiber quality through field retting.* Applied Microbiology and Biotechnology, 2024. **108**(1): p. 501.
36. Decker, A., et al., *Influence of Different Retting on Hemp Stem and Fiber Characteristics Under the East of France Climate Conditions.* Journal of natural fibers, 2024. **21**(1).
37. Konczewicz, W., M. Zimniewska, and M.A. Valera, *The selection of a retting method for the extraction of bast fibers as response to challenges in composite reinforcement.* Textile research journal, 2018. **88**(18): p. 2104-2119.
38. Grégoire, M., et al., *Analysis of the potential of hemp fibres for load bearing composite reinforcement using classical field management techniques and carded route.* Composites Part A: Applied Science and Manufacturing, 2025. **190**: p. 108658.
39. Grégoire, M., et al., *Comparing flax and hemp fibres yield and mechanical properties after scutching/hackling processing.* Industrial Crops and Products, 2021. **172**: p. 114045.
40. Dai, D., *HEMP NANOCELLULOSE: FABRICATION, CHARACTERISATION AND APPLICATION* in *School of Engineering and Design*. Brunel University
41. Zheng, G., *Numerical Investigation of Characteristic of Anisotropic Thermal Conductivity of Natural Fiber Bundle with Numbered Lumens.* Mathematical Problems in Engineering, 2014. **2014**: p. 1-8.
42. Marková, I., *Textile fiber microscopy : a practical approach*. 1st edition ed. 2019, Hoboken, NJ: Wiley.
43. Manian, A.P., M. Cordin, and T. Pham, *Extraction of cellulose fibers from flax and hemp: a review.* Cellulose, 2021. **28**(13): p. 8275-8294.
44. Chokshi, S., et al., *Chemical Composition and Mechanical Properties of Natural Fibers.* Journal of natural fibers, 2020. **ahead-of-print**(ahead-of-print): p. 1-12.
45. Abdellatef, Y., et al., *Mechanical, Thermal, and Moisture Buffering Properties of Novel Insulating Hemp-Lime Composite Building Materials.* Materials, 2020. **13**(21): p. 5000.
46. Lazić Biljana, D., et al., *Effect of chemical treatments on the chemical composition and properties of flax fibers.* Journal of the Serbian Chemical Society, 2017. **82**(1): p. 83-97.
47. Sawpan, M.A., K.L. Pickering, and A. Fernyhough, *Effect of various chemical treatments on the fibre structure and tensile properties of industrial hemp fibres.* Composites. Part A, Applied science and manufacturing, 2011. **42**(8): p. 888-895.
48. Kaczmar, J.W., J. Pach, and C. Burgstaller, *The chemically treated hemp fibres to reinforce polymers.* Polimery, 2011. **56**(11/12): p. 817-822.
49. Sosiati, H., et al., *The influence of alkali treatments on tensile strength and surface morphology of cellulose microfibrils.* Advanced Materials Research, 2015. **1123**: p. 147-150.
50. Nasrullah, A., et al., *9 - Comprehensive approach on the structure, production, processing, and application of lignin*, in *Lignocellulosic Fibre and Biomass-Based Composite Materials*, M. Jawaid, P. Md Tahir, and N. Saba, Editors. 2017, Woodhead Publishing. p. 165-178.
51. Vázquez-Vuelvas, O.F., et al., *Chapter 7 - Fungal bioprocessing of lignocellulosic materials for biorefinery*, in *Recent Advancement in Microbial*

Biotechnology, S. De Mandal and A.K. Passari, Editors. 2021, Academic Press. p. 171-208.
52. Boerjan, W., J. Ralph, and M. Baucher, *Lignin biosynthesis.* Annu Rev Plant Biol, 2003. **54**: p. 519-46.
53. Donaldson, L., B. Nanayakkara, and J. Harrington, *Wood Growth and Development*, in *Encyclopedia of Applied Plant Sciences (Second Edition)*, B. Thomas, B.G. Murray, and D.J. Murphy, Editors. 2017, Academic Press: Oxford. p. 203-210.
54. Wang, H.M., et al., *Removing pectin and lignin during chemical processing of hemp for textile applications.* Textile Research Journal, 2003. **73**(8): p. 664-669.
55. Al-Rudainy, B., et al., *Impact of Lignin Content on the Properties of Hemicellulose Hydrogels.* Polymers, 2019. **11**(1): p. 35.
56. Gutierrez, A., I.M. Rodriguez, and J.C.d. Rio, *Chemical Characterization of Lignin and Lipid Fractions in Industrial Hemp Bast Fibers Used for Manufacturing High-Quality Paper Pulps.* Journal of agricultural and food chemistry, 2006. **54**(6): p. 2138-2144.
57. Zheng, Z., et al., *Simultaneous Degumming and Extraction of a Nature Gum from Raw Hemp.* Journal of Natural Fibers, 2022. **19**(8): p. 2943-2952.
58. Zhao, T., et al., *A novel eco–friendly solid–state degumming method for extraction of hemp fibers.* Journal of Cleaner Production, 2024. **435**: p. 140549.
59. Zhang, X., et al., *Green Degumming Technology of Hemp and a Comparison between Chemical and Biological Degumming.* ACS omega, 2021. **6**(50): p. 35067-35075.
60. Yeping, X., et al., *The chemo-enzymatic modification and degumming of hemp fiber by the laccase-2,2,6,6-tetramethylpiperidine-1-oxyl radical-hemicellulase system and physico-chemical properties of the products.* Textile Research Journal, 2018. **89**: p. 2433 - 2443.
61. Ahmed, B., et al., *Degumming of Hemp Fibers Using Combined Microwave Energy and Deep Eutectic Solvent Treatment*. 2021.
62. Song, J., et al., *Processing bulk natural wood into a high-performance structural material.* Nature (London), 2018. **554**(7691): p. 224-228.
63. Xiao, S., et al., *Lightweight, strong, moldable wood via cell wall engineering as a sustainable structural material.* Science (American Association for the Advancement of Science), 2021. **374**(6566): p. 465-471.
64. Dalle Vacche, S., et al., *Valorization of Byproducts of Hemp Multipurpose Crop: Short Non-Aligned Bast Fibers as a Source of Nanocellulose.* Molecules, 2021. **26**(16).
65. Zhu, R., et al., *Novel scouring method of hemp fibers based on electrochemical techniques.* Textile Research Journal, 2021. **91**(19-20): p. 2215-2224.
66. Åkerholm, M., B. Hinterstoisser, and L. Salmén, *Characterization of the crystalline structure of cellulose using static and dynamic FT-IR spectroscopy.* Carbohydrate research, 2004. **339**(3): p. 569-578.
67. Kovalenko, V.I., *Crystalline cellulose: structure and hydrogen bonds.* Russian Chemical Reviews, 2010. **79**(3): p. 231-241.
68. Peter, Z., *Order in cellulosics: Historical review of crystal structure research on cellulose.* Carbohydr Polym, 2021. **254**: p. 117417.

69. Meyer, K.H., M. Studer, and A.J.A. Van Der Wyk, *Constitution of 'Pure' Cellulose.* Nature (London), 1949. **164**(4175): p. 786-787.
70. and, V.B. and F.R.S. PRoF. R. D. PRESTON, *FINE STRUCTURE OF CELLULOSE AND OTHER MICROFIBRILLAR SUBSTANCES.* Nature, 1955.
71. Frey-Wyssling, A., *On the crystal structure of cellulose I.* Biochimica et biophysica acta, 1955. **18**(1): p. 166-168.
72. Jablonski, M., *Intramolecular Hydrogen Bonding 2021.* Molecules, 2021. **26**(20).
73. Mukherjee, S.M., J. Sikorski, and H.J. Woods, *Micellar Structure of Native Cellulose.* Nature (London), 1951. **167**(4255): p. 821-822.
74. Jhatial, A., H. Yesuf, and B. Wagaye, *Pretreatment of Cotton*. 2020. p. 333-353.
75. Shore, J., *Cellulosics dyeing*. 1995, Bradford: Society of Dyers and Colourists.
76. Hauser, P., *Fabric Finishing*, in *Textiles and Fashion*. 2015. p. 459-473.
77. Beyene, K.A., E.K. Gebeyehu, and B.F. Adamu, *The effects of pretreatment on the surface roughness of plain-woven fabric by the Kawabata Evaluation System.* Textile Research Journal, 2023. **93**(9-10): p. 2149-2157.
78. Jhatial, A.K., H.M. Yesuf, and B.T. Wagaye, *Pretreatment of Cotton*, in *Cotton Science and Processing Technology: Gene, Ginning, Garment and Green Recycling*, H. Wang and H. Memon, Editors. 2020, Springer Singapore: Singapore. p. 333-353.
79. Maichin, P., et al., *Hemp Fiber Reinforced Geopolymer Composites: Effects of NaOH Concentration on Fiber Pre-Treatment Process.* Key Engineering Materials, 2020. **841**: p. 166-170.
80. Cruz, J. and R. Fangueiro, *Surface Modification of Natural Fibers: A Review.* Procedia Engineering, 2016. **155**: p. 285-288.
81. Roy Choudhury, A.K., *3 - Pre-treatment and preparation of textile materials prior to dyeing*, in *Handbook of Textile and Industrial Dyeing*, M. Clark, Editor. 2011, Woodhead Publishing. p. 64-149.
82. Sun, H., et al., *The improvement of dyeability of flax fibre by microwave treatment.* Pigment & resin technology, 2005. **34**(4): p. 190-196.
83. Kabir, M.M., et al., *Effects of chemical treatments on hemp fibre structure.* Applied Surface Science, 2013. **276**: p. 13-23.
84. Sepe, R., et al., *Influence of chemical treatments on mechanical properties of hemp fiber reinforced composites.* Composites Part B: Engineering, 2018. **133**: p. 210-217.
85. Tanasă, F., et al., *Modified hemp fibers intended for fiber-reinforced polymer composites used in structural applications—A review. I. Methods of modification.* Polymer Composites, 2020. **41**(1): p. 5-31.
86. Kostic, M., B. Pejic, and P. Skundric, *Quality of chemically modified hemp fibers.* Bioresour Technol, 2008. **99**(1): p. 94-9.
87. Scheibe, M., et al., *Application of Natural (Plant) Fibers Particularly Hemp Fiber as Reinforcement in Hybrid Polymer Composites - Part III. Investigations of Physical and Mechanical Properties of Composites Reinforced with Hemp Fibers.* Journal of Natural Fibers, 2024. **21**(1): p. 2414194.
88. Grifoni, D., et al., *Evaluation of Dyeing and UV Protective Properties on Hemp Fabric of Aqueous Extracts from Vegetal Matrices of Different Origin.* Fibers and Polymers, 2020. **21**(8): p. 1750-1759.

89. Guru, R., S. Panigrahi, and P. Thennarasu, *Development of Cotton, Hemp and Silk Blended Curtains for Designer Home Interiors.* Asian Journal of Applied Sciences, 2023. **16**: p. 47-54.
90. Poddar, B.J., et al., *A comprehensive review on the pretreatment of lignocellulosic wastes for improved biogas production by anaerobic digestion.* International Journal of Environmental Science and Technology, 2022. **19**(4): p. 3429-3456.
91. Brar, K.K., et al., *A paradigm shift towards production of sustainable bioenergy and advanced products from Cannabis/hemp biomass in Canada.* Biomass Conversion and Biorefinery, 2024. **14**(3): p. 3161-3182.
92. Han, H., et al., *A Study About Water/Alkali Treatments of Hemp Fiber on Ultraviolet Ageing of the Reinforced Polypropylene Composites.* Journal of polymers and the environment, 2020. **28**(10): p. 2572-2583.
93. Wawro, A., J. Batog, and W. Gieparda, *Chemical and Enzymatic Treatment of Hemp Biomass for Bioethanol Production.* Applied Sciences, 2019. **9**(24): p. 5348.
94. Kowalonek, J., H. Kaczmarek, and A. Dąbrowska, *Air plasma or UV-irradiation applied to surface modification of pectin/poly(vinyl alcohol) blends.* Applied surface science, 2010. **257**(1): p. 325-331.
95. Kalia, S., et al., *Surface modification of plant fibers using environment friendly methods for their application in polymer composites, textile industry and antimicrobial activities: A review.* Journal of environmental chemical engineering, 2013. **1**(3): p. 97-112.
96. Alves, P., et al., *Surface modification of a thermoplastic polyurethane by low-pressure plasma treatment to improve hydrophilicity.* Journal of applied polymer science, 2011. **122**(4): p. 2302-2308.
97. Daria, S., et al., *Surface modification of highly porous 3D networks via atmospheric plasma treatment.* Contributions to plasma physics (1988), 2018. **58**(5): p. 384-393.
98. Yang, J., et al., *Superhydrophobic cotton nonwoven fabrics through atmospheric plasma treatment for applications in self-cleaning and oil–water separation.* Cellulose (London), 2019. **26**(12): p. 7507-7522.
99. Thompson, R., et al., *Low-frequency plasma activation of nylon 6.* Applied surface science, 2021. **544**: p. 148929.
100. Yang, J., et al., *Fabrication of Durably Superhydrophobic Cotton Fabrics by Atmospheric Pressure Plasma Treatment with a Siloxane Precursor.* Polymers, 2018. **10**(4): p. 460.
101. Ilyushina, S., et al., *Study of the effect of plasma modification on the change of fire-resistant properties of textile materials imported by flame retardants.* Journal of physics. Conference series, 2019. **1328**(1): p. 12037.
102. Baltazar-Y-Jimenez, A. and A. Bismarck, *Surface modification of lignocellulosic fibres in atmospheric air pressure plasma.* Green chemistry : an international journal and green chemistry resource : GC, 2007. **9**(10): p. 1057-1057.
103. Sun, S., et al., *Mechanical performance of epoxy matrix composites reinforced by physically and chemically treated hemp fiber.* Polymer Composites, 2024. **45**(16): p. 15113-15124.
104. Kiruthika, A.V., *A review on physico-mechanical properties of bast fibre reinforced polymer composites.* Journal of Building Engineering, 2017. **9**: p. 91-99.

105. Olhan, S., V. Khatkar, and B.K. Behera, *Review: Textile-based natural fibre-reinforced polymeric composites in automotive lightweighting.* Journal of Materials Science, 2021. **56**(34): p. 18867-18910.
106. Alonso-Montemayor, F.J., et al., *Plasma-treated lignocellulosic fibers for polymer reinforcement. A review.* Cellulose (London), 2022. **29**(2): p. 659-683.
107. Kaur, R., et al., *Sustainable Lignin-Based Coatings Doped with Titanium Dioxide Nanocomposites Exhibit Synergistic Microbicidal and UV-Blocking Performance toward Personal Protective Equipment.* ACS Sustainable Chemistry & Engineering, 2021. **9**(33): p. 11223-11237.
108. Hemp, E.Y. *https://eastyorkshirehemp.co.uk/*.
109. Thygesen, L.G., J.B. Bilde-Sørensen, and P. Hoffmeyer, *Visualisation of dislocations in hemp fibres: A comparison between scanning electron microscopy (SEM) and polarized light microscopy (PLM).* Industrial Crops and Products, 2006. **24**(2): p. 181-185.
110. High-tech, H.
111. Rima, A., et al., *Microscopic estimation of swelling and shrinkage of hemp concrete in response to relative humidity variations.* Journal of Building Engineering, 2021. **43**: p. 102929.
112. George, M., et al., *Characterization of chemically and enzymatically treated hemp fibres using atomic force microscopy and spectroscopy.* Applied surface science, 2014. **314**: p. 1019-1025.
113. Melelli, A., et al., *The Middle Lamella of Plant Fibers Used as Composite Reinforcement: Investigation by Atomic Force Microscopy.* Molecules (Basel, Switzerland), 2020. **25**(3): p. 632.
114. Li, J. and B. Kasal, *Review on the Structure–Property Relationship of Lignocellulosic Materials Measured by Atomic Force Microscopy.* Biomacromolecules, 2025. **26**(3): p. 1404-1418.
115. Rana, M.S., H. Pota, and I. Petersen, *Improvement in the Imaging Performance of Atomic Force Microscopy: A Survey.* IEEE Transactions on Automation Science and Engineering, 2016. **14**: p. 1-21.
116. Chowdhury, S., et al., *Nanomechanical characterization of hemp fiber with atomic force microscopy.* Journal of Composite Materials, 2025. **59**(4): p. 469-478.
117. Berthomieu, C. and R. Hienerwadel, *Fourier transform infrared (FTIR) spectroscopy.* Photosynthesis research, 2009. **101**(2-3): p. 157-170.
118. Garside, P. and P. Wyeth, *Identification of Cellulosic Fibres by FTIR Spectroscopy DIFFERENTIATION OF FLAX AND HEMP BY POLARIZED ATR FTIR.* Studies in Conservation, 2013. **51**(3): p. 205-211.
119. Muchaamba, F. and R. Stephan, *A Comprehensive Methodology for Microbial Strain Typing Using Fourier-Transform Infrared Spectroscopy.* Methods and Protocols, 2024. **7**(3): p. 48.
120. Colthup, N.B., *Infrared Spectroscopy*, in *Encyclopedia of Physical Science and Technology (Third Edition)*, R.A. Meyers, Editor. 2003, Academic Press: New York. p. 793-816.
121. Agarwal, U.P., *Analysis of Cellulose and Lignocellulose Materials by Raman Spectroscopy: A Review of the Current Status.* Molecules, 2019. **24**(9): p. 1659.
122. Bumbrah, G.S. and R.M. Sharma, *Raman spectroscopy – Basic principle, instrumentation and selected applications for the characterization of drugs of abuse.* Egyptian Journal of Forensic Sciences, 2016. **6**(3): p. 209-215.

123. Das, R.S. and Y.K. Agrawal, *Raman spectroscopy: Recent advancements, techniques and applications.* Vibrational Spectroscopy, 2011. **57**(2): p. 163-176.
124. Salem, K.S., et al., *Comparison and assessment of methods for cellulose crystallinity determination.* Chemical Society reviews, 2023. **52**(18): p. 6417-6446.
125. Lee, J., et al., *Creation of crystal structure reproducing X-ray diffraction pattern without using database.* npj Computational Materials, 2023. **9**(1): p. 135.
126. Langford, J.I. and A.J.C. Wilson, *Scherrer after sixty years: A survey and some new results in the determination of crystallite size.* Journal of Applied Crystallography, 1978. **11**(2): p. 102-113.
127. Xu, F., Y.-C. Shi, and D. Wang, *X-ray scattering studies of lignocellulosic biomass: A review.* Carbohydrate Polymers, 2013. **94**(2): p. 904-917.
128. *Water contact angle.*
129. *Tensile Testing Machine.*
130. *BS EN ISO 5079:2020: Textile fibres. Determination of breaking force and elongation at break of individual fibres*. 2020, British Standards Institute.
131. *BS EN ISO 9073-18:2023: Nonwovens. Test methods: Determination of tensile strength and elongation at break using the grab tensile test*. 2024, British Standards Institute.
132. Christodoulou, M.C., et al., *Spectrophotometric Methods for Measurement of Antioxidant Activity in Food and Pharmaceuticals.* Antioxidants, 2022. **11**(11): p. 2213.
133. Manian, A.P., M. Cordin, and T. Pham, *Extraction of cellulose fibers from flax and hemp: a review.* Cellulose (London), 2021. **28**(13): p. 8275-8294.
134. Dhondt, F. and S.S. Muthu, *The Future of Hemp in the Fashion Industry*, in *Hemp and Sustainability*, F. Dhondt and S.S. Muthu, Editors. 2021, Springer Singapore: Singapore. p. 109-123.
135. Lara, L., I. Cabral, and J. Cunha, *Ecological Approaches to Textile Dyeing: A Review.* Sustainability, 2022. **14**(14): p. 8353.
136. Goñi, M.L., N.A. Gañán, and R.E. Martini, *Supercritical CO2-assisted dyeing and functionalization of polymeric materials: A review of recent advances (2015–2020).* Journal of CO2 Utilization, 2021. **54**: p. 101760.
137. Kane, F., et al., *Innovative Technologies for Sustainable Textile Coloration, Patterning, and Surface Effects*, in *Sustainability in the Textile and Apparel Industries : Production Process Sustainability*, S.S. Muthu and M.A. Gardetti, Editors. 2020, Springer International Publishing: Cham. p. 99-127.
138. Mijas, G., et al., *Study of Dyeing Process of Hemp/Cotton Fabrics by Using Natural Dyes Obtained from Rubia tinctorum L. and Calendula officialis.* Polymers, 2022. **14**(21): p. 4508.
139. Kabir, S.M.M., R. Karim, and K. Islam, *A Comparative Study on Dyeing Properties of Hemp and Cotton Fiber.* European Scientific Journal, ESJ, 2017. **13**(33).
140. Atav, R., et al., *Investigation of the dyeability and various performance properties of fabrics produced from flax and hemp fibres and their blends with cotton in comparison with cotton.* Coloration technology, 2024. **140**(3): p. 440-450.
141. Sunoj Valiaparambil Sebastian, J., et al., *Hemp Agronomy: Current Advances, Questions, Challenges, and Opportunities.* Agronomy, 2023. **13**(2): p. 475.

142. Abdelileh, M., M. Ben Ticha, and N. Meksi, *Reviving of Cotton Dyeing by Saxon Blue: Application of Microwave Irradiation to Enhance Dyeing Performances.* Fibers and polymers, 2021. **22**(7): p. 1863-1873.
143. Adeel, S., et al., *Dyeing of gamma irradiated cotton using Direct Yellow 12 and Direct Yellow 27: improvement in colour strength and fastness properties.* Cellulose (London), 2015. **22**(3): p. 2095-2105.
144. Zhianmanesh, M., et al., *Plasma surface functionalization: A comprehensive review of advances in the quest for bioinstructive materials and interfaces.* Applied Physics Reviews, 2023. **10**(2).
145. Cho, A., et al., *Plasma Treatments of Molecularly Templated Nanoporous Silica Films.* Electrochemical and Solid State Letters - ELECTROCHEM SOLID STATE LETT, 2001. **4**.
146. Pillai, R.R. and V. Thomas, *Plasma Surface Engineering of Natural and Sustainable Polymeric Derivatives and Their Potential Applications.* Polymers, 2023. **15**(2): p. 400.
147. Barbière, R., et al., *Characterisation of interfacial adhesion in hemp composites after H2O2 and non-thermal plasma treatments.* Journal of composite materials, 2021. **55**(25): p. 3751-3762.
148. Pavlovic, S.S., et al., *Impact of plasma treatment on acoustic properties of natural cellulose materials.* Cellulose (London), 2019. **26**(11): p. 6543-6554.
149. Gieparda, W., S. Rojewski, and W. Różańska, *Effectiveness of Silanization and Plasma Treatment in the Improvement of Selected Flax Fibers' Properties.* Materials, 2021. **14**(13): p. 3564.
150. Sawangrat, C., et al., *Surface Modification and Mechanical Properties Improvement of Bamboo Fibers Using Dielectric Barrier Discharge Plasma Treatment.* Polymers, 2023. **15**(7): p. 1711.
151. Ivanovska, A., et al., *Plasma Treatment as a Sustainable Method for Enhancing the Wettability of Jute Fabrics.* Sustainability (Basel, Switzerland), 2023. **15**(3): p. 2125.
152. Radetić, M., et al., *The Influence of Low-temperature Plasma and Enzymatic Treatment on Hemp Fabric Dyeability.* Fibres and Textiles in Eastern Europe, 2007. **15**: p. 93-96.
153. Luque-Agudo, V., et al., *Effect of plasma treatment on the surface properties of polylactic acid films.* Polymer Testing, 2021. **96**: p. 107097.
154. Zhu, Y., X. Ren, and C. Wu, *Influence of alkali treatment on the structure of newcell fibers.* Journal of applied polymer science, 2004. **93**(4): p. 1731-1735.
155. Lokhande, H.T. and A.S. Salvi, *Electrokinetic studies of cellulosic fibres I. Zeta potential of fibres dyed with reactive dyes.* Colloid and Polymer Science, 1976. **254**(11): p. 1030-1041.
156. Rattee, I.D., *The chemistry of dyeing.* Chemical Society reviews, 1972. **1**(2): p. 145.
157. Rattee, I.D. and M.M. Breuer, *The physical chemistry of dye adsorption*. 1974, London: Academic Press.
158. Rattee, I.D., *Bonds between dyes and fibres.* Science progress (1916), 1964. **52**(208): p. 581-592.
159. Correia, J., et al., *Surface functionalization of greige cotton knitted fabric through plasma and cationization for dyeing with reactive and acid dyes.* Cellulose (London), 2021. **28**(15): p. 9971-9990.

160. Ibrahim, N.A., B.M. Eid, and M.S. Abdel-Aziz, *Effect of plasma superficial treatments on antibacterial functionalization and coloration of cellulosic fabrics.* Applied surface science, 2017. **392**: p. 1126-1133.
161. Haji, A. and M. Naebe, *Cleaner dyeing of textiles using plasma treatment and natural dyes: A review.* Journal of Cleaner Production, 2020. **265**: p. 121866.
162. Wang, H.M. and R. Postle, *Improving the color features of hemp fibers after chemical preparation for textile applications.* Textile research journal, 2004. **74**(9): p. 781-786.
163. Juhász, L., et al., *False Morphology of Aerogels Caused by Gold Coating for SEM Imaging.* Polymers, 2021. **13**(4): p. 588.
164. Hojat, N., et al., *Automatic pore size measurements from scanning electron microscopy images of porous scaffolds.* Journal of Porous Materials, 2023. **30**(1): p. 93-101.
165. Peets, P., et al., *Reflectance FT-IR spectroscopy as a viable option for textile fiber identification.* Heritage Science, 2019. **7**(1): p. 93.
166. Rygula, A., et al., *Application of FT-Raman spectroscopy for in situdetection of microorganisms on the surface of textiles.* Journal of Environmental Monitoring, 2011. **13**(11): p. 2983-2987.
167. Uddin, M.G., M.M. Islam, and M.R. Islam, *Effects of reductive stripping of reactive dyes on the quality of cotton fabric.* Fashion and Textiles, 2015. **2**(1): p. 8.
168. *Vat dyeing of cotton piece*. Second edition. ed. 1959, Place of publication not identified: Imperial Chemical Industries Limited, Dyestuffs Division.
169. Moradkhani, G., et al., *Effects of Wet and Dry Treatments on Surface Functional Groups and Mechanical Properties of Flax Fiber Composites.* Coatings, 2023. **13**(6): p. 1036.
170. G, S.M., A.M. C, and P.L. T, *Effects of Dry Etching Plasma Treatments on Natural and Synthetics Fibers: a Comparative Study.* Materials Circular Economy, 2022. **4**(1): p. 11.
171. Palumbo, F., C. Lo Porto, and P. Favia, *Plasma Nano-Texturing of Polymers for Wettability Control: Why, What and How.* Coatings, 2019. **9**(10): p. 640.
172. Shu, Q., et al., *Atmospheric pressure argon plasma: an effective method to improve the hydrophilicity of the cellulose in paper.* Cellulose, 2023. **30**(18): p. 11767-11782.
173. Xu, J., et al., *Different Etching Mechanisms of Diamond by Oxygen and Hydrogen Plasma: a Reactive Molecular Dynamics Study.* The Journal of Physical Chemistry C, 2021. **125**(30): p. 16711-16718.
174. Kortshagen, U.R., et al., *Nonthermal Plasma Synthesis of Nanocrystals: Fundamental Principles, Materials, and Applications.* Chemical Reviews, 2016. **116**(18): p. 11061-11127.
175. Kondo, T., *The assignment of IR absorption bands due to free hydroxyl groups in cellulose.* Cellulose (London), 1997. **4**(4): p. 281-292.
176. Gerullis, S., et al., *Plasma treatment of cellulose: investigation on molecular changes using spectroscopic methods and chemical derivatization.* Cellulose, 2022. **29**(13): p. 7163-7176.
177. Geminiani, L., et al., *Differentiating between Natural and Modified Cellulosic Fibres Using ATR-FTIR Spectroscopy.* Heritage, 2022. **5**(4): p. 4114-4139.
178. Jothi Prakash, C.G. and R. Prasanth, *Approaches to design a surface with tunable wettability: a review on surface properties.* Journal of Materials Science, 2021. **56**(1): p. 108-135.

179. Ramos, S.C., et al., *Influence of polar groups on the wetting properties of vertically aligned multiwalled carbon nanotube surfaces.* Theoretical Chemistry Accounts, 2011. **130**(4): p. 1061-1069.
180. Agarwal, U.P., *Analysis of Cellulose and Lignocellulose Materials by Raman Spectroscopy: A Review of the Current Status.* Molecules, 2019. **24**(9).
181. Proniewicz, L.M., et al., *FT-IR and FT-Raman study of hydrothermally degraded groundwood containing paper.* Journal of molecular structure, 2002. **614**(1): p. 345-353.
182. Fischer2, K.S.S., *NIR FT Raman spectroscopy – a rapid analytical tool for detecting the transformation of cellulose polymorphs*Cellulose, 2000.
183. Sukhov, D.A., *Hydrogen Bonds in Natural and Mercerized Cellulose Fibres Based on Raman Spectroscopic Data.* Fibre chemistry, 2003. **35**(4): p. 277-282.
184. Fujisawa, R., et al., *Dynamical study of the water penetration process into a cellulose acetate film studied by coherent anti-Stokes Raman scattering (CARS) microspectroscopy.* Chemical Physics Letters, 2016. **655-656**: p. 86-90.
185. Godeau, G., et al., *Post-functionalization of plasma treated polycarbonate substrates: An efficient way to hydrophobic, oleophobic plastics.* Applied Surface Science, 2016. **387**: p. 28-35.
186. Staudt, J., S. Leyer, and J.K. Duchowski, *Detailed Characterization of the Effect of Application of Commercially Available Surface Treatment Agents on Textile Wetting Behavior.* Coatings, 2019. **9**(4): p. 219.
187. Fowkes, F.M., *ATTRACTIVE FORCES AT INTERFACES.* Industrial and engineering chemistry, 1964. **56**(12): p. 40-52.
188. Du, Q., et al., *Influence of hydrophobicity and roughness on the wetting and flow resistance of water droplets on solid surface: A many-body dissipative particle dynamics study.* Chemical engineering science, 2022. **249**: p. 117327.
189. Gomathi, N. and S. Neogi, *Surface modification of polypropylene using argon plasma: Statistical optimization of the process variables.* Applied surface science, 2009. **255**(17): p. 7590-7600.
190. Zhang, L., et al., *Carbon Surface Modifications by Plasma for Catalyst Support and Electrode Materials Applications.* Topics in Catalysis, 2017. **60**(12): p. 823-830.
191. Palaskar, S.S., R.D. Kale, and R.R. Deshmukh, *Application of atmospheric pressure plasma for adhesion improvement in polyurethane coating on polypropylene fabrics.* Journal of Coatings Technology and Research, 2020. **17**(2): p. 485-501.
192. Liu, J., et al., *A Reflective Fiber Optic Sensor for Surface Roughness In-Process Measurement.* Journal of Manufacturing Science and Engineering, 2002. **124**(3): p. 515-522.
193. Amin, M.N. and R.S. Blackburn, *Sustainable Chemistry Method to Improve the Wash-off Process of Reactive Dyes on Cotton.* ACS sustainable chemistry & engineering, 2015. **3**(4): p. 725-732.
194. Hegemann, D. and D. Balazs, *Nano-scale treatment of textiles using plasma technology*. 2007. p. 158-180.
195. Kamran, M., S. Adeel, and F.-u. Rehman, *Eco-Friendly Pretreatment and Dyeing of Cotton with Vat Yellow 46.* Journal of natural fibers, 2022. **19**(14): p. 9765-9775.

196. Law, A.D., C.R. McNees, and L.A. Moe, *The Microbiology of Hemp Retting in a Controlled Environment: Steering the Hemp Microbiome towards More Consistent Fiber Production.* Agronomy, 2020. **10**(4): p. 492.
197. Gregoire, M., et al., *Study of solutions to optimize the extraction of hemp fibers for composite materials.* SN Applied Sciences, 2019. **1**(10).
198. Lyu, P., et al., *Degumming methods for bast fibers—A mini review.* Industrial crops and products, 2021. **174**: p. 114158.
199. Kirk, H., et al., *A critical review of characterization and measurement of textile-grade hemp fiber.* Cellulose, 2023. **30**(14): p. 8595-8616.
200. Kanyairita, G.G., et al. *Comparison of the Efficiency of Deep Eutectic and Organic Solvents in the Extraction of Phytochemicals from Cannabis sativa L*. Separations, 2024. **11**, DOI: https://doi.org/10.3390/separations11040106.
201. Moussa, M., et al., *Toward the cottonization of hemp fibers by steam explosion. Flame-retardant fibers.* Industrial Crops and Products, 2020. **151**: p. 112242.
202. Ahmed, B., et al., *Combined effects of deep eutectic solvent and microwave energy treatments on cellulose fiber extraction from hemp bast.* Cellulose, 2023. **30**(5): p. 2895-2911.
203. Thomsen, A.B., et al., *Effects of chemical–physical pre-treatment processes on hemp fibres for reinforcement of composites and for textiles.* Industrial Crops and Products, 2006. **24**(2): p. 113-118.
204. Rombaldoni, F., et al., *Oxygen plasma treatment to reduce the dyeing temperature of wool fabrics.* Journal of applied polymer science, 2010. **118**(2): p. 1173-1183.
205. Ghoranneviss, M. and S. Shahidi, *Color intensity and wash fastness properties of dyed cotton fabric after plasma treatment.* Journal of the Textile Institute, 2017. **108**(3): p. 445-448.
206. Hamad, S.F., et al., *Exploiting Plasma Exposed, Natural Surface Nanostructures in Ramie Fibers for Polymer Composite Applications.* Materials, 2019. **12**(10): p. 1631.
207. Lim, N., A. Efremov, and K.-H. Kwon, *A Comparison of CF4, CHF3 and C4F8 + Ar/O2 Inductively Coupled Plasmas for Dry Etching Applications.* Plasma Chemistry and Plasma Processing, 2021. **41**(6): p. 1671-1689.
208. S, M.G., M.C. A, and L.T. P, *Effects of Dry Etching Plasma Treatments on Natural and Synthetics Fibers: a Comparative Study.* Materials Circular Economy, 2022. **4**(1): p. 11.
209. Stevulova, N., et al., *Properties Characterization of Chemically Modified Hemp Hurds.* Materials (Basel), 2014. **7**(12): p. 8131-8150.
210. Chukhchin, D.G., et al., *Diffractometric method for determining the degree of crystallinity of materials.* Crystallography Reports, 2016. **61**(3): p. 371-375.
211. Krässig, H.A., *Cellulose : structure, accessibility, and reactivity*. Polymer monographs ; v.11. 1993, Yverdon, Switzerland ;: Gordon and Breach Science.
212. Tavana, H., et al., *Contact angle measurements with liquids consisting of bulky molecules.* Journal of Colloid and Interface Science, 2004. **279**(2): p. 493-502.
213. Pucci, M.F., P.-J. Liotier, and S. Drapier, *Tensiometric method to reliably assess wetting properties of single fibers with resins: Validation on cellulosic reinforcements for composites.* Colloids and Surfaces A: Physicochemical and Engineering Aspects, 2017. **512**: p. 26-33.

214. Nagy, N., *Contact Angle Determination on Hydrophilic and Superhydrophilic Surfaces by Using r–θ-Type Capillary Bridges.* Langmuir, 2019. **35**(15): p. 5202-5212.
215. Ribeiro, J., et al., *Experimental Study on Mechanical Properties of Hemp Fibers Influenced by Various Parameters.* Sustainability, 2023. **15**(12): p. 9610.
216. Donaldson, L., *Autofluorescence in Plants.* Molecules, 2020. **25**(10).
217. Kitin, P., et al., *Direct fluorescence imaging of lignocellulosic and suberized cell walls in roots and stems.* AoB PLANTS, 2020. **12**(4).
218. Wang, Y., et al., *Characterization of Argon/Hydrogen Inductively Coupled Plasma for Carbon Removal over Multilayer Thin Films.* Coatings, 2023. **13**(2): p. 368.
219. Devnani, G.L., *Recent Trends in the Surface Modification of Natural Fibers for the Preparation of Green Biocomposite*, in *Green Composites*, S. Thomas and P. Balakrishnan, Editors. 2021, Springer Singapore: Singapore. p. 273-293.
220. Manaia, J.P., A.T. Manaia, and L. Rodriges, *Industrial Hemp Fibers: An Overview.* Fibers, 2019. **7**(12): p. 106.
221. Li, M., et al., *Elucidating adsorption behavior of cellulase on lignin through isolated lignin and model compounds.* Wood Science and Technology, 2022. **56**.
222. Mahlberg, R., et al., *Application of AFM on the Adhesion Studies of Oxygen-Plasma-Treated Polypropylene and Lignocellulosics.* Langmuir, 1999. **15**(8): p. 2985-2992.
223. de Farias, J.G.G., et al., *Surface lignin removal on coir fibers by plasma treatment for improved adhesion in thermoplastic starch composites.* Carbohydrate Polymers, 2017. **165**: p. 429-436.
224. Akpan, E.I., *Chemistry and Structure of Lignin*, in *Sustainable Lignin for Carbon Fibers: Principles, Techniques, and Applications*, E.I. Akpan and S.O. Adeosun, Editors. 2019, Springer International Publishing: Cham. p. 1-50.
225. Micic, M., et al., *Probing the lignin nanomechanical properties and lignin–lignin interactions using the atomic force microscopy.* Chemical Physics Letters, 2001. **347**(1): p. 41-45.
226. Muazzam, R., et al., *Plasma-based ozonolysis of lignin waste materials for the production of value-added chemicals.* Biomass Conversion and Biorefinery, 2023. **13**(7): p. 5903-5919.
227. Edwards, N.W.M., et al., *Role of surface energy and nano-roughness in the removal efficiency of bacterial contamination by nonwoven wipes from frequently touched surfaces.* Sci Technol Adv Mater, 2017. **18**(1): p. 197-209.
228. Jiang, X., et al., *A review on raw materials, commercial production and properties of lyocell fiber.* Journal of Bioresources and Bioproducts, 2020. **5**(1): p. 16-25.
229. Mozaffari, A., et al., *Argon and Argon–Oxygen Plasma Surface Modification of Gelatin Nanofibers for Tissue Engineering Applications.* Membranes, 2021. **11**(1): p. 31.
230. Yamamoto, M., et al. *Comparison of Argon and Oxygen Plasma Treatments for Ambient Room-Temperature Wafer-Scale Au–Au Bonding Using Ultrathin Au Films*. Micromachines, 2019. **10**, DOI: https://doi.org/10.3390/mi10020119.

231. Yao, L., et al., *Effect of plasma treatment and graphite/carbon black addition on bending and electromagnetic shielding of hemp fiber/polylactic acid composites.* Journal of Materials Science, 2024. **59**(36): p. 16993-17004.
232. Hua, Z.Q., et al., *Mechanisms of oxygen- and argon-RF-plasma-induced surface chemistry of cellulose.* Plasmas and Polymers, 1997. **2**(3): p. 199-224.
233. Vella, J.R., et al., *Dynamics of plasma atomic layer etching: Molecular dynamics simulations and optical emission spectroscopy.* Journal of Vacuum Science & Technology A, 2023. **41**(6).
234. Morita, K., et al., *Nanoscopic lignin mapping on cellulose nanofibers via scanning transmission electron microscopy and atomic force microscopy.* Cellulose, 2023. **30**(18): p. 11357-11367.
235. Macedo, M.J.P., et al., *Surface modification of kapok fibers by cold plasma surface treatment.* Journal of Materials Research and Technology, 2020. **9**(2): p. 2467-2476.
236. Primc, G., et al., *Recent Progress in Cellulose Hydrophobization by Gaseous Plasma Treatments.* Polymers, 2024. **16**(6): p. 789.
237. Kimura, T. and M. Noto, *Experimental study and global model of inductively coupled CF4/O2 discharges.* Journal of Applied Physics, 2006. **100**(6).
238. Bès, A., et al., *Oxygen plasma etching of hydrocarbon-like polymers: Part I Modeling.* Plasma Processes and Polymers, 2018. **15**(8): p. 1800038.
239. Greb, A., et al., *The influence of surface properties on the plasma dynamics in radio-frequency driven oxygen plasmas: Measurements and simulations.* Applied Physics Letters, 2013. **103**(24).
240. Sarangan, A., *5 - Nanofabrication*, in *Fundamentals and Applications of Nanophotonics*, J.W. Haus, Editor. 2016, Woodhead Publishing. p. 149-184.
241. Cao, Y., et al., *Atmospheric Low-Temperature Plasma-Induced Changes in the Structure of the Lignin Macromolecule: An Experimental and Theoretical Investigation.* Journal of Agricultural and Food Chemistry, 2020. **68**(2): p. 451-460.
242. Erfani Jazi, M., et al., *Structure, chemistry and physicochemistry of lignin for material functionalization.* SN Applied Sciences, 2019. **1**(9): p. 1094.
243. Lieberman, M.A. and A.J. Lichtenberg, *Principles of plasma discharges and materials processing*. 1994, New York: Wiley.
244. Zaitsev, A., et al., *Nanotexturing of plasma-polymer thin films using argon plasma treatment.* Surface and Coatings Technology, 2017. **330**: p. 196-203.
245. Huhtamäki, T., et al., *Surface-wetting characterization using contact-angle measurements.* Nature Protocols, 2018. **13**(7): p. 1521-1538.
246. de Coninck, J. and F. Dunlop, *Partial to complete wetting: A microscopic derivation of the Young relation.* Journal of Statistical Physics, 1987. **47**(5): p. 827-849.
247. Kim, D., N.M. Pugno, and S. Ryu, *Wetting theory for small droplets on textured solid surfaces.* Scientific reports, 2016. **6**(1): p. 37813-37813.
248. Mądry, K. and W. Nowicki, *Wetting between Cassie-Baxter and Wenzel regimes: a cellular model approach.* Eur Phys J E Soft Matter, 2021. **44**(11): p. 138.
249. Abbou, S., et al., *Capillary Penetration Method for Measuring Wetting Properties of Carbon Ionomer Films for Proton Exchange Membrane Fuel Cell (PEMFC) Applications.* Journal of The Electrochemical Society, 2019. **166**: p. F3227-F3233.

250. Hodak, S.K., et al., *Enhancement of the hydrophobicity of silk fabrics by SF6 plasma.* Applied surface science, 2008. **254**(15): p. 4744-4749.
251. Hubbe, M., D. Gardner, and W. Shen, *Contact Angles and Wettability of Cellulosic Surfaces: A Review of Proposed Mechanisms and Test Strategies.* BioResources, 2015. **10**.
252. Sridhar, A.S., L.A. Berglund, and J. Wohlert, *Wetting of native and acetylated cellulose by water and organic liquids from atomistic simulations.* Cellulose, 2023. **30**(13): p. 8089-8106.
253. Kostryukov, S.G., et al., *Determination of Lignin, Cellulose, and Hemicellulose in Plant Materials by FTIR Spectroscopy.* Journal of Analytical Chemistry, 2023. **78**(6): p. 718-727.
254. Kolářová, K., et al., *Effect of plasma treatment on cellulose fiber.* Cellulose, 2013. **20**(2): p. 953-961.
255. Gellerstedt, G. and G. Henriksson, *Chapter 9 - Lignins: Major Sources, Structure and Properties*, in *Monomers, Polymers and Composites from Renewable Resources*, M.N. Belgacem and A. Gandini, Editors. 2008, Elsevier: Amsterdam. p. 201-224.
256. Yun, J.H., et al., *Functional and structural insight into lignocellulosic fibers for high-areal-capacity lithium-sulfur batteries.* Journal of materials chemistry. A, Materials for energy and sustainability, 2021. **9**(34): p. 1826-18271.
257. Kabir, M.M., et al., *Impact Properties of the Chemically Treated Hemp Fibre Reinforced Polyester Composites.* Fibers and Polymers, 2020. **21**(9): p. 2098-2110.
258. Jasti, A. and S. Biswas, *Characterization of Elementary Industrial Hemp (Cannabis Sativa L.) Fiber and Its Fabric.* Journal of Natural Fibers, 2023. **20**(1): p. 2158982.
259. Maceda, A. and T. Terrazas, *Fluorescence Microscopy Methods for the Analysis and Characterization of Lignin.* Polymers, 2022. **14**(5): p. 961.
260. Horikawa, Y., *Structural diversity of natural cellulose and related applications using delignified wood.* Journal of Wood Science, 2022. **68**(1): p. 54.
261. Yan, W., et al., *Wood-derived high-performance cellulose structural materials.* e-Polymers, 2023. **23**(1).
262. Miletzky, F., A. Wagenführ, and M. Zscheile, *Wood-Based Bioeconomy*, in *The bioeconomy system*, D. Thrän and U. Moesenfechtel, Editors. 2022, Springer Berlin Heidelberg: Berlin, Heidelberg. p. 49-65.
263. Hassegawa, M., et al., *Wood-Based Products in the Circular Bioeconomy: Status and Opportunities towards Environmental Sustainability.* Land, 2022. **11**(12): p. 2131.
264. Li, T., et al., *Wood Composite as an Energy Efficient Building Material: Guided Sunlight Transmittance and Effective Thermal Insulation.* Advanced Energy Materials, 2016. **6**(22): p. 1601122.
265. Huang, Z., et al., *A conductive wood membrane anode improves effluent quality of microbial fuel cells.* Environmental Science: Water Research & Technology, 2017. **3**(5): p. 940-946.
266. Hou, D., et al., *Hydrophobic nanostructured wood membrane for thermally efficient distillation.* Science Advances, 2019. **5**(8): p. eaaw3203.
267. Zhu, H., et al., *Lightweight, conductive hollow fibers from nature as sustainable electrode materials for microbial energy harvesting.* Nano Energy, 2014. **10**: p. 268-276.

268. Bansal, R., H.C. Barshilia, and K.K. Pandey, *Nanotechnology in wood science: Innovations and applications.* International Journal of Biological Macromolecules, 2024. **262**: p. 130025.
269. Zhang, J., et al., *The emerging development of transparent wood: materials, characteristics, and applications.* Current Forestry Reports, 2022. **8**(4): p. 333-345.
270. Horikawa, Y., et al., *Development of colorless wood via two-step delignification involving alcoholysis and bleaching with maintaining natural hierarchical structure.* Journal of Wood Science, 2020. **66**(1): p. 37.
271. Tang, J., et al., *Superstrong, sustainable, origami wood paper enabled by dual-phase nanostructure regulation in cell walls.* Science Advances, 2024. **10**(30): p. eado5142.
272. Placet, V., et al., *Investigation of the internal structure of hemp fibres using optical coherence tomography and Focused Ion Beam transverse cutting.* Journal of Materials Science, 2014. **49**(24): p. 8317-8327.
273. Ranalli, P. and G. Venturi, *Hemp as a raw material for industrial applications.* Euphytica, 2004. **140**(1): p. 1-6.
274. Summerscales, J., et al., *A review of bast fibres and their composites. Part 1 – Fibres as reinforcements.* Composites Part A: Applied Science and Manufacturing, 2010. **41**(10): p. 1329-1335.
275. Celino, A., et al., *The hygroscopic behavior of plant fibers: a review.* Front Chem, 2013. **1**: p. 43.
276. Gallos, A., et al., *Lignocellulosic fibers: a critical review of the extrusion process for enhancement of the properties of natural fiber composites.* RSC Advances, 2017. **7**(55): p. 34638-34654.
277. Raja, T. and Y. D, *Analysis of the properties of a hemp fibre derived from Cannabis sativa as a renewable source.* Biomass Conversion and Biorefinery, 2023. **13**(16): p. 15149-15159.
278. Siouta, L., M. Apostolopoulou, and A. Bakolas, *Natural Fibers in Composite Materials for Sustainable Building: A State-of-the-Art Review on Treated Hemp Fibers and Hurds in Mortars.* Sustainability, 2024. **16**(23): p. 10368.
279. Ekbatani, S., et al., *Nano-engineered hierarchical natural fibre composites with localised cellulose nanocrystals and tailored interphase for improved mechanical properties.* Composites Science and Technology, 2024. **255**: p. 110719.
280. Kan, C.W., *Plasma treatments for sustainable textile processing*, in *Sustainable Apparel*. 2015. p. 49-118.
281. Sarikanat, M., et al., *The effect of argon and air plasma treatment of flax fiber on mechanical properties of reinforced polyester composite.* Journal of Industrial Textiles, 2016. **45**(6): p. 1252-1267.
282. Valášek, P., M. Müller, and V. Šleger, *Influence of Plasma Treatment on Mechanical Properties of Cellulose-based Fibres and Their Interfacial Interaction in Composite Systems.* BioResources, 2017. **12**(3).
283. Zille, A., F.R. Oliveira, and A.P. Souto, *Plasma Treatment in Textile Industry.* Plasma Processes and Polymers, 2015. **12**(2): p. 98-131.
284. Sadeghi, P., et al., *Experimental and Statistical Investigations for Tensile Properties of Hemp Fibers.* Fibers, 2024. **12**(11): p. 94.
285. Lyons, W.J., *Physical Properties of Textile Fibers. W. E. Morton and J. W. S. Hearle. Manchester and London, the Textile Institute and Butterworths, 1962.*

xxi + 608 pp. Price 105s ($14.70). Textile research journal, 1963. **33**(7): p. 580-581.
286. Tsai, P.P. and Y. Yan, *2 - The influence of fiber and fabric properties on nonwoven performance*, in *Applications of Nonwovens in Technical Textiles*, R.A. Chapman, Editor. 2010, Woodhead Publishing. p. 18-45.
287. Dai, X.Q., *10 - Fibers*, in *Biomechanical Engineering of Textiles and Clothing*, Y. Li and X.Q. Dai, Editors. 2006, Woodhead Publishing. p. 163-177.
288. Sair, S., et al., *Mechanical and thermal conductivity properties of hemp fiber reinforced polyurethane composites.* Case Studies in Construction Materials, 2018. **8**: p. 203-212.
289. Gajjar, C.R., M.W. King, and R. Guidoin, *8 - Retrieval studies for medical biotextiles*, in *Biotextiles as Medical Implants*, M.W. King, B.S. Gupta, and R. Guidoin, Editors. 2013, Woodhead Publishing. p. 182-210.
290. Jabbar, A., et al., *Oxygen plasma treatment to mitigate the shedding of fragmented fibres (microplastics) from polyester textiles.* Cleaner Engineering and Technology, 2024. **23**: p. 100851.
291. Mishra, R., J. Militky, and M. Venkataraman, *7 - Nanoporous materials*, in *Nanotechnology in Textiles*, R. Mishra and J. Militky, Editors. 2019, Woodhead Publishing. p. 311-353.
292. Mao, N., *6 - Methods for characterisation of nonwoven structure, property, and performance*, in *Advances in Technical Nonwovens*, G. Kellie, Editor. 2016, Woodhead Publishing. p. 155-211.
293. Jinka, S., et al., *Atmospheric pressure plasma treatment and breathability of polypropylene nonwoven fabric.* Journal of industrial textiles, 2013. **42**(4): p. 501-514.
294. Song, Z., et al., *Effect of porosity on the tensile strength and Micromechanisms of laminated stitched C/C-SiC composites.* Materials & Design, 2024. **247**: p. 113429.
295. G, S., A. Marino, and P. T, *Effects of Dry Etching Plasma Treatments on Natural and Synthetics Fibers: a Comparative Study.* Materials Circular Economy, 2022. **4**.
296. Zhou, P., et al., *Comparative Study of Durability Behaviors of Thermoplastic Polypropylene and Thermosetting Epoxy Exposed to Elevated Temperature, Water Immersion and Sustained Bending Loading.* Polymers, 2022. **14**(14): p. 2953.
297. Widiastuti, I., Y.R. Pratiwi, and D.N. Cahyo, *A Study on Water Absorption and Mechanical Properties in Epoxy-Bamboo Laminate Composite with Varying Immersion Temperatures.* Open Engineering, 2020. **10**(1): p. 814-819.
298. Levine, H. and L. Slade, *Water as a plasticizer: physico-chemical aspects of low-moisture polymeric systems*, in *Water Science Reviews 3: Water Dynamics*, F. Franks, Editor. 1988, Cambridge University Press: Cambridge. p. 79-185.
299. Rummani, G., et al., *Regional ultimate tensile strength and water sorption/solubility of bulk-fill and conventional resin composites: The effect of long-term water storage.* Dental Materials Journal, 2021. **40**(6): p. 1394-1402.
300. He, Z., et al., *How weak hydration interfaces simultaneously strengthen and toughen nanocellulose materials.* Extreme Mechanics Letters, 2023. **58**: p. 101947.

301. Sinko, R. and S. Keten, *Traction-separation laws and stick-slip shear phenomenon of interfaces between cellulose nanocrystals.* Journal of the Mechanics and Physics of Solids, 2015. **17**.
302. Zhang, C., et al., *Hygromechanical mechanisms of wood cell wall revealed by molecular modeling and mixture rule analysis.* Sci Adv, 2021. **7**(37): p. eabi8919.
303. Patel, P.C. and V. Kothari, *Relationship between tensile properties of fibres and nonwoven fabrics.* Indian Journal of Fibre and Textile Research, 2001. **26**: p. 398-402.
304. Rawal, A., et al., *Tensile behaviour of nonwoven structures: comparison with experimental results.* Journal of Materials Science, 2010. **45**(24): p. 6643-6652.
305. Beckermann, G.W. and K.L. Pickering, *Engineering and evaluation of hemp fibre reinforced polypropylene composites: Fibre treatment and matrix modification.* Composites Part A: Applied Science and Manufacturing, 2008. **39**(6): p. 979-988.
306. Janicki, J.C., et al., *Gauge length and temperature influence on the tensile properties of stretch broken carbon fiber tows.* Composites Part A: Applied Science and Manufacturing, 2021. **146**: p. 106426.
307. Placet, V., et al., *Diameter dependence of the apparent tensile modulus of hemp fibres: A morphological, structural or ultrastructural effect?* Composites Part A: Applied Science and Manufacturing, 2012. **43**(2): p. 275-287.
308. Kovar, R., B.S. Gupta, and Z. Kus, *4 - Stick-slip phenomena in textiles*, in *Friction in Textile Materials*, B.S. Gupta, Editor. 2008, Woodhead Publishing. p. 95-173.
309. Zhang, C., et al., *Hydrogen bonds dominated frictional stick-slip of cellulose nanocrystals.* Carbohydrate Polymers, 2021. **258**: p. 117682.
310. Fu, C., et al., *Crucial role of fiber swelling in microfibrillated cellulose extraction via ball milling.* Industrial Crops and Products, 2024. **218**: p. 118899.
311. Bai, G., et al. *Surface characteristics and dyeing properties of polyamide microfibers by plasma treatment*. in *International Conference on Advanced Fibers and Polymer Materials (ICAFPM 2005)*. 2005. Shanghai, PEOPLES R CHINA.
312. Inacio, W.P., F. Perissé Duarte Lopes, and S. Monteiro, *Diameter dependence of tensile strength by Weibull analysis: Part III sisal fiber.* Matéria (Rio de Janeiro), 2009. **15**: p. 124-130.
313. Stahlberg, R., *The phytomimetic potential of three types of hydration motors that drive nastic plant movements.* Mechanics of Materials, 2009. **41**(10): p. 1162-1171.
314. Quan, H., D. Kisailus, and M.A. Meyers, *Hydration-induced reversible deformation of biological materials.* Nature Reviews Materials, 2021. **6**(3): p. 264-283.
315. Lu, C., et al., *Structural and Mechanical Properties of Hemp Fibers: Effect of Progressive Removal of Hemicellulose and Lignin.* Journal of natural fibers, 2022. **19**(16): p. 13985-13994.
316. Singh, T., et al., *Emerging technologies for the development of wood products towards extended carbon storage and CO2 capture.* Carbon Capture Science & Technology, 2022. **4**: p. 100057.

317. Kumar, A., T. Jyske, and M. Petrič, *Delignified Wood from Understanding the Hierarchically Aligned Cellulosic Structures to Creating Novel Functional Materials: A Review.* Advanced Sustainable Systems, 2021. **5**(5): p. 2000251.
318. Agarwal, U.P., *1064 nm FT-Raman spectroscopy for investigations of plant cell walls and other biomass materials.* Front Plant Sci, 2014. **5**: p. 490.
319. Szymańska-Chargot, M., J. Cybulska, and A. Zdunek, *Sensing the structural differences in cellulose from apple and bacterial cell wall materials by Raman and FT-IR spectroscopy.* Sensors (Basel, Switzerland), 2011. **11**(6): p. 5543-5560.
320. Okuno, M., et al., *A Raman spectroscopic study of shock-wave densification of vitreous silica.* Physics and Chemistry of Minerals, 1999. **26**(4): p. 304-311.
321. Lee, C.M., et al., *Hydrogen-Bonding Network and OH Stretch Vibration of Cellulose: Comparison of Computational Modeling with Polarized IR and SFG Spectra.* J Phys Chem B, 2015. **119**(49): p. 15138-49.
322. Ahmadi, M., et al., *d-Glucose Oxidation by Cold Atmospheric Plasma-Induced Reactive Species.* ACS Omega, 2022. **7**(36): p. 31983-31998.
323. Etale, A., et al., *Cellulose: A Review of Water Interactions, Applications in Composites, and Water Treatment.* Chem Rev, 2023. **123**(5): p. 2016-2048.
324. Wohlert, M., et al., *Cellulose and the role of hydrogen bonds: not in charge of everything.* Cellulose (London), 2022. **29**(1): p. 1-23.
325. Velazquez, G., A. Herrera-Gómez, and M.O. Martín-Polo, *Identification of bound water through infrared spectroscopy in methylcellulose.* Journal of food engineering, 2003. **59**(1): p. 79-84.
326. Cichosz, S., A. Masek, and K. Dems-Rudnicka, *Original study on mathematical models for analysis of cellulose water content from absorbance/wavenumber shifts in ATR FT-IR spectrum.* Scientific Reports, 2022. **12**(1): p. 19739.
327. Khakalo, A., et al., *Delignification and Ionic Liquid Treatment of Wood toward Multifunctional High-Performance Structural Materials.* ACS Applied Materials & Interfaces, 2020. **12**(20): p. 23532-23542.